


For Reference

NOT TO BE TAKEN FROM THIS ROOM

Ex libris
UNIVERSITATIS
ALBERTAENSIS





Digitized by the Internet Archive
in 2023 with funding from
University of Alberta Library

<https://archive.org/details/Hinds1972>

THE UNIVERSITY OF ALBERTA

SURFACE TEMPERATURE EFFECTS
IN THE SLIDER BEARING

by



JOHN CHRISTOPHER HINDS

A THESIS

SUBMITTED TO THE FACULTY OF GRADUATE STUDIES AND RESEARCH
IN PARTIAL FULFILMENT OF THE REQUIREMENTS FOR THE DEGREE
OF MASTER OF SCIENCE

DEPARTMENT OF MECHANICAL ENGINEERING

EDMONTON, ALBERTA

FALL, 1972

UNIVERSITY OF ALBERTA

FACULTY OF GRADUATE STUDIES AND RESEARCH

The undersigned certify that they have read, and recommend to the Faculty of Graduate Studies and Research for acceptance, a thesis entitled "Surface Temperature Effects in the Slider Bearing," submitted by John Christopher Hinds in partial fulfilment of the requirements for the degree of Master of Science.

ABSTRACT

The effect of various temperature boundary conditions and different inlet to outlet ratios on the load carrying capacity of a plane slider bearing is analysed. The contribution of the inertia terms, and the effects of convection and dissipation are also examined. The lubricant is assumed to be incompressible, and the variation of viscosity with temperature is taken into account. From the governing equations, a set of reduced equations is first obtained by nondimensionalizing and carrying out an order of magnitude analysis. These reduced equations, together with the boundary conditions, are then transformed by use of the stream function, and the resulting equations are solved numerically. Using expressions developed, the load capacity, drag, mass flow, and average flow temperature are evaluated.

ACKNOWLEDGEMENTS

The author wishes to extend his appreciation to Dr. C. M. Rodkiewicz for his encouragement and guidance of this thesis, and also to Dr. C. Dayson of the National Research Council, who suggested the research topic.

Thanks are also extended to Mr. T. K. Chattopadhyay for his help in checking the equations, and to Mrs. Marilyn Wahl, whose skill and patience resulted in such a well typed thesis. Mr. A. Karim must also be thanked for his help in preparing the Figures, which allowed an early completion of the work.

Partial financial support for the author during the course of the work came from the National Research Council of Canada, through Grant NRC A-4198, and Grant NRC C-0083.

TABLE OF CONTENTS

CHAPTER		PAGE
I	STATEMENT OF THE PROBLEM	1
	DEFINITION OF THE PROBLEM	1
	INERTIA EFFECTS AND TEMPERATURE VARIATION IN A SLIDER BEARING	3
	REVIEW OF RELEVANT LITERATURE	5
II	THE GOVERNING EQUATIONS	8
	General Form of the Equations	8
	Reduction of the General Form of the Equations by an Order of Magnitude Analysis	10
	Transformation of the Governing Equations .	15
III	SOLUTION OF THE TRANSFORMED EQUATIONS	17
	Introduction	17
	Solution of the Momentum Equation Neglecting Inertia Terms and for Constant Viscosity .	17
	Solution of the Momentum Equation Neglecting Inertia Terms and for Variable Viscosity .	19
	Solution of the Momentum Equation Including Inertia Terms and for Variable Viscosity .	21
	Solution of the Energy Equation	23
	Method of Solution - Step by Step	26

CHAPTER	PAGE
IV DISCUSSIONS AND CONCLUSIONS	31
Introduction	31
Effects of Various Temperature Boundary	
Conditions - No Inertia	32
Influence of Inertia Terms	35
Effects of Varying Inlet to Outlet Ratio -	
No Inertia	37
Dissipation Effects - No Inertia	38
Convection Effects - No Inertia	40
Summary of Conclusions	50
Suggestions for Future Research	53
BIBLIOGRAPHY	54
APPENDIX A: TRANSFORMATION OF THE REDUCED EQUATIONS	
Transformation of the Reduced Equations	A1
Transformation of the Momentum Equation	A2
Transformation of the Energy Equation .	A3
B: ENERGY EQUATION IN FINITE DIFFERENCE FORM	
C: BEARING CHARACTERISTICS	
Dimensionless Mass Flow	C1
Dimensionless Load Capacity	C1
Dimensionless Shear Stress at Slider . .	C2
Dimensionless Drag	C2
Dimensionless Heat Convected into Bearing	C3
Dimensionless Heat Convected Out of Bearing	C3
Dimensionless Heat Flux Across Pad . . .	C4
Dimensionless Heat Flux Across Slider .	C4

CHAPTER	PAGE
APPENDIX C: Dimensionless Heat Flux Across Slider . .	C4
Dimensionless Heat Conducted Through Pad	C4
Dimensionless Heat Conducted Through Slider	C5
Average Flow Temperature	C5
APPENDIX D: CURVES FOR CHAPTER IV	
APPENDIX E: TABLES FOR CHAPTER IV	
APPENDIX F: COMPUTER PROGRAMS	
Program to Solve for Case of Constant Viscosity and Including Inertia Terms	F1
Program to Solve for Case of Variable Viscosity and Including Inertia Terms	F8

LIST OF TABLES

TABLE		PAGE
1a	Effect of Cooling Slider - No Inertia (i) $T_p = 100^\circ\text{F}$, $PE = 1.0$, $P_e = 5.0$ (ii) $T_p = 100^\circ\text{F}$, $PE = 1.0$, $P_e = 10.0$	E1
1b	Effect of Heating Pad - No Inertia (i) $T_s = 100^\circ\text{F}$, $PE = 1.0$, $P_e = 5.0$ (ii) $T_s = 100^\circ\text{F}$, $PE = 1.0$, $P_e = 10.0$	E2
1c	Effect of Cooling Slider and Heating Pad - No Inertia (i) $T_s + T_p = 350^\circ\text{F}$, $PE = 1.0$, $P_e = 5.0$ (ii) $T_s + T_p = 350^\circ\text{F}$, $PE = 1.0$, $P_e = 10.0$. .	E3
1d	Effect of Boundary Temps. on Load Capacity for the same T_s/T_p ratio (i) $T_s/T_p = 2.0$, $PE = 1.0$, 5.0 (ii) $T_s/T_p = 0.5$, $PE = 1.0$, 5.0	E4
2a	Influence of Inertia Terms (i) Viscosity Constant (ii) $T_s = 200^\circ\text{F}$, $T_p = 100^\circ\text{F}$, $P = 59.64$, $PE = 0.5357$	E5
2b	Influence of Inertia Terms $P = 59.64$, $PE = 0.5357$ (i) $T_s = 150^\circ\text{F}$, $T_p = 150^\circ\text{F}$ (ii) $T_s = 100^\circ\text{F}$, $T_p = 200^\circ\text{F}$	E7
2c	% Increase in Load Capacity Due to the Presence of Inertia Terms	E8
3a	Varying Inlet to Outlet Ratio - No Inertia $T_s = 150^\circ\text{F}$, $T_p = 150^\circ\text{F}$, $PE = 1.0$ (i) $P_e = 6.0$ (ii) $P_e = 1.25$ (iii) $P_e = 0.10$	E9
3b	Varying Inlet to Outlet Ratio - No Inertia $T_s = 200^\circ\text{F}$, $T_p = 100^\circ\text{F}$, $PE = 1.0$ (i) $P_e = 6.0$ (ii) $P_e = 1.25$ (iii) $P_e = 0.10$	E10
3c	Varying Inlet to Outlet Ratio - No Inertia $T_s = 100^\circ\text{F}$, $T_p = 200^\circ\text{F}$, $PE = 1.0$ (i) $P_e = 6.0$ (ii) $P_e = 1.25$ (iii) $P_e = 0.10$	E11

TABLE

PAGE

4a	Dissipation Effects - No Inertia (i) $T_s/T_p = 0.5$, $P_e = 5.0$, (ii) $T_s/T_p = 1.0$, $P_e = 5.0$, (iii) $T_s/T_p = 2.0$, $P_e = 5.0$	E12
4b	Dissipation Effects - No Inertia (i) $T_s/T_p = 0.5$, $P_e = 10.0$ (ii) $T_s/T_p = 1.0$, $P_e = 10.0$ (iii) $T_s/T_p = 2.0$, $P_e = 10.0$	E14
4c	Dissipation Effects - No Inertia (i) $T_s/T_p = 0.5$, $P_e = 15.0$ (ii) $T_s/T_p = 1.0$, $P_e = 15.0$ (iii) $T_s/T_p = 2.0$, $P_e = 15.0$	E16
4d	Dissipation Effects - No Inertia (i) $T_s/T_p = 0.5$, $P_e = 20.0$ (ii) $T_s/T_p = 1.0$, $P_e = 20.0$ (iii) $T_s/T_p = 2.0$, $P_e = 20.0$	E18
5a	Convection Effects - No Inertia (i) $T_s/T_p = 0.5$, $PE = 0.39$ (ii) $T_s/T_p = 1.0$, $PE = 0.39$ (iii) $T_s/T_p = 2.0$, $PE = 0.39$	E20
5b	Convection Effects - No Inertia (i) $T_s/T_p = 0.5$, $PE = 1.59$ (ii) $T_s/T_p = 1.0$, $PE = 1.59$ (iii) $T_s/T_p = 2.0$, $PE = 1.59$	E21
5c	Convection Effects - No Inertia (i) $T_s/T_p = 0.5$, $PE = 10.89$ (ii) $T_s/T_p = 1.0$, $PE = 10.89$ (iii) $T_s/T_p = 2.0$, $PE = 10.89$	E22
5d	Convection Effects - No Inertia (i) $T_s/T_p = 0.5$, $PE = 20.33$, (ii) $T_s/T_p = 1.0$, $PE = 20.33$ (iii) $T_s/T_p = 2.0$, $PE = 20.33$	E23
5e	Convection Effects - No Inertia (i) $T_s/T_p = 0.5$, $PE = 43.06$ (ii) $T_s/T_p = 1.0$, $PE = 43.06$ (iii) $T_s/T_p = 2.0$, $PE = 43.06$	E24

LIST OF FIGURES

FIGURE		PAGE
1	Slider Bearing Geometry	3
2	Marching Scheme for Solving Energy Equation . .	26
3	Grid Network	B6
4	Velocity Distribution at Various Sections Along Length of Bearing $T_s = 200^{\circ}\text{F}$, $T_p = 100^{\circ}\text{F}$ - No Inertia	D1
5	Velocity Distribution at Various Sections Along Length of Bearing $T_s = 100^{\circ}\text{F}$, $T_p = 100^{\circ}\text{F}$ - No Inertia	D2
6	Velocity Distribution at Various Sections Along Length of Bearing $T_s = 50^{\circ}\text{F}$, $T_p = 100^{\circ}\text{F}$ - No Inertia	D3
7	Temperature Distribution at Various Sections Along Length of Bearing $T_s = 200^{\circ}\text{F}$, $T_p = 100^{\circ}\text{F}$ - No Inertia	D4
8	Pressure Distribution At Various Sections Along Length of Bearing - No Inertia	D5
9	Shear Stress Distribution at Various Sections Along Length of Bearing - No Inertia	D6
10	Load Capacity Versus T_s/T_p - Slider Cooled . .	D7
11	Load Capacity Versus T_s/T_p - Pad Heated	D8
12	Load Capacity Versus T_s/T_p - Slider Cooled and Pad Heated	D9

FIGURE		PAGE
13	Drag Versus T_s/T_p - Slider Cooled	D10
14	Drag Versus T_s/T_p - Pad Heated	D11
15	Effect of Boundary Temperatures on Load Capacity for the Same T_s/T_p Ratio - No Inertia	D12
16	Velocity Distribution at Various Sections Along Length of Bearing $Re^* = 0.5$ - No Inertia	D13
17	Velocity Distribution at Various Sections Along Length of Bearing $Re^* = 0.5$ - Inertia Included	D14
18	Temperature Distribution at Various Sections Along Length of Bearing $Re^* = 0.5$ - No Inertia	D15
19	Temperature Distribution at Various Sections Along Length of Bearing $Re^* = 0.5$ - Inertia Included	D16
20	Pressure Distribution at Various Sections Along Length of Bearing	D17
21	Shear Stress Distribution at Various Sections Along Length of Bearing	D18
22	Plot of Load Capacity Versus Reynolds No. - Comparison With Previous Works	D19
23	Plot of Load Capacity Versus Reynolds No. for Various Temperature Boundary Conditions	D20
24	Velocity Distribution at Various Sections Along Length of Bearing $\bar{h}_r = 1.75$ - No Inertia	D21
25	Velocity Distribution at Various Sections Along Length of Bearing $\bar{h}_r = 2.25$ - No Inertia	D22

FIGURE		PAGE
26	Velocity Distribution at Various Sections Along Length of Bearing $\bar{h}_r = 2.75$ - No Inertia	D23
27	Temperature Distribution at Various Sections Along Length of Bearing $\bar{h}_r = 1.75$ - No Inertia	D24
28	Temperature Distribution at Various Sections Along Length of Bearing $\bar{h}_r = 2.25$ - No Inertia	D25
29	Temperature Distribution at Various Sections Along Length of Bearing $\bar{h}_r = 2.75$ - No Inertia	D26
30	Pressure Distribution at Various Sections Along Length of Bearing - No Inertia	D27
31	Shear Stress Distribution at Various Sections Along Length of Bearing - No Inertia	D28
32	Load Capacity Versus Inlet to Outlet Ratio $T_s = 200^\circ\text{F}$, $T_p = 100^\circ\text{F}$ - No Inertia	D29
33	Load Capacity Versus Inlet to Outlet Ratio $T_s = 150^\circ\text{F}$, $T_p = 150^\circ\text{F}$ - No Inertia	D30
34	Load Capacity Versus Inlet to Outlet Ratio $T_s = 100^\circ\text{F}$, $T_p = 200^\circ\text{F}$ - No Inertia	D31
35	Load Capacity Versus Inlet to Outlet Ratio for Various Temperature Boundary Conditions - No Inertia	D32
36	Velocity Distribution at Various Sections Along Length of Bearing $PE = 1.27$ - No Inertia	D33
37	Velocity Distribution at Various Sections Along Length of Bearing $PE = 5.08$ - No Inertia	D34

FIGURE		PAGE
38	Velocity Distribution at Various Sections Along Length of Bearing $PE = 20.33$ - No Inertia	D35
39	Temperature Distribution at Various Sections Along Length of Bearing $PE = 1.27$ - No Inertia	D36
40	Temperature Distribution at Various Sections Along Length of Bearing $PE = 5.08$ - No Inertia	D37
41	Temperature Distribution at Various Sections Along Length of Bearing $PE = 20.33$ - No Inertia	D38
42	Pressure Distribution at Various Sections Along Length of Bearing - No Inertia	D39
43	Shear Stress Distribution at Various Sections Along Length of Slider - No Inertia	D40
44	Load Capacity Versus PE for Various Values of P_e . $T_s = 55^\circ\text{F}$, $T_p = 110^\circ\text{F}$ - No Inertia . . .	D41
45	Load Capacity Versus PE for Various Values of P_e . $T_s = 82.5^\circ\text{F}$, $T_p = 82.5^\circ\text{F}$ - No Inertia . .	D42
46	Load Capacity Versus PE for Various Values of P_e . $T_s = 100^\circ\text{F}$, $T_p = 55^\circ\text{F}$ - No Inertia . . .	D43
47	Velocity Distribution at Various Sections Along Length of Bearing $P_e = 1.0$ - No Inertia	D44
48	Velocity Distribution at Various Sections Along Length of Bearing $P_e = 5.0$ - No Inertia	D45
49	Velocity Distribution at Various Sections Along Length of Bearing $P_e = 20.0$ - No Inertia	D46

FIGURE		PAGE
50	Temperature Distribution at Various Sections Along Length of Bearing $P_e = 1.0$ - No Inertia	D47
51	Temperature Distribution at Various Sections Along Length of Bearing $P_e = 5.0$ - No Inertia	D48
52	Temperature Distribution at Various Sections Along Length of Bearing $P_e = 20.0$ - No Inertia	D49
53	Pressure Distribution at Various Sections Along Length of Bearing - No Inertia	D50
54	Shear Stress Distribution at Various Sections Along Length of Slider - No Inertia	D51
55	Load Capacity Versus P_e for Various Values of PE. $T_s/T_p = 0.5$ - No Inertia	D52
56	Load Capacity Versus P_e for Various Values of PE. $T_s/T_p = 1.0$ - No Inertia	D53
57	Load Capacity Versus P_e for Various Values of PE. $T_s/T_p = 2.0$ - No Inertia	D54
58	Viscosity Temperature relationship for medium and for light oil	D55

LIST OF SYMBOLS

- a = coefficient in difference equations (3.21) and (A.12)
 A_1 = integral expression of equations (3.13)
 A_2 = integral expression of equations (3.13)
 A_3 = integral expression of equations (3.13)
 A_4 = integral expression of equations (3.13)
 A_5 = integral expression of equations (3.20)
 A_6 = integral expression of equations (3.20)
 b = coefficient in difference equations (3.21) and (A.12)
 B_1 = expression for constant in equations (3.12) and (3.19)
 B_2 = expression for constant in equations (3.12) and (3.19)
 c = coefficient in difference equations (3.21) and (A.12)
 C_1 = coeff. in equations (3.2), (3.9) and (3.16)
 C_2 = coeff. in equations (3.2), (3.9) and (3.16)
 C_3 = coeff. in equations (3.2), (3.9) and (3.16)
 C_p = specific heat of lubricant at constant pressure
 d = coeff. in difference equations (3.21) and (A.12)
 D_1 = expression for constant in equations (3.6), (3.11)
 and (3.18)
 D_2 = expression for constant in equations (3.6), (3.11)
 and (3.18)
 \bar{D} = dimensionless drag, $Dh_o/\mu_r UL$
 E = type of Eckert number, $U^2/C_p T_r$

F = correction due to the presence of inertia terms, as described by equation (3.15)

h = film thickness determined by equation (2.6)

h_i = inlet spacing between bearing members

h_o = outlet spacing between bearing members

\bar{h} = dimensionless film thickness

\bar{h}_r = ratio of inlet to outlet

i = parameter indicating sectional location along \bar{x} direction of grid

j = parameter indicating sectional location along \bar{y} direction of grid

L = length of bearing

$m = \bar{h}_r - 1$

M = number of sectional locations along \bar{x} direction of grid

N = number of sectional locations along \bar{y} direction of grid

p = gauge pressure

\bar{p} = dimensionless pressure, $pRe^*/\rho U^2$

P = Prandtl number, $\mu_r C_p / K$

q_p = heat flux at pad

q_s = heat flux at slider

\bar{q}_p = dimensionless heat flux at pad, $q_p h_o / K T_r$

\bar{q}_s = dimensionless heat flux at slider, $q_s h_o / K T_r$

Q_e = heat convected out of bearing

\bar{Q}_e = dimensionless heat convected out of bearing, $\frac{Q_e}{(\rho C_p T_r U h_o)}$

Q_i = heat convected into bearing

\bar{Q}_i = dimensionless heat convected into bearing, $\frac{Q_i}{(\rho C_p T_r U h_o)}$

Q_p = heat conducted through pad

\bar{Q}_p = dimensionless heat conducted through pad, $Q_p h_o / \kappa T_r L$

Q_s = heat conducted through slider

\bar{Q}_s = dimensionless heat conducted through slider, $Q_s h_o / \kappa T_r L$

Re^* = modified Reynolds number, $\frac{\rho U L}{\mu_r} \left(\frac{h_o}{L}\right)^2$

T = lubricant temperature

T_b = average flow temperature

T_p = temperature at interface between lubricant and pad

T_s = temperature at interface between lubricant and slider

T_r = reference temperature, $(T_s + T_p) / 2.0$

\bar{T} = dimensionless temperature, T / T_r

u = velocity in x-direction

\bar{u} = dimensionless velocity in x-direction, u / U

U = velocity of slider

v = velocity in y-direction

\bar{v} = dimensionless velocity in \bar{y} -direction

V = reference velocity in y-direction

W = load capacity of bearing

\bar{W} = dimensionless load capacity of bearing, $\frac{W h_o^2}{\mu_r U L}$

\bar{W}_L = dimensionless load capacity of bearing, $\frac{W h_o^2}{6 \mu_r U L}$

x = longitudinal coordinate

\bar{x} = dimensionless longitudinal coordinate, x / L

$\Delta \bar{x}$ = grid spacing in \bar{x} direction

y = transverse coordinate

\bar{y} = dimensionless transverse coordinate, $y/h(x)$

$\Delta \bar{y}$ = grid spacing in \bar{y} direction

GREEK LETTERS

β = temperature coefficient of viscosity

κ = thermal conductivity of lubricant

ρ = density of lubricant

Ψ = stream function

$\bar{\Psi}$ = dimensionless stream function, Ψ/Ψ_c

Ψ_c = rate of mass flow through bearing

$\bar{\Psi}_c$ = dimensionless mass flow, $\frac{\Psi_c}{\rho U h_0}$

τ = shear stress at a point in the fluid

τ_0 = shear stress at slider

$\bar{\tau}_0$ = dimensionless shear stress at slider, $\frac{\tau_0 h_0}{\mu_r U}$

μ = viscosity of lubricant

$\bar{\mu}$ = dimensionless viscosity of lubricant, μ/μ_r

μ_r = reference viscosity of lubricant

CHAPTER I

STATEMENT OF THE PROBLEM

The purpose of the present investigation, is to study the effects of various temperature boundary conditions, on the load-carrying capacity of a plane slider bearing.

DEFINITION OF PROBLEM

Up to now, not much work has been carried out on methods for increasing the load-carrying capacity of slider bearings. Some of the work done by Tahara [1] and a few others, have been concerned with removing the heat generated in a lubricating film, by use of a coolant forced through the bottom of the bearing pad. The reasoning was that cooling the lubricant would not only prevent overheating, but would also increase the load-carrying capacity of the bearing. The fact that cooling the lubricant increases its viscosity is well known, but it should also be borne in mind that a more viscous lubricant would also tend to increase the dissipative effects in the bearing. We can see therefore that the main factor contributing to the load capacity is not simply the bulk flow temperature.

It is possible to obtain a better understanding of the contributions to load capacity, if we consider the physical aspects of the operation of a slider bearing. The main

requirement for the operation of any bearing, is that the bearing must be able to support a load. In the case of fluid film bearings, this requirement means that the lubricant must be under pressure. For shafts operating at very low speeds, and under heavy loads, this pressure is usually supplied from outside; and these bearings are known as externally pressurized or hydrostatic bearings. In the case of bearings operating at higher speeds, and under average loads, the pressure is usually supplied by the revolving motion of the shaft which drags lubricant into the bearing. These types of bearings are usually referred to as hydrodynamic bearings, and are the ones of interest in this study.

When the lubricant enters the bearing, the tapered shape of the pad surface (See Fig. 1) forces the fluid close to it to flow parallel to this inclined surface. In reaction to this constraint, the fluid exerts a pressure on the bearing pad. This pressure builds up to a maximum around the middle of the bearing then decreases to the ambient pressure at the bearing outlet.

The amount of load a bearing can carry is influenced by the inlet to outlet ratio, h_i/h_o . It has been shown [2] that the load capacity rises to a maximum for $h_i/h_o = 2.2$ then falls gradually. For h_i/h_o fixed, the load which the

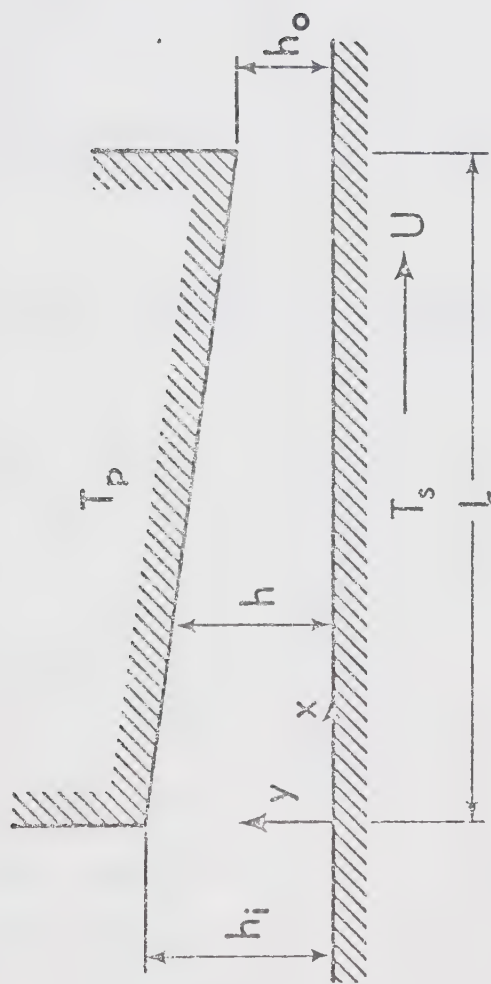


Fig. 1 Slider Bearing Geometry

bearing can support is determined by the thickness of the lubricant film. For the same load the thicker the film the larger the load the bearing can carry. This is because it will require a larger load on the bearing in order for the film thickness to return to its original value. Our attempts at increasing the load capacity should therefore be concerned with increasing the thickness of the lubricant film for a given load. This can be accomplished most effectively by cooling the slider, or by cooling the bearing pad.

INERTIA EFFECTS AND TEMPERATURE VARIATION IN A SLIDER BEARING

The Reynolds equation is based on the assumption that the inertia forces are negligible compared to the viscous forces [3]. The importance of the inertia terms relative to the viscous terms in the equation of motion, can be characterized by a dimensionless parameter referred to as the modified Reynolds number, Re^* .

In the operation of most bearings, Re^* , is very small, therefore the inertia effects could be easily ignored. However, for bearings operating at high speeds, or where the viscosity of the lubricant is very low (e.g. for gas bearings), Re^* may reach values near to or exceeding unity. Thus, in such a case, the inertia forces become comparable in magnitude to the viscous forces and may no longer be ignored. If the

Reynolds number becomes greater than a certain critical value, turbulence will develop, and the governing equations will have to be correspondingly modified.

Another assumption made in classical hydrodynamic lubrication, is that the temperature variation in the lubricant film is negligible. The viscosity is then taken as being constant throughout the film, and equal to the inlet oil viscosity. This results in the uncoupling of the momentum and the energy equations, which greatly simplifies the solution of the problem. Under most operating conditions though, the energy generated by viscous dissipation causes a significant rise in the lubricant film temperature. This results in a corresponding decrease in viscosity. Hence, the solution assuming viscosity at the inlet oil temperature will be in error. Wilcock [4] and Rosenblatt [5] conclude from their experiments, that in fact the average value of viscosity corresponding to that of the outlet oil should be taken. Several authors have attempted to include the viscosity variation, by allowing the viscosity to vary in the X direction only. This results in a much simpler form of the momentum and the energy equations.

The temperature distribution within the bearing, depends largely on the thermal boundary conditions imposed on the film. If both boundaries were taken as adiabatic, all the heat generated by viscous dissipation would have to be carried out by the fluid. The effect of this would be to decrease the average lubricant viscosity, thus reducing the

load carrying capacity of the bearing. If the boundaries were not adiabatic though, some of the heat generated would be transferred across the bearing faces, and the resulting decrease in load carrying capacity would not be as great.

REVIEW OF RELEVANT LITERATURE

The equations of motion for the slider bearing, yield two non-linear partial differential equations; and over the years, several authors have investigated the influence of the non-linear inertia terms using approximate methods.

Slezkin and Targ [6] averaged the inertia terms across the film thickness. This allowed the resulting equation to be readily integrated, since the inertia terms became a function of x only. Other authors [7,8] have employed this technique to obtain solutions for various bearing configurations.

Kahlert [9] assumed that the inertia forces were small compared to the viscous forces. He then included the influence of the inertia terms by a small correction to the results obtained from the purely viscous consideration.

Snyder [10] obtained a more exact solution, by taking into account the variation of the inertia effects across the film as well as in the direction of flow. In his method, the stream function is expressed as a power series in δ , which is a function of film thickness; while the coefficients are assumed to be functions of η , which in turn is a function of both x and y . These coefficients are obtained by solving a

set of differential equations. In his solution, Snyder solved for only the first two terms of the power series. More recently, Rodkiewicz and Anwar [11] found that it was necessary to retain at least four terms of the series expansion, in order to improve the accuracy at higher modified Reynolds numbers.

In all of the previous references, the solutions were obtained assuming constant viscosity. Other researchers have taken into account the variation of the lubricant viscosity, for various boundary conditions on the film temperature. Hunter and Zienkiewicz [12] considered two different boundary conditions on the temperature.

(1) Both boundaries having the same temperature.

(2) Both boundaries adiabatic.

In their analysis, they neglected the inertia terms, and also the lateral convection term in the energy equation.

Snyder [13] studied the overall temperature variations across the lubricant film. The slider surface was taken as an isothermal surface, and the stationary surface as adiabatic. From his analysis, he concluded that the consequences of the variations of viscosity cannot be neglected for high Prandtl number lubricants. The most complete investigation so far has been carried out by Hahn and Kettleborough [14], who used matrix methods. They retained the inertia terms in the momentum equation, and the convective terms in the energy equation. Also, the viscosity of the lubricant was regarded as a function of temperature and pressure, and the density a

function of temperature. The temperature boundary conditions were obtained by equating the heat fluxes at the solid-liquid interfaces. They concluded that it was desirable to cool the bearing surfaces, since this would increase the load carrying capacity of the bearings. It was also found that the temperature at the moving surface was reasonably constant, even though the heat flux varied considerably.

CHAPTER II

THE GOVERNING EQUATIONS

GENERAL FORM OF THE EQUATIONS

The equations governing the steady, laminar flow of an incompressible lubricant through an infinite slider bearing, as shown in Fig. I, are the momentum equations in the x and y directions, (Eqs. (2.1) and (2.2) respectively), the energy equation, Eq. (2.3), and the continuity equation, Eq. (2.4). In order to solve these equations, it is also necessary to specify the boundary conditions as presented in Eqs. (2.5).

For our problem, the boundary conditions on velocity are obtained by satisfying the conditions of no-slip at the pad and at the slider; while the boundary conditions on the temperature, are obtained from the compatibility conditions at the said two interfaces.

The general form of the equations may now be listed as follows:

Momentum equations

$$\rho \left[u \frac{\partial u}{\partial x} + v \frac{\partial u}{\partial y} \right] = - \frac{\partial p}{\partial x} + 2 \frac{\partial}{\partial x} \left(\mu \frac{\partial u}{\partial x} \right) + \frac{\partial}{\partial y} \left(\mu \frac{\partial u}{\partial y} \right) + \frac{\partial}{\partial y} \left(\mu \frac{\partial v}{\partial x} \right)$$

(2.1)

$$\rho \left[v \frac{\partial v}{\partial y} + u \frac{\partial v}{\partial x} \right] = - \frac{\partial p}{\partial y} + 2 \frac{\partial}{\partial y} \left(\mu \frac{\partial v}{\partial y} \right) + \frac{\partial}{\partial x} \left(\mu \frac{\partial u}{\partial y} \right) + \frac{\partial}{\partial x} \left(\mu \frac{\partial v}{\partial x} \right) \quad (2.2)$$

Energy equation

$$\rho C_p \left[u \frac{\partial T}{\partial x} + v \frac{\partial T}{\partial y} \right] = \frac{\partial}{\partial x} \left(k \frac{\partial T}{\partial x} \right) + \frac{\partial}{\partial y} \left(k \frac{\partial T}{\partial y} \right) + \mu \left\{ 2 \left[\left(\frac{\partial u}{\partial x} \right)^2 + \left(\frac{\partial v}{\partial y} \right)^2 \right] + \left[\frac{\partial v}{\partial x} + \frac{\partial u}{\partial y} \right]^2 - \frac{2}{3} \left[\frac{\partial u}{\partial x} + \frac{\partial v}{\partial y} \right]^2 \right\} \quad (2.3)$$

Continuity equation

$$\frac{\partial u}{\partial x} + \frac{\partial v}{\partial y} = 0 \quad (2.4)$$

Boundary conditions:

$$y=0; u=U, v=0$$

$$y=h; u=0, v=0$$

$$y=0; T=T_s$$

$$y=h; T=T_p$$

$$\int_0^L \left(\frac{dp}{dx} \right) dx = 0$$

The equation used for the film thickness is

$$h = h_o + (h_i - h_o) (L-x)/L \quad (2.6)$$

REDUCTION OF THE GENERAL FORM OF THE EQUATIONS
BY AN ORDER OF MAGNITUDE ANALYSIS

Because of the large number of terms in the Governing Equations (2.1) through (2.4), it would be very difficult to obtain a satisfactory solution. In order to simplify the problem, the given equations will be nondimensionalized, and an order of magnitude analysis carried out. It would then be possible to retain only the most important terms, and obtain solutions for the derived set of reduced equations.

Before proceeding with the nondimensionalization, a list of some of the usual assumptions made is in order:

- (1) The lubricant film is very thin i.e. $h/L \ll 1$.
- (2) The density, thermal conductivity, and specific heat of the lubricant are constant.
- (3) The effects of thermal and elastic distortions are negligible.
- (4) Cavitation effects may be ignored.
- (5) The temperature distribution at the inlet is linear.

Selecting appropriate reference quantities, the variables can be expressed as follows:

$$\begin{array}{ll}
 x = \bar{x}L & T = \bar{T}T_r \\
 y = \bar{y}h & h = \bar{h}h_o \\
 u = \bar{u}U & h_i = \bar{h}_r h_o \\
 v = \bar{v}V & \mu = \bar{\mu} \mu_r \\
 p = \bar{p} \rho U^2 / \text{Re}^* & \text{where } T_r = (T_s + T_p)/2
 \end{array}$$

By substituting these transformed variables into the governing equations, and with some rearranging, it is possible to compare the relative magnitudes of the various terms.

Upon transforming the x derivative, we obtain

$$\begin{aligned}
 \frac{\partial}{\partial x} &= \frac{\partial}{\partial \bar{x}} \frac{\partial \bar{x}}{\partial x} + \frac{\partial}{\partial \bar{y}} \frac{\partial \bar{y}}{\partial x} \\
 &= \frac{\partial}{\partial \bar{x}} \left(\frac{1}{L} \right) + \frac{\partial}{\partial \bar{y}} \frac{\partial}{\partial x} \left(\frac{y}{h} \right) \\
 &= \frac{1}{L} \frac{\partial}{\partial \bar{x}} + y \left(\frac{-1}{h^2} \right) \frac{\partial h}{\partial x} \frac{\partial}{\partial \bar{y}} \\
 &= \frac{1}{L} \frac{\partial}{\partial \bar{x}} + \left(\frac{y}{h} \right) \left(\frac{-1}{h} \right) \frac{\partial h}{\partial x} \frac{\partial}{\partial \bar{y}} ,
 \end{aligned}$$

From Eq. (2.6),

$$\begin{aligned}
 h &= h_o + (h_i - h_o) (L-x)/L \\
 \frac{\partial h}{\partial x} &= -(h_i - h_o)/L \\
 &= -(h_i/h_o - 1)h_o/L \\
 &= -(\bar{h}_r - 1)h_o/L \\
 \frac{\partial}{\partial x} &= \frac{1}{L} \left[\frac{\partial}{\partial \bar{x}} + \bar{y} \frac{(\bar{h}_r - 1)}{\bar{h}} \frac{\partial}{\partial \bar{y}} \right]
 \end{aligned}$$

Writing $\frac{\partial}{\partial x^*} = \frac{\partial}{\partial \bar{x}} + \bar{y} \frac{(\bar{h}_r - 1)}{\bar{h}} \frac{\partial}{\partial \bar{y}}$

$$\frac{\partial}{\partial x} = \frac{1}{L} \frac{\partial}{\partial x^*} \tag{2.7}$$

Similarly for the y derivative,

$$\begin{aligned}
 \frac{\partial}{\partial \bar{y}} &= \frac{\partial}{\partial \bar{x}} \frac{\partial \bar{x}}{\partial \bar{y}} + \frac{\partial}{\partial \bar{y}} \frac{\partial \bar{y}}{\partial \bar{y}} \\
 &= \frac{\partial}{\partial \bar{x}} 0 + \frac{\partial}{\partial \bar{y}} \left(\frac{1}{h} \right) \\
 \frac{\partial}{\partial \bar{y}} &= \frac{1}{h_0 \bar{h}} \frac{\partial}{\partial \bar{y}}
 \end{aligned} \tag{2.8}$$

For the continuity equation, we get

$$\frac{U}{L} \frac{\partial \bar{u}}{\partial \bar{x}^*} + \frac{V}{h_0 \bar{h}} \frac{\partial \bar{v}}{\partial \bar{y}} = 0$$

$$\text{i.e.} \quad \frac{\partial \bar{u}}{\partial \bar{x}^*} + \left(\frac{VL}{Uh_0} \right) \frac{1}{\bar{h}} \frac{\partial \bar{v}}{\partial \bar{y}} = 0$$

In the above equation, $\frac{\partial \bar{u}}{\partial \bar{x}^*}$, $\frac{\partial \bar{v}}{\partial \bar{y}}$, and \bar{h} are all of order [1]. Consequently, we must have $\frac{VL}{Uh_0} = 0[1]$ also. Choosing $\frac{VL}{Uh_0} = 1$ We can write $V = Uh_0/L$

The momentum equations become

$$\begin{aligned}
 \bar{h}^2 \text{Re}^* \left[\bar{u} \frac{\partial \bar{u}}{\partial \bar{x}^*} + \frac{\bar{v}}{\bar{h}} \frac{\partial \bar{u}}{\partial \bar{y}} \right] &= \bar{h}^2 \left[- \frac{\partial \bar{p}}{\partial \bar{x}^*} + 2 \left(\frac{h_0}{L} \right)^2 \frac{\partial}{\partial \bar{x}^*} \left(\bar{\mu} \frac{\partial \bar{u}}{\partial \bar{x}^*} \right) + \right. \\
 &\quad \left. \left(\frac{h_0}{L} \right)^2 \frac{\partial}{\partial \bar{y}} \left(\bar{\mu} \frac{\partial \bar{v}}{\partial \bar{x}^*} \right) \right] + \frac{\partial}{\partial \bar{y}} \left(\bar{\mu} \frac{\partial \bar{u}}{\partial \bar{y}} \right)
 \end{aligned} \tag{2.9}$$

$$\begin{aligned}
 \bar{h}^2 \text{Re}^* \left(\frac{h_0}{L} \right)^2 \left[\frac{\bar{v}}{\bar{h}} \frac{\partial \bar{v}}{\partial \bar{y}} + \bar{u} \frac{\partial \bar{v}}{\partial \bar{x}^*} \right] &= \left[- \bar{h} \frac{\partial \bar{p}}{\partial \bar{y}} + \left(\frac{h_0}{L} \right)^2 \frac{\partial}{\partial \bar{y}} \left(\bar{\mu} \frac{\partial \bar{v}}{\partial \bar{y}} \right) \right. \\
 &\quad \left. + \left(\frac{h_0}{L} \right)^2 \bar{h} \frac{\partial}{\partial \bar{x}^*} \left(\bar{\mu} \frac{\partial \bar{u}}{\partial \bar{y}} \right) + \bar{h}^2 \left(\frac{h_0}{L} \right)^4 \frac{\partial}{\partial \bar{x}^*} \left(\bar{\mu} \frac{\partial \bar{v}}{\partial \bar{x}^*} \right) \right]
 \end{aligned} \tag{2.10}$$

and the energy equation yields

$$\begin{aligned}
 \left[\bar{u} \frac{\partial \bar{T}}{\partial x^*} + \frac{\bar{v}}{\bar{h}} \frac{\partial \bar{T}}{\partial \bar{y}} \right] &= \frac{1}{P \operatorname{Re}^*} \left(\frac{h_o}{L} \right)^2 \frac{\partial^2 \bar{T}}{\partial x^{*2}} + \frac{1}{P \operatorname{Re}^*} \frac{1}{h^2} \frac{\partial^2 \bar{T}}{\partial \bar{y}^2} \\
 &+ \frac{E}{\operatorname{Re}^*} \left(\frac{h_o}{L} \right)^2 \frac{1}{\mu} \left\{ \left[\left(\frac{\partial \bar{u}}{\partial x^*} \right)^2 + \left(\frac{\partial \bar{v}}{\partial \bar{y}} \right)^2 \frac{1}{\bar{h}^2} \right] + \left[\left(\frac{h_o}{L} \right) \frac{\partial \bar{v}}{\partial x^*} + \left(\frac{L}{h_o} \right) \frac{\partial \bar{u}}{\partial \bar{y}} \right]^2 \right. \\
 &\left. - 2/3 \left[\frac{\partial \bar{u}}{\partial x^*} + \frac{1}{\bar{h}} \frac{\partial \bar{v}}{\partial \bar{y}} \right]^2 \right\} \quad (2.11)
 \end{aligned}$$

One of our earlier assumptions was that the lubricating film was very thin, ie. $h/L \ll 1$. From this assumption, it follows that $(h/L)^2 \ll 1$, and $L/h \gg 1$. With these facts in mind, it is possible to retain only those terms with the larger coefficients. We are thus able to obtain a set of reduced equations, which are to be solved for a given set of boundary conditions:

For the momentum equation in the \bar{y} direction we get

$$\frac{\partial \bar{p}}{\partial \bar{y}} = - \bar{h} \operatorname{Re}^* \left(\frac{h_o}{L} \right)^2 \left[\frac{\bar{v}}{\bar{h}} \frac{\partial \bar{v}}{\partial \bar{y}} + \bar{u} \frac{\partial \bar{v}}{\partial x^*} \right] \quad (2.12)$$

Now both $\frac{\bar{v}}{\bar{h}} \frac{\partial \bar{v}}{\partial \bar{y}} + \bar{u} \frac{\partial \bar{v}}{\partial x^*}$ and \bar{h} are of order [1].

$$\text{Therefore } \frac{\partial \bar{p}}{\partial \bar{y}} \text{ is of order } \left[\operatorname{Re}^* \left(\frac{h_o}{L} \right)^2 \right] \quad (2.13)$$

which is very small, even for modified Reynolds numbers as large as 1. We see then that for our problem, the pressure

gradient in the \bar{y} direction is not important, and can be taken to equal 0.

$$\frac{\partial \bar{p}}{\partial \bar{y}} = 0 \quad (2.14)$$

Thus \bar{p} is not a function of \bar{y} , but of \bar{x} alone. The other equations when reduced give

$$\bar{h}^2 \text{Re}^* \left[\bar{u} \frac{\partial \bar{u}}{\partial \bar{x}^*} + \frac{\bar{v}}{\bar{h}} \frac{\partial \bar{u}}{\partial \bar{y}} \right] = - \bar{h}^2 \frac{\partial \bar{p}}{\partial \bar{x}} + \frac{\partial}{\partial \bar{y}} \left(\bar{u} \frac{\partial \bar{u}}{\partial \bar{y}} \right) \quad (2.15)$$

$$\bar{h}^2 \text{Pr} \text{Re}^* \left[\bar{u} \frac{\partial \bar{T}}{\partial \bar{x}^*} + \frac{\bar{v}}{\bar{h}} \frac{\partial \bar{T}}{\partial \bar{y}} \right] = \frac{\partial^2 \bar{T}}{\partial \bar{y}^2} + \text{Pr} \text{E} \bar{u} \left(\frac{\partial \bar{u}}{\partial \bar{y}} \right)^2 \quad (2.16)$$

$$\bar{h} \frac{\partial \bar{u}}{\partial \bar{x}^*} + \frac{\partial \bar{v}}{\partial \bar{y}} = 0 \quad (2.17)$$

In the above, the dimensionless parameters are:

$$\left. \begin{aligned} \text{Re}^* &= \frac{\rho U L}{\mu_r} \left(\frac{h_o}{L} \right)^2 \\ \text{Pr} &= \frac{\mu_r C_p}{\kappa} \\ \text{E} &= \frac{U^2}{C_p T_r} \end{aligned} \right\} \quad (2.18)$$

and the boundary conditions become:

$$\left. \begin{aligned} \bar{y} = 0; \bar{u} = 1; \bar{v} = 0 \\ \bar{y} = 1; \bar{u} = 0, \bar{v} = 0 \end{aligned} \right\} \quad (2.19)$$

$$\int_0^1 \frac{d\bar{p}}{d\bar{x}} d\bar{x} = 0 \quad (2.20)$$

$$\left. \begin{aligned} \bar{T}(\bar{x}, 0) &= \frac{2T_s/T_p}{[1 + T_s/T_p]} \\ \bar{T}(\bar{x}, 1) &= \frac{2}{[1 + T_s/T_p]} \\ \bar{T}(0, \bar{y}) &= \bar{T}(0, 0) + [\bar{T}(0, 1) - \bar{T}(0, 0)] \bar{y} \end{aligned} \right\} \quad (2.21)$$

The expression derived for the dimensionless film thickness is,

$$\bar{h} = \bar{h}_r - \bar{x} [\bar{h}_r - 1] \quad (2.22)$$

TRANSFORMATION OF THE GOVERNING EQUATIONS

In order to reduce the number of dependent variables, thus simplifying computations, we can resort to using the stream function. Writing,

$$\left. \begin{aligned} \Psi_c &= \int_0^{h(x)} \rho u \, dy \\ \bar{\Psi} &= \Psi / \Psi_c \\ \bar{\Psi}_c &= \Psi_c / (\rho U h_0) \\ \bar{u} &= \frac{\bar{\Psi}}{\bar{h}} \quad \frac{\partial \bar{\Psi}}{\partial \bar{y}} \\ \bar{v} &= -\bar{\Psi}_c \left[\frac{\partial \bar{\Psi}}{\partial \bar{x}} + \frac{(\bar{h}_r - 1)}{\bar{h}} \bar{y} \frac{\partial \bar{\Psi}}{\partial \bar{y}} \right] \end{aligned} \right\} \quad (2.23)$$

The continuity equation is identically satisfied, and $\bar{\Psi}_c$ represents the mass flow through the bearing.

Expressions (2.15) and (2.16), (see Appendix A), and Equations (2.19) now become

$$\begin{aligned} \text{Re}^* \bar{h} \bar{\Psi}_c \left[\frac{\partial \bar{\Psi}}{\partial \bar{y}} \left\{ \frac{\partial}{\partial \bar{x}} \left(\frac{\partial \bar{\Psi}}{\partial \bar{y}} \right) + \frac{(\bar{h}_r - 1)}{\bar{h}} \frac{\partial \bar{\Psi}}{\partial \bar{y}} \right\} - \frac{\partial \bar{\Psi}}{\partial \bar{x}} \frac{\partial^2 \bar{\Psi}}{\partial \bar{y}^2} \right] \\ = - \frac{\bar{h}^3}{\bar{\Psi}_c} \frac{d\bar{p}}{d\bar{x}} + \frac{\partial}{\partial \bar{y}} \left(\bar{\mu} \frac{\partial^2 \bar{\Psi}}{\partial \bar{y}^2} \right) \end{aligned} \quad (2.24)$$

$$\begin{aligned} \bar{h} \bar{\Psi}_c P \text{Re}^* \left[\frac{\partial \bar{\Psi}}{\partial \bar{y}} \frac{\partial \bar{T}}{\partial \bar{x}} - \frac{\partial \bar{\Psi}}{\partial \bar{x}} \frac{\partial \bar{T}}{\partial \bar{y}} \right] = \frac{\partial^2 \bar{T}}{\partial \bar{y}^2} \\ + P E \left(\frac{\bar{\Psi}_c}{\bar{h}} \right)^2 \bar{\mu} \left(\frac{\partial^2 \bar{\Psi}}{\partial \bar{y}^2} \right)^2 \end{aligned} \quad (2.25)$$

$$\left. \begin{aligned} \bar{y} = 0; \quad \bar{\Psi} = 0, \quad \frac{\partial \bar{\Psi}}{\partial \bar{y}} &= \frac{\bar{h}}{\bar{\Psi}_c} \\ \bar{y} = 1; \quad \bar{\Psi} = 1, \quad \frac{\partial \bar{\Psi}}{\partial \bar{y}} &= 0 \end{aligned} \right\} \quad (2.26)$$

Expressions (2.20) through (2.22) however, remain the same.

It can be seen from the above equations and the boundary conditions, that in general, the solution to our problem depends on the following dimensionless groups:

$$\bar{h}_r, P \text{Re}^*, P E, \text{Re}^*, \text{ and } T_s/T_p.$$

CHAPTER III

SOLUTION OF THE TRANSFORMED EQUATIONS

INTRODUCTION

Because of the non-linear nature of the momentum Equation (2.24), and the coupling with the energy Equation (2.25) through the viscosity, the solution of the problem can present some difficulty. For modified Reynolds numbers much less than unity [11], solutions were obtained neglecting the inertia terms; while for modified Reynolds numbers in the vicinity of unity, solutions were obtained including the inertia terms.

SOLUTION OF THE MOMENTUM EQUATION NEGLECTING INERTIA TERMS AND FOR CONSTANT VISCOSITY

Neglecting the inertia terms, and for constant viscosity, the momentum Equation (2.24) becomes

$$\frac{\partial^3 \bar{\Psi}}{\partial \bar{Y}^3} = \frac{\bar{h}^3}{\bar{\Psi}_c} \frac{d\bar{p}}{d\bar{x}} \quad (3.1)$$

Upon integrating the above equation three times with respect to \bar{Y} , we obtain the following expression

$$\bar{\Psi} = \frac{\bar{h}^3}{\bar{\Psi}_c} \frac{d\bar{p}}{d\bar{x}} \frac{\bar{Y}^3}{6} + C_1 (\bar{x}) \frac{\bar{Y}^2}{2} + C_2 (\bar{x}) \bar{Y} + C_3 (\bar{x}) \quad (3.2)$$

The coeffs. $C_1(\bar{x})$, $C_2(\bar{x})$, and $C_3(\bar{x})$ of Equation (3.2) are determined from the following three boundary conditions.

$$\begin{aligned}\bar{y} &= 0; & \bar{\Psi} &= 0 \\ \bar{y} &= 1; & \bar{\Psi} &= 1 \\ \frac{\partial \bar{\Psi}}{\partial \bar{y}} &= 0\end{aligned}\tag{3.3}$$

which yield

$$\begin{aligned}C_1(\bar{x}) &= -2 \left[1 + \frac{\bar{h}^3}{\bar{\Psi}_c} \frac{d\bar{p}}{d\bar{x}} \frac{1}{3} \right] \\ C_2(\bar{x}) &= 2 + \frac{\bar{h}^3}{\bar{\Psi}_c} \frac{d\bar{p}}{d\bar{x}} \frac{1}{6} \\ C_3(\bar{x}) &= 0\end{aligned}\tag{3.4}$$

The fourth boundary condition, $\bar{y} = 0$, $\frac{\partial \bar{\Psi}}{\partial \bar{y}} = \frac{\bar{h}}{\bar{\Psi}_c}$ allows us to obtain an expression for the pressure gradient, $\frac{d\bar{p}}{d\bar{x}}$.

$$\frac{d\bar{p}}{d\bar{x}} = D_1(\bar{x}) - D_2(\bar{x}) \bar{\Psi}_c\tag{3.5}$$

where $D_1(\bar{x})$ and $D_2(\bar{x})$ are given by the expressions of Equation (3.6) below

$$\begin{aligned}D_1(\bar{x}) &= 6.0/\bar{h}^2 \\ D_2(\bar{x}) &= 12.0/\bar{h}^3\end{aligned}\tag{3.6}$$

The dimensionless mass flow, $\bar{\Psi}_c$, is found by substituting the expression for $\frac{d\bar{p}}{d\bar{x}}$ of Equation (3.5),

into the integral Equation (2.20), yielding

$$\bar{\Psi}_c = \int_0^1 D_1(\bar{x}) d\bar{x} / \int_0^1 D_2(\bar{x}) d\bar{x} \quad (3.7)$$

SOLUTION OF THE MOMENTUM EQUATION NEGLECTING INERTIA TERMS AND FOR VARIABLE VISCOSITY

When the inertia terms are neglected, but variable viscosity is preserved, the momentum Equation (2.24) yields.

$$\frac{\partial}{\partial \bar{y}} \left(\bar{\mu} \frac{\partial^2 \bar{\Psi}}{\partial \bar{y}^2} \right) = \frac{\bar{h}^3}{\bar{\Psi}_c} \frac{d\bar{p}}{d\bar{x}} \quad (3.8)$$

The above equation is integrated three times with respect to \bar{y} , whence the following equation is obtained.

$$\begin{aligned} \bar{\Psi} = & \frac{\bar{h}^3}{\bar{\Psi}_c} \frac{d\bar{p}}{d\bar{x}} \int_0^{\bar{y}} \left(\int_0^{\bar{y}} \frac{\bar{y}}{\bar{\mu}} d\bar{y} \right) d\bar{y} + C_1(\bar{x}) \int_0^{\bar{y}} \left(\int_0^{\bar{y}} \frac{1}{\bar{\mu}} d\bar{y} \right) d\bar{y} \\ & + C_2(\bar{x}) \bar{y} + C_3(\bar{x}) \end{aligned} \quad (3.9)$$

The coeffs. $C_1(\bar{x})$, $C_2(\bar{x})$, and $C_3(\bar{x})$ of Equation (3.9) are determined from the boundary conditions as listed in (3.3). These become:

$$\begin{aligned}
C_1(\bar{x}) &= \left[1 - \frac{\bar{h}^3}{\bar{\Psi}_c} \frac{d\bar{p}}{d\bar{x}} (A_1(\bar{x}, 1) - A_2(\bar{x}, 1)) \right] / \\
&\quad \left[A_3(\bar{x}, 1) - A_4(\bar{x}, 1) \right] \\
C_2(\bar{x}) &= - \left[\frac{\bar{h}^3}{\bar{\Psi}_c} \frac{d\bar{p}}{d\bar{x}} A_2(\bar{x}, 1) + C_1(\bar{x}) A_4(\bar{x}, 1) \right] \\
C_3(\bar{x}) &= 0
\end{aligned} \tag{3.10}$$

The fourth boundary condition allows us to determine an expression for $\frac{d\bar{p}}{d\bar{x}}$ in the same form as Equation (3.5).

$D_1(\bar{x})$, and $D_2(\bar{x})$ now become:

$$\begin{aligned}
D_1(\bar{x}) &= -1.0/\bar{h}^2 [A_2(\bar{x}, 1) - B_2(\bar{x})] \\
D_2(\bar{x}) &= B_1(\bar{x})/\bar{h}^3 [A_2(\bar{x}, 1) - B_2(\bar{x})]
\end{aligned} \tag{3.11}$$

An expression for $\bar{\Psi}_c$ is likewise obtained, and retains the same form as it does in Equation (3.7). In the above,

$$\begin{aligned}
B_1(\bar{x}) &= A_4(\bar{x}, 1)/[A_3(\bar{x}, 1) - A_4(\bar{x}, 1)] \\
B_2(\bar{x}) &= A_4(\bar{x}, 1)[A_1(\bar{x}, 1) - A_2(\bar{x}, 1)]/[A_3(\bar{x}, 1) - A_4(\bar{x}, 1)]
\end{aligned} \tag{3.12}$$

[[]]

and

$$\begin{aligned}
 A_1(\bar{x}, 1) &= \int_0^1 \left(\int_0^{\bar{y}} \frac{\bar{y}}{\bar{\mu}} d\bar{y} \right) d\bar{y} \\
 A_2(\bar{x}, 1) &= \int_0^1 \frac{\bar{y}}{\bar{\mu}} d\bar{y} \\
 A_3(\bar{x}, 1) &= \int_0^1 \left(\int_0^{\bar{y}} \frac{1}{\bar{\mu}} d\bar{y} \right) d\bar{y} \\
 A_4(\bar{x}, 1) &= \int_0^1 \frac{1}{\bar{\mu}} d\bar{y}
 \end{aligned} \tag{3.13}$$

We are now in a position to evaluate $C_1(\bar{x})$ and $C_2(\bar{x})$, provided the viscosity distribution is known.

SOLUTION OF THE MOMENTUM EQUATION INCLUDING INERTIA TERMS AND FOR VARIABLE VISCOSITY

The momentum Equation (2.24) can be rewritten as follows:

$$\frac{\partial}{\partial \bar{y}} \left(\bar{\mu} \frac{\partial^2 \bar{\Psi}}{\partial \bar{y}^2} \right) = F(\bar{\Psi}) + \frac{\bar{h}^3}{\bar{\Psi}_c} \frac{d\bar{p}}{d\bar{x}} \tag{3.14}$$

where

$$F(\bar{\Psi}) = \text{Re}^* \bar{h} \bar{\Psi}_c \left[\frac{\partial \bar{\Psi}}{\partial \bar{y}} \left\{ \frac{\partial}{\partial \bar{x}} \left(\frac{\partial \bar{\Psi}}{\partial \bar{y}} \right) + \frac{\bar{h}_r^{-1}}{\bar{h}} \frac{\partial \bar{\Psi}}{\partial \bar{y}} \right\} - \frac{\partial \bar{\Psi}}{\partial \bar{x}} \frac{\partial^2 \bar{\Psi}}{\partial \bar{y}^2} \right] \tag{3.15}$$

Integrating Eq. (3.14) we obtain

$$\begin{aligned} \bar{\Psi} = & \frac{\bar{h}^3}{\bar{\Psi}_c} \frac{d\bar{p}}{d\bar{x}} \int_0^{\bar{Y}} \left(\int_0^{\bar{Y}} \frac{\bar{Y}}{\bar{\mu}} d\bar{Y} \right) d\bar{Y} + \int_0^{\bar{Y}} \left(\int_0^{\bar{Y}} \frac{1}{\bar{\mu}} \int_0^{\bar{Y}} F(\bar{\Psi}) d\bar{Y} \right) d\bar{Y} \\ & + C_1(\bar{x}) \int_0^{\bar{Y}} \left(\int_0^{\bar{Y}} \frac{1}{\bar{\mu}} d\bar{Y} \right) d\bar{Y} + C_2(\bar{x}) \bar{Y} + C_3(\bar{x}) \end{aligned} \quad (3.16)$$

where,

$$\begin{aligned} C_1(\bar{x}) &= \left[1 + A_6(\bar{x}, 1) - A_5(\bar{x}, 1) - \frac{\bar{h}^3}{\bar{\Psi}_c} \frac{d\bar{p}}{d\bar{x}} [A_1(\bar{x}, 1) \right. \\ &\quad \left. - A_2(\bar{x}, 1)] \right] / \left[A_3(\bar{x}, 1) - A_4(\bar{x}, 1) \right] \\ C_2(\bar{x}) &= - \left[A_6(\bar{x}, 1) + \frac{\bar{h}^3}{\bar{\Psi}_c} \frac{d\bar{p}}{d\bar{x}} A_2(\bar{x}, 1) + C_1(\bar{x}) A_4(\bar{x}, 1) \right] \\ C_3(\bar{x}) &= 0 \end{aligned} \quad (3.17)$$

The pressure gradient, $\frac{d\bar{p}}{d\bar{x}}$, has the same form as expressed by Equation (3.5), where now

$$\begin{aligned} D_1(\bar{x}) &= -1.0/\bar{h}^2 [A_2(\bar{x}, 1) - B_2(\bar{x})] \\ D_2(\bar{x}) &= B_1(\bar{x})/\bar{h}^3 [A_2(\bar{x}, 1) - B_2(\bar{x})] \end{aligned} \quad (3.18)$$

In the above,

$$B_1(\bar{x}) = A_6(\bar{x},1) + A_4(\bar{x},1) [1 + A_6(\bar{x},1) - A_5(\bar{x},1)] / [A_3(\bar{x},1) - A_4(\bar{x},1)]$$

$$B_2(\bar{x}) = A_4(\bar{x},1) \cdot [A_1(\bar{x},1) - A_2(\bar{x},1)] / [A_3(\bar{x},1) - A_4(\bar{x},1)]$$
(3.19)

and,

$$A_5(\bar{x},1) = \int_0^1 \left(\int_0^{\bar{Y}} \left(\frac{1}{\bar{\mu}} \int_0^{\bar{Y}} F(\bar{\Psi}) d\bar{y} \right) d\bar{y} \right) d\bar{y}$$

$$A_6(\bar{x},1) = \int_0^1 \left(\frac{1}{\bar{\mu}} \int_0^{\bar{Y}} F(\bar{\Psi}) d\bar{y} \right) d\bar{y}$$
(3.20)

Thus, providing us with the viscosity distribution, would allow $C_1(\bar{x})$ and $C_2(\bar{x})$ to be evaluated.

SOLUTION OF THE ENERGY EQUATION

For the case of variable viscosity, it is necessary to obtain the viscosity distribution, before the stream function can be computed. This is accomplished by first solving the Energy Equation (2.25) together with the boundary conditions (2.21), using the Crank-Nicholson method. The viscosity distribution is then obtained by interpolation from a set of data which had been previously read in.

In the numerical process, (See Appendix B), the derivatives are replaced by the central finite difference

approximations, and the terms are rearranged to obtain the following equation.

$$a_{i,j} \bar{T}_{i+1,j-1} + b_{i,j} \bar{T}_{i+1,j} + c_{i,j} \bar{T}_{i+1,j+1} = d_{i,j} \quad (3.21)$$

where $a_{i,j}$, $b_{i,j}$, $c_{i,j}$ and $d_{i,j}$ are defined in Appendix B.

It should be noted that the coefficients $a_{i,j}$, $b_{i,j}$, and $c_{i,j}$ are known from the solution of the momentum equation alone. However, $d_{i,j}$ in addition depends on the temperature at the preceding section. The temperature distribution at the inlet is given by the last of Equations (2.21). Using these initial values, and marching from section to section along the bearing, one obtains the complete temperature distribution.

For the numerical procedure, the square grid presented below was employed, with the spacing interval in the \bar{x} and the \bar{y} directions taken as 0.1 and 0.05 respectively.

For $i = 1$, Equation (3.21) becomes,

$$a_{1,j} \bar{T}_{2,j-1} + b_{1,j} \bar{T}_{2,j} + c_{1,j} \bar{T}_{2,j+1} = d_{1,j} \quad (3.22)$$

Using values of j from 2 to $N-1$, the above equation yields a linear system of $N-2$ equations with $N-2$ unknowns.

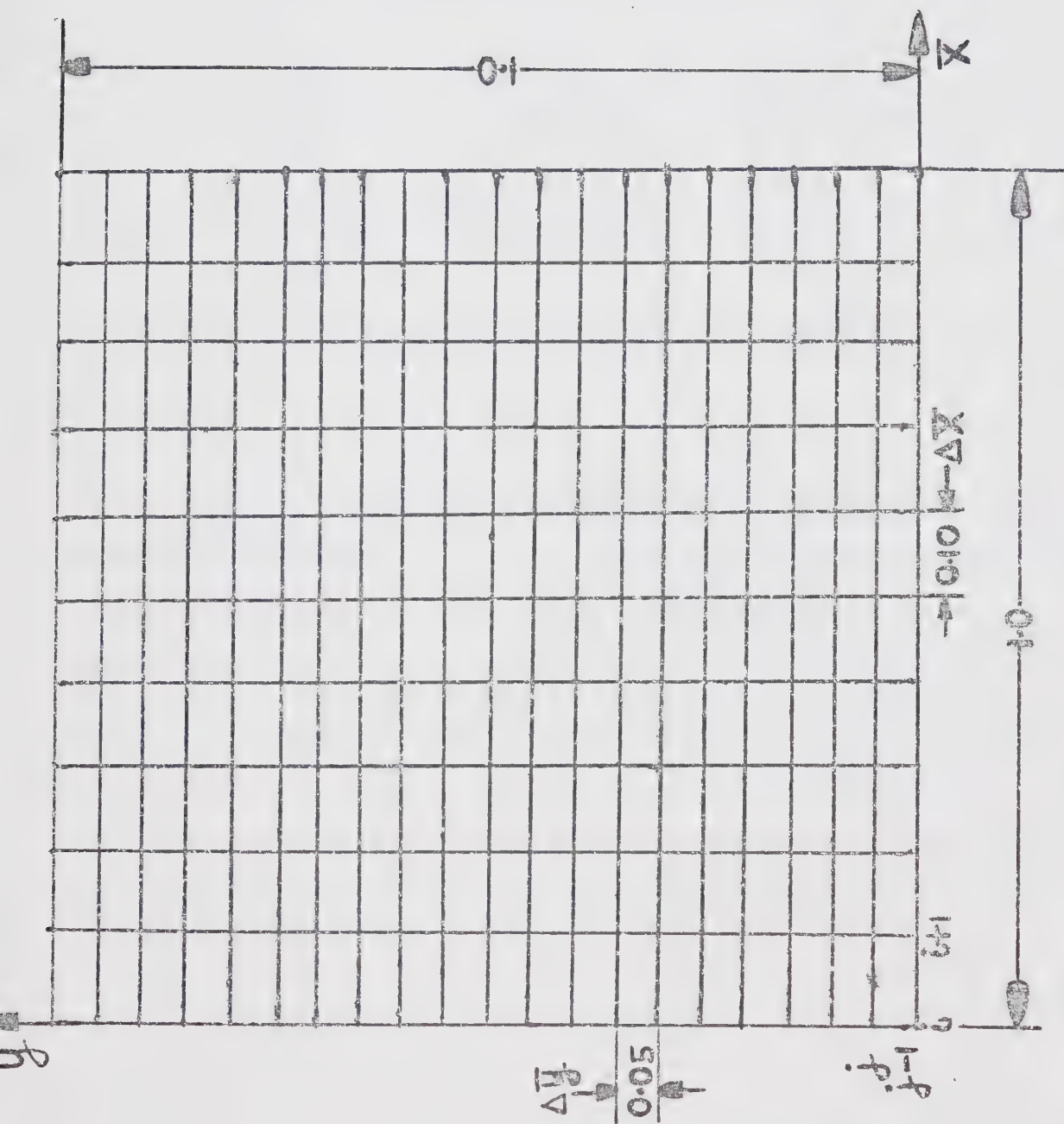


FIG. 2 Marching Scheme for solving Energy Equation

$$a_{1,2}\bar{T}_{2,1} + b_{1,2}\bar{T}_{2,2} + c_{1,2}\bar{T}_{2,3} = d_{1,2}$$

$$a_{1,3}\bar{T}_{2,2} + b_{1,3}\bar{T}_{2,3} + c_{1,3}\bar{T}_{2,4} = d_{1,3}$$

$$a_{1,4}\bar{T}_{2,3} + b_{1,4}\bar{T}_{2,4} + c_{1,4}\bar{T}_{2,5} = d_{1,4}$$

$$a_{1,N-3}\bar{T}_{2,N-4} + b_{1,N-3}\bar{T}_{2,N-3} + c_{1,N-3}\bar{T}_{2,N-2} = d_{1,N-3}$$

$$a_{1,N-2}\bar{T}_{2,N-3} + b_{1,N-2}\bar{T}_{2,N-2} + c_{1,N-2}\bar{T}_{2,N-1} = d_{1,N-2}$$

$$a_{1,N-1}\bar{T}_{2,N-2} + b_{1,N-1}\bar{T}_{2,N-1} + c_{1,N-1}\bar{T}_{2,N} = d_{1,N-1}$$

(3.23)

Since the boundary conditions $\bar{T}(I,1)$ and $\bar{T}(I,N)$ are known for $I = 1, 2, \dots, M$, the system of Equations (3.23) can be rewritten in matrix form. The matrix is tridiagonal and of order $N-2$. It was solved directly, by using the method of triangular decomposition [15]. After $\bar{T}_{2,j}$ ($j = 2, 3, \dots, N-1$) was evaluated, the temperature distribution throughout the grid was obtained by repeating the above procedure for each successive section.

METHOD OF SOLUTION - STEP BY STEP

In the general case, the solution of our problem requires that we solve Eqs. (2.24) and (2.25), together with the boundary conditions as stated in Eqs. (2.21) and (2.26). Since Eqs. (2.24) and (2.25) are coupled through the viscosity, an iterative method is used, which involves a back and forth movement between these two equations, until the temperature distribution converges to within a prescribed error bound. Solutions are obtained for the case in which inertia terms are not important, and also for the case when these terms are important. For the latter case, the solution neglecting the inertia terms is used as a first approximation, then these terms are included by use of a correcting procedure. The method of solution is as outlined in the following steps.

- (1) Evaluate $D_1(\bar{x})$ and $D_2(\bar{x})$ by using Eqs. (3.6).
- (2) Find the mass flow by use of Eq. (3.7).
- (3) Use Eq. (3.5) to determine the pressure gradient,

$$\frac{d\bar{p}}{d\bar{x}}.$$
- (4) Determine the value of the coeffs. $C_1(\bar{x})$ and $C_2(\bar{x})$ by using Eqs. (3.4).
- (5) From Eq. (3.2), evaluate the stream function distribution.
- (6) Obtain the temperature distribution by solving Eq. (2.25) for constant viscosity.

- (7) Evaluate $A_1(\bar{x},1)$ through $A_4(\bar{x},1)$ by use of Eqs. (3.13)
- (8) Use Eqs. (3.12) to find $B_1(\bar{x})$ and $B_2(\bar{x})$.
- (9) Determine $D_1(\bar{x})$ and $D_2(\bar{x})$ by use of Eqs. (3.11).
- (10) Find the mass flow by use of Eq. (3.7).
- (11) Use Eq. (3.5) to compute the pressure gradient,

$$\frac{d\bar{p}}{d\bar{x}}.$$
- (12) Evaluate the coeffs. $C_1(\bar{x})$ and $C_2(\bar{x})$ by use of Eqs. (3.10).
- (13) Obtain the stream function distribution by using Eq. (3.9).
- (14) Determine the temperature distribution by solving Eq. (2.25).
- (15) If the convergence criteria on the temperature is satisfied after the first iteration go to step (17).
- (16) If the convergence criteria on the temperature is not satisfied, after the first iteration go to step (7).
- (17) Evaluate the bearing characteristics and print results.
- (18) If inertia terms are not important, go to step (33).
- (19) If inertia terms are important continue.
- (20) Use Eq. (3.15) to find the correction for the presence of inertia terms.

- (21) Evaluate $A_1(\bar{x},1)$ through $A_6(\bar{x},1)$ by use of Eqs. (3.13) and (3.20).
- (22) Use Eqs. (3.19) to find $B_1(\bar{x})$ and $B_2(\bar{x})$.
- (23) Compute $D_1(\bar{x})$ and $D_2(\bar{x})$ by using Eqs. (3.18).
- (24) Determine the mass flow by use of Eq. (3.7).
- (25) Use Eq. (3.5) to find the pressure gradient, hence determine the pressure distribution.
- (26) Evaluate the coeffs. $C_1(\bar{x})$ and $C_2(\bar{x})$ by use of Eqs. (3.17).
- (27) Obtain the stream function distribution by use of Eq. (3.16).
- (28) If the convergence criteria on the pressure is satisfied go to step (30).
- (29) Go to step (20).
- (30) Solve Eq. (2.26) for the temperature distribution.
- (31) If the convergence criteria on the temperature is not satisfied after the first iteration, go to step (20).
- (32) Evaluate the bearing characteristics and print results.
- (33) Solution completed.

CHAPTER IV

RESULTS AND CONCLUSIONS

INTRODUCTION

In order to understand more fully the various factors which contribute to the load capacity, the Momentum Eq. (2.24) together with the Energy Eq. (2.25) are solved for several different cases, which are as follows:

(a) The momentum equation neglecting inertia terms, together with the energy equation are solved for various boundary conditions on temperature. Sample results are listed in Tables 1a through 1d, and graphs are presented in Figs. 4 through 15.

(b) Assuming constant viscosity, the momentum equation is first solved for various values of modified Reynolds number. Afterwards, it is solved together with the energy equation, for three different temperature boundary conditions, but this time retaining the viscosity variation with temperature. Tables 2a through 2c list some sample results, and graphs are presented in Figs. 16 through 23.

(c) Considering variable viscosity, the momentum equation neglecting inertia terms, together with the energy equation, are solved for various values of inlet to outlet ratio, \bar{h}_r , Sample results are listed in tables 3a through 3c, and graphs are presented in Figs. 24 through 35.

(d) Neglecting the inertia terms, the momentum equation together with the energy equation are solved for three different T_s/T_p ratios, and for constant Pe ; while at the same time retaining the viscosity variation with temperature. In this case, the results obtained enable us to examine the effects of dissipation on the load capacity of the bearing. Graphs are plotted in Figs. 36 through 46, and sample results are listed in tables 4a through 4d.

(e) In order to examine the effects of convection terms on the load capacity of the bearing, a method similar to that in (d) was undertaken, but this time keeping PE constant instead of Pe . Graphs illustrating results are then plotted in Figs. 47 through 57, while sample results are presented in tables 5a through 5e.

EFFECTS OF VARIOUS TEMPERATURE

BOUNDARY CONDITIONS - NO INERTIA

Figs. 4 through 6 plot the velocity distributions for the following boundary conditions: (i) $T_s = 200^\circ\text{F}$, $T_p = 100^\circ\text{F}$, (ii) $T_s = 100^\circ\text{F}$, $T_p = 100^\circ\text{F}$ and (iii) $T_s = 50^\circ\text{F}$, $T_p = 100^\circ\text{F}$. All the dimensionless groups have the same values, and these boundary conditions were chosen to find out what happens to the load capacity when the slider is cooled. It is possible to get some idea of what the pressure distributions for the three different boundary conditions are like, by examining their velocity and temperature profiles.

If we first examine the shape of the velocity distribution at various sections, as illustrated in any of Figs. 4, 5, or 6, we see that the profile changes from concave inwards at the entrance to convex outwards at the exit. This is readily explained, because the pressure gradient, which is positive at the inlet, passes through zero around the mid-section of the bearing, then becomes negative at the exit. Also, by examining only the inlet and outlet velocity profiles of Figs. 4 through 6, we can tell which pressure distributions are higher. It is reasonable to expect that large positive pressure gradients at the bearing inlet would tend to cause backflow, while large negative pressure gradients at the exit would cause the velocity profile at this section to be more convex outwards.

These two effects can be clearly seen in Fig. 6. Note that the outlet velocity profile becomes more convex outwards as the slider is cooled, indicating an increased mass flow rate. The temperature distribution for the case $T_s = 200^\circ\text{F}$, $T_p = 100^\circ\text{F}$ appears in Fig. 7, whence the rise in temperature as the lubricant flows through the bearing is readily seen. Plots of the pressure distribution for the three cases appear in Fig. 8, and agree with what we were led to expect from observations just made.

Fig. 9 presents plots of the shear stress distribution at the slider for the three cases being studied. Since $\bar{\tau} = \frac{\bar{\mu}}{h} \frac{\partial \bar{u}}{\partial y}$, then the shear stress at the slider depends on both the viscosity and the velocity gradient at the said interface.

Examination of Figs. 4 through 6 show that the magnitude of the velocity gradient at the slider decreases as the slider temperature decreases; but since the viscosity rises quite rapidly with decreasing temperature, it is very likely that the colder slider will cause larger shear stresses to be developed. This is indeed the case as can be seen from the curves plotted in Fig. 9.

Note that for the colder slider temperatures, the velocity gradient passes through zero, then becomes positive towards the bearing outlet. This explains why the shear stress curves cross each other, and approach zero at points at or just before the outlet.

Figs. 10 through 12 present curves of load capacity versus T_s/T_p for the following cases: (i) T_p fixed at 100°F, slider cooled. (ii) T_s fixed at 100°F, pad heated (iii) $T_s + T_p$ fixed at 350°F, slider cooled and at the same time pad heated. Comparison of these curves show that providing Pe , PE , and \bar{h}_r are the same, the load capacity for each of the three cases just mentioned, and for the same T_s/T_p ratio are quite close, although the actual boundary conditions differ greatly. It can also be seen that the divergence becomes smaller in the range $0.5 \leq T_s/T_p \leq 2.0$, which includes the normal operating range of most bearings.

Figs. 13 and 14 present curves of drag versus T_s/T_p for the first two cases listed in the previous paragraph. Applying a similar reasoning, it is seen that the difference in drag is quite small for the range $0.5 \leq T_s/T_p \leq 2.0$. The

actual divergence in load capacity, drag, etc. for the same T_s/T_p ratio is due to the differences in viscosity distribution which follows because of variations in the temperature boundary conditions. Fig. 15 shows the influence of the actual temperature boundary conditions on load capacity, for two different T_s/T_p ratios. It is seen that both larger and smaller values of T_s+T_p tend to cause greater divergence in the load capacity values, but this divergence is much more pronounced for the smaller T_s/T_p ratio.

INFLUENCE OF INERTIA TERMS

Figs. 16 and 17 present the velocity distributions for the cases where inertia terms are not included and where they are included respectively. It is seen that when the inertia terms are included, the velocity gradient at the inlet is close to zero near to the pad, but it is slightly greater than zero at a similar point for the inertia-less case. Thus the pressure gradient at the inlet when inertia terms are included, should be slightly larger than for the case of no inertia. However, the difference in the outlet velocity profiles is not easily discernible, so we would expect the pressure gradients at this section to be quite close.

Temperature distributions for the two cases being discussed are presented in Figs. 18 and 19 respectively. The temperature profiles are quite close, and there are no significant differences between the two. It is possible

though for both cases, to observe the heating of the lubricant as it flows through the bearing.

Fig. 20 presents curves of the pressure distribution; whence it is seen that inclusion of the inertia terms gives a slightly higher pressure distribution, which in turn yields a larger load-capacity. Fig. 21 presents the shear stress distribution for $Re^* = 0.5$ and for the cases with and without the inertia terms. It should be noted that although inclusion of the inertia terms gives a higher pressure distribution, it also causes slightly larger shear stresses at the slider.

Fig. 22 compares the results of the present work with those of Rodkiewicz and Anwar [11], and Woodhead and Kettleborough [15]. It is of interest to note that the curve for the present work is almost parallel to the one obtained in [11]. Taking the results of [15] as a standard, it is seen that the present results are quite good for small and for large values of Re^* , and the error rises to a maximum of 1% for Re^* around 0.6.

Fig. 23 presents curves showing the influence of the inertia terms on load capacity for different temperature boundary conditions, while table 2c lists the actual values of the percentage increase in load capacity. It should be noted that the largest errors made in neglecting the inertia terms occur when the bearing operates under normal conditions, ie. when $T_s/T_p > 1.0$. For constant viscosity and for $Re^* = 1.0$, the percentage increase in load capacity is 7.95%,

which is a bit less than the value of 8.9% given in [11].

EFFECTS OF VARYING INLET TO OUTLET RATIO - NO INERTIA

Figs. 24 through 26 present the velocity distributions for the following cases respectively: (i) $\bar{h}_r = 1.75$ (ii) $\bar{h}_r = 2.25$ (iii) $\bar{h}_r = 2.75$. Notice that as \bar{h}_r increases, the backflow at the inlet of the bearing increases continuously, while the velocity profile at the outlet becomes more convex outwards. These observations would lead us to expect a rise in the pressure distribution as \bar{h}_r increases from 1.75 to 2.75. However, we must first take a look at the temperature distributions.

Figs. 27 through 29 present plots of the temperature distributions for the three values of \bar{h}_r under consideration. The respective profiles are quite similar, so that the temperature distribution does not seem to have contributed much to the differences observed in the respective velocity distributions.

As shown by the curves of Fig. 30, the expectation of a continuous rise in the pressure profiles with \bar{h}_r is only partly correct. What can be readily seen is that for positive gradients, the smaller the value of \bar{h}_r the larger the pressure, while for negative gradients the reverse is now true.

Fig. 31 presents plots of the shear stress distribution for the values of \bar{h}_r under consideration. It should be noted that the magnitude of the shear stress decreases as

\bar{h}_r increases. In dimensionless form, the shear stress at the slider can be represented as follows: $\bar{\tau}_0 = \left(\bar{\mu} \frac{\partial \bar{u}}{\partial \bar{y}} \right)_{\bar{y}=0}$. Since the slider temperatures are all the same, and \bar{h} the sectional gradients $\left(\frac{\partial \bar{u}}{\partial \bar{y}} \right)_{\bar{y}=0}$ for the three values of \bar{h}_r are not too different, then differences in the shear stress profiles will be influenced mainly by the variations in $1/\bar{h}$. Since \bar{h} is proportional to \bar{h}_r , then $1/\bar{h} \propto 1/\bar{h}_r$. So that increasing \bar{h}_r should cause numerically smaller values of shear stress at the slider. This is indeed the result, as can be seen from the curves of Fig. 31.

Figs. 32 through 34 plot curves of load capacity versus \bar{h}_r , for constant Pe, but for different temperature boundary conditions; while Fig. 35 compares curves with different temperature boundary conditions, but for constant Pe. For all these figures, it should be noted that the load capacity always rises to a maximum for $2.00 \leq \bar{h}_r \leq 2.25$, then falls gradually.

DISSIPATION EFFECTS - NO INERTIA

Figs. 36 through 38 plot the velocity distributions for PE = 1.27, 5.08 and 20.33 respectively; while other dimensionless groups have the same values. Upon examining these figures, we find that the velocity profiles become more convex outwards as PE increases, indicating a rise in mass flow. This trend might lead one to expect an increase in load capacity also, but this conclusion cannot be made without first examining the temperature distributions.

If we now examine the temperature distributions of Figs. 39 through 41, we find that the differences among the three are quite pronounced, with the temperature profiles rising continuously as PE increases. The pressure gradient is directly proportional to the lubricant viscosity, which decreases with increasing temperature. Thus the increasing mass flow as PE increases is counterbalanced by the drop in lubricant viscosity; and whether the load capacity rises or falls with PE, will depend on the combined influence of these two factors.

The curves of Fig. 42 show that the pressure profile gets smaller as PE increases. So that the reduction in viscosity seems to have had a much greater effect on the load capacity, than the small rise in mass flow of the lubricant.

The shear stress is given by $\bar{\tau}_0 = \frac{\bar{\mu}}{\bar{h}} \frac{\partial \bar{u}}{\partial \bar{y}}$, and since the lubricant in contact with the slider has a constant viscosity, then the shear stress at the slider is proportional to the velocity gradient at the said interface. Examination of Figs. 36 through 38 show that the velocity gradient at the slider are all negative, and that the magnitude of the gradient at any section decreases as PE increases; so that the effect of increasing dissipation is to decrease the drag on the slider. Results for the shear stress are plotted in Fig. 43, and agree quite well with the observations just made.

Figs. 44 through 46 plot curves of load capacity versus PE for constant P_e , but for different temperature boundary conditions. In all cases, it can be seen that

increasing PE, ie increasing dissipation, causes a reduction in the load-carrying capacity of a bearing.

CONVECTION EFFECTS - NO INERTIA

Figs. 47 through 49 present velocity distributions for $Pe = 1.0, 5.0, \text{ and } 20.0$ respectively. Upon examining their velocity profiles, we find that there is not much difference among them, so that here the mass flow won't be important in explaining the variations in the pressure profiles. However, after examining the temperature distributions of Figs. 50 through 52, we find that the difference in the profiles is now quite pronounced, with the temperature profiles becoming smaller as Pe increases from 1.0 to 20.0.

These results agree with findings made by a few previous researchers. Rodkiewicz and Anwar [11] found that for a high Prandtl No. lubricant, neglecting the convective terms in the energy equation caused a considerable rise in the lubricant film temperature; and a similar finding was made by Snyder [10]. Both groups concluded that for high Prandtl No. flows, it was necessary to retain both of the convective terms in the energy equation

The pressure gradient is directly proportional to the lubricant viscosity, which increases with decreasing temperature. We should therefore expect that the pressure distribution curves would become larger as Pe increases. This expectation is proved correct by the results plotted on the curves of Fig. 53.

Again, since the viscosity is constant all along the slider, then the shear stress at the slider is proportional to the value of the velocity gradient, $\frac{\partial \bar{u}}{\partial y}$, at the said interface. Figs. 47 through 49 show that the velocity gradients at the slider are all negative, and that the magnitude of the gradient at any section increases as Pe increases; so that the effect of increasing Pe is to increase the drag on the slider. Fig. 54 plots the shear stress distributions for the values of Pe under consideration, and it is seen that the results agree quite well with what we expected.

Figs. 55 through 57 plot curves of load capacity versus Pe for constant PE , but for different temperature boundary conditions. In all cases, it can be seen that increasing Pe , ie increasing convection, causes an increase in the load carrying capacity of a bearing.

SAMPLE CALCULATIONS

In order to indicate the physical significance of the dimensionless results, a sample calculation for the case of the cooled slider is presented below. This is followed by selected numerical results in tabular form. The following relationships have been used.

$$W = \frac{\bar{W}\mu_r UL}{h_o^2} \quad (4.1)$$

$$D = \frac{\bar{D}\mu_r UL}{h_o} \quad (4.2)$$

$$\Psi_c = \bar{\Psi}_c \rho U h_o \quad (4.3)$$

$$Pe = \frac{\rho C_p}{\kappa} \frac{U h_o^2}{L} \quad (4.4)$$

$$PE = \frac{U_r C_p}{\kappa} \frac{U^2}{C_p T_r} \quad (4.5)$$

where $L = 2"$, $\bar{h}_r = 2.0$, $\rho = 8.1875 \times 10^{-5} \frac{\text{lbf} - \text{sec}^2}{\text{in}^4}$,

$C_p = 1.7886 \times 10^2 \frac{\text{Btu} - \text{in}}{\text{lbf} - \text{sec}^2 - ^\circ\text{F}}$, and $\kappa = 1.7508 \times 10^{-6}$

$\frac{\text{Btu}}{\text{sec} - ^\circ\text{F} - \text{in}}$ were assumed.

Following are the three cases for the cooled slider considered:

(i) Assuming $T_s = 200^\circ\text{F}$, $T_p = 100^\circ\text{F}$, $Pe = 20.0$ and $PE = 1.0$, we obtain $T_r = (T_s + T_p)/2.0 = 150^\circ\text{F}$ and find respective absolute viscosity

$$\mu_r = 0.3276 \times 10^{-5} \frac{\text{lbf} - \text{sec}}{\text{in}^2}$$

Having these, we find from (4.5) the velocity of the slider, namely,

$$U = 8.64 \times 10^2 \text{ in/sec}$$

Now from the above given value of the Peclect number

$$Pe = 20.0 = 8.37 \times 10^3 \frac{U h_o^2}{L}$$

the value of h_o can be computed

$$h_o = 2.35 \times 10^{-3} \text{ in}$$

Under these conditions, from (4.1), (4.2), and (4.3) we obtain

$$\begin{aligned} W &= 111.2 \text{ lbf/in}^2 \\ D &= -1.39 \text{ lbf/in} \\ \psi_c &= 3.11 \times 10^{-2} \frac{\text{lbm}}{\text{in} - \text{sec}} \end{aligned} \quad (4.6)$$

(ii) Similarly for $T_s = 50^\circ\text{F}$, $T_p = 100^\circ\text{F}$, $Pe = 20.0$ and $PE = 1.0$ we obtain the following:

$$\begin{aligned} T_r &= 75^\circ\text{F} \\ \mu_r &= 0.25798 \times 10^{-4} \frac{\text{lbf} - \text{sec}}{\text{in}^2} \\ U &= 2.177 \times 10^2 \text{ in/sec} \\ h_o &= 4.684 \times 10^{-3} \text{ in} \end{aligned}$$

Under these conditions (4.1), (4.2) and (4.3) now yield

$$\begin{aligned} W &= 113 \text{ lbf/in}^2 \\ D &= -1.945 \text{ lbf/in} \\ \psi_c &= 2.77 \times 10^2 \frac{\text{lbm}}{\text{in} - \text{sec}} \end{aligned} \quad (4.7)$$

(iii) Assuming $T_s = 50^\circ\text{F}$, $T_p = 100^\circ\text{F}$, $Pe = 20.0$ and $h_o = 2.34 \times 10^{-3} \text{ in}$, and using relationship (4.4)

$$Pe = 20.0 = 8.37 \times 10^3 \frac{U h_o^2}{L}$$

the value of U can be computed

$$U = 8.64 \times 10^2 \text{ in/sec}$$

$T_r = 75^\circ\text{F}$, from which we find the respective absolute viscosity, namely,

$$\mu_r = 0.258 \times 10^{-4} \frac{\text{lbf} \cdot \text{sec}}{\text{in}^2}$$

We can now compute the value of PE by using (4.5)

$$\text{PE} = 61.25 \frac{\mu_r U^2}{T_r} = 15.75$$

Under the above conditions, from the relationships (4.1), (4.2) and (4.3) we now obtain

$$W = 1,219 \text{ lbf/in}^2$$

$$D = -9.42 \text{ lbf/in} \quad (4.8)$$

$$\Psi_c = 5.65 \times 10^{-2} \frac{\text{lbm}}{\text{in} \cdot \text{sec}}$$

The above format has been used to obtain the following numerical results:

- (a) Slider cooled
- (b) Pad heated
- (c) Increasing PE
- (d) Increasing Pe

while the influence of the inertia terms on the load capacity of a slider bearing is also investigated.

(a) Slider Cooled - $T_p = 100^\circ\text{F}$

$T_s = 200^\circ\text{F}$		$T_s = 50^\circ\text{F}$		$T_s = 50^\circ\text{F}$	
$Pe = 20.0, PE = 1.0$		$Pe = 20.0, PE = 1.0$		$Pe = 20.0, PE = 15.75$	
$U = 8.643 \times 10^2$	in/sec	$U = 2.177 \times 10^2$	in/sec	$U = 8.643 \times 10^2$	in/sec
$h_o = 2.3537 \times 10^{-3}$	in	$h_o = 4.684 \times 10^{-3}$	in	$h_o = 2.3537 \times 10^{-3}$	in
$\bar{W} = 0.10870$		$\bar{W} = 0.22013$		$\bar{W} = 0.15146$	
$\bar{D} = -0.5782$		$\bar{D} = -0.81215$		$\bar{D} = -.49758$	
$\bar{\psi}_C = 0.48381$		$\bar{\psi}_C = 0.85908$		$\bar{\psi}_C = 0.87790$	
$\bar{W} = 111.2$	lb f/in^2	$W = 113$	lb f/in^2	$\bar{W} = 1,219$	lb f/in^2
$D = -1.39$	lb f/in	$D = -1.945$	lb f/in	$D = -9.42$	lb f/in
$\psi_C = 3.11 \times 10^{-2}$	$\frac{\text{lbm}}{\text{in-sec}}$	$\psi_C = 2.77 \times 10^{-2}$	$\frac{\text{lbm}}{\text{in-sec}}$	$\psi_C = 5.65 \times 10^{-2}$	$\frac{\text{lbm}}{\text{in-sec}}$

(b) Pad Heated - $T_s = 100^\circ\text{F}$

$T_p = 50^\circ\text{F}$	$T_p = 200^\circ\text{F}$	$T_p = 200^\circ\text{F}$
Pe = 20.0, PE = 1.0	Pe = 20.0, PE = 1.0	Pe = 20.0, PE = 0.06
$U = 2.178 \times 10^2 \text{ in/sec}$	$U = 8.643 \times 10^2 \text{ in/sec}$	$U = 2.178 \times 10^2 \text{ in/sec}$
$h_o = 4.685 \times 10^{-3} \text{ in}$	$h_o = 2.3537 \times 10^{-3}$	$h_o = 4.685 \times 10^{-3} \text{ in}$
$\bar{W} = 0.10995$	$\bar{W} = 0.23685$	$\bar{W} = 0.24782$
$\bar{D} = -0.58787$	$\bar{D} = -0.82949$	$\bar{D} = -0.87915$
$\bar{\psi}_c = 0.4969$	$\bar{\psi}_c = 0.87827$	$\bar{\psi}_c = 0.87649$
$W = 56.50 \text{ lbf/in}^2$	$W = 242 \text{ lbf/in}^2$	$W = 16.17 \text{ lbf/in}^2$
$D = -1.41 \text{ lbf/in}$	$D = -1.995 \text{ lbf/in}$	$D = -0.2675 \text{ lbf/in}$
$\psi_c = 1.604 \times 10^{-2} \frac{\text{lbm}}{\text{in-sec}}$	$\psi_c = 5.66 \times 10^{-2} \frac{\text{lbm}}{\text{in-sec}}$	$\psi_c = 2.83 \times 10^{-2} \frac{\text{lbm}}{\text{in-sec}}$

(c) Influence of $PE - T_s = 110^\circ F$, $T_p = 55^\circ F$

$Pe = 20.0$, $PE = 1.27$	$Pe = 20.0$, $PE = 20.33$	$Pe = 80.0$, $PE = 20.33$
$U_r = 2.9766 \times 10^2 \text{ in/sec}$	$U_r = 1.19 \times 10^3 \text{ in/sec}$	$U_r = 1.191 \times 10^3$
$h_o = 4.01 \times 10^{-3} \text{ in}$	$h_o = 2.005 \times 10^{-3} \text{ in}$	$h_o = 4.01 \times 10^{-3} \text{ in}$
$\bar{W} = 0.10834$	$W = 0.05622$	$\bar{W} = 0.076768$
$\bar{D} = -1.644$	$\bar{D} = -0.3411$	$\bar{D} = -0.47113$
$\bar{\psi}_c = 0.49419$	$\bar{\psi}_c = 0.55075$	$\bar{\psi}_c = 0.52802$
$W = 77.7 \text{ lbf/in}^2$	$W = 645 \text{ lbf/in}^2$	$W = 220 \text{ lbf/in}^2$
$D = -1.644 \text{ lbf/in}$	$D = -7.85 \text{ lbf/in}$	$D = -5.39 \text{ lbf/in}$
$\psi_c = 1.89 \times 10^{-2} \frac{\text{lbm}}{\text{in-sec}}$	$\psi_c = 4.15 \times 10^{-2} \frac{\text{lbm}}{\text{in-sec}}$	$\psi_c = 2.83 \times 10^{-2} \frac{\text{lbm}}{\text{in-sec}}$

(d) Influence of $Pe - T_s = 150^\circ F$, $T_p = 75^\circ F$

$Pe = 1.0$, $PE = 6.1799$	$Pe = 2.50$, $PE = 6.1799$	$Pe = 2.5$, $PE = 38.6$
$U_r = 1.199 \times 10^3$ in/sec	$U_r = 1.199 \times 10^3$ in/sec	$U_r = 2.995 \times 10^3$ in/sec
$h_o = 4.467 \times 10^{-4}$ in	$h_o = 7.065 \times 10^{-4}$ in	$h_o = 4.467 \times 10^{-4}$ in
$\bar{W} = 0.065964$	$\bar{W} = 0.067969$	$\bar{W} = 0.030973$
$\bar{D} = -0.33806$	$\bar{D} = -0.35272$	$\bar{D} = -0.14462$
$\bar{\psi}_C = 0.51777$	$\bar{\psi}_C = 0.51907$	$\bar{\psi}_C = 0.57742$
$W = 6,262$ lbf/in ²	$W = 2580$ lbf/in ²	$W = 7,340$ lbf/in ²
$D = -14.35$ lbf/in	$D = -9.47$ lbf/in	$D = -15.35$ lbf/in
$\psi_C = 0.877 \times 10^{-2}$ $\frac{lbm}{in-sec}$	$\psi_C = 1.39 \times 10^{-2}$ $\frac{lbm}{in-sec}$	$\psi_C = 2.437 \times 10^2$ $\frac{lbm}{in-sec}$

(e) Influence of Inertia Terms

$$- T_s = 200^\circ\text{F}, T_p = 100^\circ\text{F}, \text{Re}^* = 0.5$$

Inertia Terms Not Included

Inertia Terms Included

$$\bar{W} = 0.12686$$

$$\bar{W} = 0.1333$$

$$\bar{D} = -0.6644$$

$$\bar{D} = -0.6876$$

$$\bar{\Psi}_c = 0.5389$$

$$\bar{\Psi}_c = 0.5261$$

$$\underline{W = 46.8 \text{ lbf/in}^2}$$

$$\underline{W = 49.2 \text{ lbf/in}^2}$$

$$D = -0.534 \text{ lbf/in}$$

$$D = -0.553 \text{ lbf/in}$$

$$\Psi_c = 5.57 \times 10^{-2} \frac{\text{lbm}}{\text{in-sec}}$$

$$\Psi_c = 5.43 \times 10^{-2} \frac{\text{lbm}}{\text{in-sec}}$$

SUMMARY OF CONCLUSIONS

The main conclusions of the analysis may now be listed as follows.

(1) Decreasing the slider temperature to pad temperature ratio of a slider bearing causes an increase in both the dimensionless load capacity and the dimensionless drag, irrespective of whether the slider is cooled or the pad is heated. For the range $0.5 \leq T_s/T_p \leq 2.0$, the dimensionless values of the load capacity, drag, and mass flow depend strongly on the T_s/T_p ratio, but weakly on the actual values of the temperature boundary conditions.

(2) Although cooling the slider causes an increase in the load a bearing can carry, heating the pad for the case considered causes the bearing to be able to support less load. This difference is readily explained by using the following reasoning.

For a bearing operating at a fixed speed and having a constant film thickness, the load is proportional to the product of the dimensionless load capacity and the reference viscosity. When the slider is cooled, both the values of the dimensionless load capacity and the reference viscosity increase, thus causing an overall increase in the load which the bearing can carry. However, for the heated pad, although there is an increase in the dimensionless load capacity, the value of the reference viscosity decreases, which for the case under consideration causes a drop in the load which the bearing can support. For both cases, the rate of mass

flow through the bearing increases, while for the cooled slider alone there is an increase in the drag.

(3) Neglecting the inertia terms in the momentum equation results in a smaller value being obtained for the load which the bearing can carry, and this error increases as Re^* increases. The largest errors made in neglecting the inertia terms occur for the larger T_s/T_p ratios. For $T_s = 200^\circ\text{F}$, $T_p = 100^\circ\text{F}$, and $Re^* = 0.5$, the value of the error is approximately 5% of the value obtained when the inertia terms are included, and this error rises to approximately 10% of the true load for $Re^* = 1.0$.

(4) When the inlet to outlet ratio, \bar{h}_r , of a plane slider bearing is increased, the load which the bearing can carry rises to a maximum then falls gradually. The observed maxima were in the range $2.00 \leq \bar{h}_r \leq 2.25$.

(5) Increasing PE, brought about by varying the speed of the slider causes a drop in the dimensionless values of the load capacity and drag.

However, with our choice of reference temperature, and for the sample example presented, the load the bearing can carry increases about three times as PE goes from 1.27 to 20.33. This result can be explained by using the following reasoning. When a bearing operates at a varying speed and for a constant film thickness, the load it can carry is proportional to the product of the dimensionless load capacity and the slider velocity assuming that the reference viscosity remains constant. For the larger value of PE, although the

value of the dimensionless load capacity decreases, the higher velocity offsets this decrease thus resulting in a larger value for the load which the bearing is able to support. A similar argument can be used to explain the larger drag. The increased dissipation caused by higher velocities would give a lower reference viscosity than the one used in our calculations, so that the actual values of the load and drag would be smaller than those now evaluated.

(6) Increasing Pe at constant speed, brought about by an increase in the film thickness results in larger values for the dimensionless load capacity and drag. However, the actual load the bearing can carry decreases as Pe increases, and the drag behaves likewise. The reason for this drop in load capacity can be understood from the following argument. When a slider bearing operates at constant speed and for a varying film thickness h_o , the load it can carry is proportional to the product of the dimensionless load capacity and $\frac{1}{h_o^2}$, assuming the reference viscosity remains constant. For the larger value of Pe , although the value of the dimensionless load capacity increases, $\frac{1}{h_o^2}$ decreases because of an increase in h_o . For the sample example presented this drop in $\frac{1}{h_o^2}$ offsets the rise in the dimensionless load capacity, resulting in a smaller value of load which the bearing can sustain. A similar reasoning can be used to explain the smaller value obtained for the drag. The reduced dissipation caused by the larger film

thickness would give a somewhat larger value for the reference viscosity, so that the actual magnitudes of the load and drag would be larger than those now obtained.

SUGGESTIONS FOR FUTURE RESEARCH

The present theoretical work has clearly shown that it is possible to considerably increase the load a slider bearing can carry by maintaining a low slider temperature to pad temperature ratio. It is suggested to design and build an apparatus to verify and find the range of applicability of the theory. The main feature of the design should be that a high viscosity layer next to the slider.

One of the assumptions made in Chapter II was that the effects of thermal and elastic distortions were to be neglected in the analysis. However, for extreme cases examined, the difference in the temperature boundary conditions were so large that this assumption may not be strictly correct. The net result of thermal distortion would be to cause changes in the clearance between the slider and the pad, which directly affects the lubricant film thickness, and thus would cause changes in the load capacity, drag, etc. It is proposed to find the conditions at which these effects can still be neglected.

BIBLIOGRAPHY

BIBLIOGRAPHY

1. Tahara, H., "Forced Cooling of a Slider Bearing of Infinite Length." *Lubrication Engineering*, Vol. 21, No. 5, 1965, p. 193-200.
2. Radzimovsky, E. I., "Lubrication of Bearings." The Ronald Press Company, New York, 1959, p. 87.
3. Reynolds, O., "On the Theory of Lubrication." *Philosophical Transaction of the Royal Society of London*, Part I, Vol. 177, 1886 p. 157.
4. Wilcock, D. F., "Predicting Sleeve Bearing Performance." *Proc. Conference on Lubrication and Wear*, *Instn. Mech. Engrs.*, London, p. 82.
5. Rosenblatt, M., and Wilcock, D. F., "Oil Flow, Key Factor in Sleeve Bearing Performance." *Trans. ASME*, Vol. 74, 1952, p. 849.
6. Slezkin, N. A., and Targ, S. M., "The Generalized Equations of Reynolds," *Compte Rendus De L'Academie des Science USSR*, Vol. 54, 1946, p. 205.
7. Osterle, J. F., Chou, Y. T., and Saibel, E. A., "Effect of Lubricant Inertia in Journal-Bearing Lubrication." *Journal of Applied Mechanics*, *ASME Trans.* Vol. 79, 1957, p. 449.
8. Osterle, F., and Saibel, E., "On the Effect of Lubricant Inertia in Hydrodynamic Lubrication." *Journal of Applied Mathematics and Physics*, *ZAMP*, Vol. 6, 1955, p. 334.
9. Kahlert, W., "Der Einfluss der Tragheitskrafte bei der Hydrodynamischen Shniermitteltheorie," *Ingenieur-Archiv*, Vol. 16, 1948, p. 321.
10. Snyder, W. T., "The Non-Linear Hydrodynamic Slider Bearing." *Journal of Basic Engineering*, *Trans. ASME Series D*, Vol. 85, 1963, p. 429.

11. Rodkiewicz, C. M., and Anwar, M. I., "Inertia and Convective Effects in Hydrodynamic Lubrication of a Slider Bearing." *Journal of Lubrication Technology*, April 1971, p. 313.
12. Hunter, W. B., and Zienkiewicz, O. C. "Effect of Temperature Variation Across the Lubricating Films in the Theory of Hydrodynamic Lubrication." *Journ. Mech. Eng. Sci.*, Vol. 2, No. 1, 1960, p. 52.
13. Snyder, W. T., "Temperature Variations Across the Lubricant Film in Hydrodynamic Lubrication." *App. Sci. Res. Section A*, Vol. 14, July 1963. p.1.
14. Hahn, E. J., and Kettleborough, C. F., "Solution for the Pressure and Temperature in an Infinite Slider Bearing of Arbitrary Profile." *Journal of Lubrication Technology*, Oct. 1967, p. 445.
15. Woodhead, R. W., and Kettleborough, C. F., "Solution of Navier-Stokes Equations for the Non-linear Hydrodynamic Slider by Matrix Algebra Methods," *Journal Mechanical Engineering Science*, Vol. 5, No. 2., 1963.

APPENDIX A

TRANSFORMATION OF THE REDUCED EQUATIONS

APPENDIX A

TRANSFORMATION OF THE REDUCED EQUATIONS

In order to simplify computations, the governing Equations (2.15) through (2.17) are transformed by use of the stream function.

Writing $\rho u = \frac{\partial \Psi}{\partial y}$, $\rho v = -\frac{\partial \Psi}{\partial x}$ and $\bar{\Psi} = \frac{\Psi}{\Psi_c}$; it is possible

for us to obtain expressions for \bar{u} and \bar{v} in terms of the stream function.

$$\text{Now } \frac{\partial}{\partial x} = \frac{1}{L} \left[\frac{\partial}{\partial \bar{x}} + \bar{y} \frac{(\bar{h}_{r-1})}{\bar{h}} \frac{\partial}{\partial \bar{y}} \right]$$

$$\text{and } \frac{\partial}{\partial y} = \frac{1}{h_o} \frac{1}{\bar{h}} \frac{\partial}{\partial \bar{y}}$$

For the u component,

$$\rho U \bar{u} = \frac{\Psi_c}{h_o} \frac{\partial \bar{\Psi}}{\partial \bar{y}} \frac{1}{\bar{h}} \quad \bar{u} = \frac{\Psi_c}{\rho U h_o} \frac{1}{\bar{h}} \frac{\partial \bar{\Psi}}{\partial \bar{y}}$$

$$\text{ie. } \bar{u} = \frac{\bar{\Psi}_c}{\bar{h}} \frac{\partial \bar{\Psi}}{\partial \bar{y}} \quad (\text{A.1})$$

Similarly for the v component,

$$\frac{U h_o}{\rho L} \bar{v} = -\frac{\Psi_c}{L} \left(\frac{\partial \bar{\Psi}}{\partial \bar{x}} + \bar{y} \frac{(\bar{h}_{r-1})}{\bar{h}} \frac{\partial \bar{\Psi}}{\partial \bar{y}} \right)$$

$$\bar{v} = - \frac{\bar{\psi}_c}{\rho U h_0} \left(\frac{\partial \bar{\Psi}}{\partial \bar{x}} + \bar{y} \frac{(\bar{h}_{r-1})}{\bar{h}} \frac{\partial \bar{\Psi}}{\partial \bar{y}} \right)$$

$$\bar{v} = - \bar{\psi}_c \left(\frac{\partial \bar{\Psi}}{\partial \bar{x}} + \bar{y} \frac{(\bar{h}_{r-1})}{\bar{h}} \frac{\partial \bar{\Psi}}{\partial \bar{y}} \right) \quad (A.2)$$

where $\bar{\psi}_c$ is the dimensionless mass flow.

TRANSFORMATION OF THE MOMENTUM EQUATION

Substituting for \bar{u} and \bar{v} into Eq. (2.15) we obtain

$$\bar{h}^2 \text{Re}^* \left[\left(\frac{\bar{\psi}_c}{\bar{h}} \right) \frac{\partial \bar{\Psi}}{\partial \bar{y}} \frac{\partial}{\partial \bar{x}} + \left(\frac{\bar{\psi}_c}{\bar{h}} \right) \frac{\partial \bar{\Psi}}{\partial \bar{y}} - \left(\frac{\bar{\psi}_c}{\bar{h}} \right) \frac{\partial \bar{\Psi}}{\partial \bar{x}} + \frac{(\bar{h}_{r-1})}{\bar{h}} \bar{y} \frac{\partial \bar{\Psi}}{\partial \bar{y}} \right]$$

$$\frac{\partial}{\partial \bar{y}} \left(\frac{\bar{\psi}_c}{\bar{h}} \frac{\partial \bar{\Psi}}{\partial \bar{y}} \right) = -\bar{h}^2 \frac{\partial \bar{p}}{\partial \bar{x}} + \frac{\partial}{\partial \bar{y}} \left[\bar{\mu} \frac{\partial}{\partial \bar{y}} \left(\frac{\bar{\psi}_c}{\bar{h}} \frac{\partial \bar{\Psi}}{\partial \bar{y}} \right) \right]$$

$$\text{i.e. } \bar{h}^2 \text{Re}^* \left[\frac{\bar{\psi}_c}{\bar{h}} \left\{ \frac{\partial \bar{\Psi}}{\partial \bar{y}} \frac{\partial}{\partial \bar{x}} + \left(\frac{\bar{\psi}_c}{\bar{h}} \frac{\partial \bar{\Psi}}{\partial \bar{y}} \right) + \frac{\partial \bar{\Psi}}{\partial \bar{y}} \bar{y} \frac{(\bar{h}_{r-1})}{\bar{h}} \frac{\partial}{\partial \bar{y}} \right. \right.$$

$$\left. \left. \left(\frac{\bar{\psi}_c}{\bar{h}} \frac{\partial \bar{\Psi}}{\partial \bar{y}} \right) - \frac{\partial \bar{\Psi}}{\partial \bar{x}} \frac{\partial}{\partial \bar{y}} \left(\frac{\bar{\psi}_c}{\bar{h}} \frac{\partial \bar{\Psi}}{\partial \bar{y}} \right) - \frac{(\bar{h}_{r-1})}{\bar{h}} \bar{y} \frac{\partial \bar{\Psi}}{\partial \bar{y}} \frac{\partial}{\partial \bar{y}} \left(\frac{\bar{\psi}_c}{\bar{h}} \frac{\partial \bar{\Psi}}{\partial \bar{y}} \right) \right\} \right]$$

$$= -\bar{h}^2 \frac{\partial \bar{p}}{\partial \bar{x}} + \frac{\bar{\psi}_c}{\bar{h}} \frac{\partial}{\partial \bar{y}} \left(\bar{\mu} \frac{\partial^2 \bar{\Psi}}{\partial \bar{y}^2} \right)$$

$$\bar{h} \text{Re}^* \bar{\psi}_c \left[\frac{\partial \bar{\Psi}}{\partial \bar{y}} \left\{ \frac{\partial \bar{\Psi}}{\partial \bar{y}} \frac{\bar{\psi}_c}{\bar{h}} \frac{(\bar{h}_{r-1})}{\bar{h}} + \frac{\bar{\psi}_c}{\bar{h}} \frac{\partial}{\partial \bar{x}} \left(\frac{\partial \bar{\Psi}}{\partial \bar{y}} \right) \right\} + \frac{\bar{\psi}_c}{\bar{h}} \frac{(\bar{h}_{r-1})}{\bar{h}} \right.$$

$$\left. \bar{y} \frac{\partial \bar{\Psi}}{\partial \bar{y}} \frac{\partial^2 \bar{\Psi}}{\partial \bar{y}^2} - \frac{\bar{\psi}_c}{\bar{h}} \frac{\partial \bar{\Psi}}{\partial \bar{x}} \frac{\partial^2 \bar{\Psi}}{\partial \bar{y}^2} - \frac{\bar{\psi}_c}{\bar{h}} \frac{(\bar{h}_{r-1})}{\bar{h}} \bar{y} \frac{\partial \bar{\Psi}}{\partial \bar{y}} \frac{\partial^2 \bar{\Psi}}{\partial \bar{y}^2} \right]$$

$$\begin{aligned}
&= -\bar{h}^2 \frac{\partial \bar{p}}{\partial \bar{x}} + \frac{\bar{\Psi}_c}{\bar{h}} \frac{\partial}{\partial \bar{y}} \left(\bar{\mu} \frac{\partial^2 \bar{\Psi}}{\partial \bar{y}^2} \right) \\
\text{i.e. } \bar{h} \operatorname{Re}^* \bar{\Psi}_c &\left[\left(\frac{\partial \bar{\Psi}}{\partial \bar{y}} \right)^2 \frac{(\bar{h}_{r-1})}{\bar{h}} + \frac{\partial \bar{\Psi}}{\partial \bar{y}} \frac{\partial}{\partial \bar{x}} \left(\frac{\partial \bar{\Psi}}{\partial \bar{y}} \right) - \frac{\partial \bar{\Psi}}{\partial \bar{x}} \frac{\partial^2 \bar{\Psi}}{\partial \bar{y}^2} \right] \\
&= -\frac{\bar{h}^3}{\bar{\Psi}_c} \frac{\partial \bar{p}}{\partial \bar{x}} + \frac{\partial}{\partial \bar{y}} \left(\bar{\mu} \frac{\partial^2 \bar{\Psi}}{\partial \bar{y}^2} \right) \quad (\text{A.3})
\end{aligned}$$

TRANSFORMATION OF THE ENERGY EQUATION

Likewise for the Energy Eq. (2.16) we get

$$\begin{aligned}
&\bar{h}^2 P \operatorname{Re}^* \left[\frac{\bar{\Psi}_c}{\bar{h}} \frac{\partial \bar{\Psi}}{\partial \bar{y}} \left(\frac{\partial \bar{T}}{\partial \bar{x}} + \bar{y} \frac{(\bar{h}_{r-1})}{\bar{h}} \frac{\partial \bar{T}}{\partial \bar{y}} \right) - \frac{\bar{\Psi}_c}{\bar{h}} \left(\frac{\partial \bar{\Psi}}{\partial \bar{x}} + \bar{y} \frac{(\bar{h}_{r-1})}{\bar{h}} \right. \right. \\
&\left. \left. \frac{\partial \bar{\Psi}}{\partial \bar{y}} \right) \frac{\partial \bar{T}}{\partial \bar{y}} \right] = \frac{\partial^2 \bar{T}}{\partial \bar{y}^2} + PE \left(\frac{\bar{\Psi}_c}{\bar{h}} \right)^2 \bar{\mu} \left(\frac{\partial^2 \bar{\Psi}}{\partial \bar{y}^2} \right)^2 \\
&\bar{h} \bar{\Psi}_c P \operatorname{Re}^* \left[\frac{\partial \bar{\Psi}}{\partial \bar{y}} \frac{\partial \bar{T}}{\partial \bar{x}} + \frac{\partial \bar{\Psi}}{\partial \bar{y}} \bar{y} \frac{(\bar{h}_{r-1})}{\bar{h}} \frac{\partial \bar{T}}{\partial \bar{y}} - \frac{\partial \bar{\Psi}}{\partial \bar{x}} \frac{\partial \bar{T}}{\partial \bar{y}} - \frac{\partial \bar{\Psi}}{\partial \bar{y}} \bar{y} \right. \\
&\left. \frac{(\bar{h}_{r-1})}{\bar{h}} \frac{\partial \bar{T}}{\partial \bar{y}} \right] = \frac{\partial^2 \bar{T}}{\partial \bar{y}^2} + PE \left(\frac{\bar{\Psi}_c}{\bar{h}} \right)^2 \bar{\mu} \left(\frac{\partial^2 \bar{\Psi}}{\partial \bar{y}^2} \right)^2 \\
\text{i.e. } \bar{h} \bar{\Psi}_c P \operatorname{Re}^* &\left[\frac{\partial \bar{\Psi}}{\partial \bar{y}} \frac{\partial \bar{T}}{\partial \bar{x}} - \frac{\partial \bar{\Psi}}{\partial \bar{x}} \frac{\partial \bar{T}}{\partial \bar{y}} \right] = \frac{\partial^2 \bar{T}}{\partial \bar{y}^2} + PE \\
&\left(\frac{\bar{\Psi}_c}{\bar{h}} \right)^2 \bar{\mu} \left(\frac{\partial^2 \bar{\Psi}}{\partial \bar{y}^2} \right)^2 \quad (\text{A.4})
\end{aligned}$$

APPENDIX B

ENERGY EQUATION IN FINITE DIFFERENCE FORM

APPENDIX B

ENERGY EQUATION IN FINITE DIFFERENCE FORM

The energy Equation (2.25) is rewritten in finite difference form, by replacing the derivatives of the temperature by their central finite difference approximations. Let $\Delta \bar{x}$ and $\Delta \bar{y}$ represent the grid spacing in the \bar{x} and \bar{y} directions as shown in Fig. 3.

Considering the point $i+1/2, j$, the energy equation can be rewritten as follows:

$$\begin{aligned} \bar{h}_{i+1/2} \bar{\Psi}_c \text{ P Re}^* & \left[- \left(\frac{\partial \bar{\Psi}}{\partial \bar{y}} \right)_{i+1/2,j} \left(\frac{\partial \bar{T}}{\partial \bar{x}} \right)_{i+1/2,j} - \left(\frac{\partial \bar{\Psi}}{\partial \bar{x}} \right)_{i+1/2,j} \left(\frac{\partial \bar{T}}{\partial \bar{y}} \right)_{i+1/2,j} \right] \\ & = \left(\frac{\partial^2 \bar{T}}{\partial \bar{y}^2} \right)_{i+1/2,j} + \left(\frac{\bar{\Psi}_c}{\bar{h}_{i+1/2}} \right)^2 \text{ P.E. } \bar{\mu}_{i+1/2,j} \left(\frac{\partial^2 \bar{\Psi}}{\partial \bar{y}^2} \right)_{i+1/2,j}^2 \end{aligned} \quad (\text{B.1})$$

Where,

$$\bar{h}_{i+1/2} = (\bar{h}_i + \bar{h}_{i+1})/2.0 \quad (\text{B.2})$$

$$\left(\frac{\partial \bar{\Psi}}{\partial \bar{y}} \right)_{i+1/2,j} = \frac{1}{2} \left[\left(\frac{\partial \bar{\Psi}}{\partial \bar{y}} \right)_{i,j} + \left(\frac{\partial \bar{\Psi}}{\partial \bar{y}} \right)_{i+1,j} \right] \quad (\text{B.3})$$

$$\left(\frac{\partial \bar{\Psi}}{\partial \bar{x}} \right)_{i+1/2,j} = \frac{1}{2} \left[\left(\frac{\partial \bar{\Psi}}{\partial \bar{x}} \right)_{i,j} + \left(\frac{\partial \bar{\Psi}}{\partial \bar{x}} \right)_{i+1,j} \right] \quad (\text{B.4})$$

$$\bar{\mu}_{i+1/2,j} = \frac{1}{2} \left(\bar{\mu}_{i,j} + \bar{\mu}_{i+1,j} \right) \quad (\text{B.5})$$

$$\left[\left(\frac{\partial^2 \bar{\Psi}}{\partial \bar{Y}^2} \right)_{i+1/2,j} \right]^2 = \left[\frac{1}{2} \left\{ \left(\frac{\partial^2 \bar{\Psi}}{\partial \bar{Y}^2} \right)_{i,j} + \left(\frac{\partial^2 \bar{\Psi}}{\partial \bar{Y}^2} \right)_{i+1,j} \right\} \right]^2 \quad (\text{B.6})$$

$$\left(\frac{\partial \bar{T}}{\partial \bar{x}} \right)_{i+1/2,j} = \frac{\bar{T}_{i+1,j} - \bar{T}_{i,j}}{\Delta \bar{x}} + O[\Delta \bar{x}^2] \quad (\text{B.7})$$

$$\begin{aligned} \left(\frac{\partial \bar{T}}{\partial \bar{y}} \right)_{i+1/2,j} &= \frac{1}{2} \left[\frac{\bar{T}_{i,j+1} - \bar{T}_{i,j-1}}{2\Delta \bar{y}} + \frac{\bar{T}_{i+1,j+1} - \bar{T}_{i+1,j-1}}{2\Delta \bar{y}} \right] \\ &\quad + O[\Delta \bar{y}^2] \end{aligned} \quad (\text{B.8})$$

$$\begin{aligned} \left(\frac{\partial^2 \bar{T}}{\partial \bar{y}^2} \right)_{i+1/2,j} &= \frac{1}{2} \left[\frac{\bar{T}_{i,j+1} - 2\bar{T}_{i,j} + \bar{T}_{i,j-1}}{\Delta \bar{y}^2} \right. \\ &\quad \left. + \frac{\bar{T}_{i+1,j+1} - 2\bar{T}_{i+1,j} + \bar{T}_{i+1,j-1}}{\Delta \bar{y}^2} \right] + O[\Delta \bar{y}^2] \end{aligned} \quad (\text{B.9})$$

For $i = 1,$

$$\left(\frac{\partial \bar{\Psi}}{\partial \bar{x}}\right)_{i,j} = \left[4 \bar{\Psi}_{i+1,j} - 3 \bar{\Psi}_{i,j} - \bar{\Psi}_{i+2,j} \right] / 2 \Delta \bar{x} + O[\Delta \bar{x}^2]$$

For $i = M$

$$\left(\frac{\partial \bar{\Psi}}{\partial \bar{x}}\right)_{i,j} = \left[\bar{\Psi}_{i-2,j} + 3 \bar{\Psi}_{i,j} - 4 \bar{\Psi}_{i-1,j} \right] / 2 \Delta \bar{x} + O[\Delta \bar{x}^2] \quad (B.10)$$

For $1 < i < M$

$$\left(\frac{\partial \bar{\Psi}}{\partial \bar{x}}\right)_{i,j} = (\bar{\Psi}_{i+1,j} - \bar{\Psi}_{i-1,j}) / 2 \Delta \bar{x} + O[\Delta \bar{x}^2]$$

Now substituting Equations (A.2) through (A.9) into Equation (A.1) we obtain,

$$\begin{aligned} & \frac{\bar{h}_{i+1/2} \bar{\Psi}_c^{P.Re*}}{\Delta \bar{x}} \left(\frac{\partial \bar{\Psi}}{\partial \bar{y}}\right)_{i+1/2,j} \left[\bar{T}_{i+1,j} - \bar{T}_{i,j} \right] - \frac{\bar{h}_{i+1/2} \bar{\Psi}_c^{P.Re*}}{4 \Delta \bar{y}} \\ & \left(\frac{\partial \bar{\Psi}}{\partial \bar{x}}\right)_{i+1/2,j} \left[\bar{T}_{i,j+1} - \bar{T}_{i,j-1} + \bar{T}_{i+1,j+1} - \bar{T}_{i+1,j-1} \right] = \frac{1}{2 \Delta \bar{y}^2} \\ & \left[\bar{T}_{i,j+1} - 2 \bar{T}_{i,j} + \bar{T}_{i,j-1} + \bar{T}_{i+1,j+1} - 2 \bar{T}_{i+1,j} + \bar{T}_{i+1,j-1} \right] \\ & + \left(\frac{\bar{\Psi}_c}{\bar{h}_{i+1/2}}\right)^2 PE \bar{\mu}_{i+1/2,j} \left(\frac{\partial^2 \bar{\Psi}}{\partial \bar{y}^2}\right)_{i+1/2,j}^2 \end{aligned}$$

After rearranging the terms, the previous equation becomes

$$\begin{aligned}
 & \bar{T}_{i+1,j-1} \left[\frac{\bar{h}_{i+1/2} \bar{\psi}_c}{4\Delta\bar{y}} \left(\frac{\partial \bar{\psi}}{\partial \bar{x}} \right)_{i+1/2,j} - \frac{1}{2\text{Pre}^* \Delta\bar{y}^{-2}} \right] + \bar{T}_{i+1,j} \\
 & \left[\frac{\bar{h}_{i+1/2} \bar{\psi}_c}{\Delta\bar{x}} \left(\frac{\partial \bar{\psi}}{\partial \bar{y}} \right)_{i+1/2,j} + \frac{1}{\text{P.Re}^* \Delta\bar{y}^{-2}} \right] - \bar{T}_{i+1,j+1} \left[\frac{\bar{h}_{i+1/2} \bar{\psi}_c}{4\Delta\bar{y}} \right. \\
 & \left. \left(\frac{\partial \bar{\psi}}{\partial \bar{x}} \right)_{i+1/2,j} + \frac{1}{2\text{Pre}^* \Delta\bar{y}^{-2}} \right] = \bar{T}_{i,j-1} \left[\frac{1}{2\text{Pre}^* \Delta\bar{y}^{-2}} - \frac{\bar{h}_{i+1/2} \bar{\psi}_c}{4\Delta\bar{y}} \right. \\
 & \left. \left(\frac{\partial \bar{\psi}}{\partial \bar{x}} \right)_{i+1/2,j} \right] + \bar{T}_{i,j} \left[\frac{\bar{h}_{i+1/2} \bar{\psi}_c}{\Delta\bar{x}} \left(\frac{\partial \bar{\psi}}{\partial \bar{y}} \right)_{i+1/2,j} - \frac{1}{\text{Pre}^* \Delta\bar{y}^{-2}} \right] \\
 & + \bar{T}_{i,j+1} \left[\frac{\bar{h}_{i+1/2} \bar{\psi}_c}{4\Delta\bar{y}} \left(\frac{\partial \bar{\psi}}{\partial \bar{x}} \right)_{i+1/2,j} \right. \\
 & \left. + \frac{1}{2\text{Pre}^* \Delta\bar{y}^{-2}} \right] + \left(\frac{\bar{\psi}_c}{\bar{h}_{i+1/2}} \right)^2 \frac{E}{\text{Re}^*} \bar{\mu}_{i+1/2,j} \left(\frac{\partial^2 \bar{\psi}}{\partial \bar{y}^2} \right)_{i+1/2,j}^2
 \end{aligned}$$

The above equation can finally be rewritten as follows

$$a_{i,j} \bar{T}_{i+1,j-1} + b_{i,j} \bar{T}_{i+1,j} + c_{i,j} \bar{T}_{i+1,j+1} = d_{i,j} \quad (\text{B.11})$$

where

$$a_{i,j} = \left[\frac{\bar{h}_{i+1/2} \bar{\psi}_c}{4\Delta\bar{y}} \left(\frac{\partial \bar{\psi}}{\partial \bar{x}} \right)_{i+1/2,j} - \frac{1}{2\text{Pre}^* \Delta\bar{y}^{-2}} \right] \quad (\text{B.12})$$

$$b_{i,j} = \left[\frac{\bar{h}_{i+1/2} \bar{\psi}_c}{\Delta\bar{x}} \left(\frac{\partial \bar{\psi}}{\partial \bar{y}} \right)_{i+1/2,j} + \frac{1}{\text{Pre}^* \Delta\bar{y}^{-2}} \right] \quad (\text{B.13})$$

$$c_{i,j} = - \left[\frac{\bar{h}_{i+1/2} \bar{\psi}_c}{4 \Delta \bar{y}} \left(\frac{\partial \bar{\psi}}{\partial \bar{x}} \right)_{i+1/2,j} + \frac{1}{2 P \cdot \text{Re}^* \Delta \bar{y}^{-2}} \right] \quad (\text{B.14})$$

$$d_{i,j} = - a_{i,j} \bar{T}_{i,j-1} + \left[b_{i,j} - \frac{2}{P \cdot \text{Re}^* \Delta \bar{y}^{-2}} \right] \bar{T}_{i,j} - c_{i,j}$$

$$\bar{T}_{i,j+1} + \frac{E}{\text{Re}^*} \left(\frac{\bar{\mu}_{i,j} + \bar{\mu}_{i+1,j}}{8} \right) \left[\left(\frac{\partial^2 \bar{\psi}}{\partial \bar{y}^{-2}} \right)_{i+1/2,j} \frac{\bar{\psi}_c}{\bar{h}_{i+1/2}} \right]^2 \quad (\text{B.15})$$

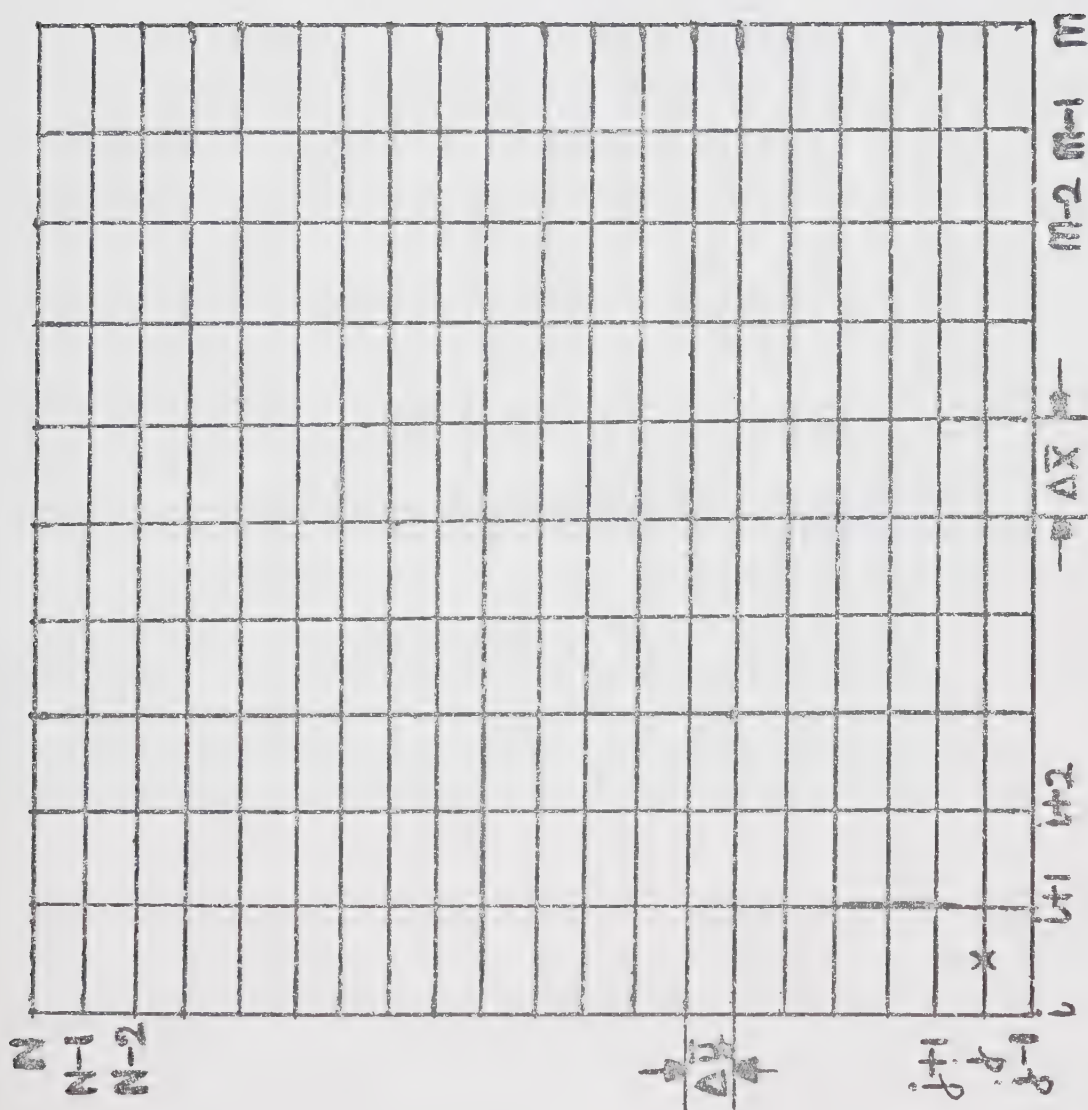


FIG.3 Grid Network

APPENDIX C
EQUATIONS FOR BEARING CHARACTERISTICS

APPENDIX C

BEARING CHARACTERISTICS

By substituting dimensionless variables for the dimensional ones, it is possible to obtain dimensionless equations for all the characteristics of the bearing operation.

Dimensionless Mass Flow

$$\Psi_C = \int_0^h \rho u \, dy \quad (C.1)$$

After substituting dimensionless variables in the above equation we obtain

$$\Psi_C = (\rho U h_0) \bar{h} \int_0^1 \bar{u} \, d\bar{y}$$

$$\frac{\Psi_C}{(\rho U h_0)} = \bar{h} \int_0^1 \bar{u} \, d\bar{y}$$

$$\bar{\Psi}_C = \bar{h} \int_0^1 \bar{u} \, d\bar{y} \quad (C.2)$$

Dimensionless Load Capacity

$$W = \int_0^L p \, dx \quad (C.3)$$

Again nondimensionalizing we have,

$$W = \frac{\rho U^2 L}{\text{Re} \star L} \int_0^1 \bar{p} \, d\bar{x}$$

$$W = \frac{\mu_r U L}{h_0^2} \int_0^1 \bar{p} \, d\bar{x}$$

$$\frac{Wh_o^2}{\mu_r UL} = \int_0^1 \bar{p} \, d\bar{x}$$

$$\text{i.e.} \quad \bar{W} = \int_0^1 \bar{p} \, d\bar{x} \quad (C.4)$$

Dimensionless Shear Stress at Slider

$$\tau_o = \mu \left(\frac{\partial u}{\partial y} \right)_{y=0} \quad (C.5)$$

$$\text{ie.} \quad \tau_o = \frac{U\mu_r}{h_o} \frac{\bar{\psi}_c}{\bar{h}^2} \left[\bar{\mu} \left(\frac{\partial^2 \bar{\psi}}{\partial \bar{y}^2} \right) \right]_{\bar{y}=0}$$

$$\frac{\tau_o h_o}{\mu_r U} = \frac{\bar{\psi}_c}{\bar{h}^2} \left[\bar{\mu} \left(\frac{\partial^2 \bar{\psi}}{\partial \bar{y}^2} \right) \right]_{\bar{y}=0}$$

$$\bar{\tau}_o = \frac{\bar{\psi}_c}{\bar{h}^2} \left[\bar{\mu} \frac{\partial^2 \bar{\psi}}{\partial \bar{y}^2} \right]_{\bar{y}=0} \quad (C.6)$$

Dimensionless Drag

$$D = \int_0^L \tau_{y=0} \, dx \quad (C.7)$$

$$D = \int_0^L \left(\mu \frac{\partial u}{\partial y} \right)_{y=0} \, dx$$

$$D = \frac{\mu_r UL}{h_o} \bar{\psi}_c \int_0^1 \left[\bar{\mu} \left(\frac{\partial^2 \bar{\psi}}{\partial \bar{y}^2} \right) \right]_{\bar{y}=0} \frac{1}{\bar{h}^2} \, d\bar{x}$$

$$\frac{D h_o}{\mu_r UL} = \bar{\psi}_c \int_0^1 \left[\bar{\mu} \frac{\partial^2 \bar{\psi}}{\partial \bar{y}^2} \right]_{\bar{y}=0} \frac{1}{\bar{h}^2} \, d\bar{x}$$

$$\bar{D} = \bar{\Psi}_c \int_0^1 \left[\bar{\mu} \frac{\partial^2 \bar{\Psi}}{\partial \bar{Y}^2} \right]_{\bar{Y}=0} \frac{1}{\bar{h}^2} d\bar{x} \quad (C.8)$$

Dimensionless Heat Convected into Bearing

$$Q_i = \int_0^h \rho C_p \mu_i T_i dy \quad (C.9)$$

$$Q_i = \rho C_p T_r U h_o \bar{\Psi}_c \frac{\bar{h}}{\bar{h}} \int_0^1 \left(\bar{T} \frac{\partial \bar{\Psi}}{\partial \bar{Y}} \right)_{\bar{x}=0} d\bar{y}$$

ie.
$$\frac{Q_i}{(\rho C_p T_r U h_o)} = \bar{\Psi}_c \int_0^1 \left(\bar{T} \frac{\partial \bar{\Psi}}{\partial \bar{Y}} \right)_{\bar{x}=0} d\bar{y}$$

$$\bar{Q}_i = \bar{\Psi}_c \int_0^1 \left(\bar{T} \frac{\partial \bar{\Psi}}{\partial \bar{Y}} \right)_{\bar{x}=0} d\bar{y} \quad (C.10)$$

Dimensionless Heat Convected out of Bearing

$$Q_e = \int_0^h \rho C_p u_e T_e dy \quad (C.11)$$

$$Q_e = (\rho C_p T_r U h_o) \bar{\Psi}_c \frac{\bar{h}}{\bar{h}} \int_0^1 \left(\bar{T} \frac{\partial \bar{\Psi}}{\partial \bar{Y}} \right)_{\bar{x}=1} d\bar{y}$$

$$\frac{Q_e}{[\rho C_p T_r U h_o]} = \bar{\Psi}_c \int_0^1 \left(\bar{T} \frac{\partial \bar{\Psi}}{\partial \bar{Y}} \right)_{\bar{x}=1} d\bar{y}$$

$$\bar{Q}_e = \bar{\Psi}_c \int_0^1 \left(\bar{T} \frac{\partial \bar{\Psi}}{\partial \bar{Y}} \right)_{\bar{x}=1} d\bar{y} \quad (C.12)$$

Dimensionless Heat Flux Across Pad

$$q_p = - \left[K \frac{dT}{dy} \right]_{y=h} \quad (C.13)$$

$$= - \frac{KT_r}{h_o} \frac{1}{\bar{h}} \left(\frac{d\bar{T}}{d\bar{y}} \right)_{\bar{y}=1}$$

$$\frac{q_p h_o}{KT_r} = - \frac{1}{\bar{h}} \left(\frac{d\bar{T}}{d\bar{y}} \right)_{\bar{y}=1}$$

$$\bar{q}_p = - \frac{1}{\bar{h}} \left(\frac{d\bar{T}}{d\bar{y}} \right)_{\bar{y}=1} \quad (C.14)$$

Dimensionless Heat Flux Across Slider

$$q_s = - K \left(\frac{dT}{dy} \right)_{y=0} \quad (C.15)$$

$$= \frac{KT_r}{h_o} \frac{1}{\bar{h}} \left(\frac{d\bar{T}}{d\bar{y}} \right)_{\bar{y}=0}$$

i.e. $\frac{q_s h_o}{KT_r} = \frac{1}{\bar{h}} \left(\frac{d\bar{T}}{d\bar{y}} \right)_{\bar{y}=0}$

$$\bar{q}_s = \frac{1}{\bar{h}} \left(\frac{d\bar{T}}{d\bar{y}} \right)_{\bar{y}=0} \quad (C.16)$$

Dimensionless Heat Conducted Through Pad

$$Q_p = \int_0^L q_p dx \quad (C.17)$$

$$= \frac{LKT_r}{h_o} \int_0^1 \bar{q}_p d\bar{x}$$

$$\frac{Q_p h_o}{LKT_r} = \int_0^1 \bar{q}_p d\bar{x}$$

$$\bar{Q}_p = \int_0^1 \bar{q}_p d\bar{x} \quad (C.18)$$

Dimensionless Heat Conducted Through Slider

$$Q_s = \int_0^L q_s dx \quad (C.19)$$

$$= \frac{LKT_r}{h_o} \int_0^1 \bar{q}_s d\bar{x}$$

$$\frac{Q_s h_o}{LKT_r} = \int_0^1 \bar{q}_s d\bar{x}$$

$$\bar{Q}_s = \int_0^1 \bar{q}_s d\bar{x} \quad (C.20)$$

Average Flow Temperature

$$T_b = \frac{\int_0^L \frac{\int_0^{h_o} u \rho T dy}{\int_0^{h_o} \rho u dy} dx}{\int_0^L dx} = \frac{\int_0^1 \frac{\rho U T_r h_o}{\rho U h_o} \frac{\bar{h}}{\bar{h}} \frac{\int_0^1 \bar{u} \bar{T} d\bar{y}}{\int_0^1 \bar{u} d\bar{y}} d\bar{x}}{\int_0^1 d\bar{x}}$$

$$T_b = T_r \int_0^1 \frac{\int_0^1 \bar{u} \bar{T} d\bar{y}}{\int_0^1 \bar{u} d\bar{y}} d\bar{x} \quad (C.21)$$

APPENDIX D
FIGURES FOR CHAPTER IV

$\bar{h}_r = 2.0$
 $T_s = 200^\circ F$
 $P_e = 20.0$

$T_p = 100^\circ F$
 $PE = 1.0$

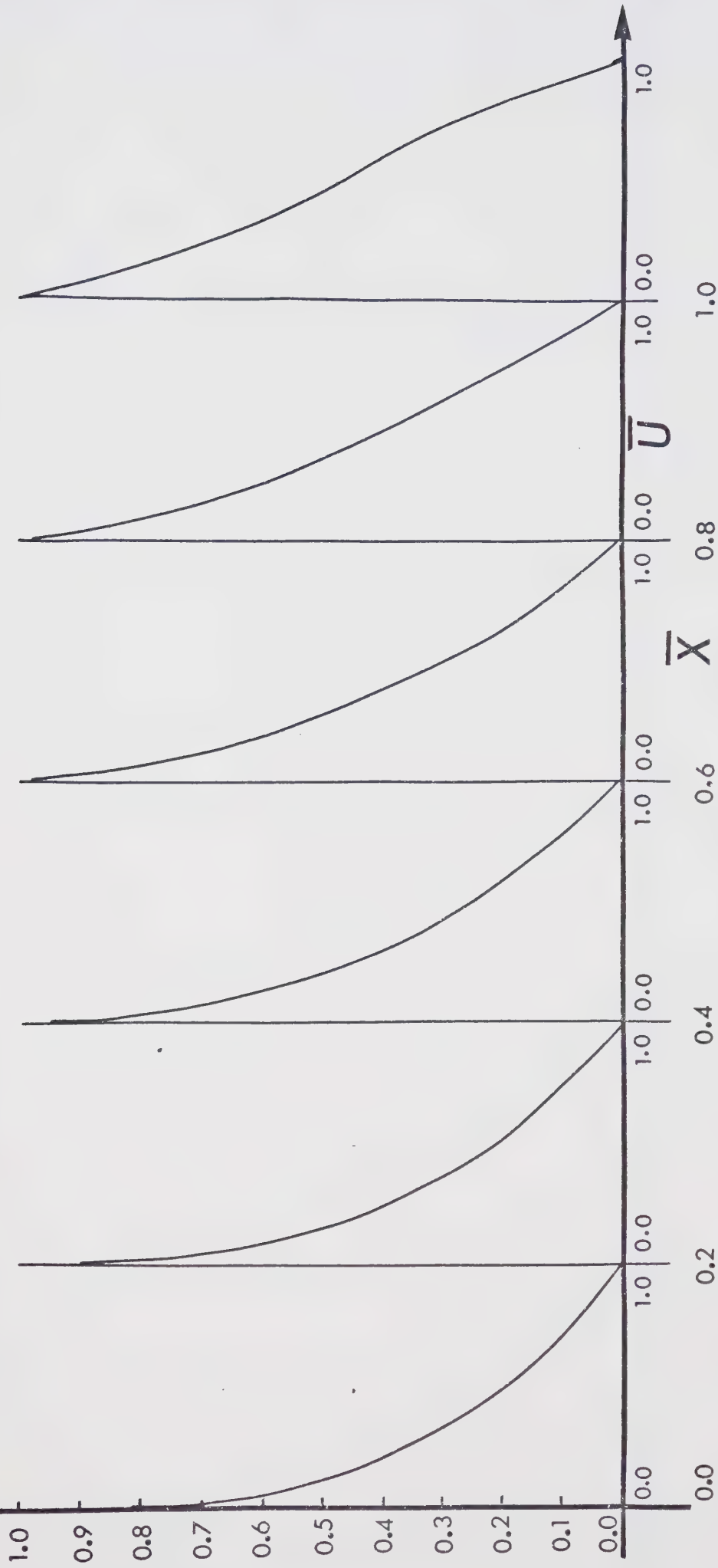


FIG.4 Velocity Distribution at various sections along
 length of bearing — No Inertia

$\bar{h}_r = 2.0$
 $T_s = 100^\circ\text{F}$
 $P_e = 20.0$

$T_p = 100^\circ\text{F}$
 $PE = 1.0$

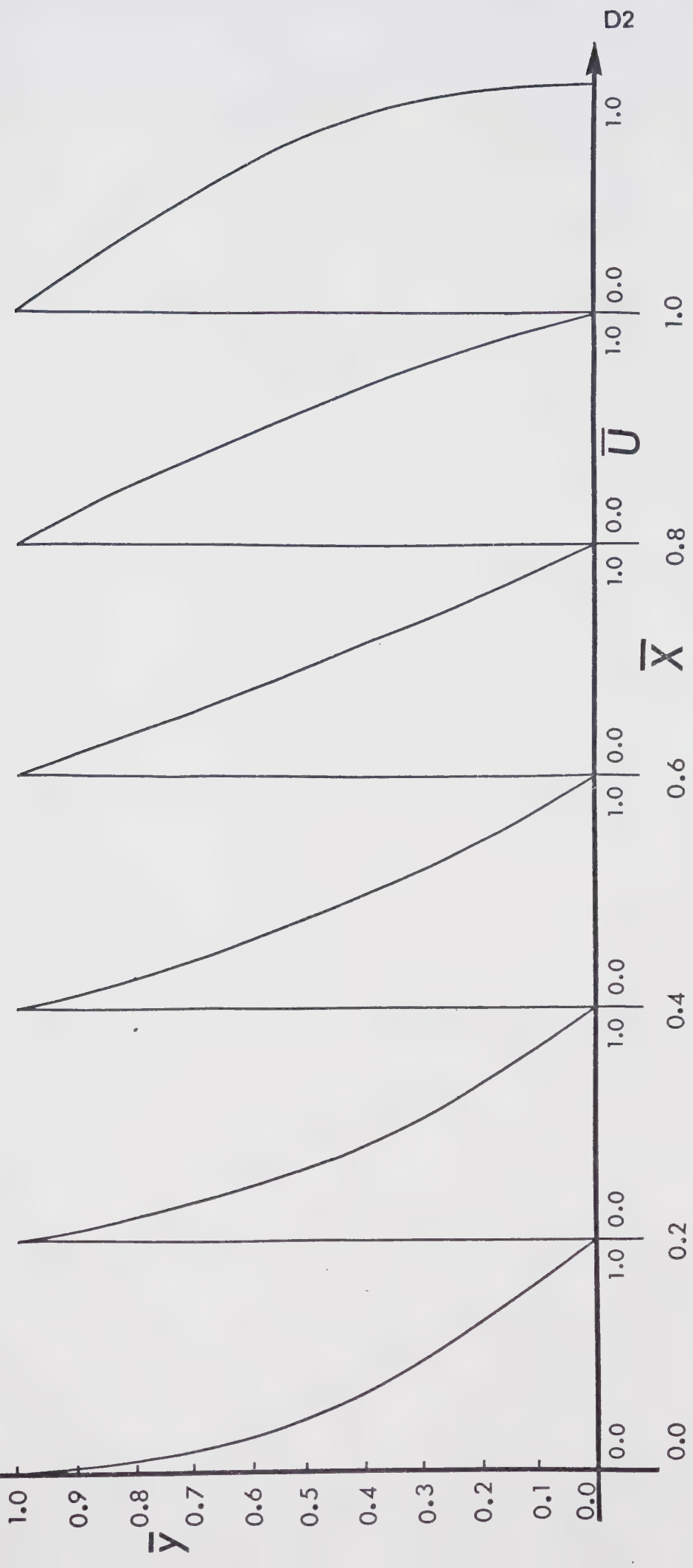


FIG.5 Velocity Distribution at various sections along length of bearing — No Inertia

$\bar{h}_r = 2.0$
 $T_s = 50^\circ F$
 $P_e = 20.0$

$T_p = 100^\circ F$
 $PE = 1.0$

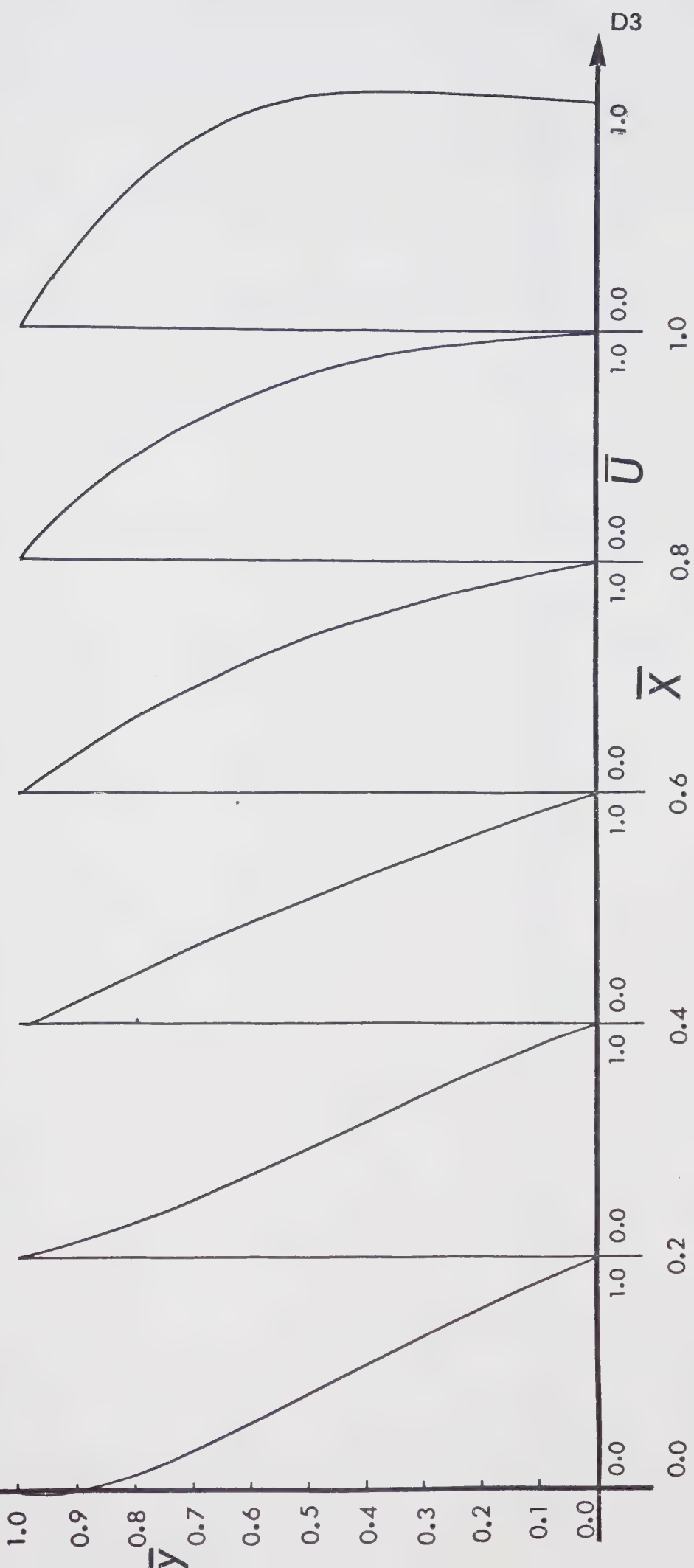


FIG.6 Velocity Distribution at various sections along length of bearing — No Inertia

$$\bar{h}_r = 2.0$$

$$P_e = 20.0$$

$$PE = 1.0$$

$$T_s = 200^\circ F$$

$$T_p = 100^\circ F$$

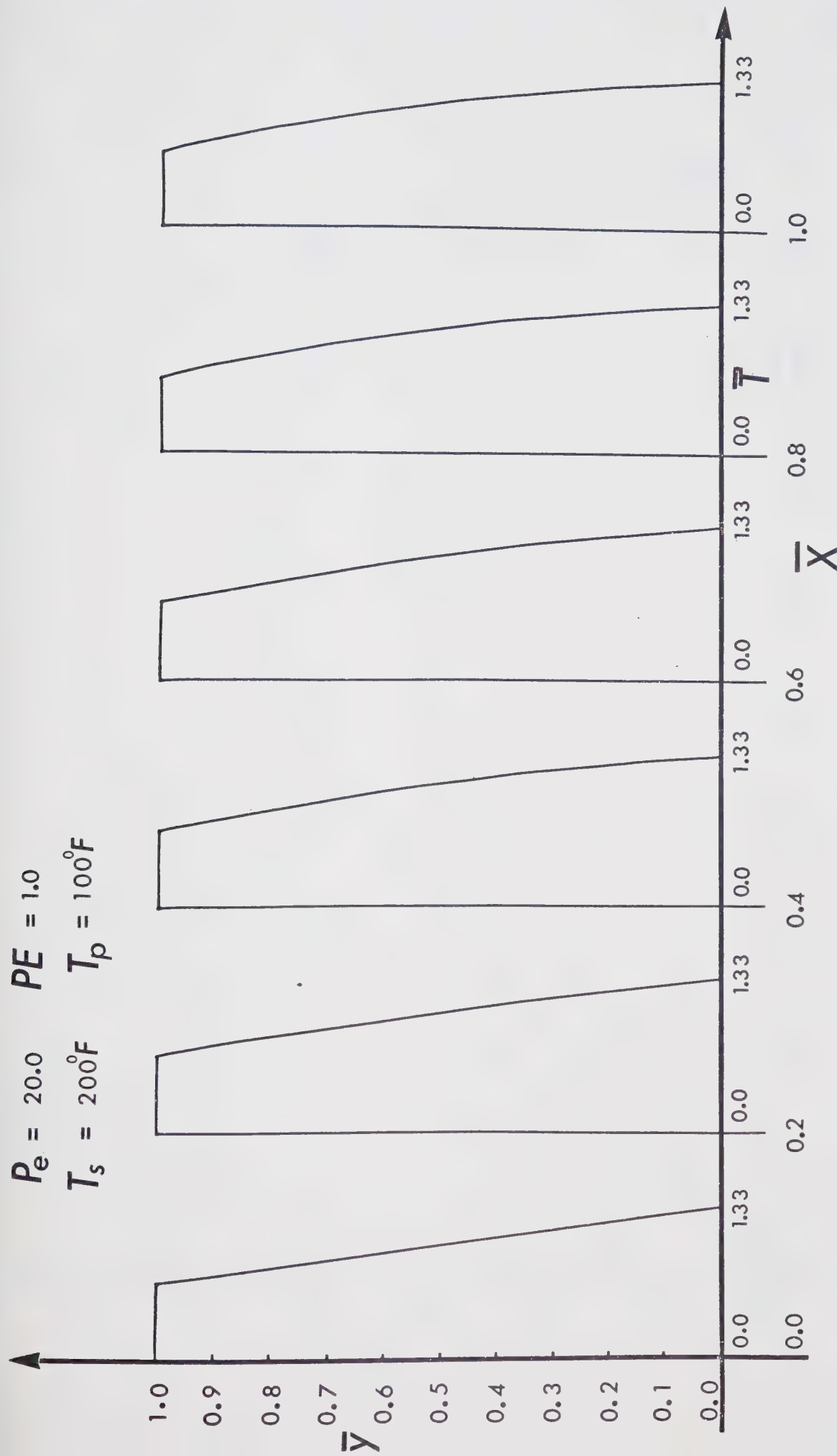


FIG.7 Temperature Distribution at various sections along length of bearing - No Inertia

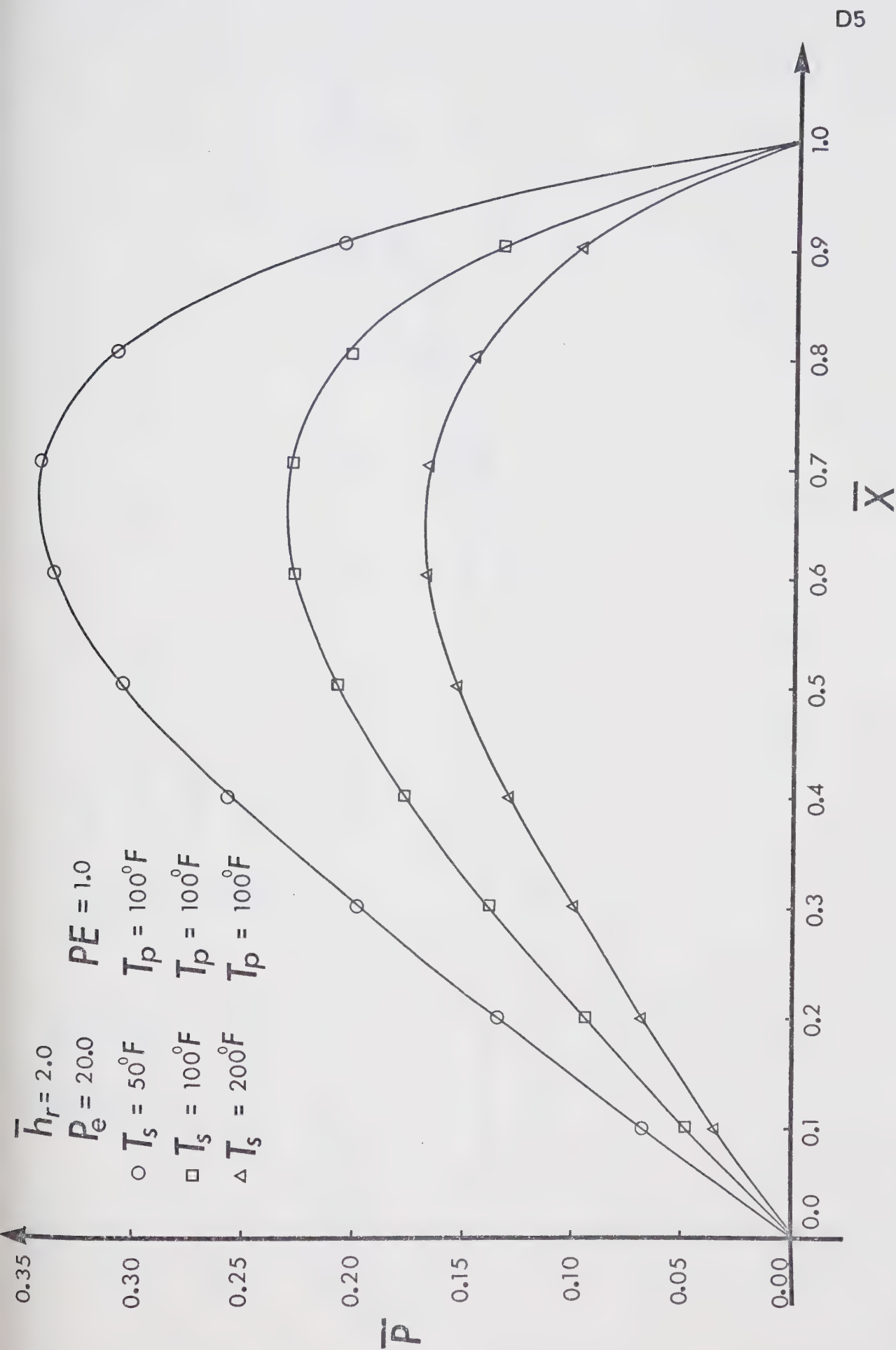


FIG.8 Pressure Distribution at various sections along length of bearing — No Inertia

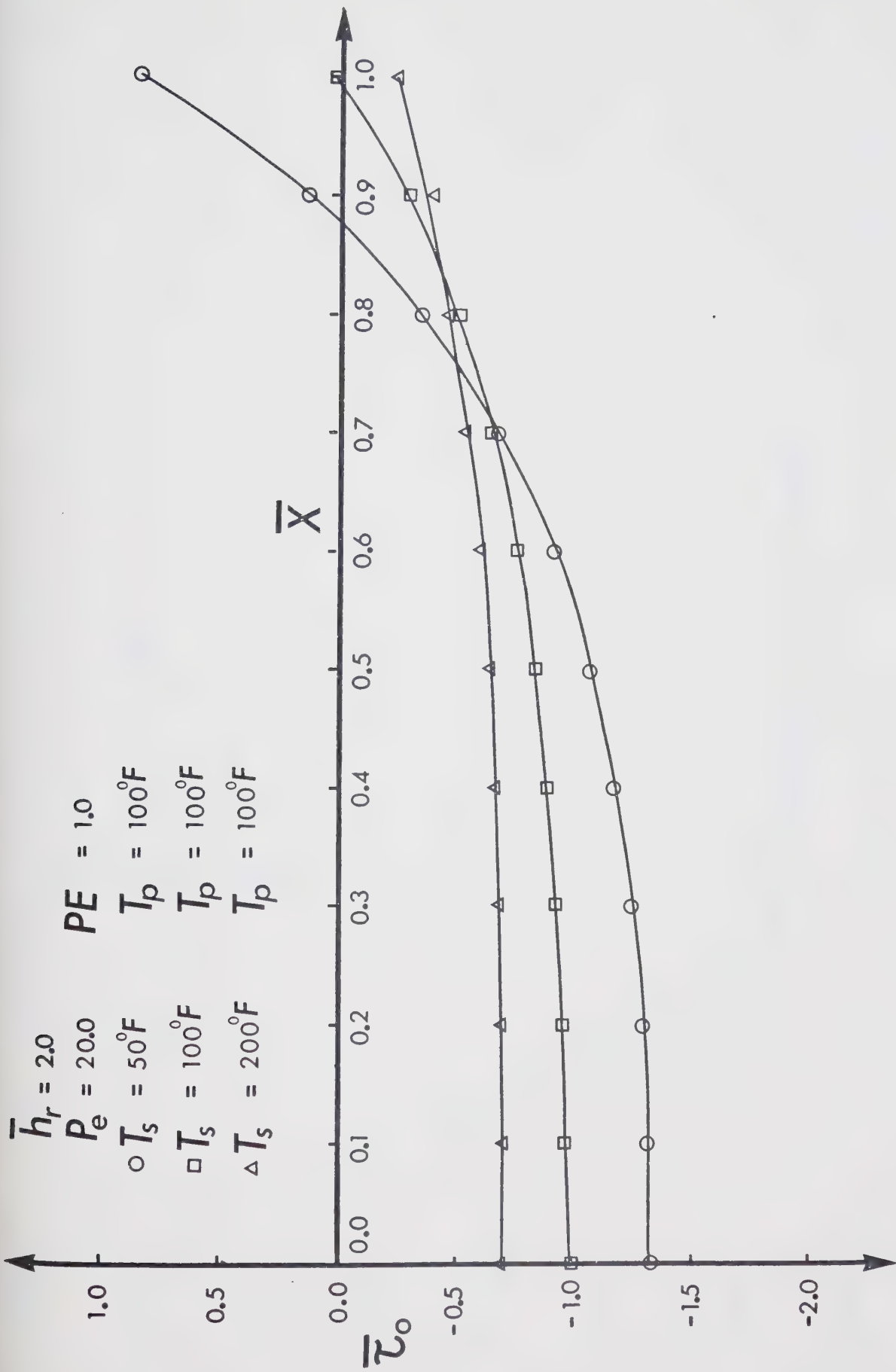


FIG.9 Shear Stress Distribution at various sections along length of slider — No Inertia

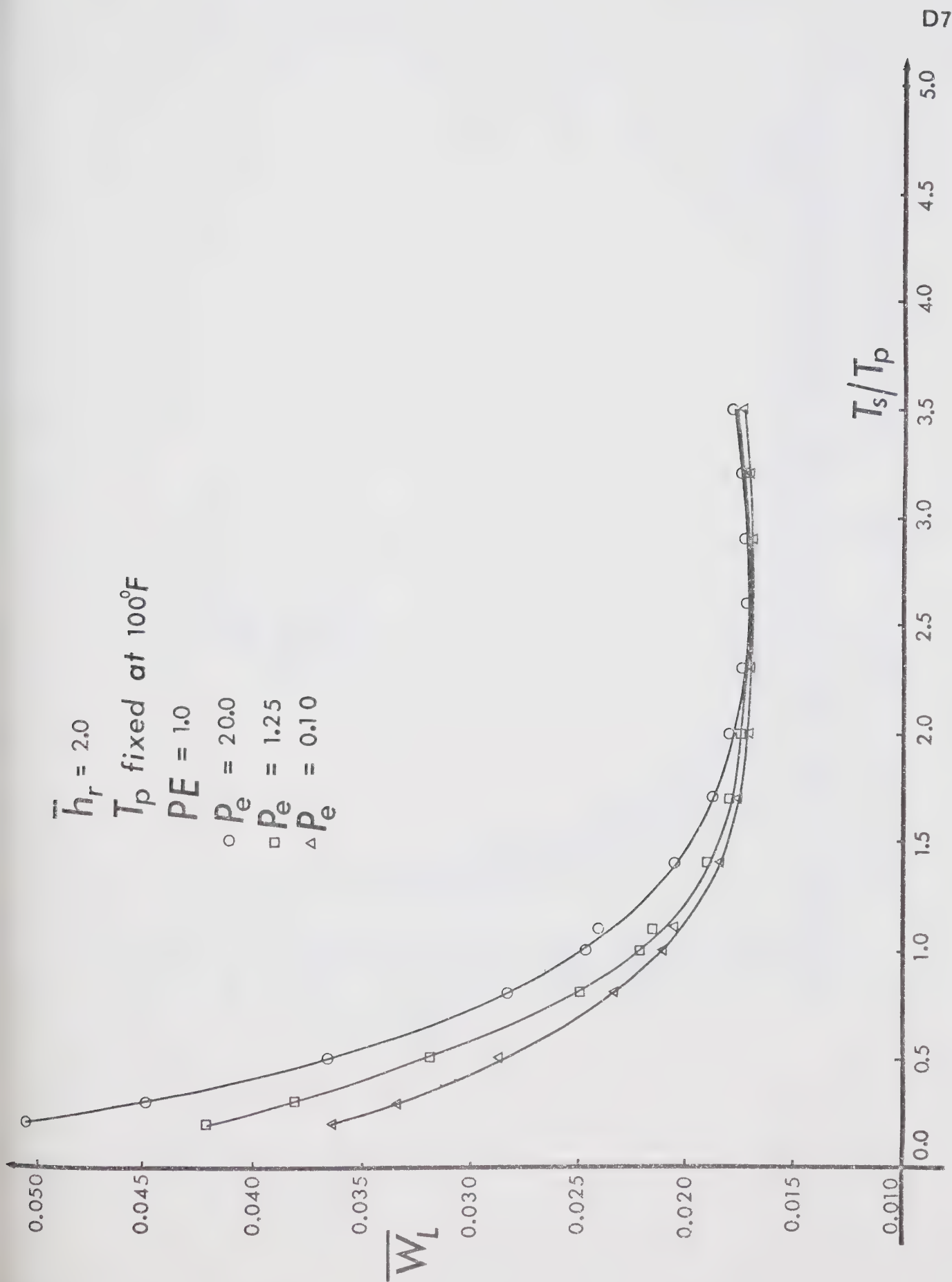


FIG. 7.0 Load Capacity versus T_s/T_p — Slider Cooled

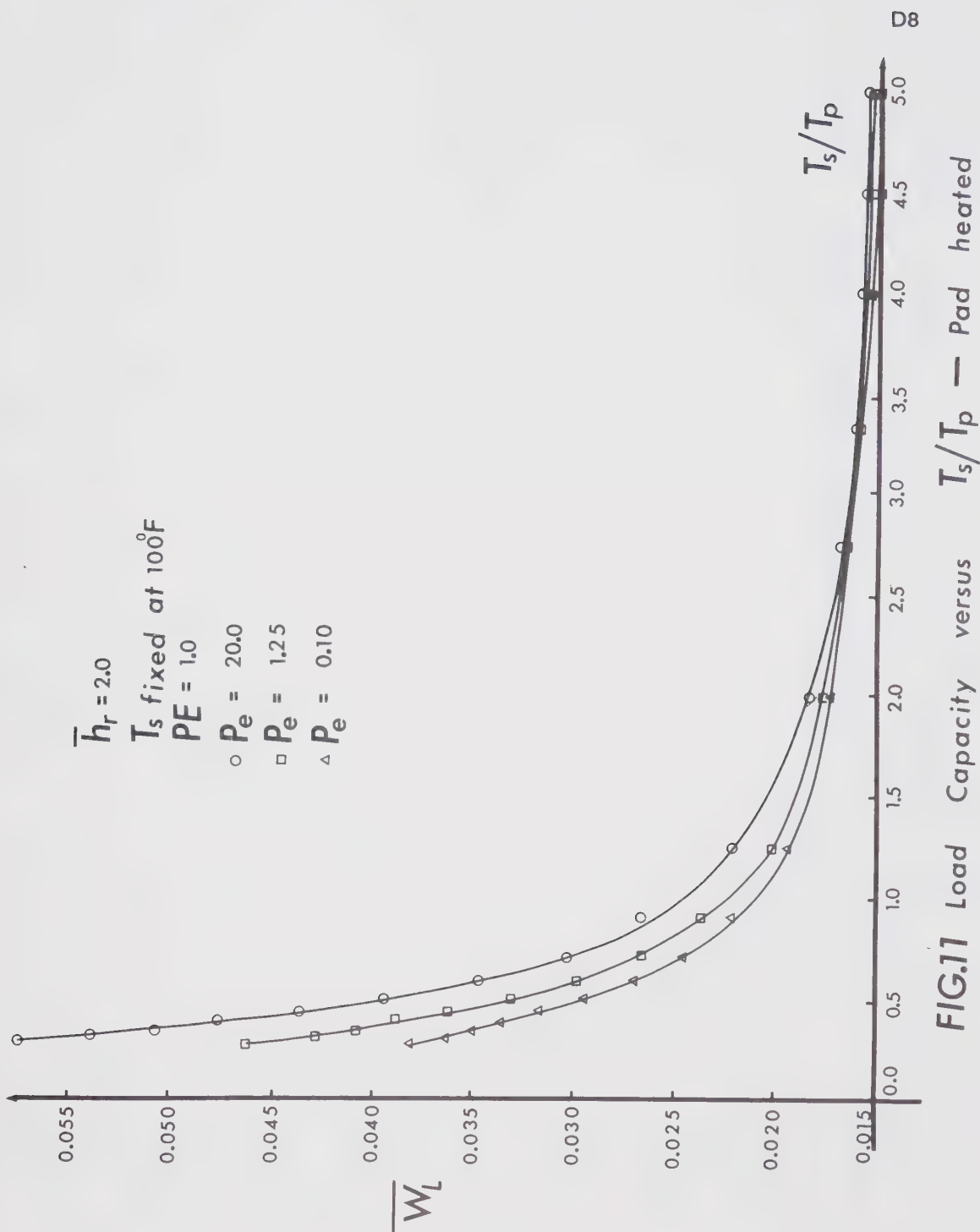
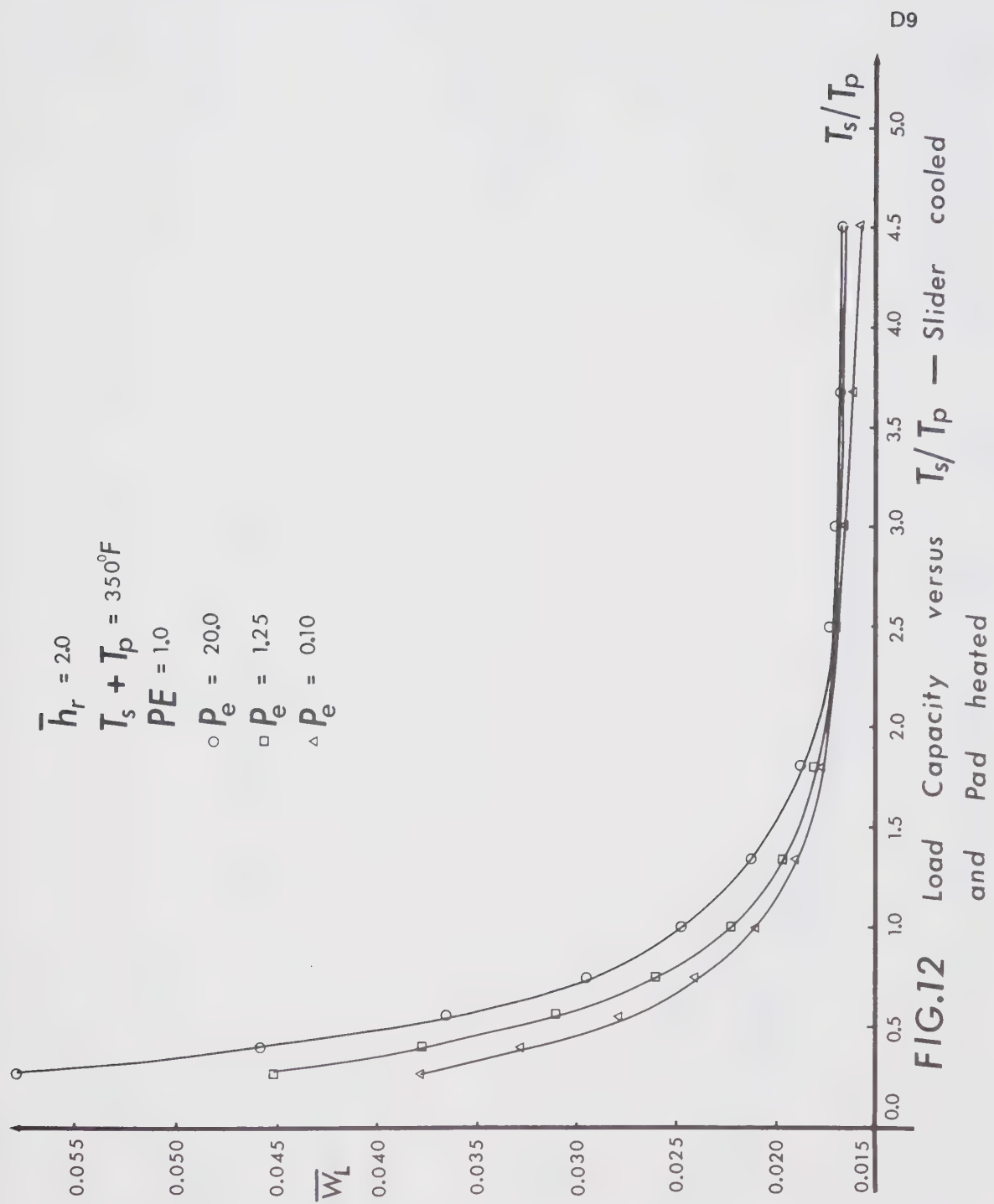


FIG.11 Load Capacity versus T_s/T_p — Pad heated



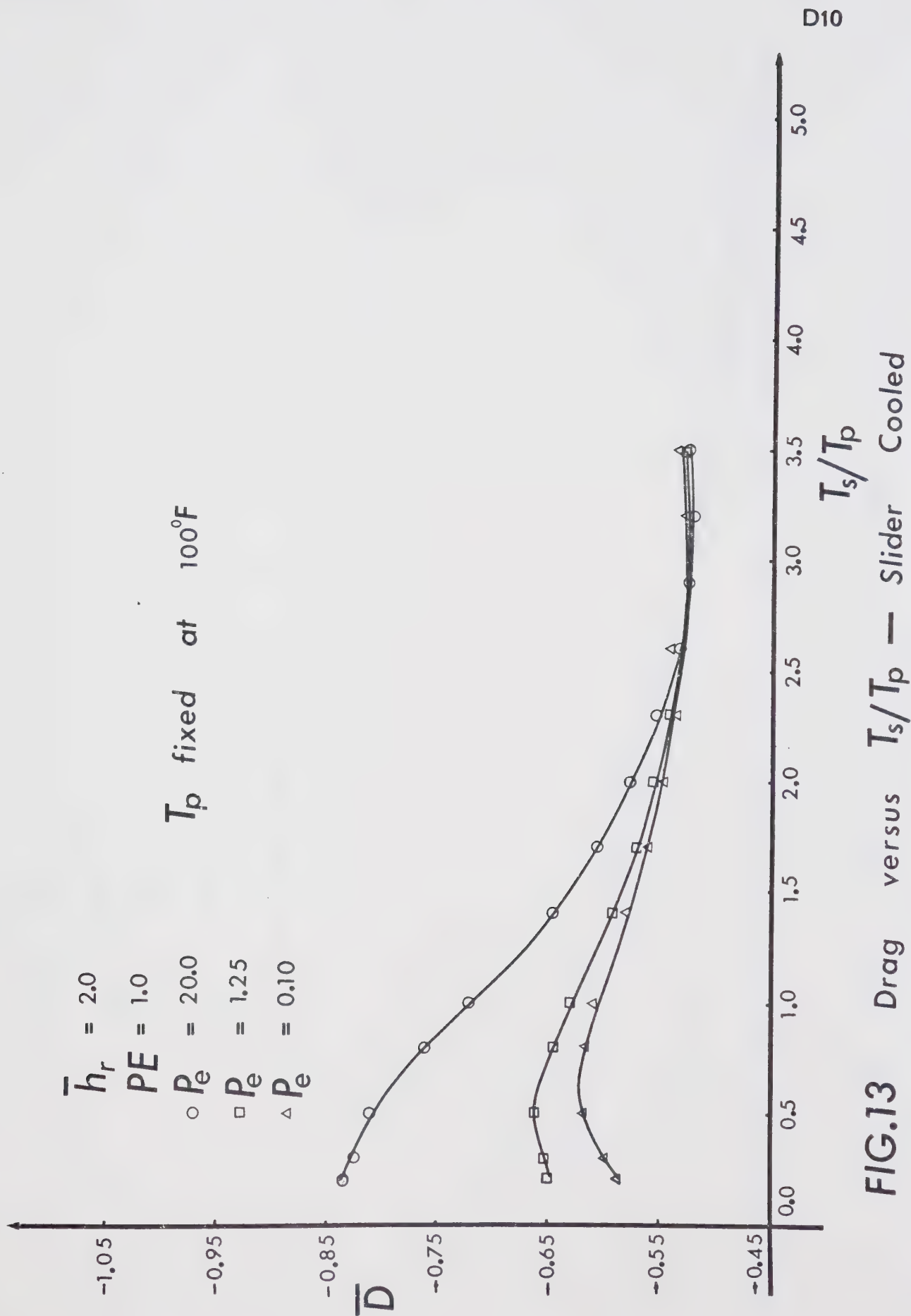


FIG.13 Drag versus T_s/T_p — Slider Cooled

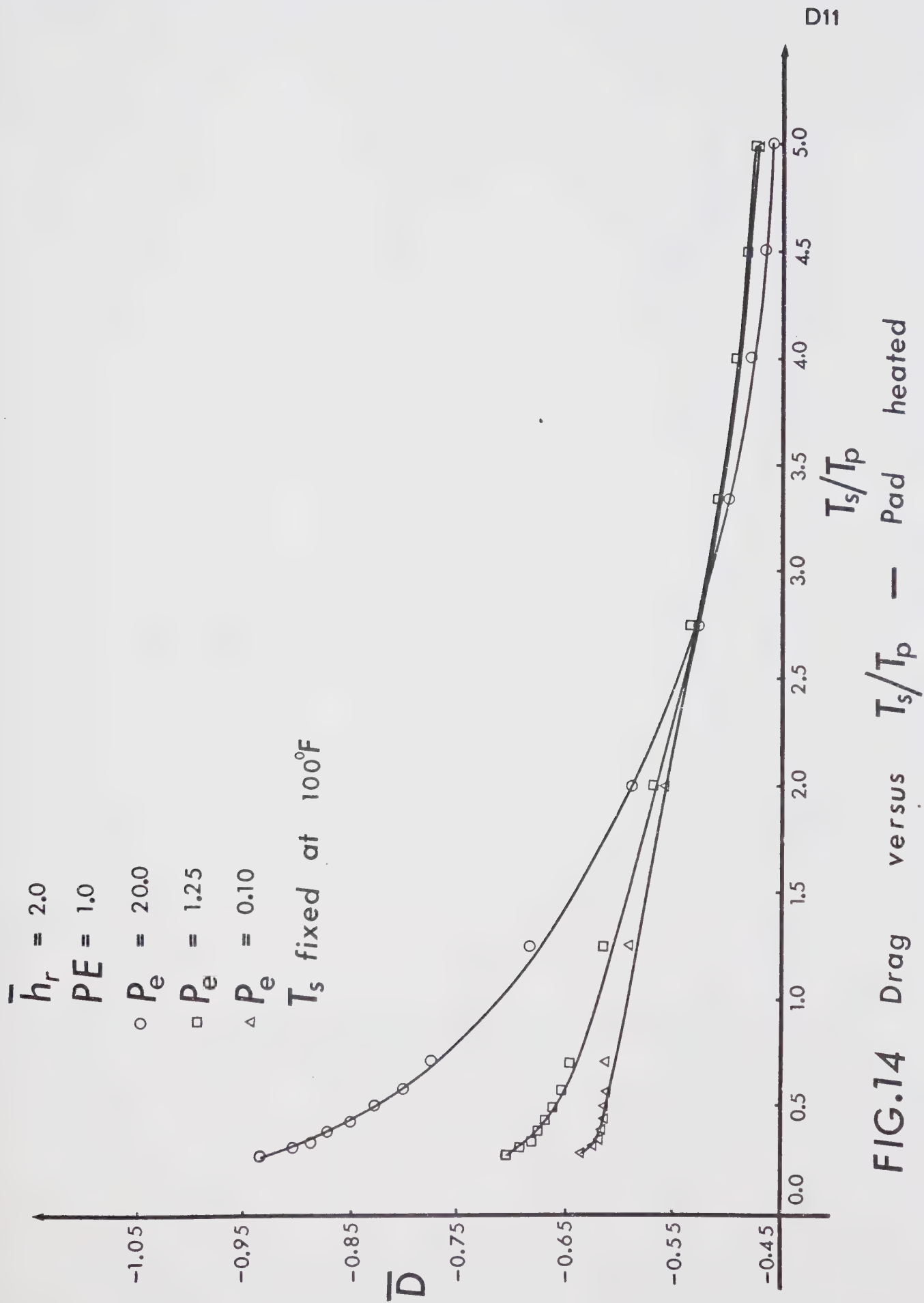


FIG.14 Drag versus T_s/T_p — Pad heated

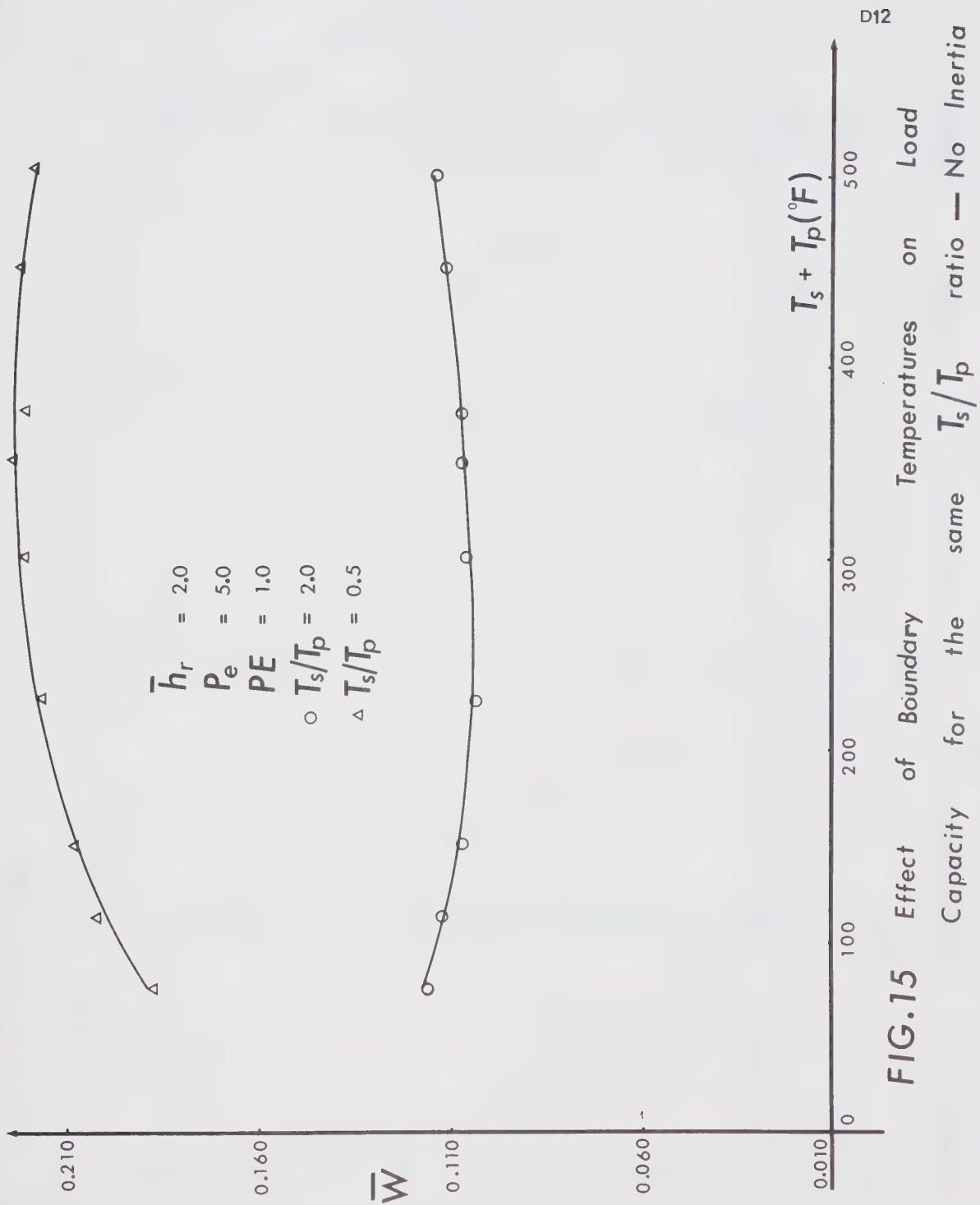


FIG. 15 Effect of Boundary Capacity for the same T_s/T_p ratio — No Inertia

$$\begin{aligned}\bar{h}_r &= 2.0 & R_e^* &= 0.5 \\ T_s &= 200^\circ\text{F} & T_p &= 100^\circ\text{F} \\ P &= 59.64 & PE &= 0.5357\end{aligned}$$

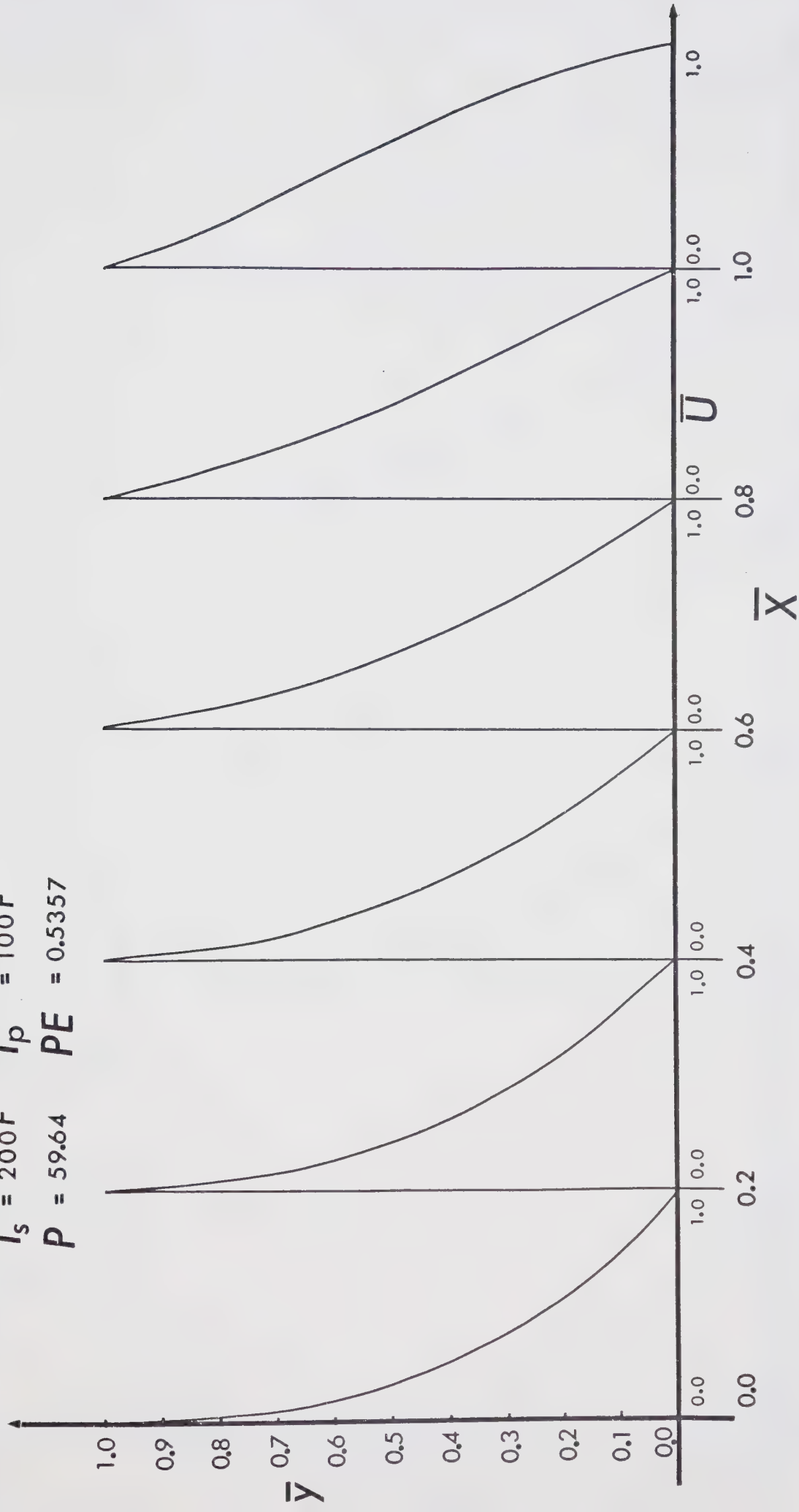


FIG.16 Velocity Distribution at various sections along length of bearing — No Inertia

$\bar{h}_r = 2.0$
 $T_s = 200^\circ\text{F}$
 $P = 59.64$

$R_e^* = 0.5$

$T_p = 100^\circ\text{F}$

$PE = 0.5357$

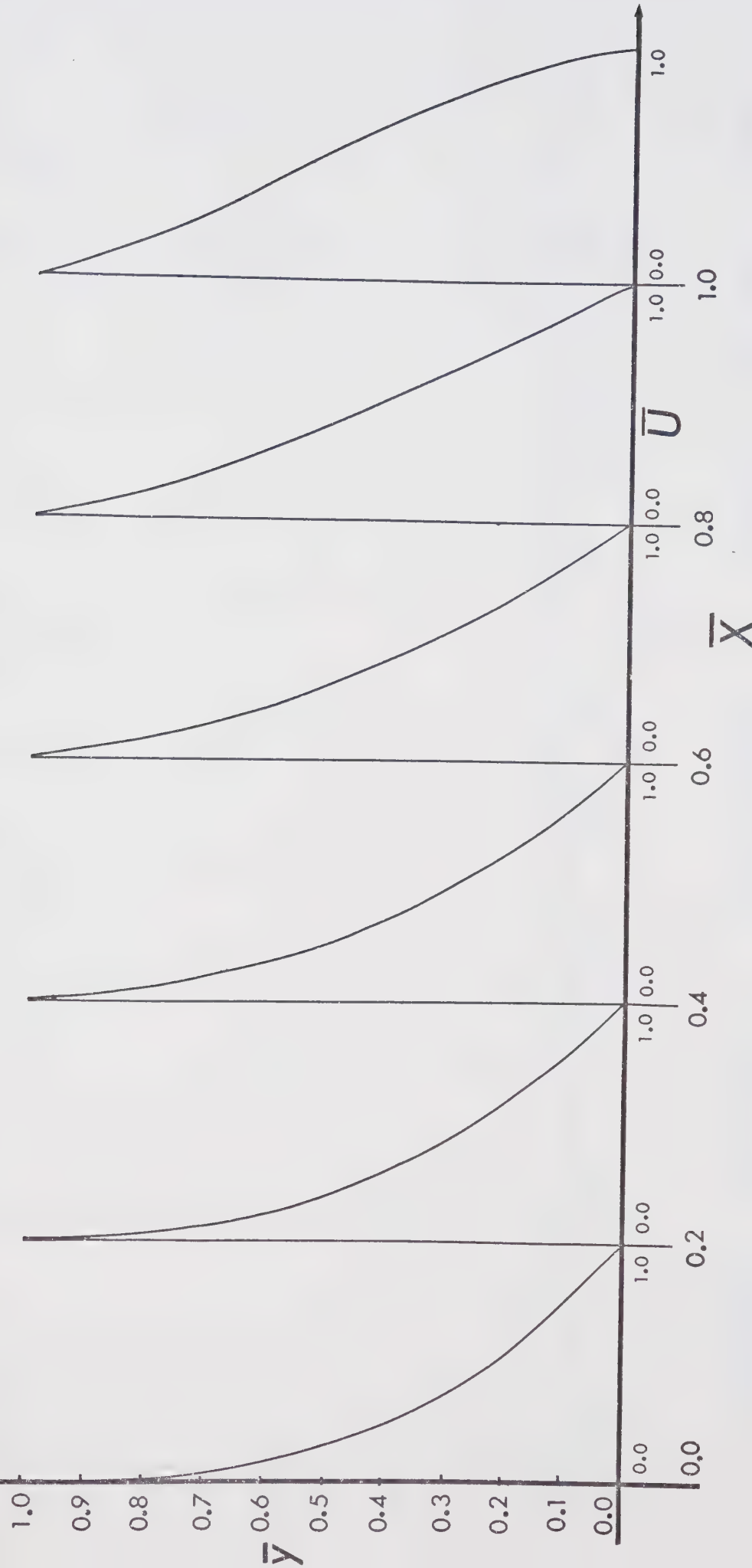


FIG.17 Velocity Distribution at various sections along length of bearing — Inertia Included

$\bar{h}_r = 2.0$
 $P = 59.64$
 $T_s = 200^\circ\text{F}$

$R_e^* = 0.5$
 $PE = 0.5357$
 $T_p = 100^\circ\text{F}$

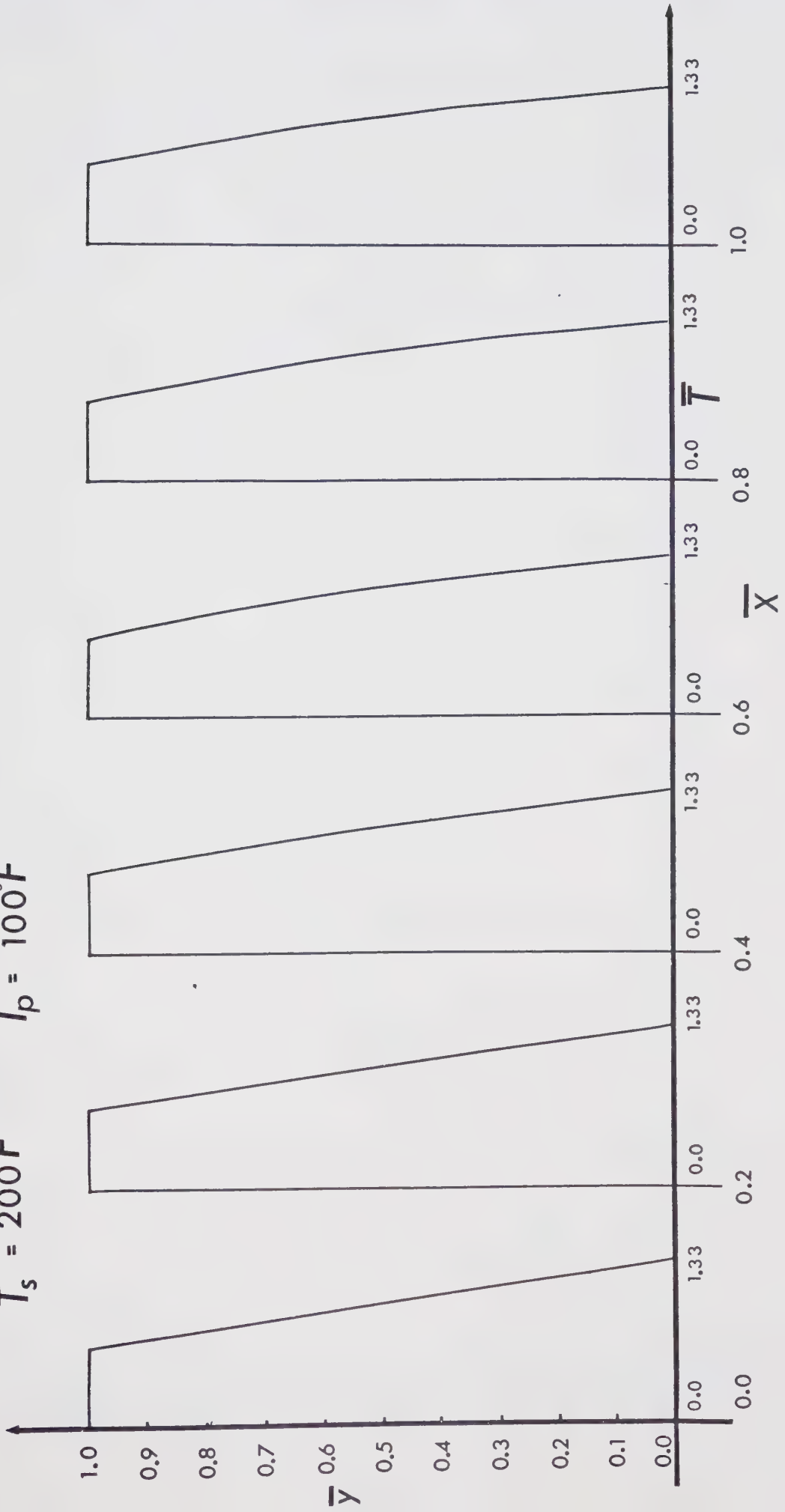


FIG.18 Temperature Distribution at various sections along length of bearing — No Inertia

$\bar{h}_r = 2.0$
 $P = 59.64$
 $T_s = 200^\circ\text{F}$

$R_e^* = 0.5$
 $PE = 0.5357$
 $T_p = 100^\circ\text{F}$

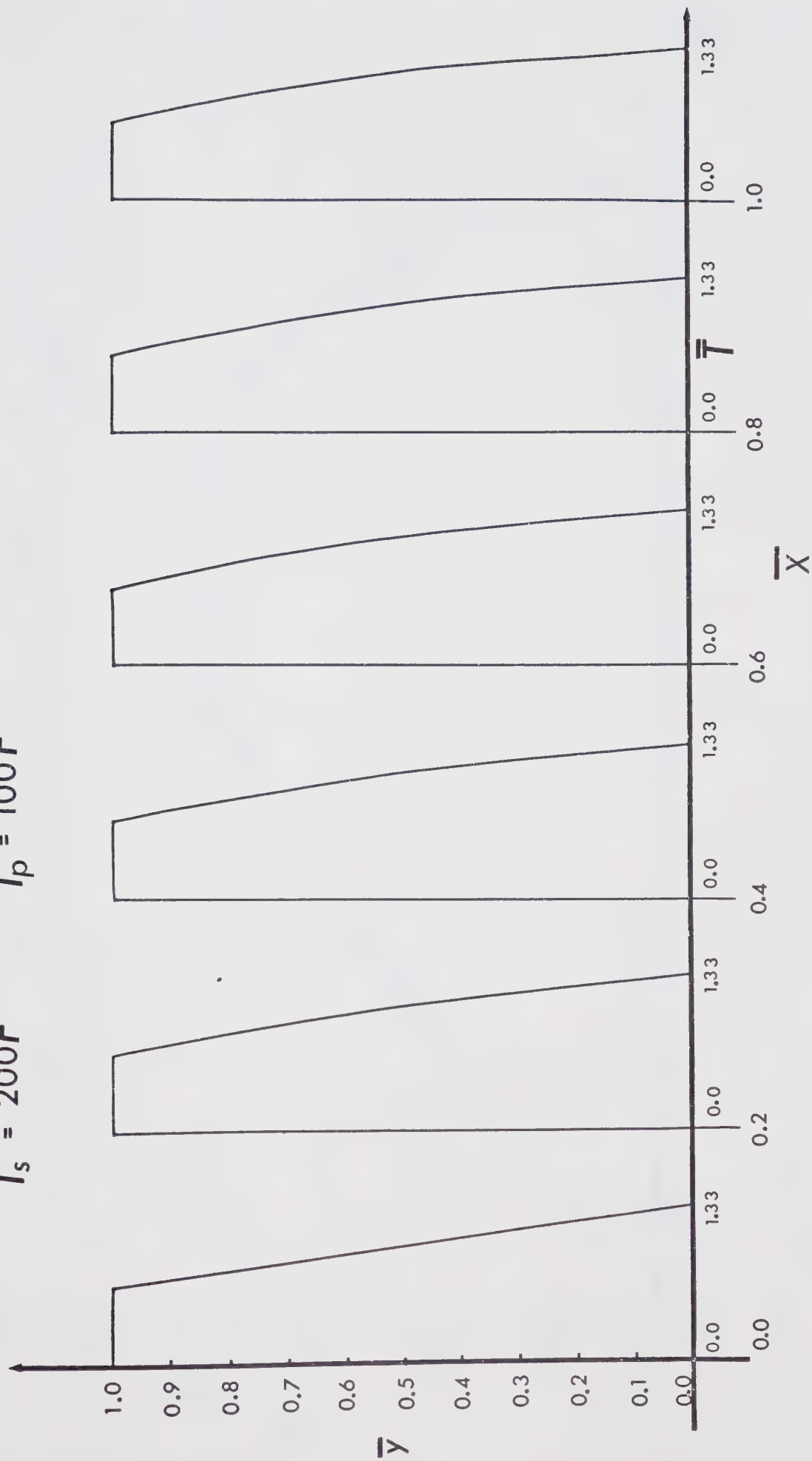
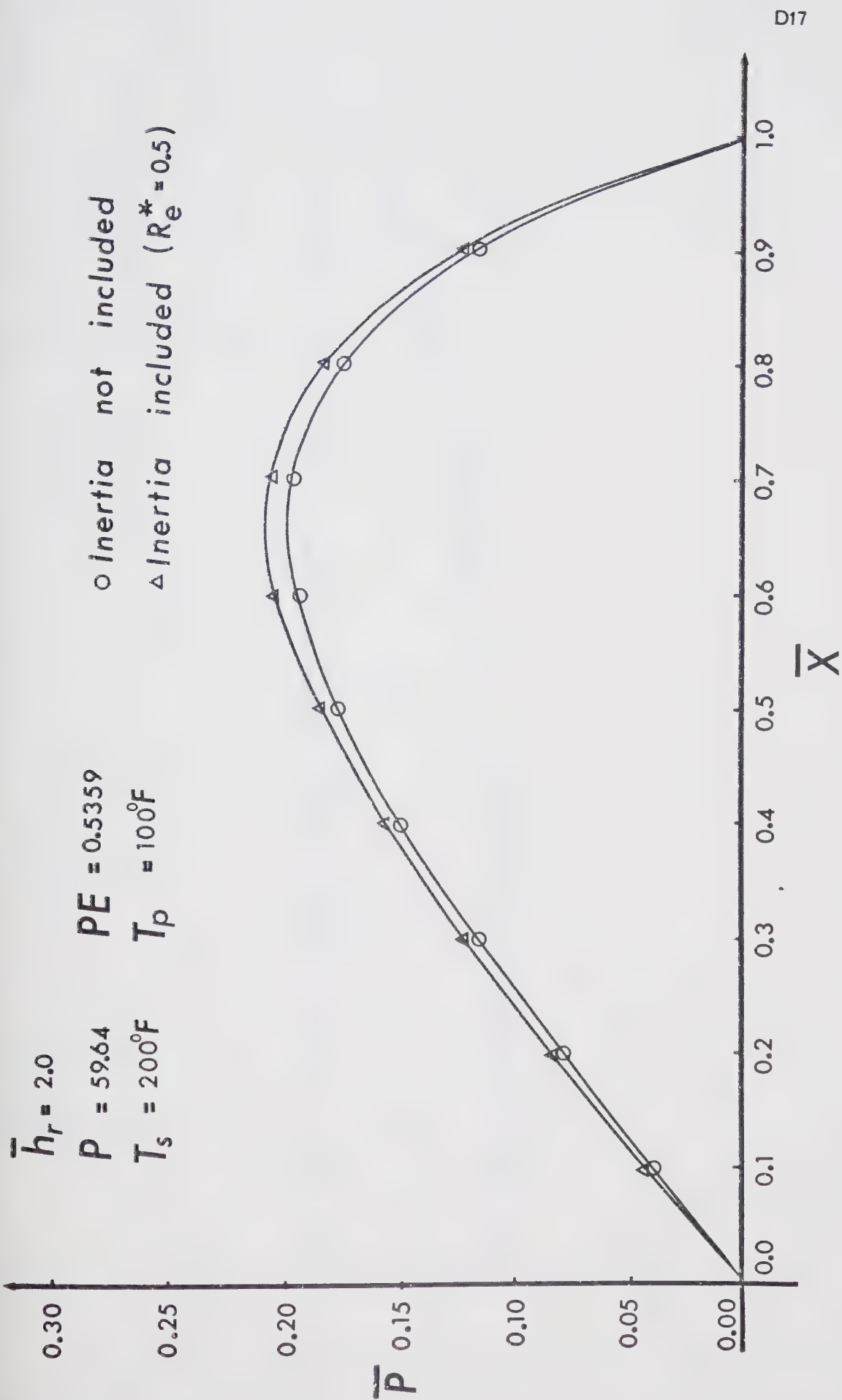


FIG.19 Temperature Distribution at various sections along length of bearing — Inertia included



D17

FIG. 20 Pressure Distribution at various sections along length of bearing

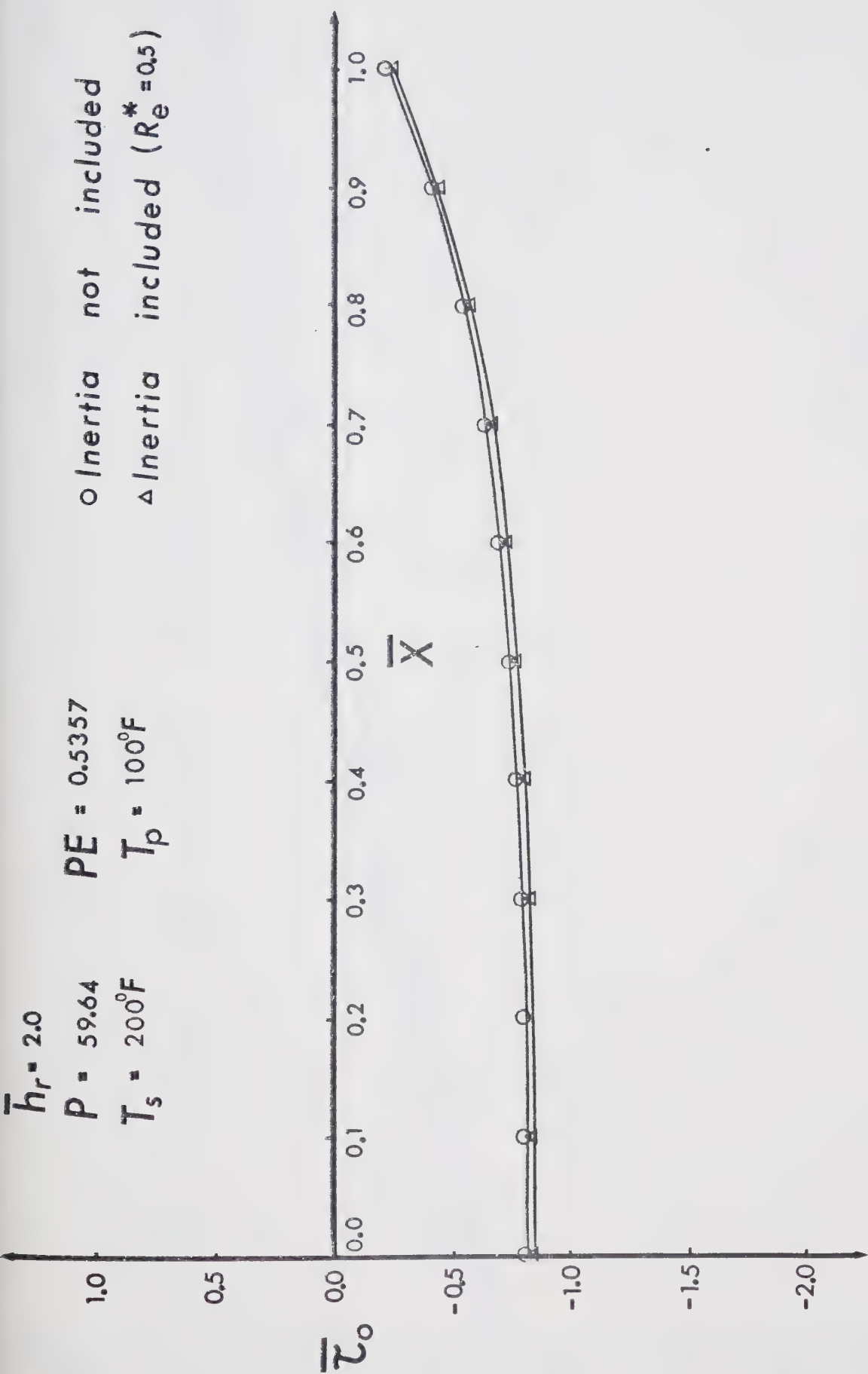


FIG.21 Shear Stress Distribution at various sections along length of slider

□ RODKIEWICZ & ANWAR

△ WOODHEAD & KETTLEBOROUGH

○ PRESENT WORK

All solutions for constant viscosity

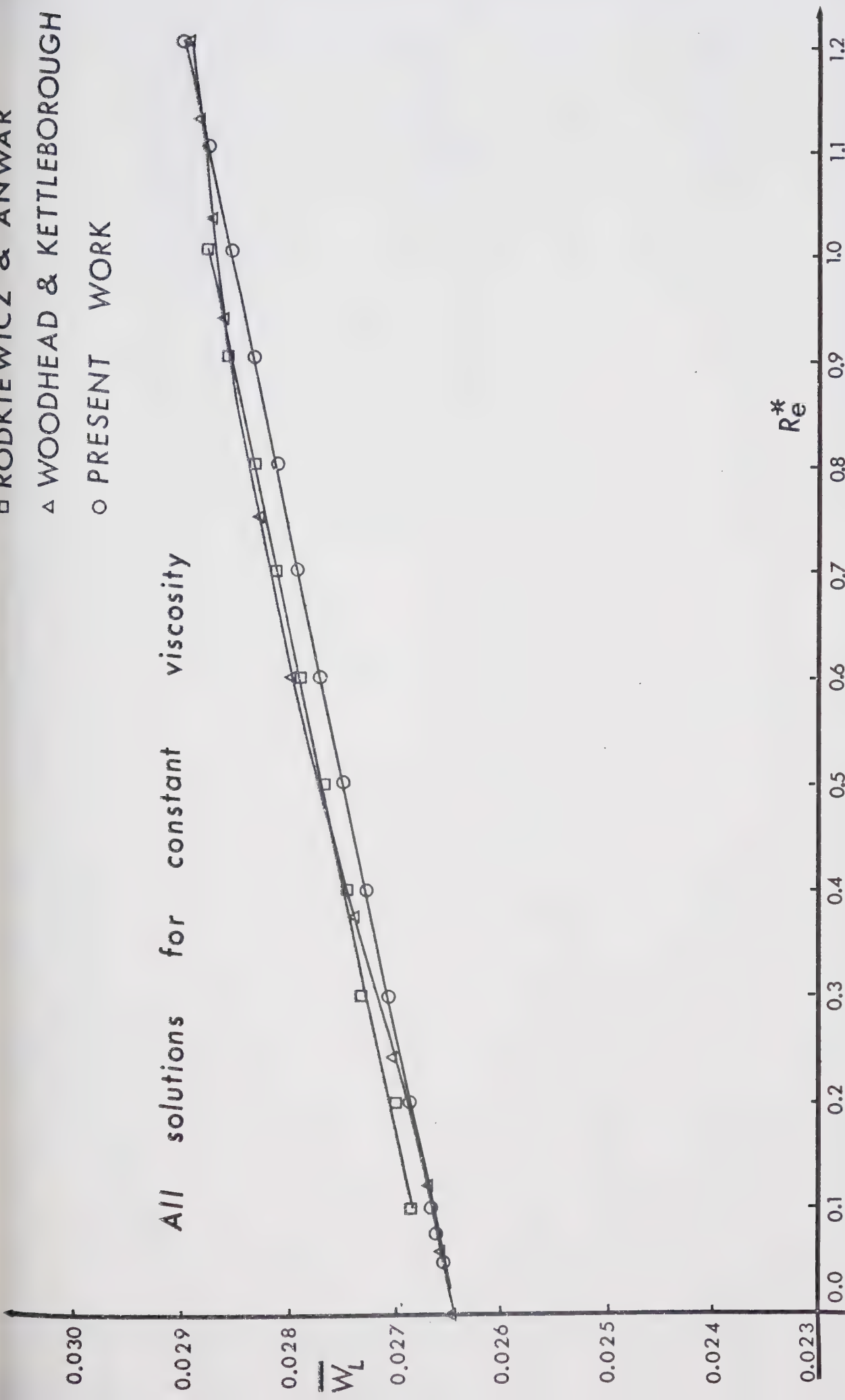


FIG.22

Plot of Load Capacity versus Reynolds No. —
Comparison with previous works

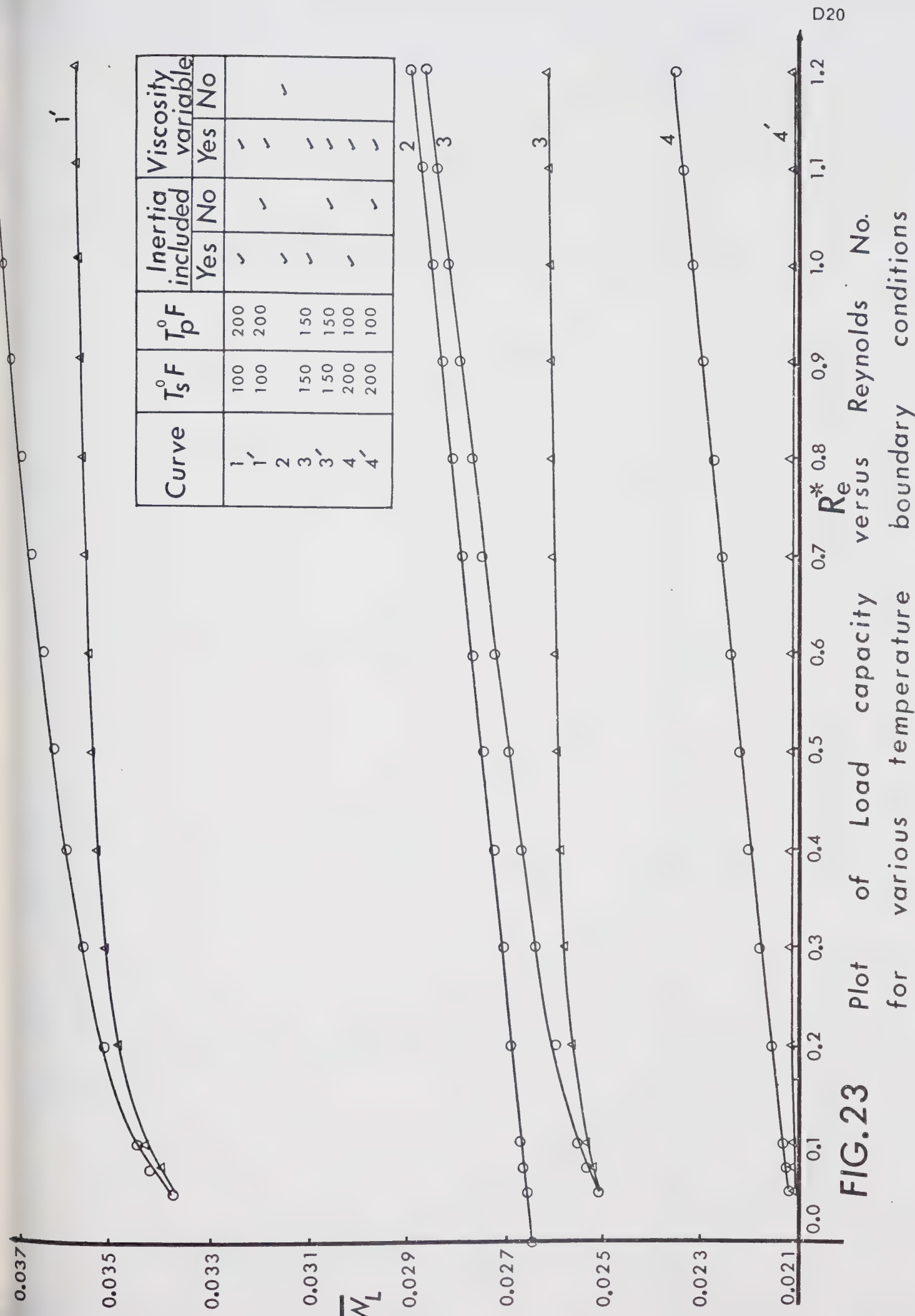


FIG. 23 Plot of Load capacity versus Re^* for various temperature boundary conditions

$$P_e = 200 \quad P_e = 1.0$$

$$T_s = 200^\circ\text{F} \quad T_p = 100^\circ\text{F}$$

$$h_r = 1.75$$

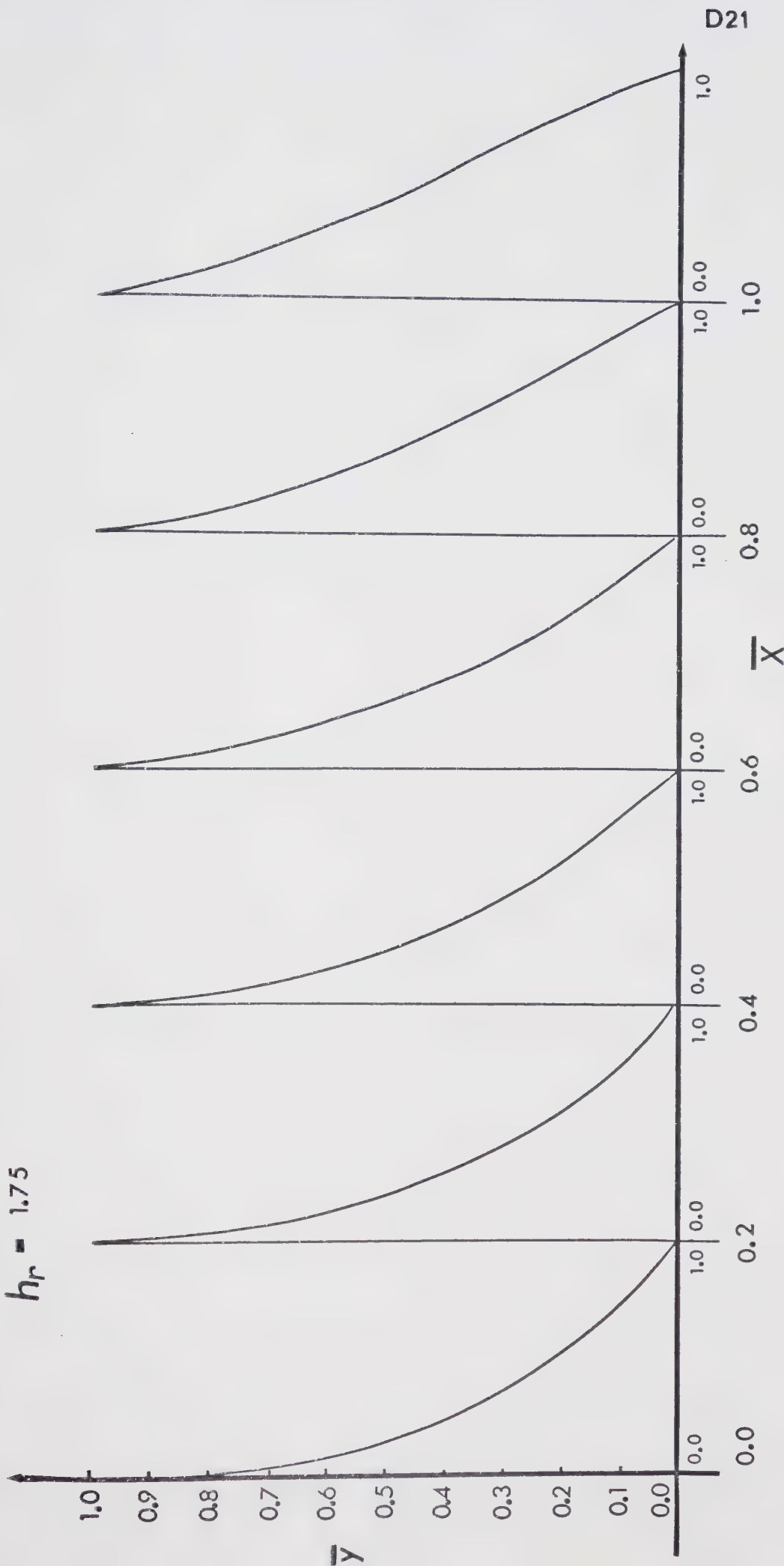


FIG.24 Velocity Distribution at various sections along length of bearing — No Inertia

$P_e = 20.0$
 $T_s = 200^\circ\text{F}$
 $h_r = 2.25$

$PE = 1.0$
 $T_p = 100^\circ\text{F}$

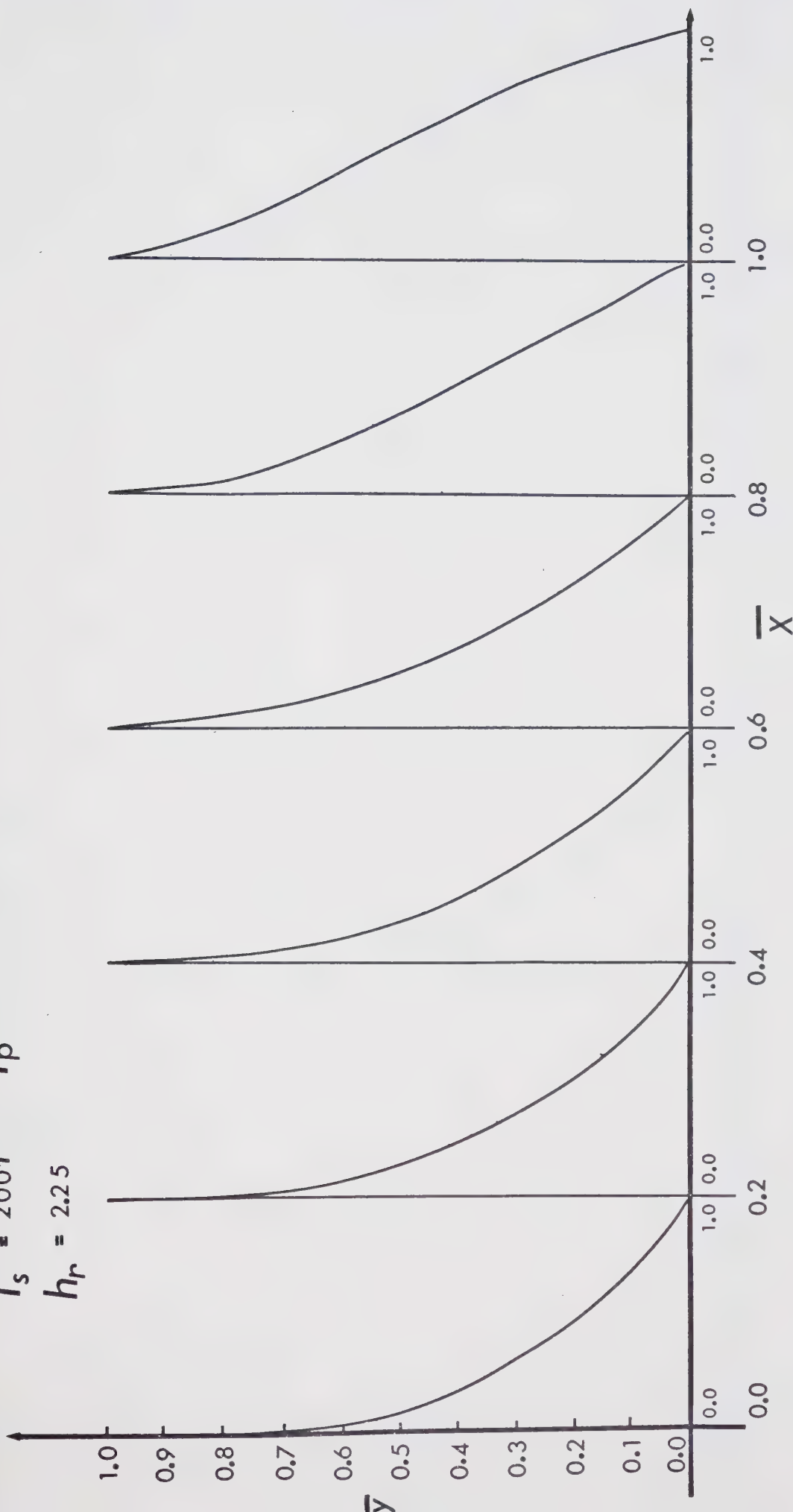


FIG.25 Velocity Distribution at various sections along
 length of bearing — No Inertia

$$\begin{aligned} \bar{h}_r &= 2.75 & PE &= 1.0 \\ P_e &= 20.0 & T_p &= 100^\circ\text{F} \\ T_s &= 200^\circ\text{F} \end{aligned}$$

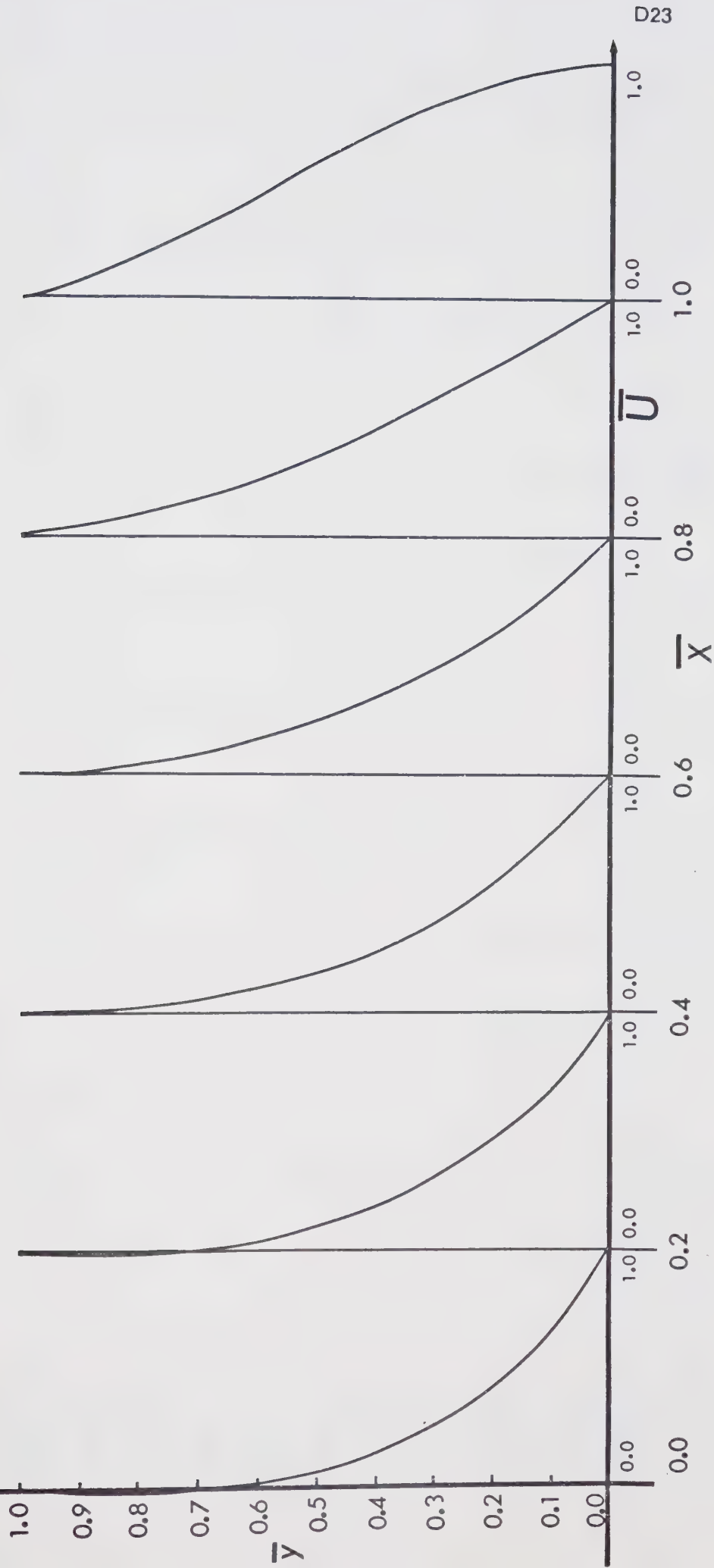


FIG.2.26 Velocity Distribution at various sections along length of bearing — No Inertia

$$P_e = 20.0 \quad PE = 1.0$$

$$T_s = 200^\circ F \quad T_p = 100^\circ F$$

$$\bar{h}_r = 1.75$$

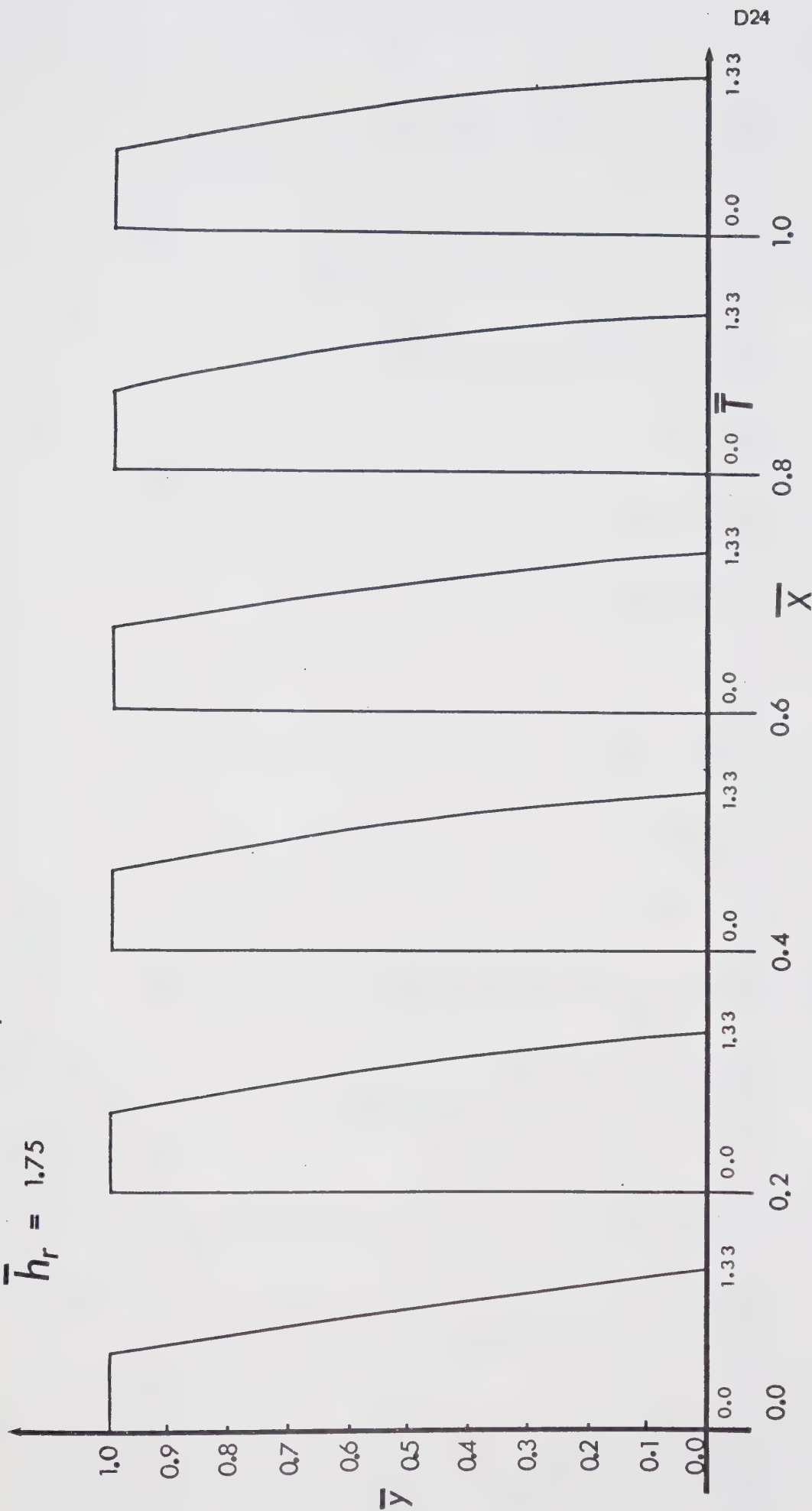
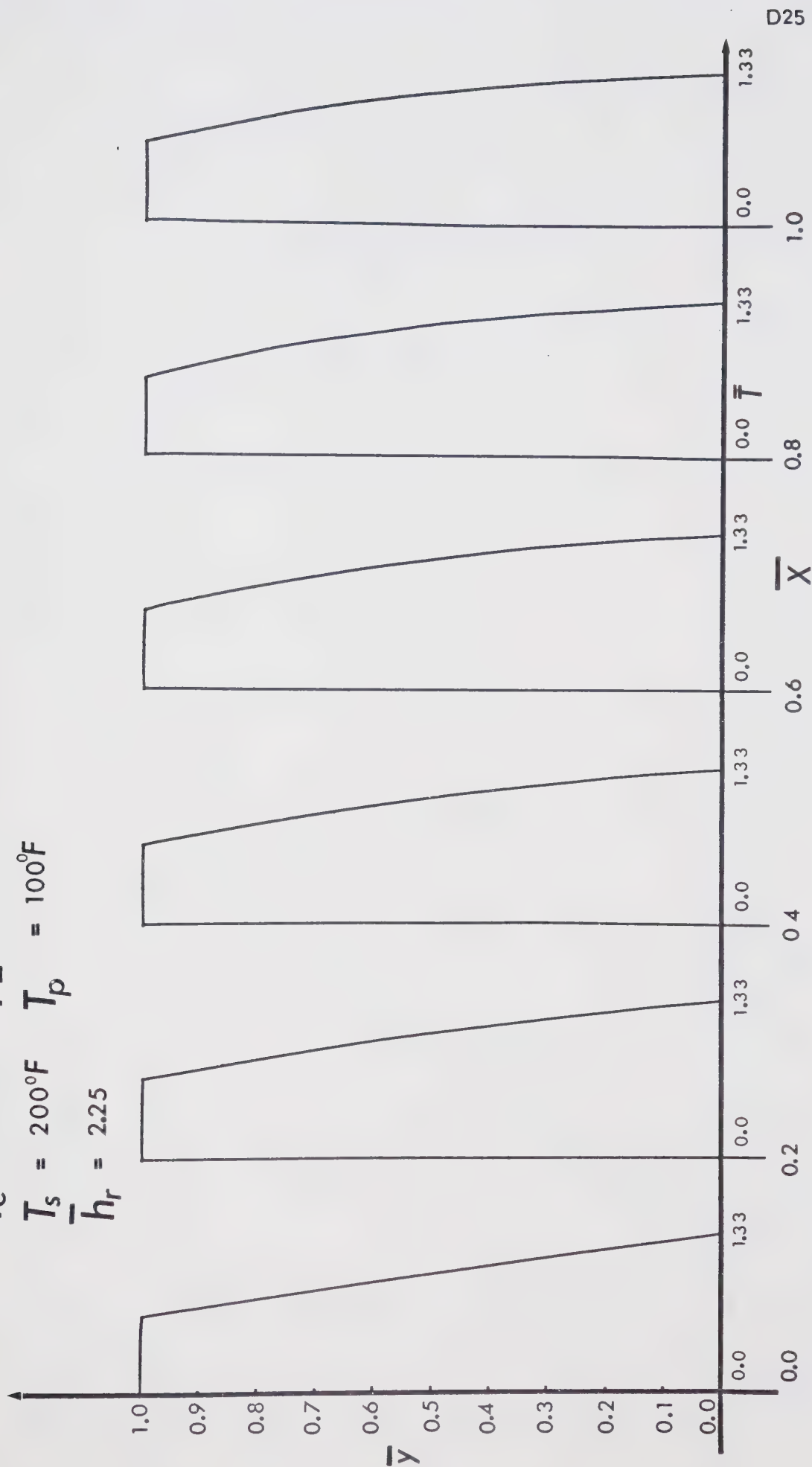


FIG.27 Temperature Distribution at various sections along length of bearing — No Inertia

$$P_e = 20.0 \quad PE = 1.0$$

$$T_s = 200^\circ F \quad T_p = 100^\circ F$$

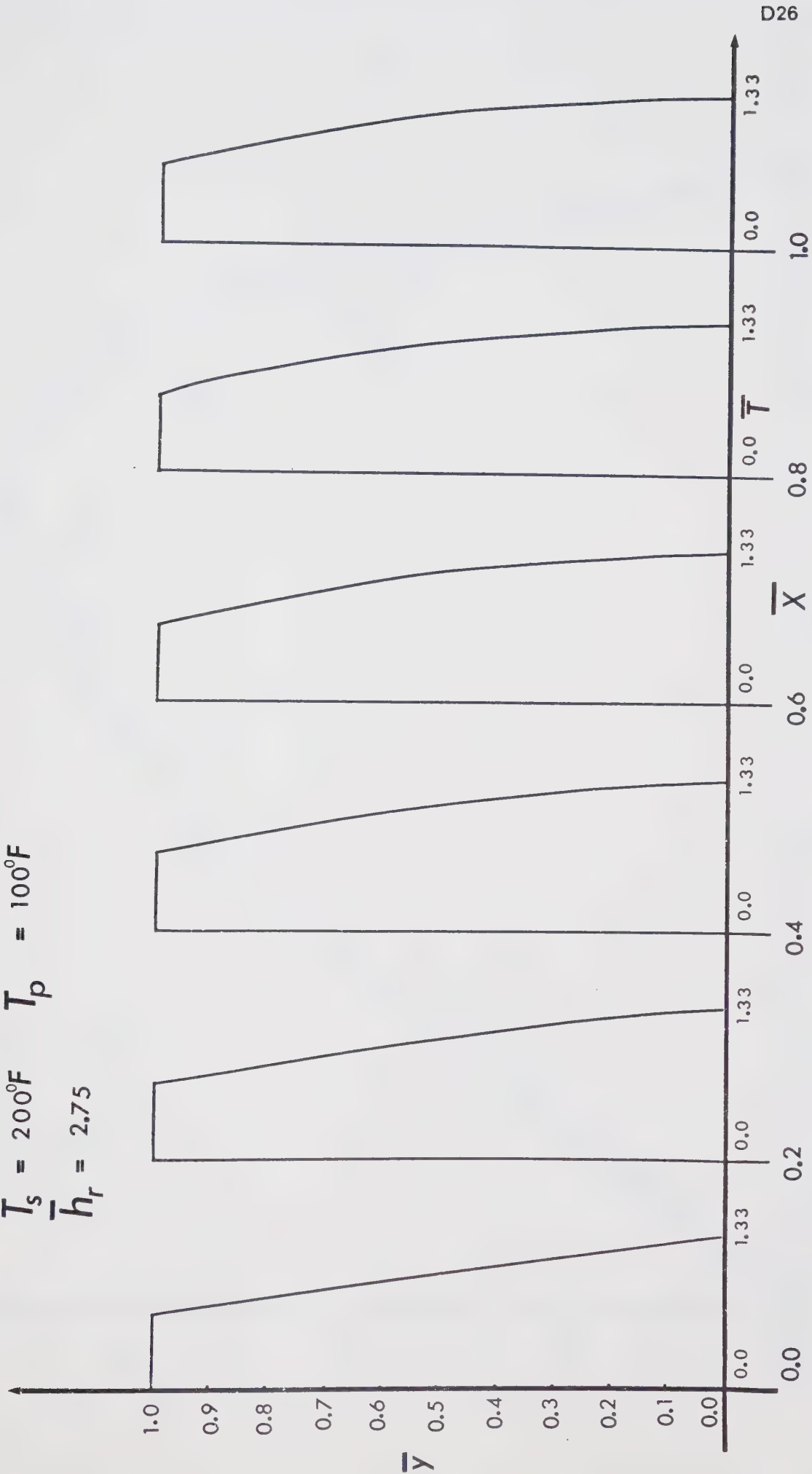
$$\bar{h}_r = 2.25$$



D25

FIG.28 Temperature of length of bearing — No Inertia Distribution at various sections along

$P_e = 20.0$ $PE = 1.0$
 $T_s = 200^\circ F$ $T_p = 100^\circ F$
 $\bar{h}_r = 2.75$



D26

FIG. 29 Temperature Distribution at various sections along length of bearing — No Inertia

$P_e = 20.0$ $PE = 1.0$
 $T_s = 200^\circ F$ $T_p = 100^\circ F$

$\bar{h}_r = 1.75$
 $\square \bar{h}_r = 2.25$
 $\triangle \bar{h}_r = 2.75$

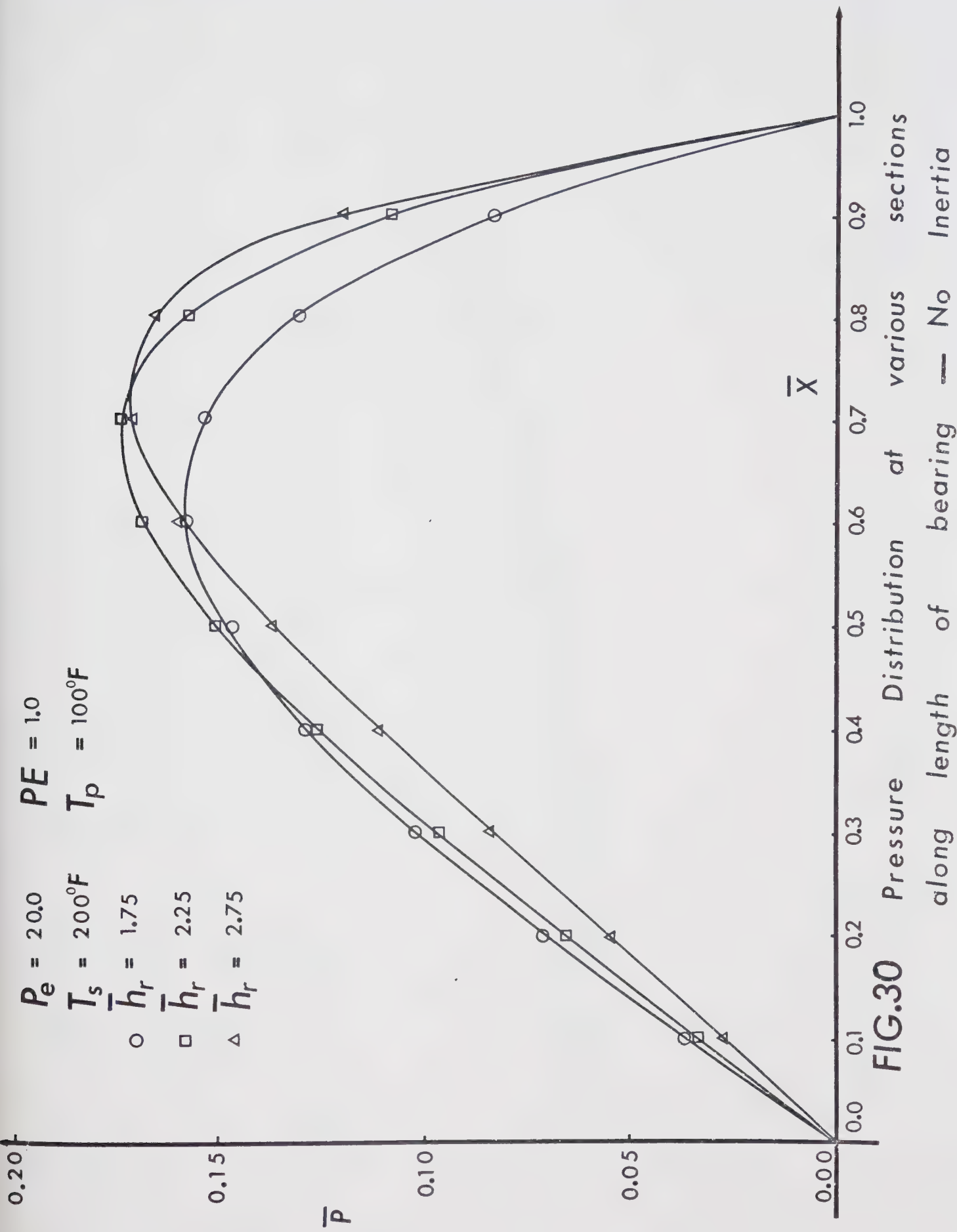


FIG.30

Pressure Distribution at various sections along length of bearing — No Inertia

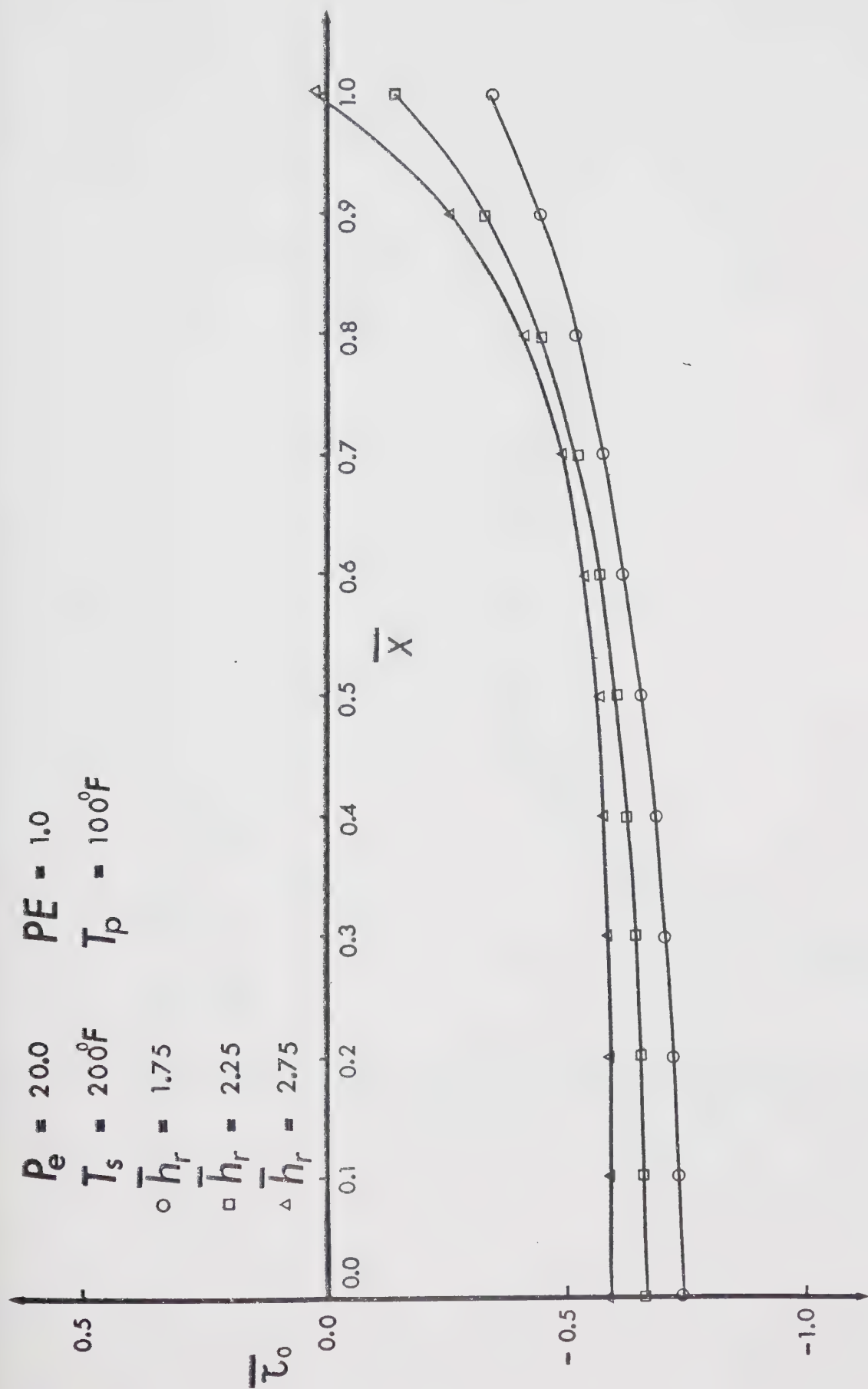


FIG. 31 Shear stress along length of slider at various sections — No inertia

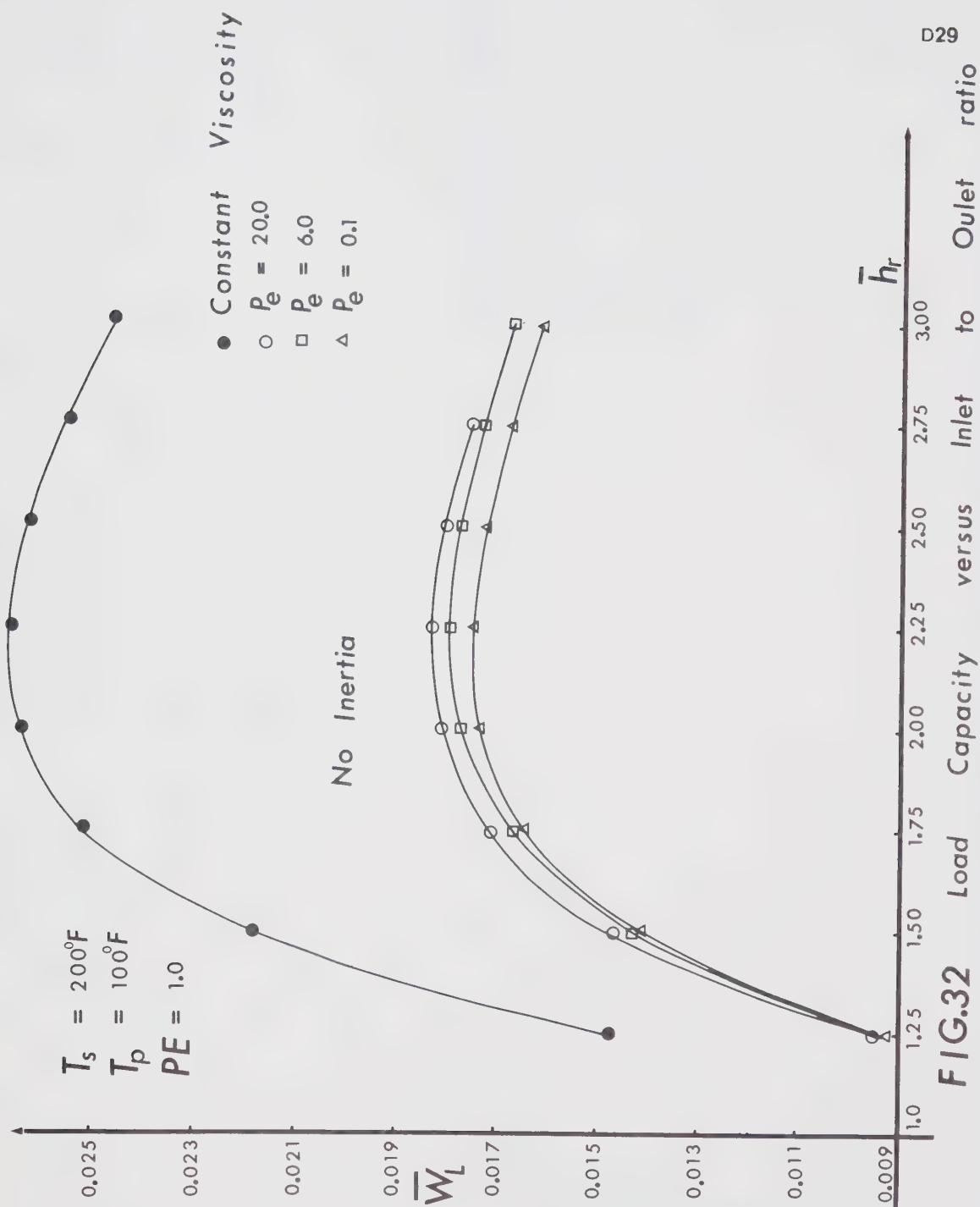


FIG. 32

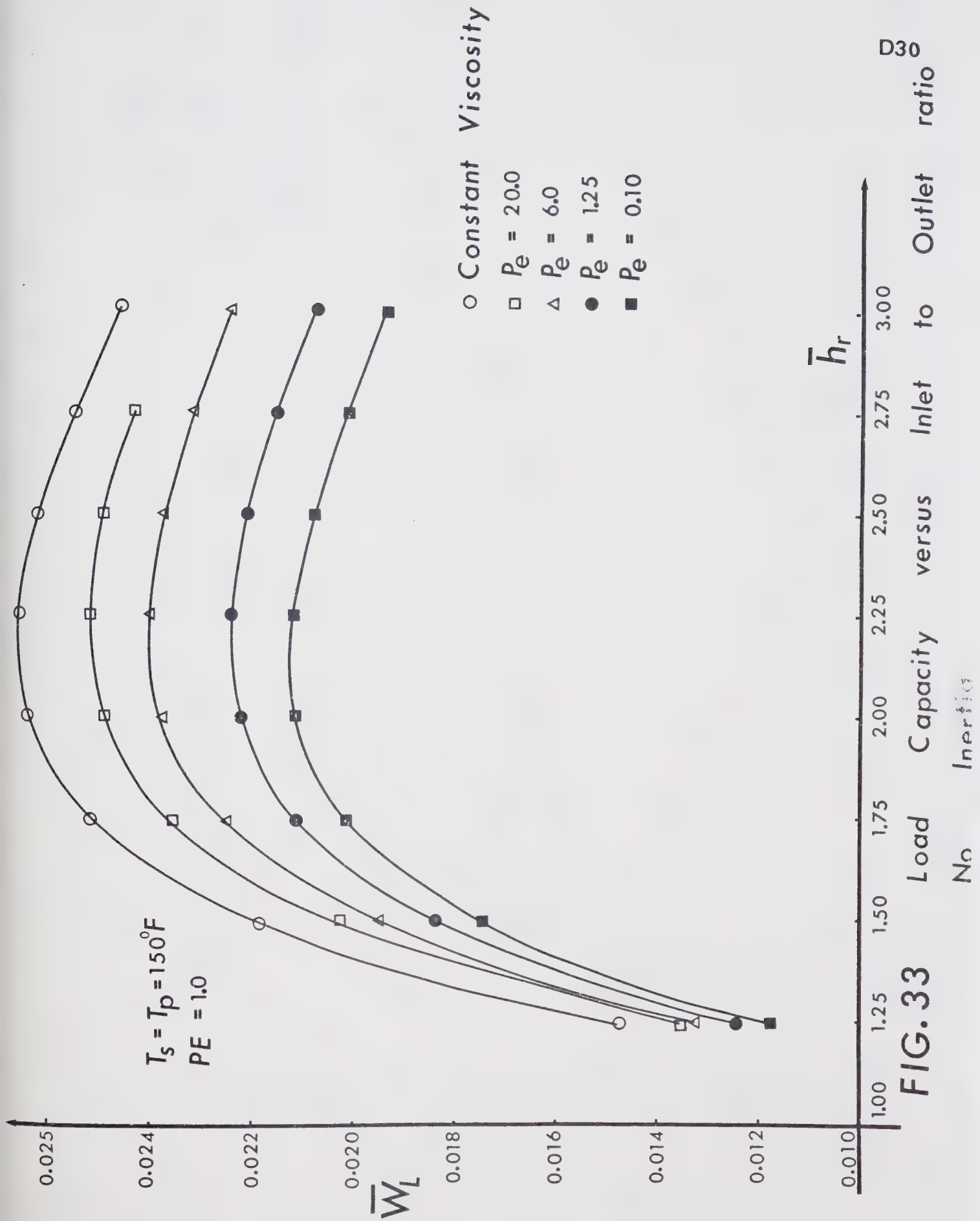


FIG. 33

$P_e = 20.0$
 $P_e = 6.0$
 $P_e = 1.25$
 $P_e = 0.10$
 Constant Viscosity

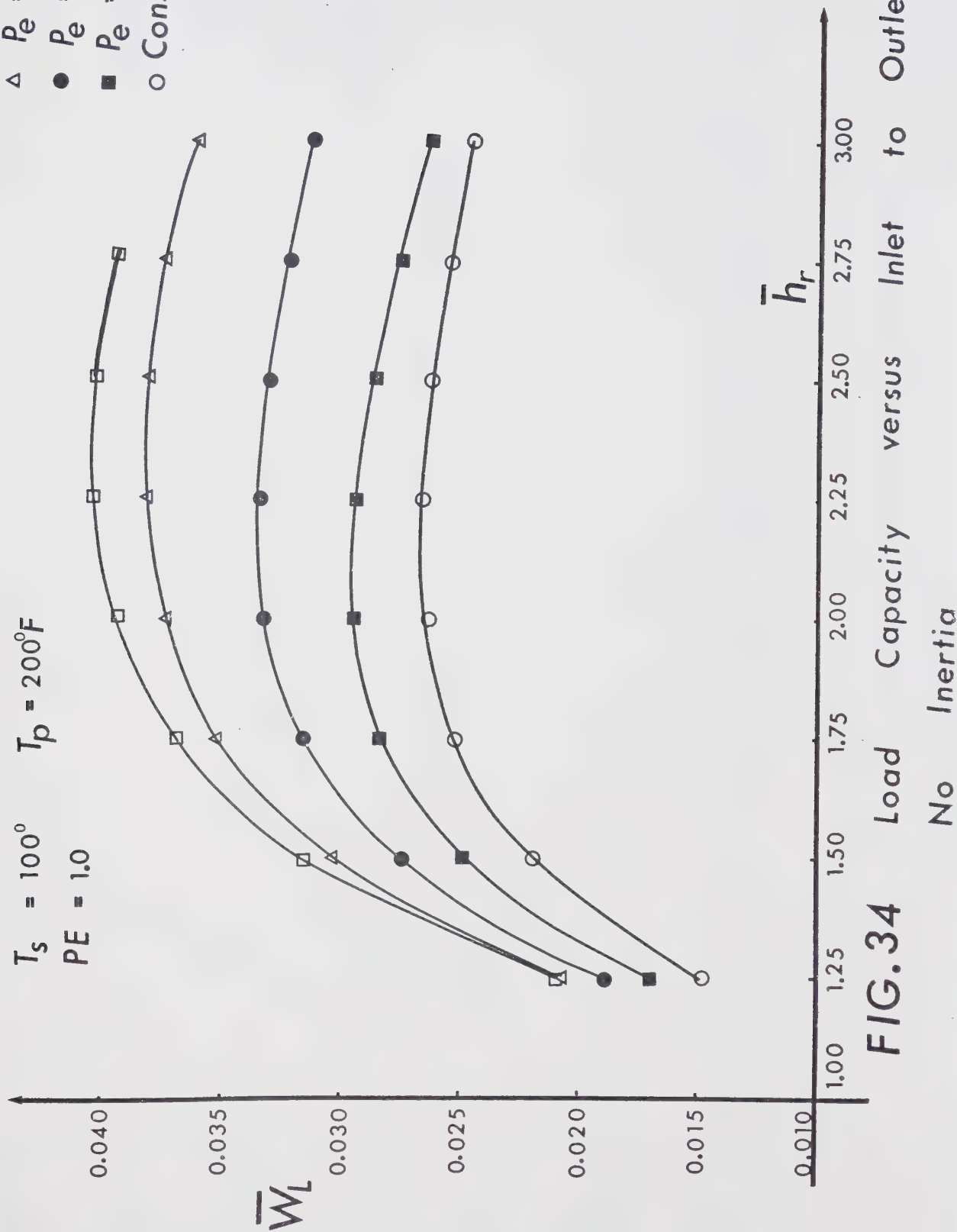


FIG. 34

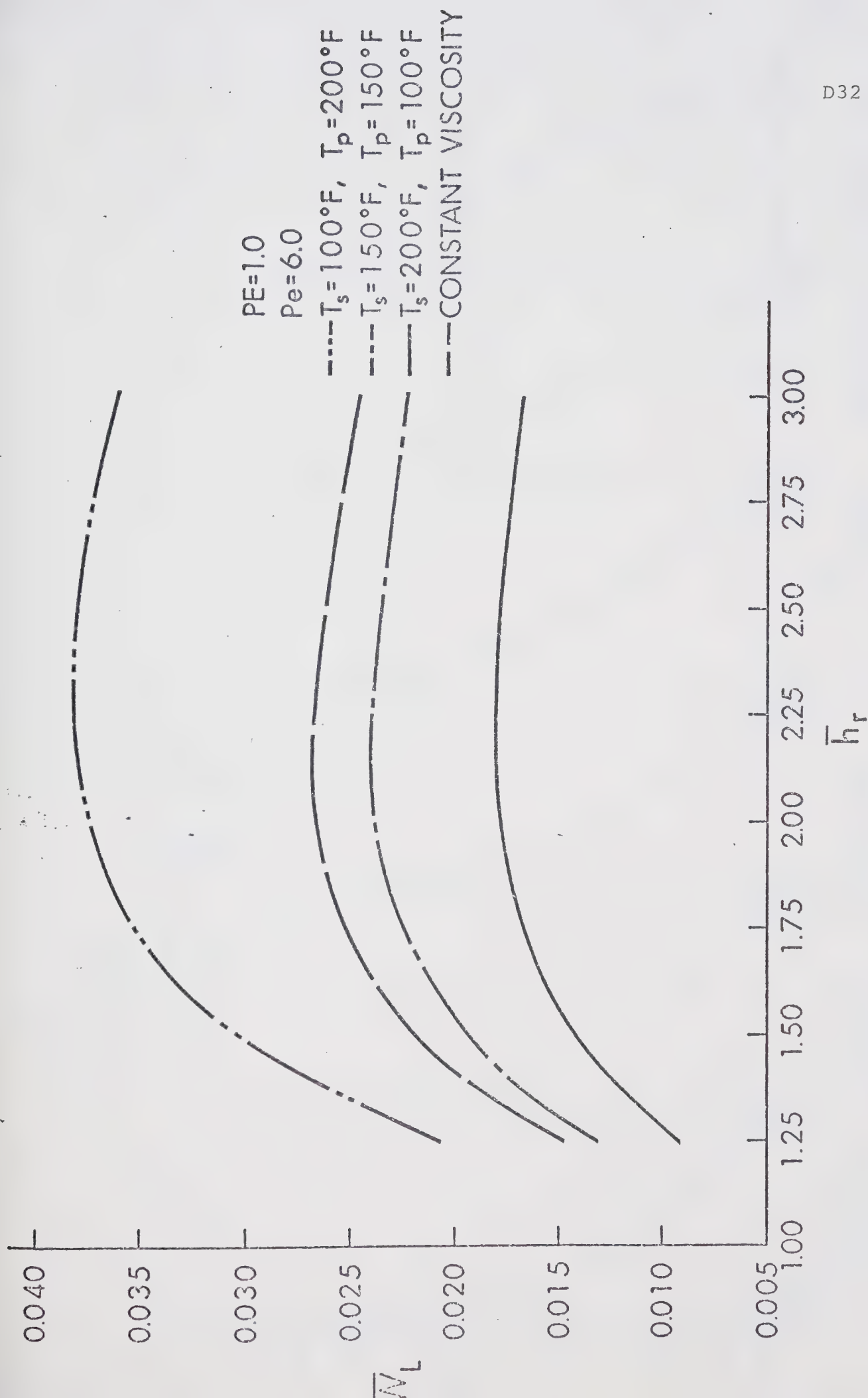


Fig. 35 Load Capacity Versus Inlet to Outlet Ratio

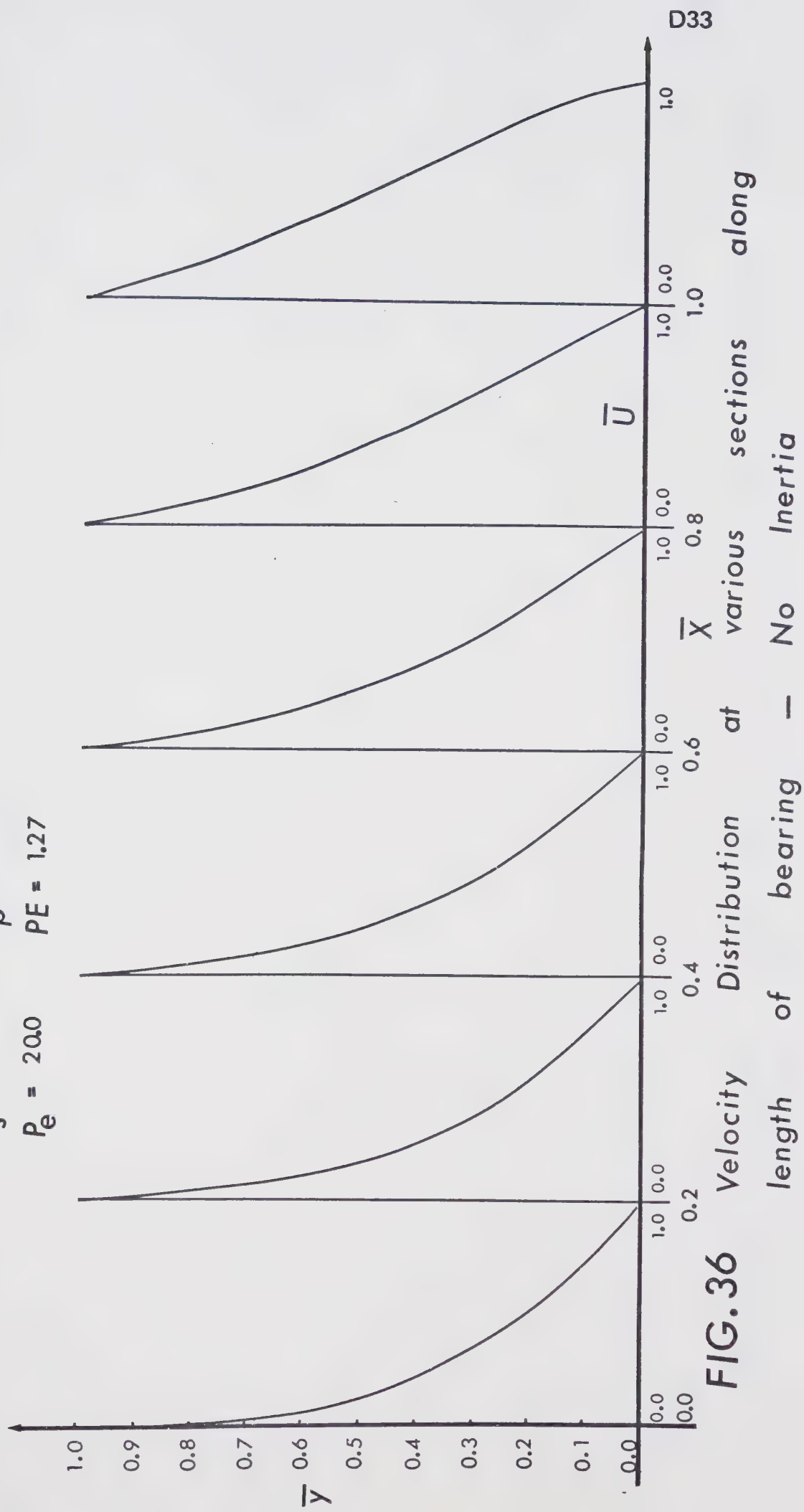
$$\bar{h}_r = 2.0$$

$$T_s = 110^\circ\text{F}$$

$$P_e = 20.0$$

$$T_p = 55^\circ\text{F}$$

$$PE = 1.27$$



$\bar{h}_r = 2.0$
 $T_s = 110^\circ\text{F}$
 $P_e = 20.0$

$T_p = 55^\circ\text{F}$
 $PE = 5.08$

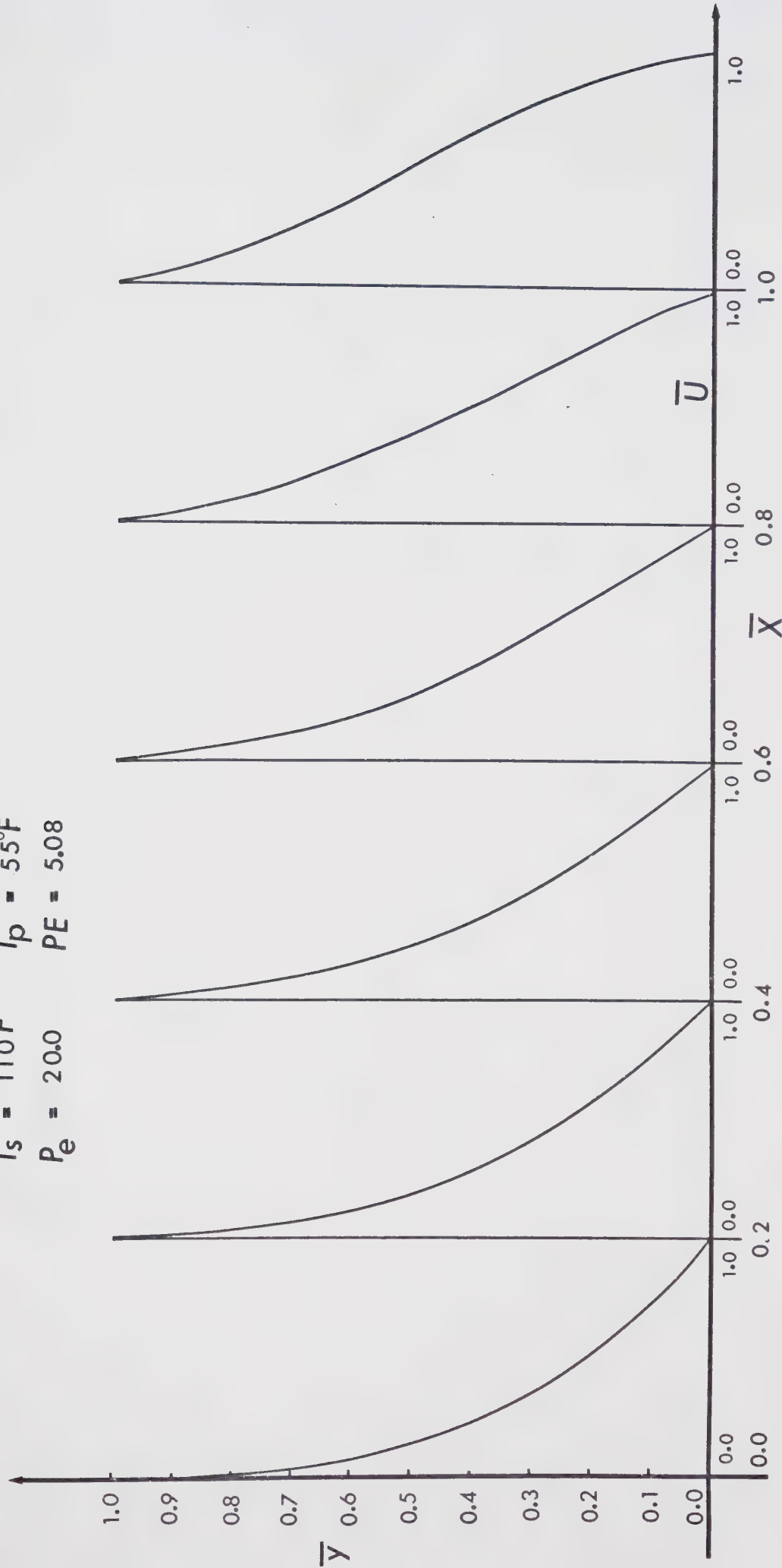


FIG.37 Velocity Distribution at various sections along length of bearing — No Inertia

$\bar{h}_r = 2.0$
 $T_s = 110^\circ\text{F}$
 $P_e = 20.0$

$T_p = 55^\circ\text{F}$
 $PE = 20.33$

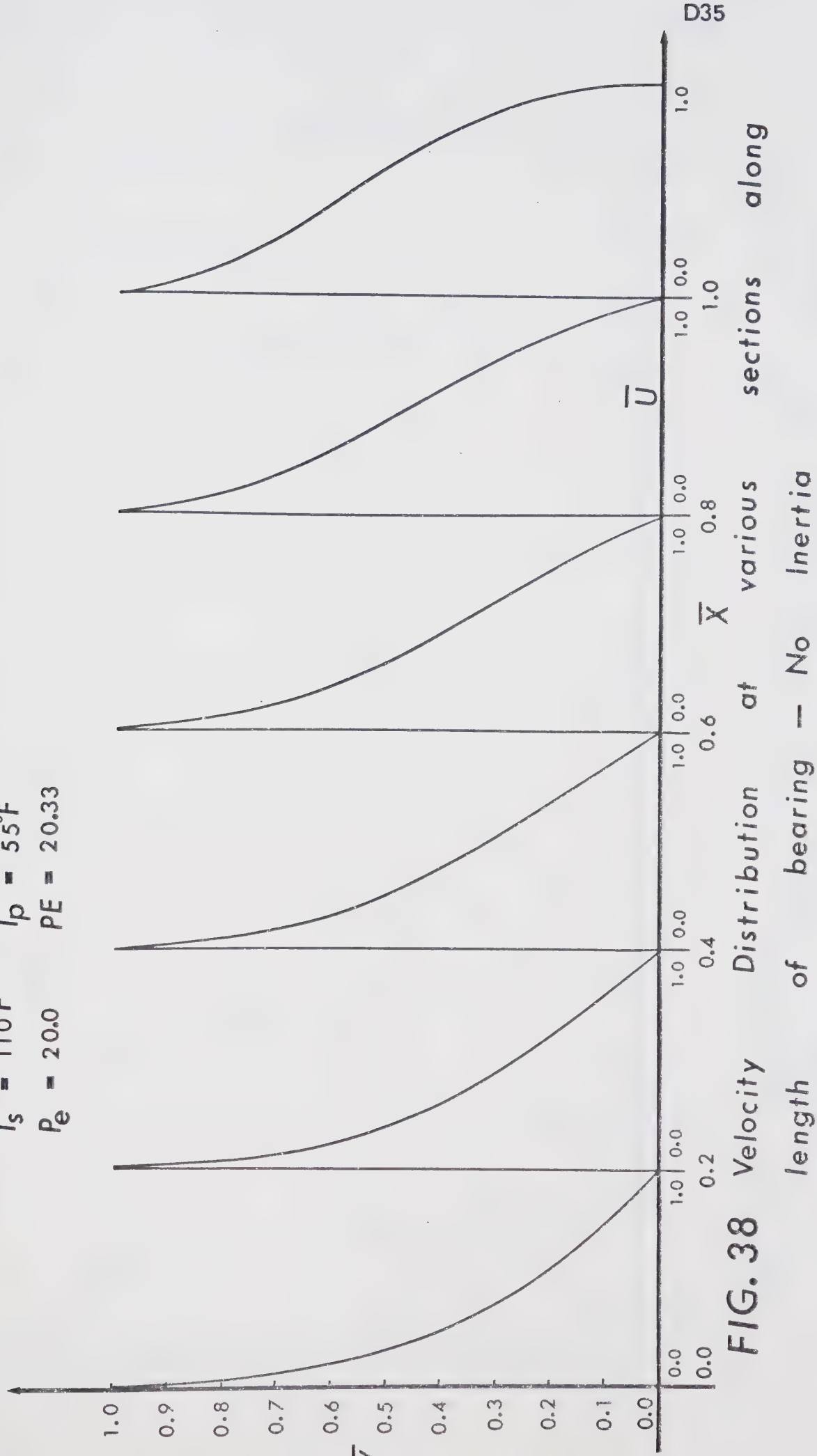


FIG. 38

$\bar{h}_r = 2.0$
 $T_s = 110^\circ\text{F}$
 $P_e = 20.0$

$T_p = 55^\circ\text{F}$
 $PE = 1.27$

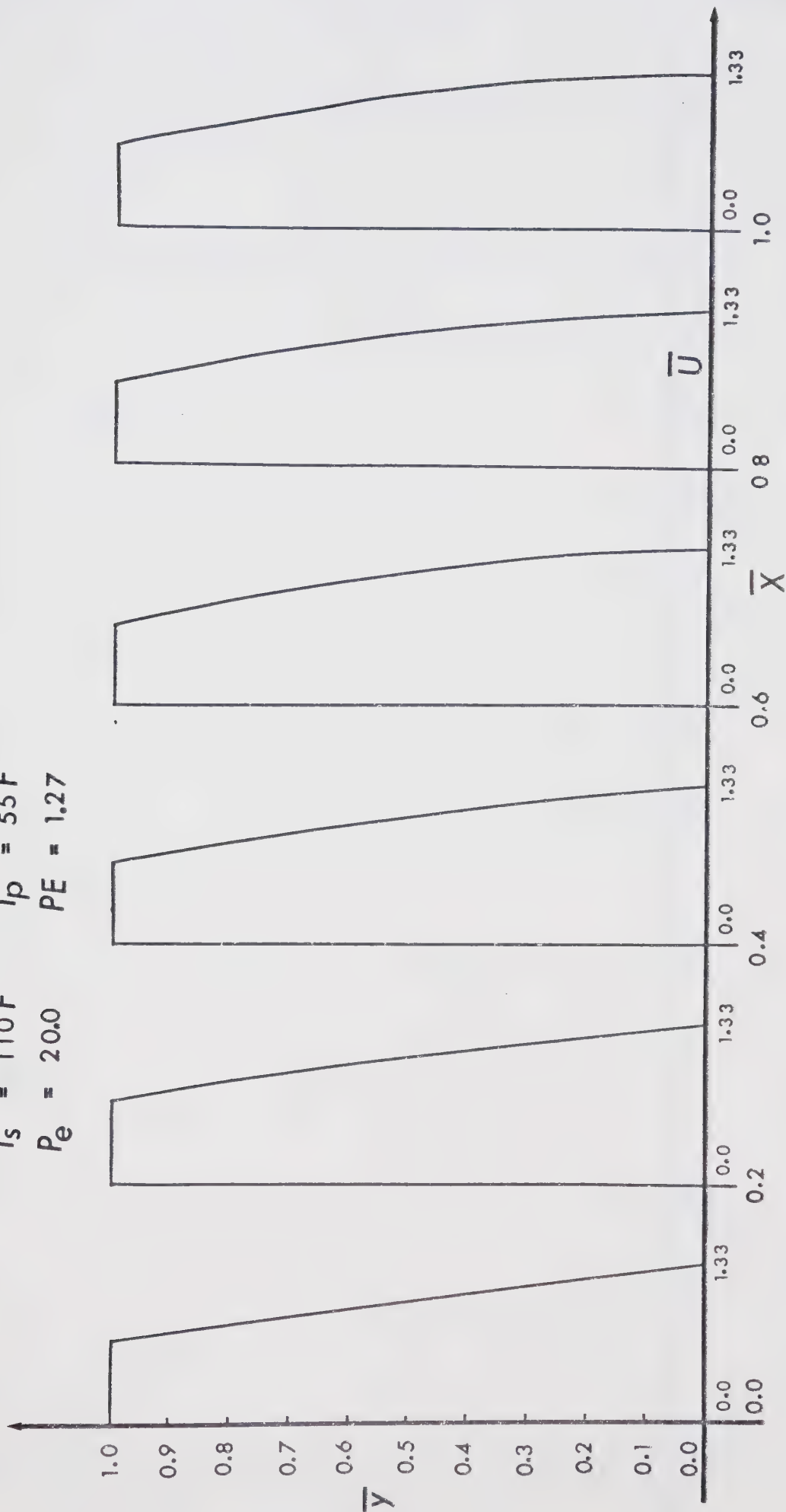


FIG. 39 Temperature Distribution at various sections along length of bearing — No Inertia

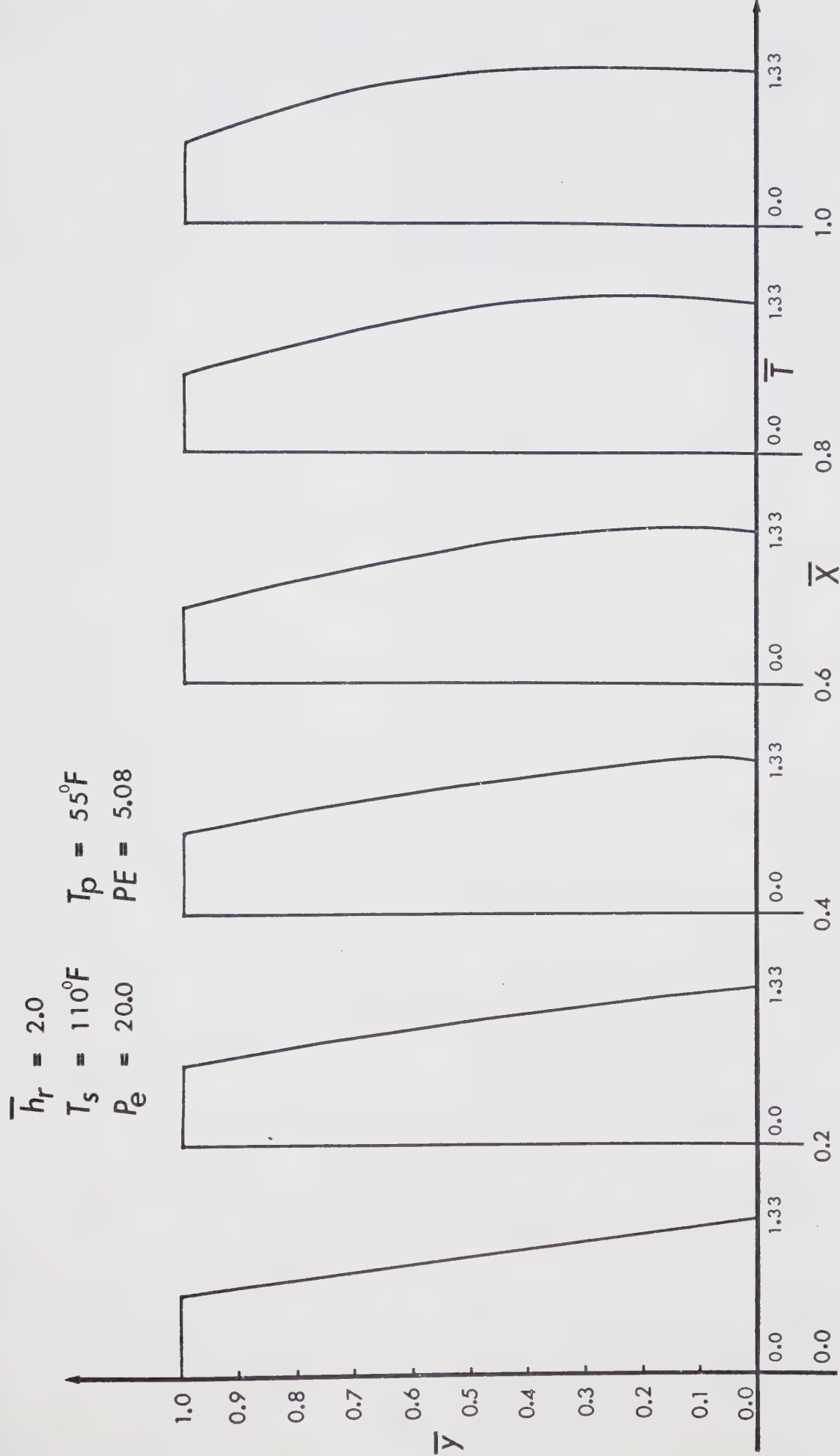
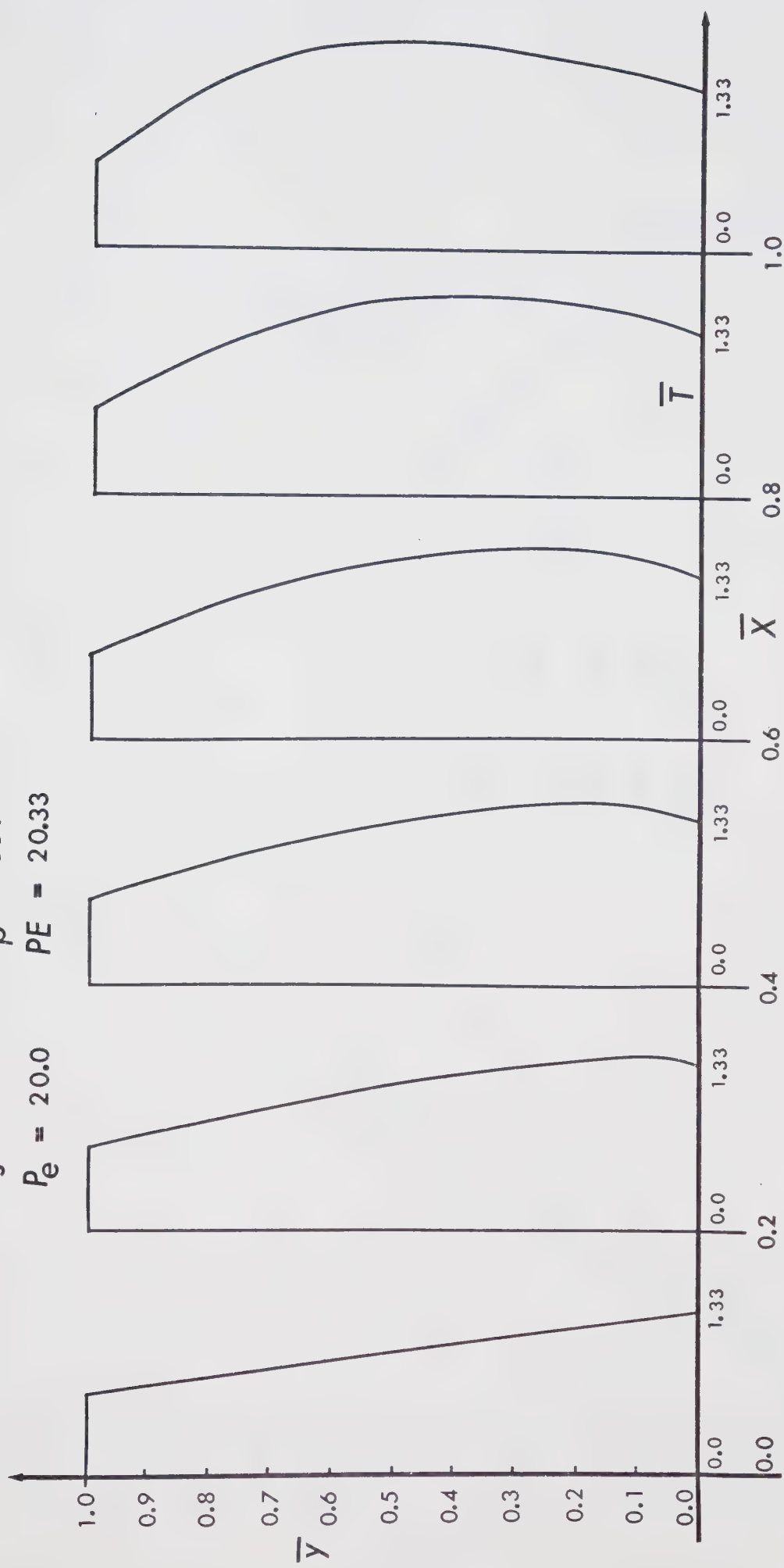


FIG. 40 Temperature Distribution at various sections along length of bearing — No Inertia

$\bar{h}_r = 2.0$
 $T_s = 110^\circ\text{F}$
 $P_e = 20.0$

$T_p = 55^\circ\text{F}$
 $PE = 20.33$



D38

Temperature Distribution at various sections
 along length of bearing — No Inertia

FIG.41

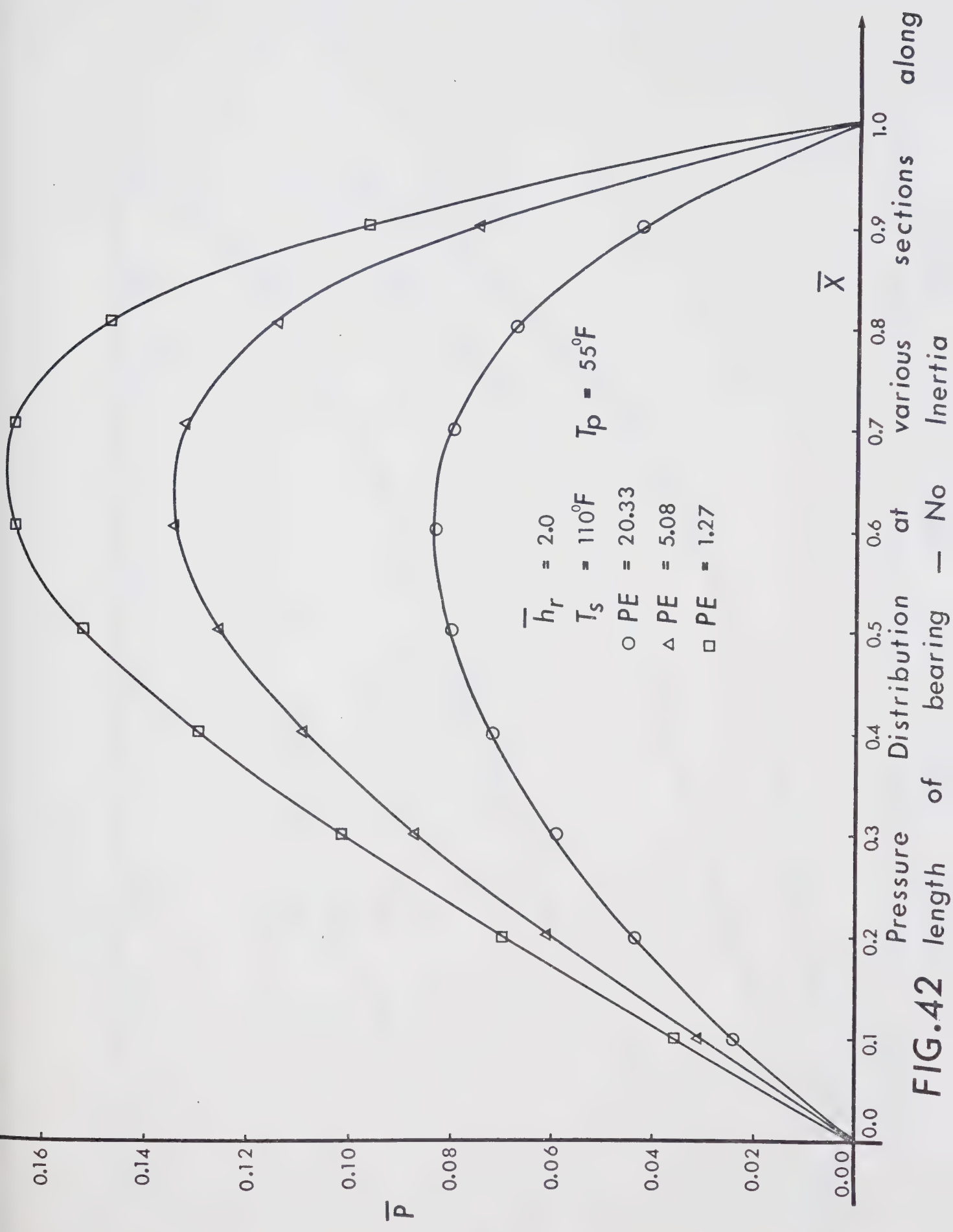


FIG.42

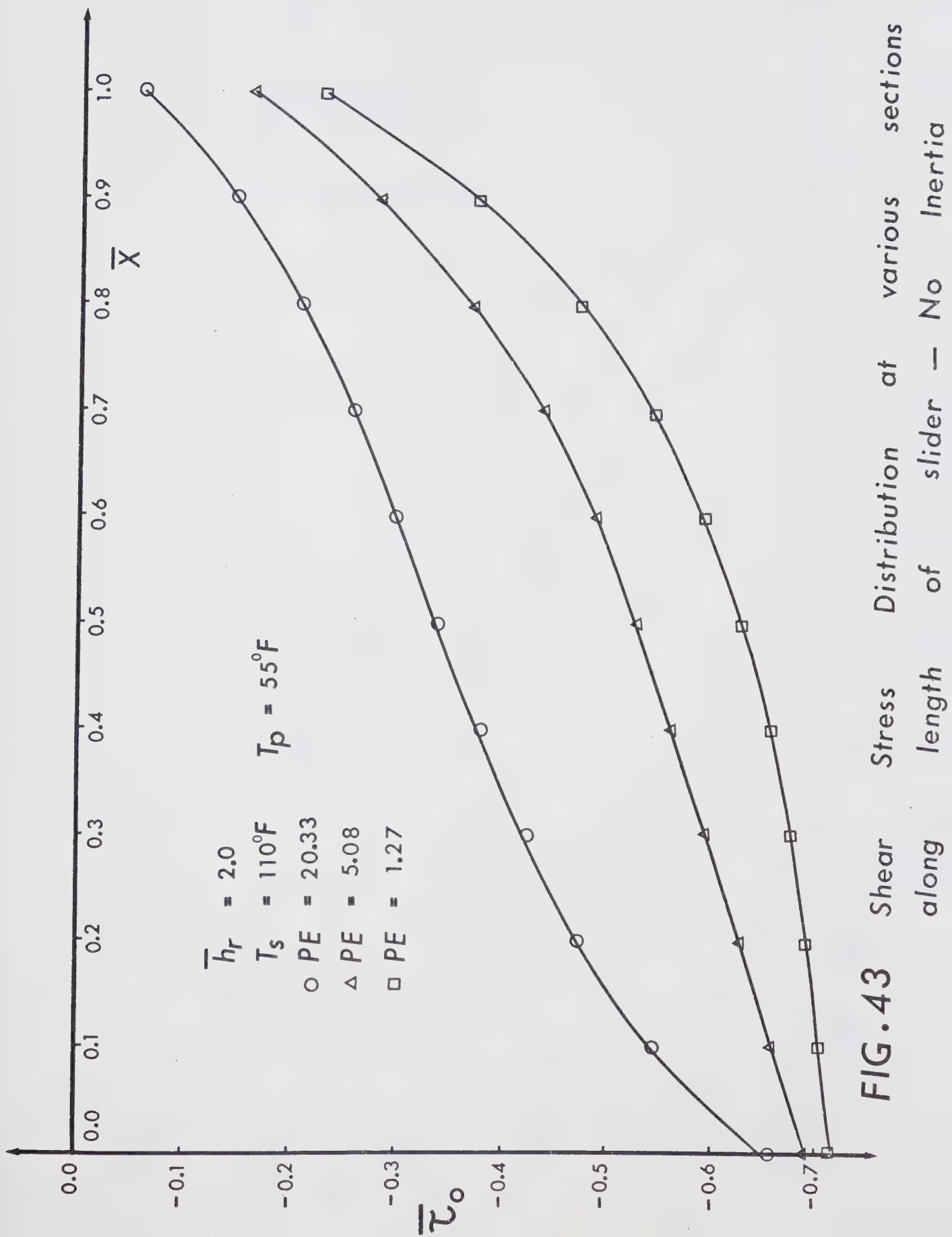


FIG. 43 Shear Stress Distribution along length of slider at various sections — No Inertia

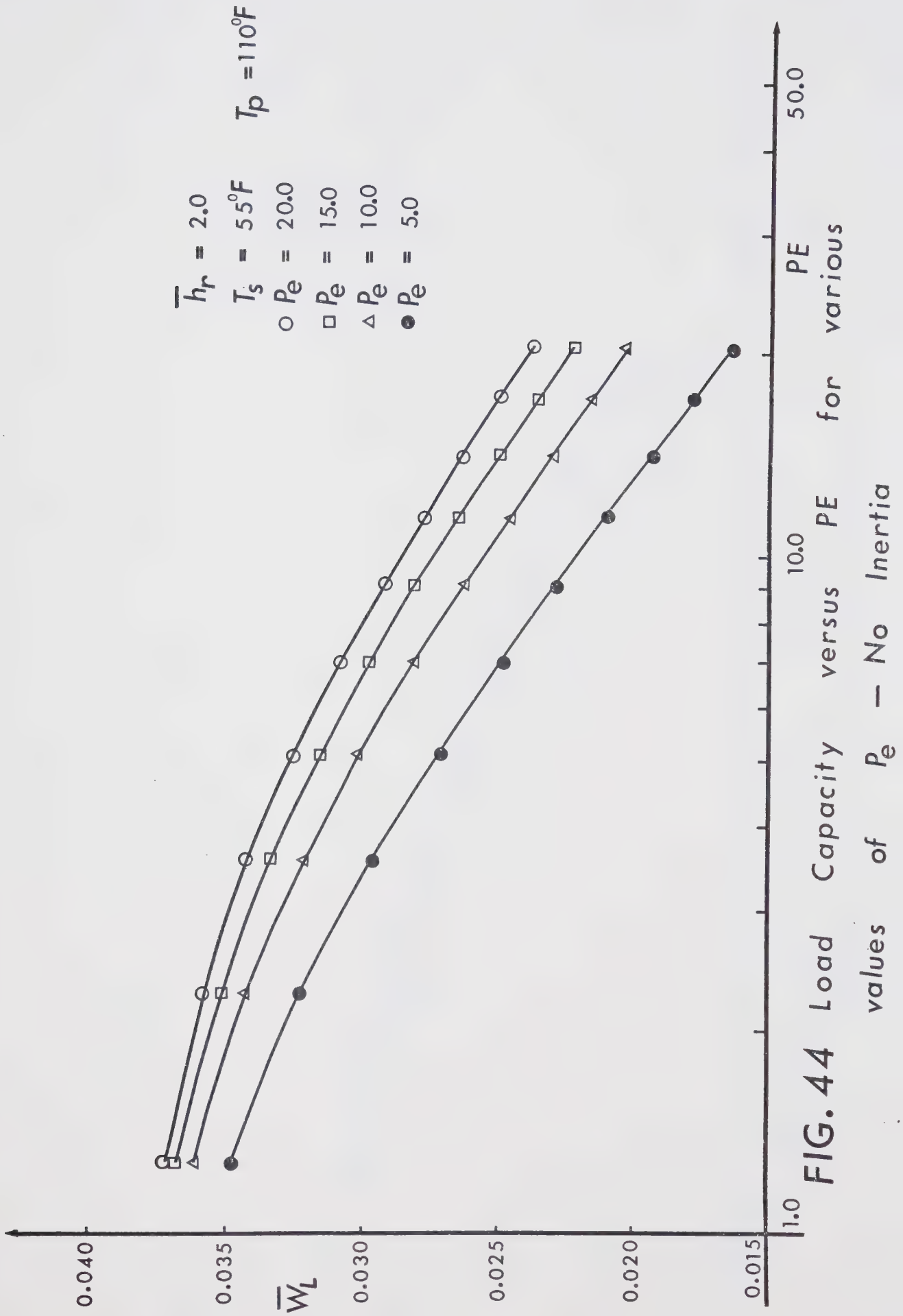


FIG. 44 Load Capacity versus PE for various values of P_e - No Inertia

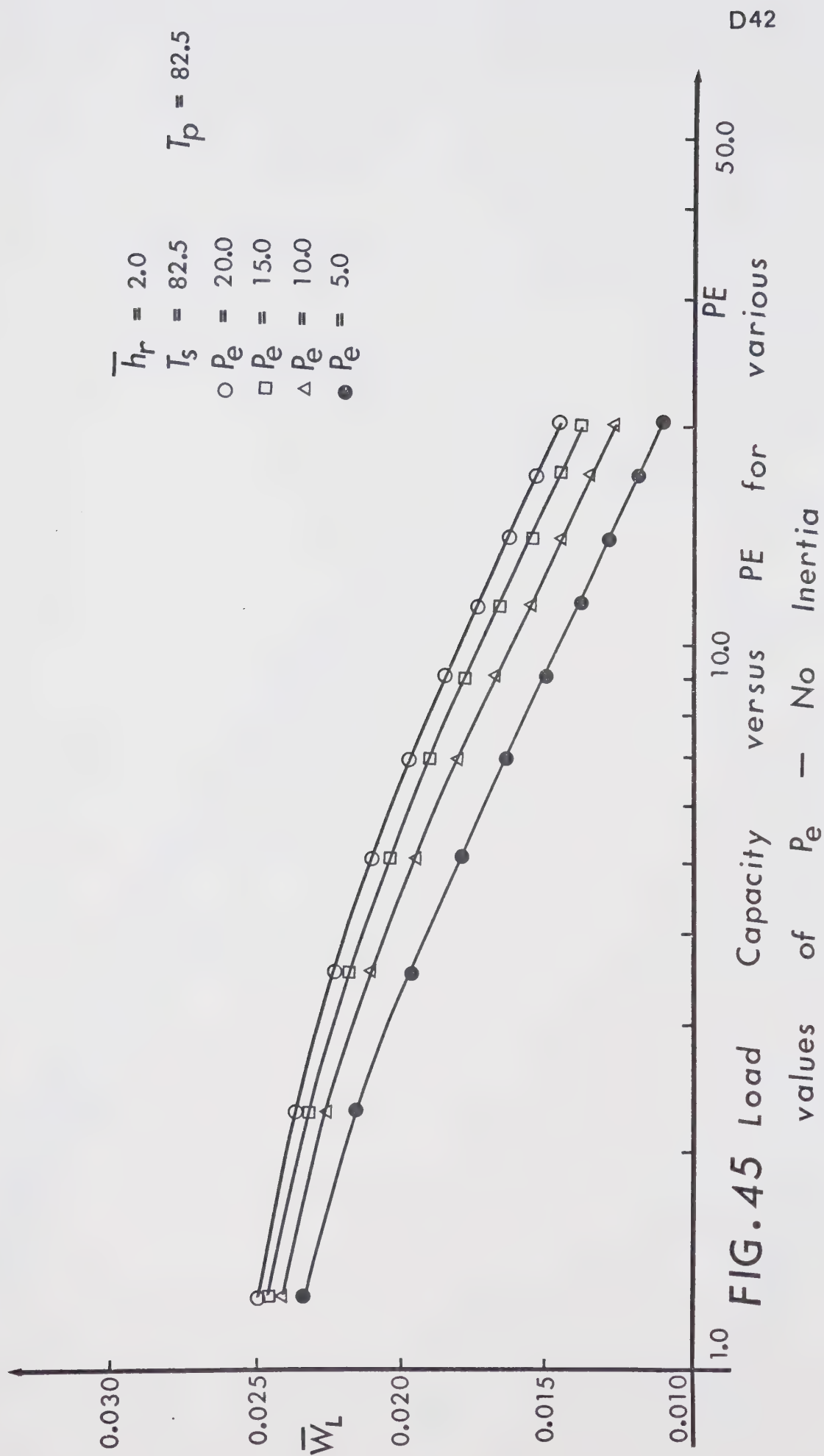


FIG. 45

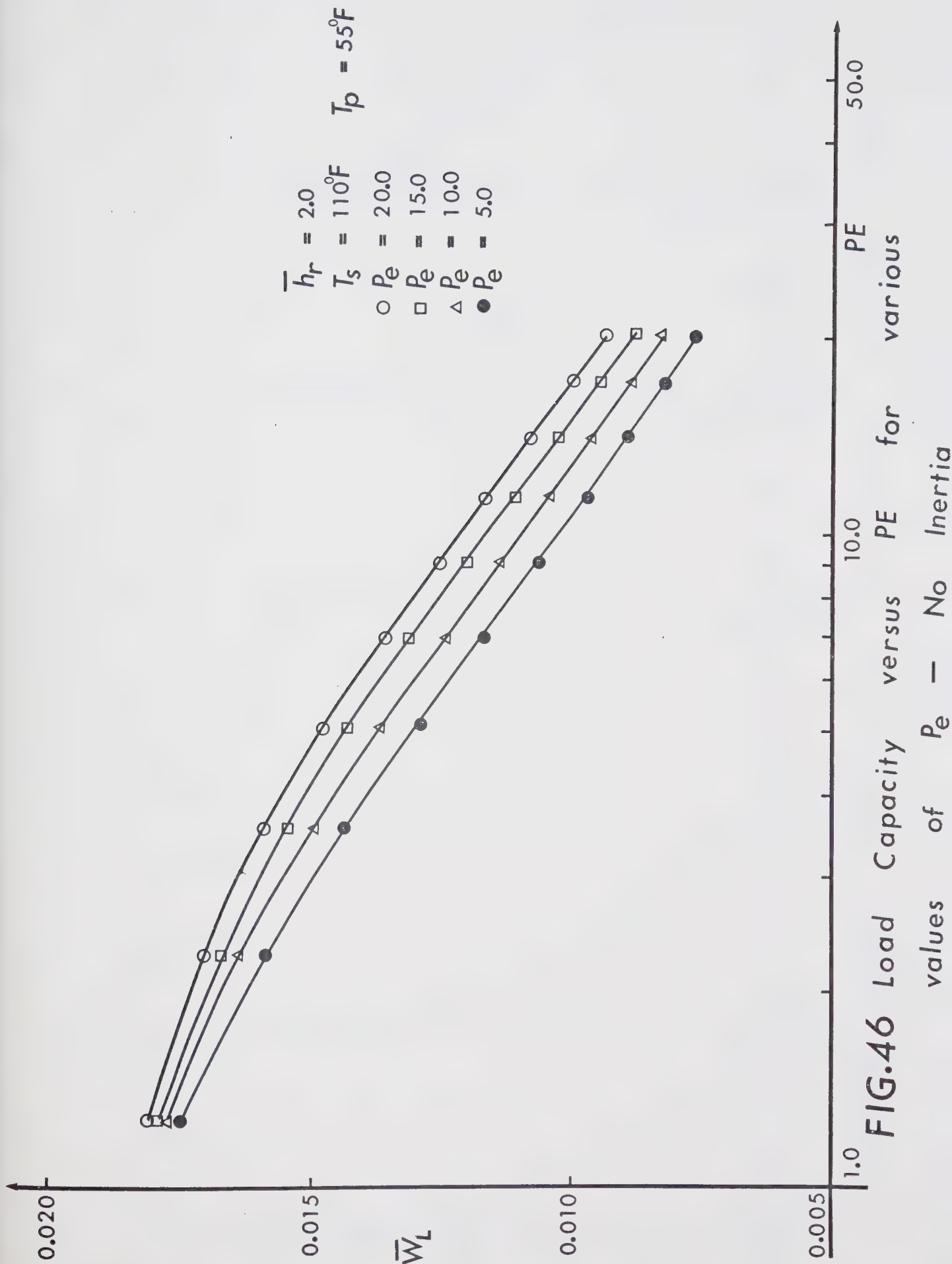


FIG.46 Load Capacity versus PE for various values of P_e - No Inertia

$\bar{h}_r = 2.0$
 $T_s = 110^\circ\text{F}$
 $P_e = 1.0$
 $T_p = 55^\circ\text{F}$
 $PE = 20.33$

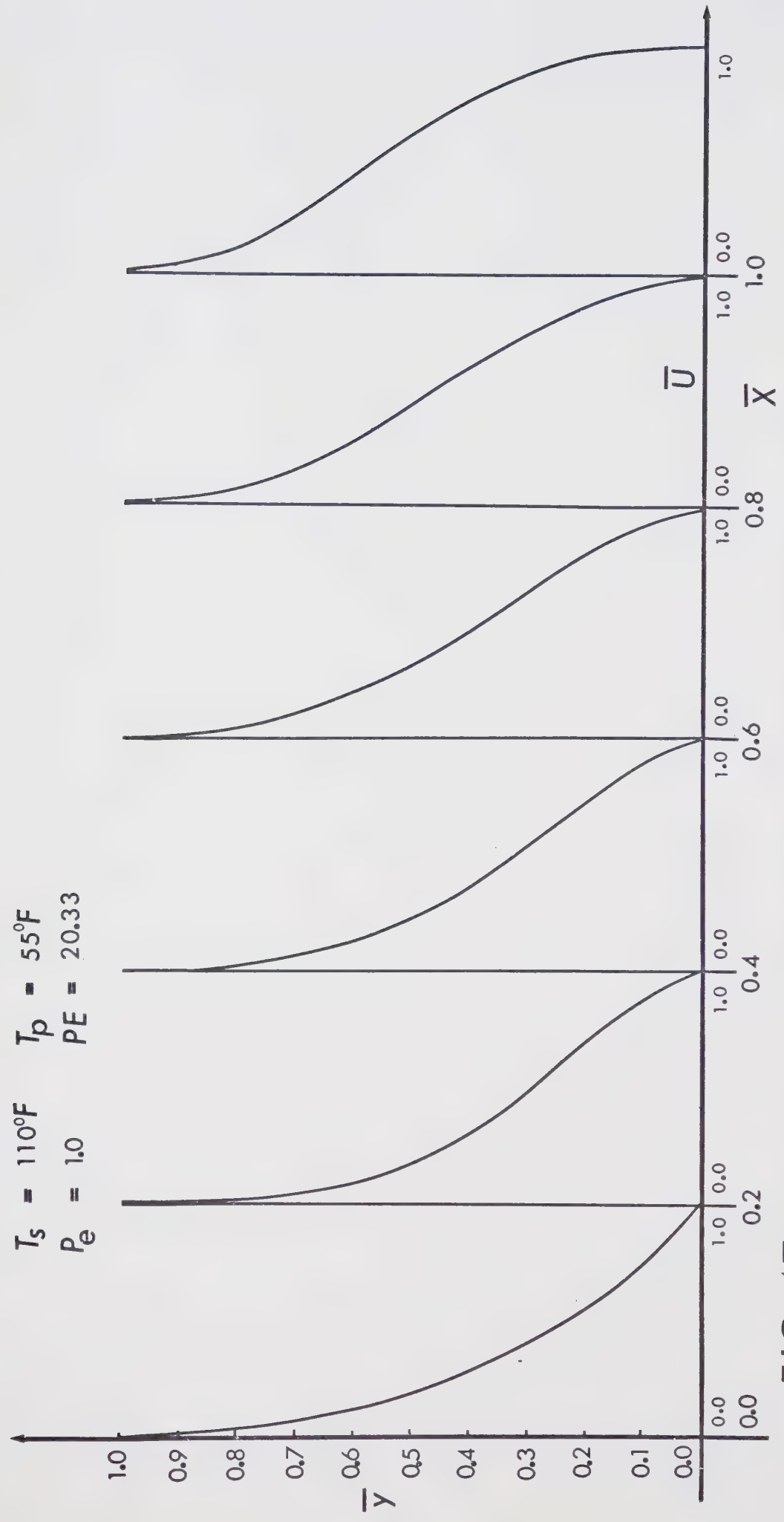


FIG. 47 Velocity Distribution at various sections along length of bearing — No Inertia

$\bar{h}_r = 2.0$
 $T_s = 110^\circ F$
 $P_e = 5.0$
 $T_p = 55^\circ F$
 $PE = 20.33$

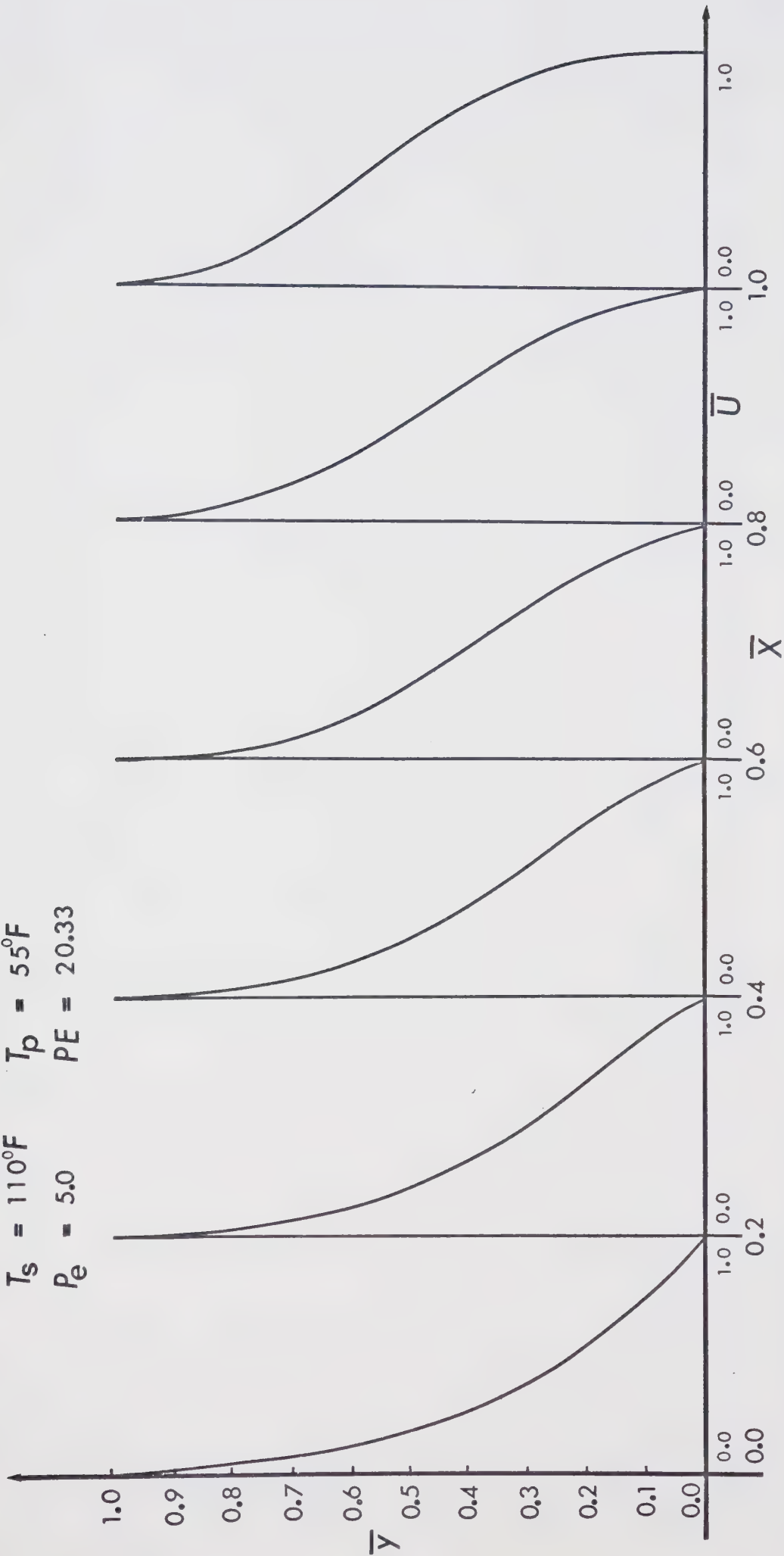


FIG.48 Velocity Distribution at various sections along
 of bearing — No Inertia

$\bar{h}_r = 2.0$
 $T_s = 110^\circ\text{F}$
 $P_e = 20.0$

$T_p = 55^\circ\text{F}$
 $PE = 20.33$

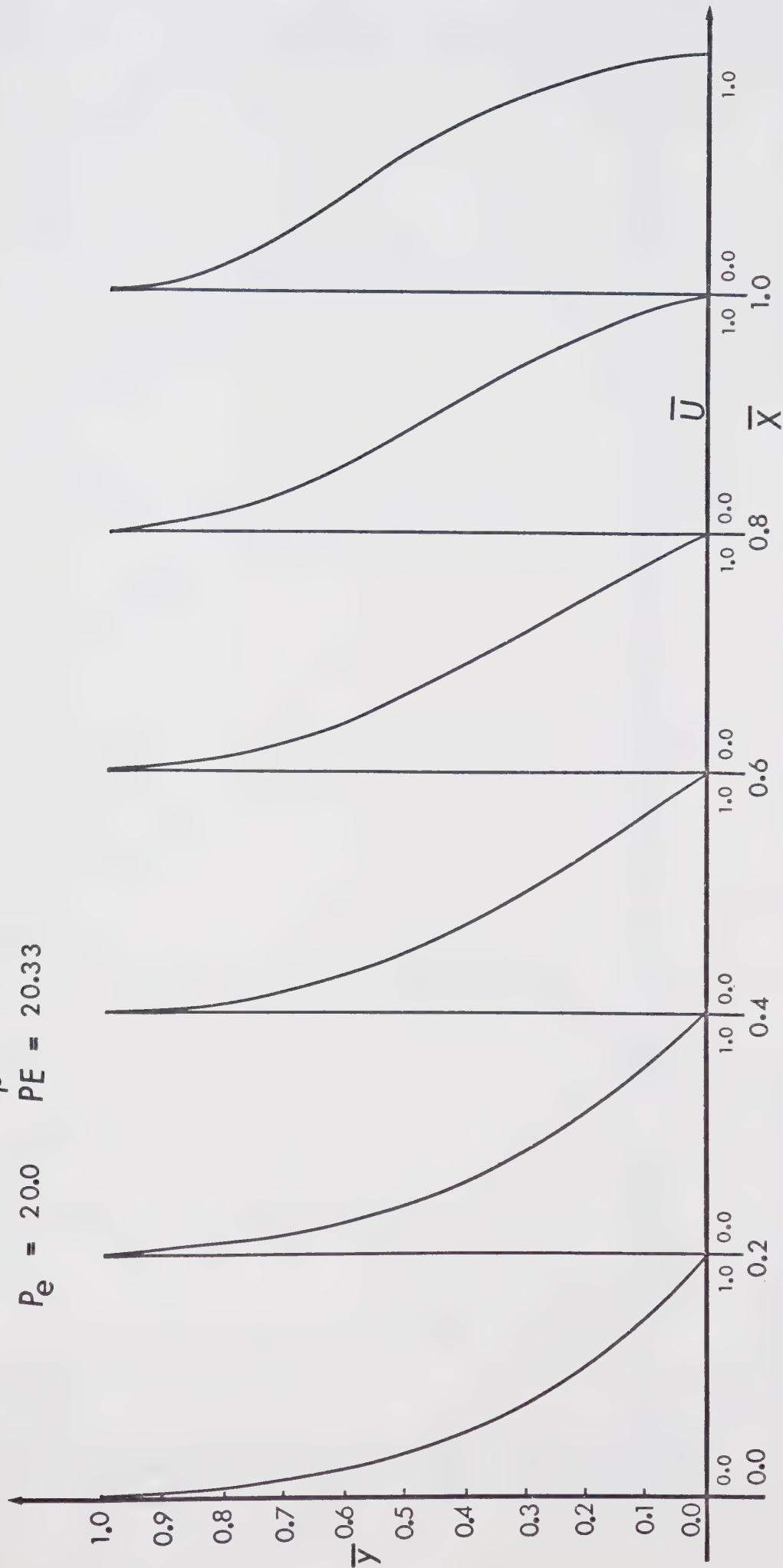


FIG. 49 Velocity Distribution at various sections along length of bearing No Inertia

$\bar{h}_r = 20$
 $T_s = 110^\circ\text{F}$
 $P_e = 1.0$

$T_p = 55^\circ\text{F}$
 $PE = 20.33$

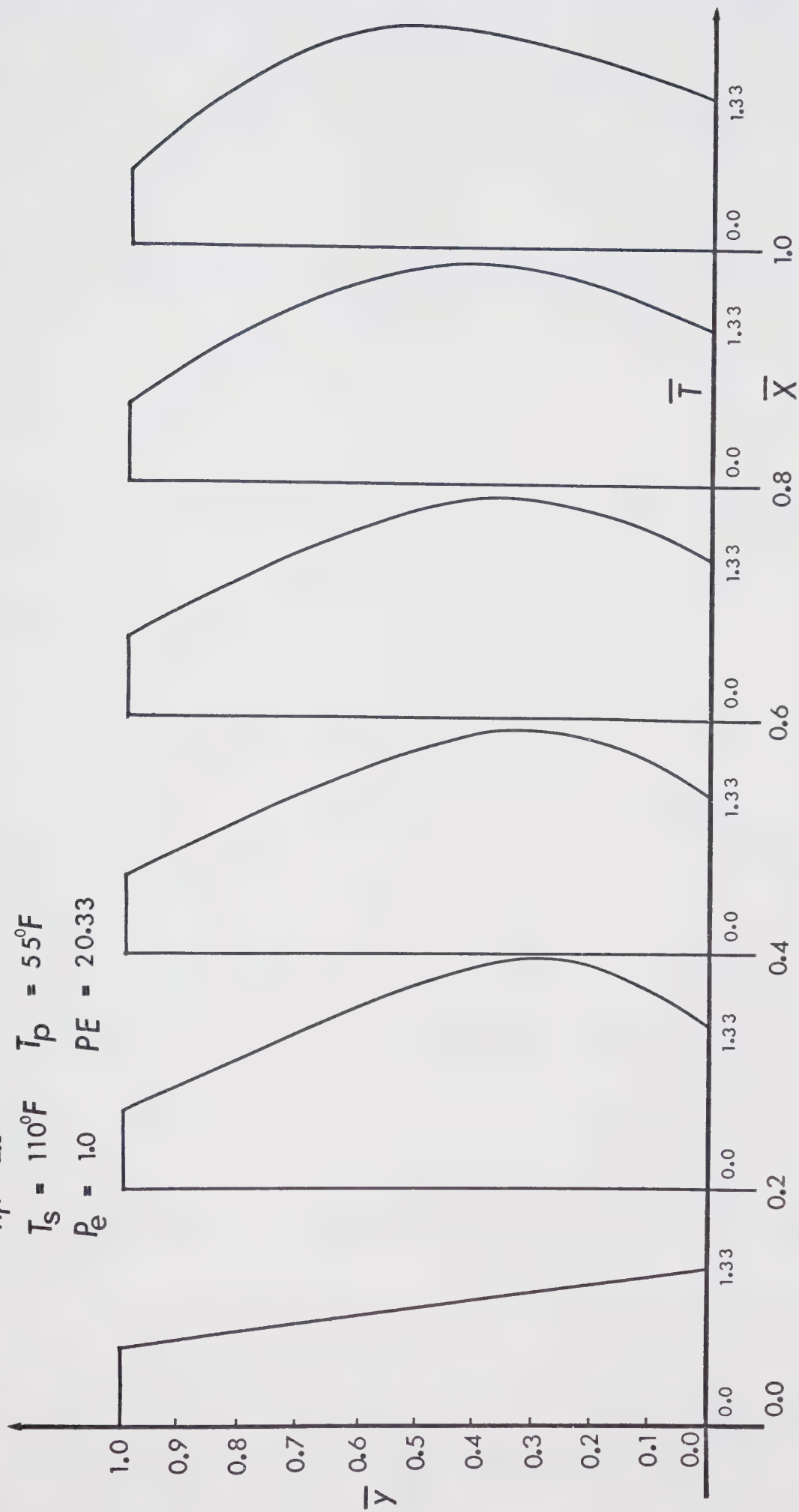


FIG. 50 Temperature Distribution at various sections along length of bearing — No Inertia

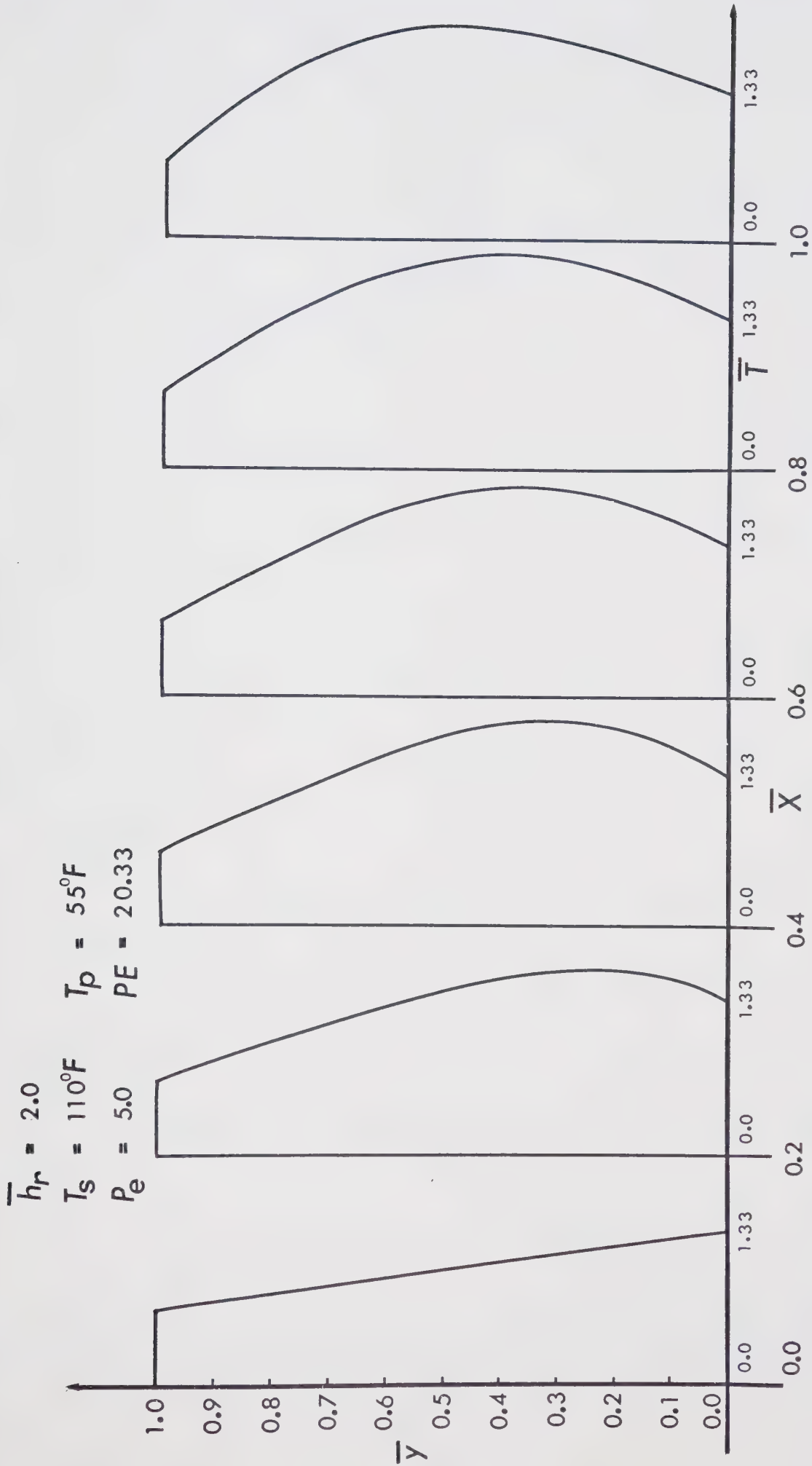


FIG. 51 Temperature Distribution at various sections along length of bearing — No Inertia

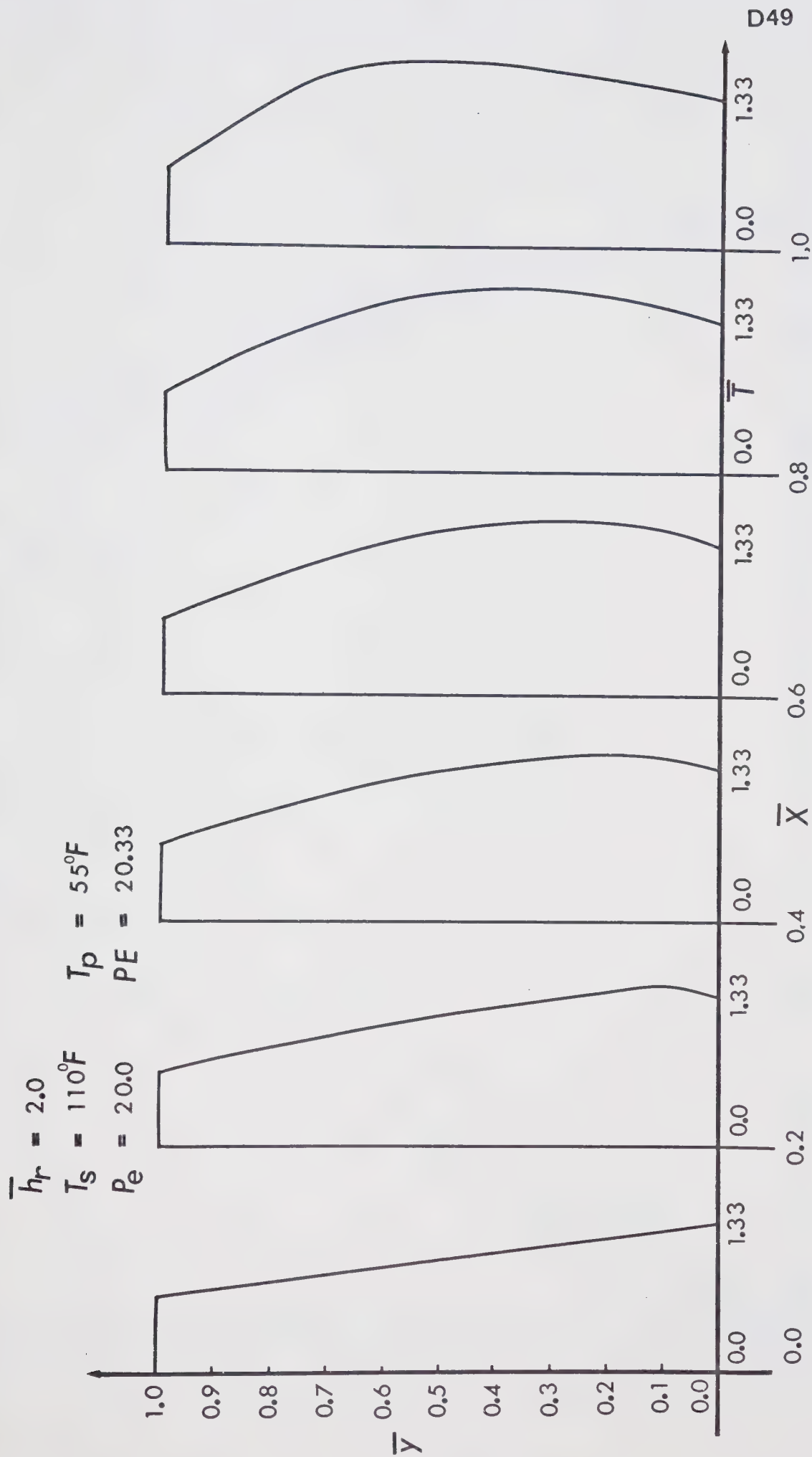


FIG. 52 Temperature Distribution at various sections along length of bearing — No Inertia

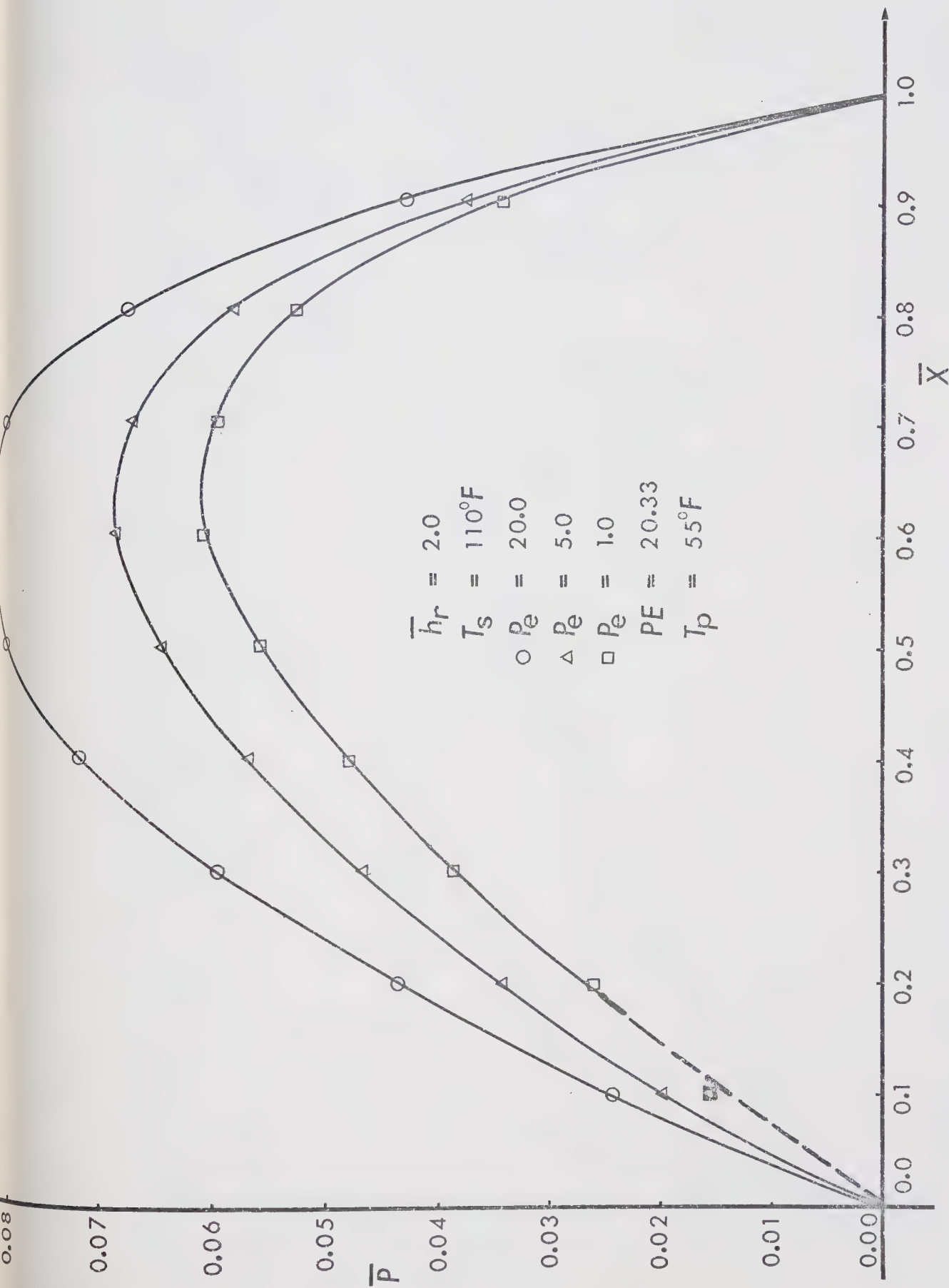


FIG. 53 Pressure Distribution at various sections along length of bearing — No Inertia

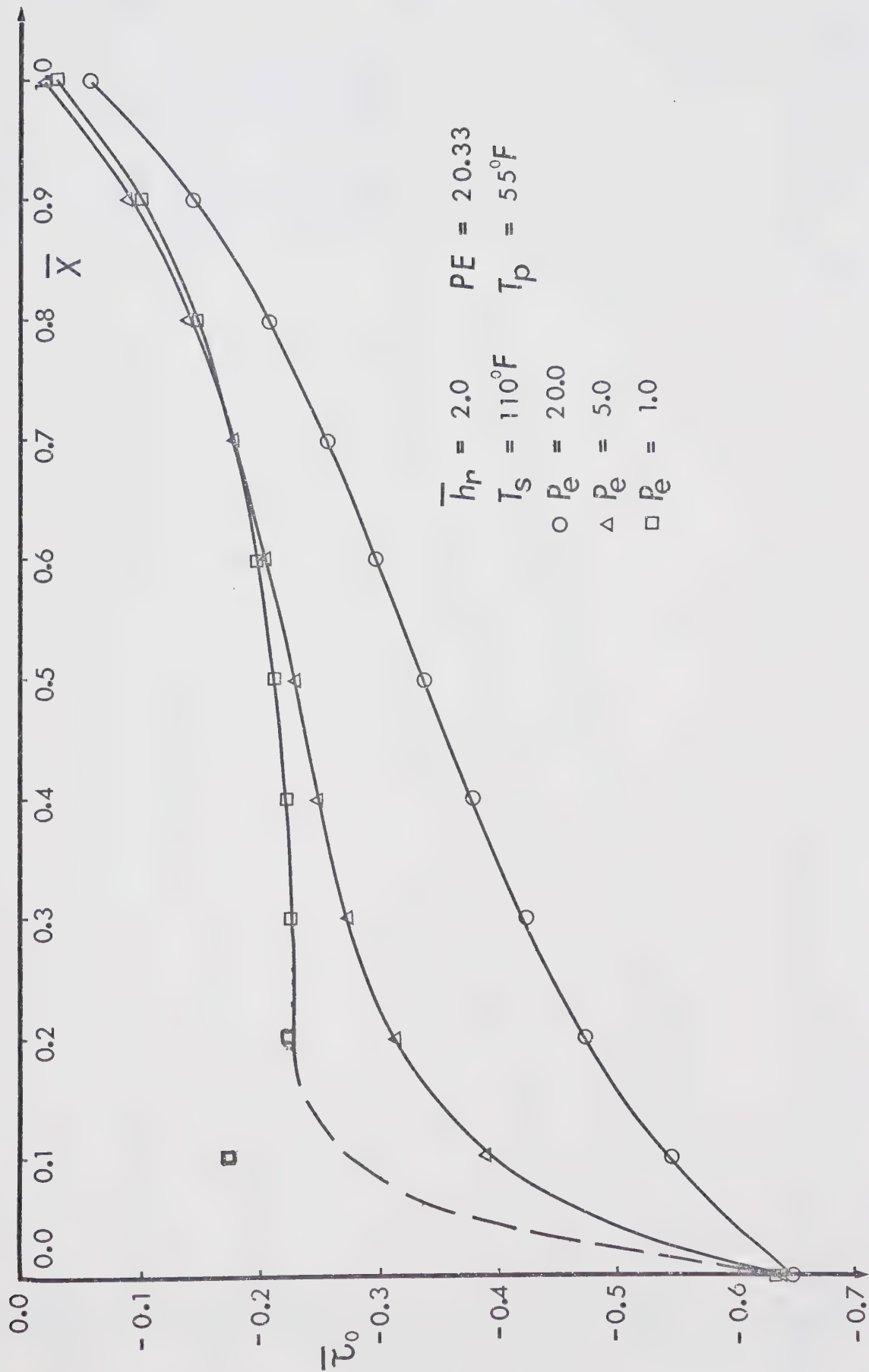


FIG. 5.4 Shear Stress Distribution along length of slider at various sections — No Inertia

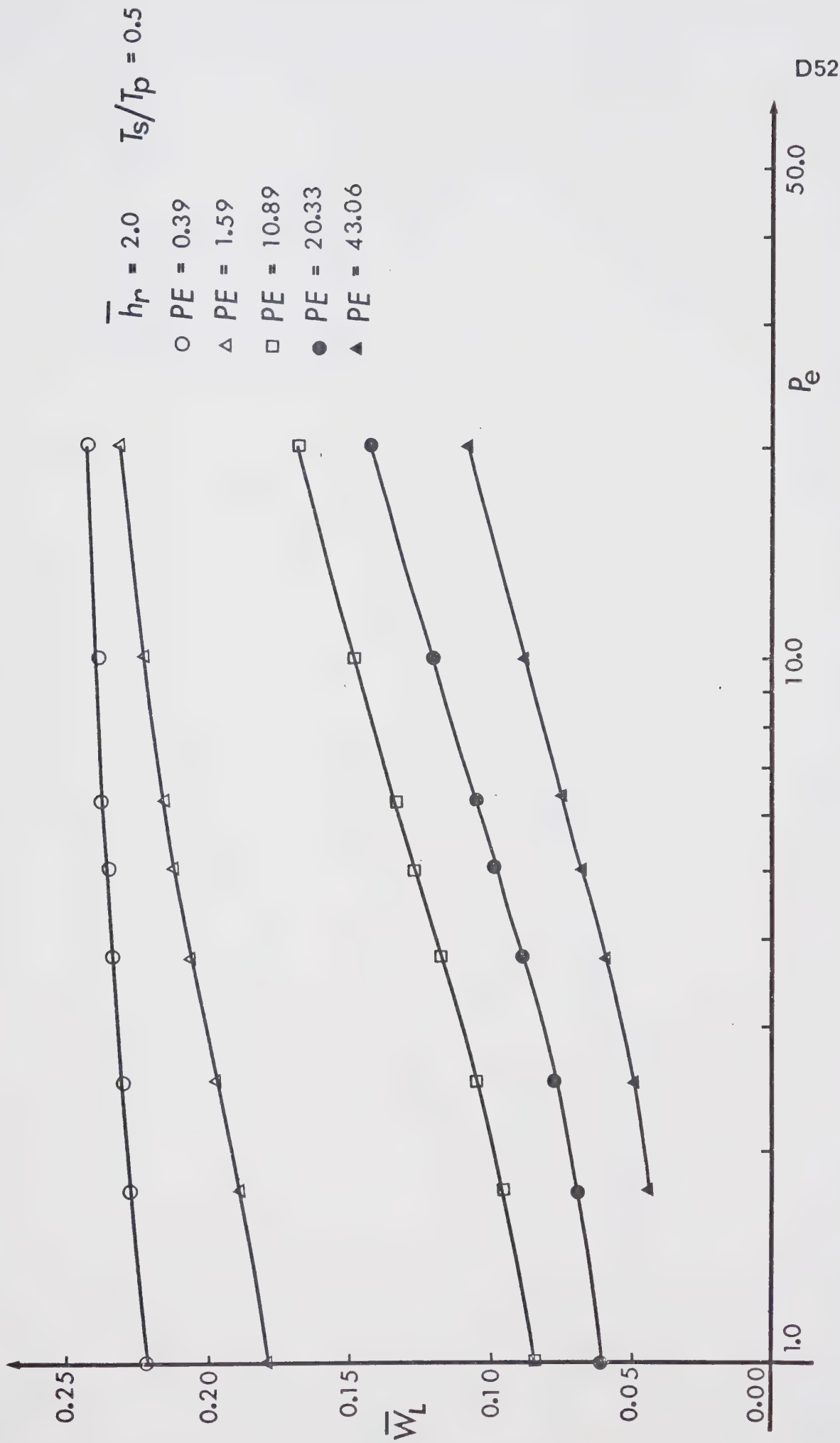


FIG. 55 Load Capacity versus P_e for various values of PE — No Inertia

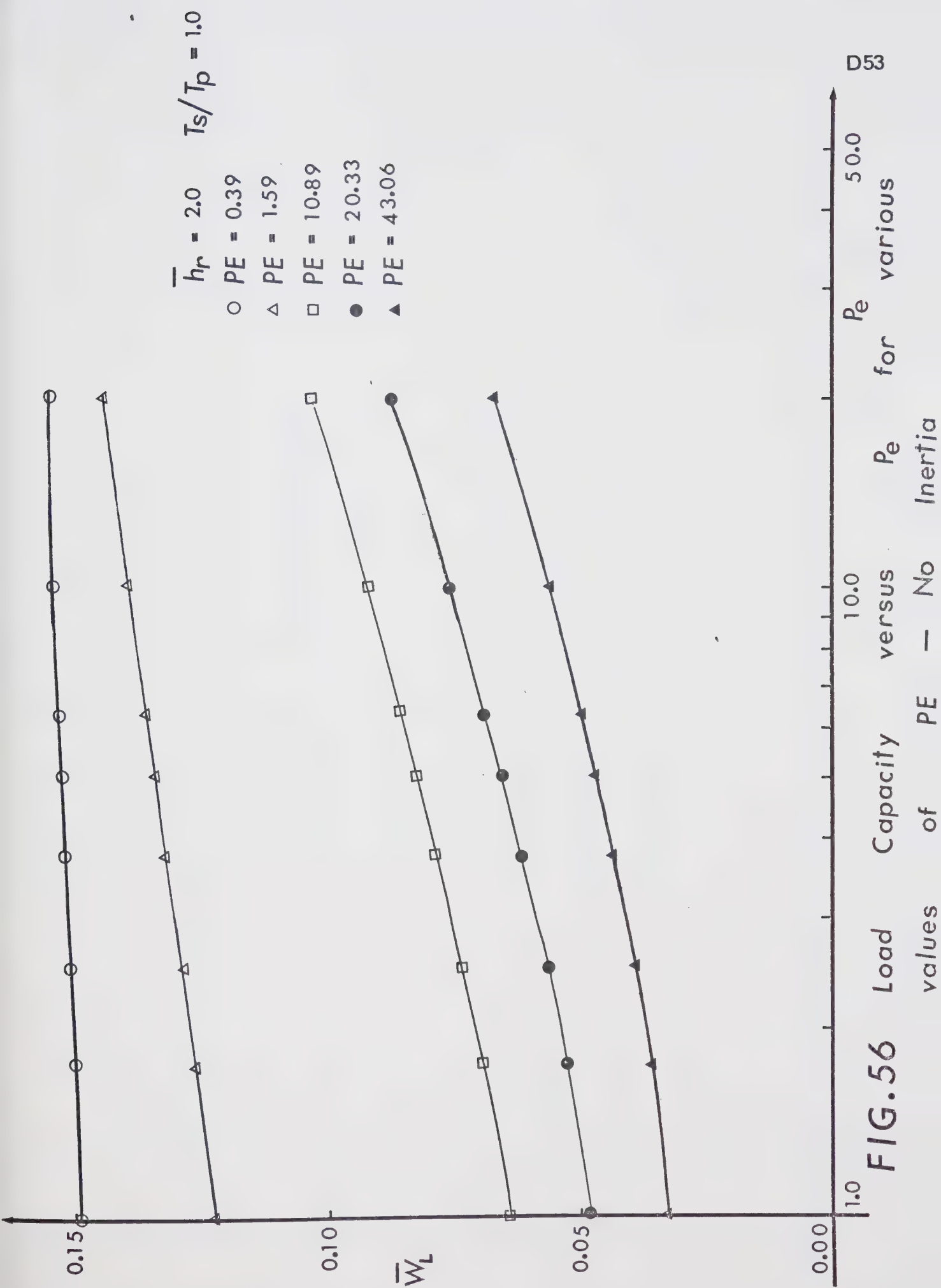
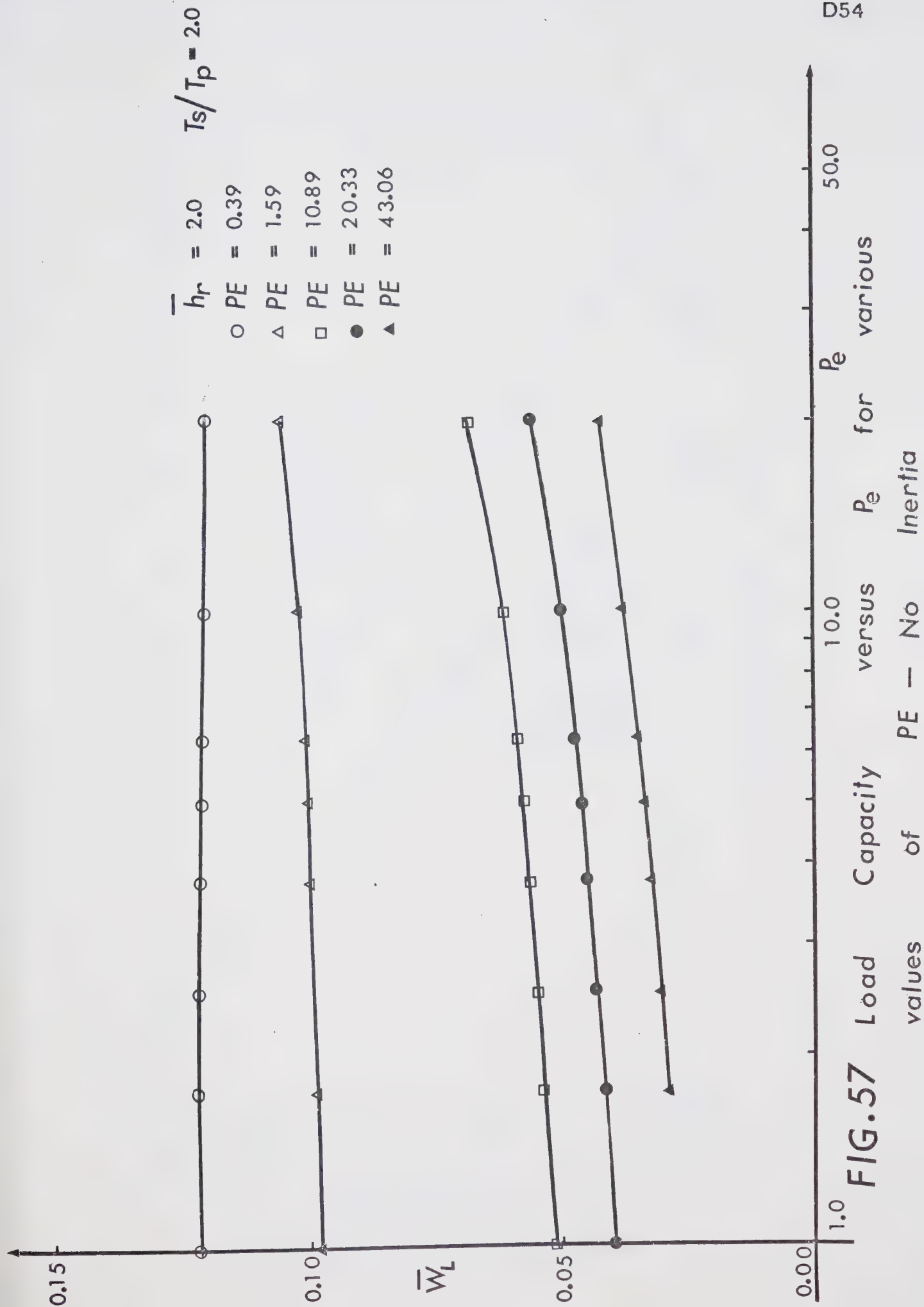


FIG. 56



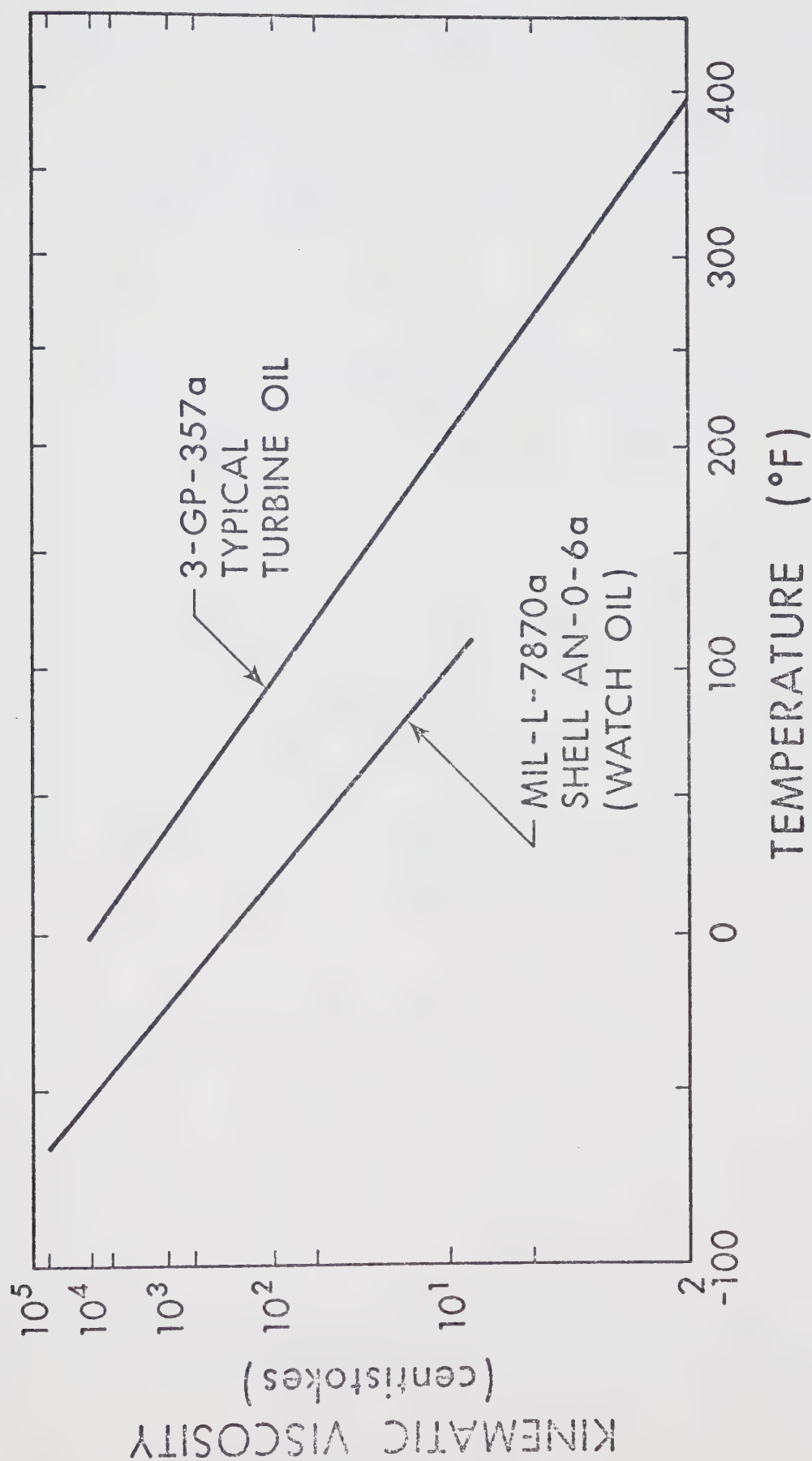


Fig. 58. Viscosity Temperature relationships for medium and for light oil

APPENDIX E
TABLES FOR CHAPTER IV

TABLE 1a
EFFECT OF COOLING SLIDER - NO INERTIA

(i)	T_p = 100°F	PE = 1.0	P_e = 5.0		
$T_s / (°F)$	T_s / T_p	\bar{W}	\bar{D}	\bar{y}	$T_b (°F)$
350	3.50	0.10686	-0.52803	0.41305	309.69
320	3.20	0.10430	-0.52235	0.41832	284.26
290	2.90	0.10365	-0.52603	0.42747	258.99
260	2.60	0.10446	-0.53811	0.43993	233.82
230	2.30	0.10411	-0.54576	0.45677	208.66
200	2.00	0.10618	-0.56244	0.48231	183.74
170	1.70	0.10998	-0.58287	0.51891	159.16
140	1.40	0.11809	-0.61372	0.56994	135.16
110	1.10	0.13734	-0.66794	0.64391	112.08
100	1.00	0.14117	-0.66856	0.67176	104.47
80	0.80	0.16075	-0.69874	0.73876	89.79
50	0.50	0.20833	-0.73298	0.85609	68.56
30	0.30	0.25468	-0.73761	0.93640	54.74
20	0.20	0.28639	-0.74353	0.97425	47.89
(ii)	T_p = 100°F	PE = 1.0	P_e = 10.0		
350	3.50	0.10543	-0.52622	0.41543	309.20
320	3.20	0.10343	-0.52166	0.42047	283.77
290	2.90	0.10301	-0.52635	0.42948	258.41
260	2.60	0.10407	-0.54011	0.44151	233.11
230	2.30	0.10438	-0.54990	0.45786	207.85
200	2.00	0.10725	-0.56985	0.48301	182.79
170	1.70	0.11165	-0.59436	0.51887	158.05
140	1.40	0.12078	-0.63159	0.56986	133.88
110	1.10	0.14152	-0.69586	0.64472	110.60
100	1.00	0.14509	-0.69533	0.67282	102.99
80	0.80	0.16582	-0.73328	0.73994	88.26
50	0.50	0.21477	-0.77508	0.85906	67.00
30	0.30	0.26380	-0.78445	0.94035	53.18
20	0.20	0.29745	-0.79175	0.97875	46.31

TABLE 1b

EFFECT OF HEATING PAD - NO INERTIA

(i)	$T_s = 100^\circ\text{F}$	$PE = 1.0$	$P_e = 5.0$	
T_p ($^\circ\text{F}$)	T_s/T_p	\bar{W}	$\bar{\psi}_c$	T_b ($^\circ\text{F}$)
20.0	5.00	0.09226	0.38552	86.67
22.2	4.50	0.09273	0.39285	86.95
25.0	4.00	0.09367	0.40315	87.30
30.0	3.33	0.09606	0.42110	88.03
36.4	2.75	0.10037	0.44428	89.08
50.0	2.00	0.10753	0.49547	91.63
80.0	1.25	0.12676	0.60667	98.78
110.0	0.91	0.15054	0.70059	107.59
140.0	0.71	0.17277	0.77751	117.06
170.0	0.59	0.19707	0.83114	127.18
200.0	0.50	0.22185	0.87267	137.20
230.0	0.44	0.24471	0.90143	147.38
260.0	0.39	0.26628	0.92054	157.50
290.0	0.35	0.28208	0.93512	167.49
320.0	0.31	0.29894	0.94584	177.53
350.0	0.29	0.31641	0.95245	187.59
(ii)	$T_s = 100^\circ\text{F}$	$PE = 1.0$	$P_e = 10.0$	
20.0	5.00	0.09075	0.38871	86.74
22.2	4.50	0.09106	0.39630	86.97
25.0	4.00	0.09293	0.40579	87.30
30.0	3.33	0.09557	0.42337	87.95
36.4	2.75	0.10040	0.44603	88.86
50.0	2.00	0.10861	0.49612	91.13
80.0	1.25	0.12983	0.60688	97.67
110.0	0.91	0.15536	0.70068	105.90
140.0	0.71	0.17822	0.77972	114.92
170.0	0.59	0.20390	0.83497	124.56
200.0	0.50	0.23035	0.87727	134.08
230.0	0.44	0.25450	0.90671	143.73
260.0	0.39	0.27821	0.92680	153.32
290.0	0.35	0.29551	0.94135	162.77
320.0	0.31	0.31366	0.95222	172.24
350.0	0.29	0.33362	0.95930	181.68

TABLE 1c
EFFECT OF COOLING SLIDER AND HEATING PAD - NO INERTIA

(i) $T_s + T_p = 350^\circ\text{F}$		$PE = 1.0$		$P_e = 5.0$		
T_s ($^\circ\text{F}$)	T_p ($^\circ\text{F}$)	T_s/T_p	\bar{W}	\bar{D}	\bar{y}_c	T_b ($^\circ\text{F}$)
300.0	50.00	6.00	0.098232	-0.44374	0.35408	262.26
286.4	63.63	4.50	0.09922	-0.46821	0.37487	251.76
275.0	75.00	3.67	0.09988	-0.48804	0.39376	243.27
262.5	87.50	3.00	0.10143	-0.51141	0.41756	234.14
250.0	100.0	2.50	0.10344	-0.53500	0.44485	225.38
225.0	125.0	1.80	0.10979	-0.58156	0.50862	209.12
200.0	150.0	1.33	0.12183	-0.62684	0.58494	194.89
175.0	175.0	1.00	0.14110	-0.67023	0.67186	182.82
150.0	200.0	0.75	0.16824	-0.70426	0.76085	172.35
125.0	225.0	0.56	0.20623	-0.73299	0.84409	163.00
100.0	250.0	0.40	0.25727	-0.76130	0.91513	153.99
75.00	275.0	0.27	0.31873	-0.78823	0.97108	145.00
50.00	300.0	0.17	0.39116	-0.81890	1.01270	135.46

(ii) $T_s + T_p = 350^\circ\text{F}$		$PE = 1.0$		$P_e = 10.0$		
T_s ($^\circ\text{F}$)	T_p ($^\circ\text{F}$)	T_s/T_p	\bar{W}	\bar{D}	\bar{y}_c	T_b ($^\circ\text{F}$)
300.0	50.00	6.00	0.09537	-0.43740	0.35815	262.49
286.4	63.63	4.50	0.09692	-0.46349	0.37820	251.77
275.0	75.00	3.67	0.09823	-0.48510	0.39662	243.08
262.5	87.50	3.00	0.10051	-0.51087	0.41981	233.70
250.0	100.0	2.50	0.10333	-0.53739	0.44624	224.67
225.0	125.0	1.80	0.11129	-0.59169	0.50890	207.78
200.0	150.0	1.33	0.12488	-0.64658	0.58482	192.89
175.0	175.0	1.00	0.14524	-0.69733	0.67231	180.23
150.0	200.0	0.75	0.17329	-0.74051	0.76295	169.28
125.0	225.0	0.56	0.21349	-0.77690	0.84822	159.48
100.0	250.0	0.40	0.26822	-0.81363	0.92109	150.02
75.0	275.0	0.27	0.33713	-0.85034	0.97768	140.52
50.0	300.0	0.17	0.42113	-0.89337	1.01880	130.39

TABLE 1d

EFFECT OF LUBRICANT TEMP ON LOAD CAPACITY

T_s ($^{\circ}\text{F}$)	T_p ($^{\circ}\text{F}$)	$T_s + T_p$ ($^{\circ}\text{F}$)	\bar{W}	\bar{V}_C	T_b ($^{\circ}\text{F}$)
350	175	525	0.11465	0.50617	321.09
300	150	450	0.11231	0.49709	275.46
250	125	375	0.10817	0.48886	229.59
233.34	116.67	350	0.10797	0.49040	213.77
200	100	300	0.10618	0.48231	183.74
150	75	225	0.10445	0.48241	137.70
100	50	150	0.10753	0.49547	91.63
75	37.5	112.5	0.11285	0.51310	68.59
50	25	75	0.11683	0.53914	45.55
175	350	525	0.22010	0.84798	262.50
150	300	450	0.22318	0.85768	225.00
125	250	375	0.22167	0.86622	171.39
116.67	233.34	350	0.22457	0.87073	159.62
100	200	300	0.22185	0.87267	137.20
75	150	225	0.21673	0.87154	102.88
50	100	150	0.20830	0.85609	68.56
37.5	75	112.5	0.20279	0.83610	51.41
25	50	75	0.18825	0.80689	34.17

TABLE 2a
INFLUENCE OF INERTIA TERMS

(i) Viscosity Constant				
Re^*	\bar{W}	\bar{D}	$\bar{\psi}_C$	
0.0	0.15886	-0.77267	0.66663	
0.05	0.15948	-0.77697	0.66518	
0.075	0.15978	-0.77911	0.66446	
0.10	0.16009	-0.78125	0.66374	
0.20	0.16134	-0.78932	0.66103	
0.30	0.16258	-0.79722	0.65838	
0.40	0.16384	-0.80484	0.65582	
0.50	0.16509	-0.81219	0.65334	
0.60	0.16636	-0.81928	0.65096	
0.70	0.16763	-0.82611	0.64866	
0.80	0.16891	-0.83269	0.64644	
0.90	0.17019	-0.83902	0.64430	
1.00	0.17148	-0.84512	0.64224	
1.10	0.17278	-0.85099	0.64026	
1.20	0.17409	-0.85662	0.63835	

(ii) $T_s = 200^\circ F$ $T_p = 100^\circ F$ $P = 59.64$ $PE = 0.5357$				
Re^*	\bar{W}^0	\bar{W}^*	\bar{D}^*	$\bar{\psi}_C^*$ T_b^*
0.0	0.12671	0.12671	-0.66414	0.53432 179.62
0.05	0.12671	0.12734	-0.66663	0.53292 179.68
0.075	0.12669	0.12764	-0.66707	0.53290 179.68
0.10	0.12673	0.12800	-0.66814	0.53268 179.64
0.20	0.12692	0.12951	-0.67346	0.53126 179.46

TABLE 2a (Continued)

Re *	\bar{W}^O	\bar{W}^*	\bar{D}^*	\bar{y}_C	T_b^*
0.30	0.12699	0.13088	-0.67855	0.52958	179.36
0.40	0.12695	0.13215	-0.68323	0.52782	179.33
0.50	0.12686	0.13333	-0.68762	0.52606	179.34
0.60	0.12674	0.13448	-0.69180	0.52431	179.36
0.70	0.12662	0.13563	-0.69583	0.52254	179.40
0.80	0.12651	0.13676	-0.69971	0.52081	179.45
0.90	0.12640	0.13790	-0.70350	0.51910	179.50
1.00	0.12630	0.13903	-0.70718	0.51741	179.56
1.10	0.12622	0.14016	-0.71076	0.51576	179.62
1.20	0.12613	0.14128	-0.71423	0.51414	179.68

O - Inertia not included

* - Inertia included

INFLUENCE OF INERTIA TERMS

E7

(i) $T_s = 150^\circ\text{F}$		T_p	\bar{W}^*	\bar{D}^*	\bar{y}^*	$T_b (^{\circ}\text{F})^*$
			W			
0.0		0.15042	0.15042	-0.72243	0.66840	154.79
0.05		0.15042	0.15231	-0.73500	0.66653	154.06
0.075		0.15148	0.15096	-0.72652	0.66690	154.79
0.10		0.15223	0.15336	-0.74214	0.66598	153.50
0.20		0.15401	0.15636	-0.76263	0.66317	152.25
0.30		0.15494	0.15854	-0.77679	0.66027	151.66
0.40		0.15553	0.16038	-0.78823	0.65748	151.32
0.50		0.15594	0.16204	-0.79816	0.65482	151.10
0.60		0.15625	0.16362	-0.80715	0.65225	150.95
0.70		0.15651	0.16513	-0.81548	0.64978	150.83
0.80		0.15670	0.16659	-0.82329	0.64741	150.74
0.90		0.15686	0.16803	-0.83070	0.64511	150.67
1.00		0.15700	0.16945	-0.83776	0.64289	150.62
1.10		0.15711	0.17085	-0.84453	0.64074	150.57
1.20		0.15721	0.17224	-0.85104	0.63865	150.53
(ii) $T_s = 100^\circ\text{F}$		T_p	W	D	y	$T_b (^{\circ}\text{F})$
0.0		0.20254	0.20254	-0.77764	0.80801	135.70
0.05		0.20254	0.20301	-0.78324	0.80699	135.68
0.075		0.20490	0.20560	-0.80131	0.80823	134.18
0.10		0.20633	0.20726	-0.81521	0.80869	133.13
0.20		0.20923	0.21111	-0.85204	0.80767	130.93
0.30		0.21074	0.21363	-0.87661	0.80542	129.92
0.40		0.21176	0.21567	-0.89633	0.80297	129.32
0.50		0.21252	0.21750	-0.91342	0.80055	128.90
0.60		0.21310	0.21917	-0.92896	0.79822	128.58
0.70		0.21357	0.22077	-0.94325	0.79595	128.32
0.80		0.21396	0.22233	-0.95677	0.79369	128.10
0.90		0.21432	0.22389	-0.96966	0.79147	127.92
1.00		0.21464	0.22541	-0.98200	0.78932	127.75
1.10		0.21493	0.22692	-0.99383	0.78720	127.59
1.20		0.21518	0.22842	-1.00520	0.78512	127.45
o	-	Inertia not included				
*	-	Inertia included				

o - Inertia not included
 * - Inertia included

TABLE 2c
% INCREASE IN LOAD CAPACITY DUE TO PRESENCE OF INERTIA TERMS

T_s (°F)	T_p (°F)	Re [*]	\bar{W}^O	\bar{W}^*	$\bar{W}^* - \bar{W}^O$	% increase in load capacity
200	100	0.2	0.12692	0.12951	0.00259	2.04
200	100	0.4	0.12695	0.13215	0.00520	4.10
200	100	0.6	0.12674	0.13448	0.00774	6.11
200	100	0.8	0.12651	0.13676	0.01025	8.12
200	100	1.0	0.12630	0.13903	0.01273	10.07
Constant						
		0.2	0.15886	0.16134	0.00248	1.56
		0.4	0.15886	0.16384	0.00498	3.14
		0.6	0.15886	0.16636	0.00750	4.72
		0.8	0.15886	0.16891	0.01005	6.34
		1.0	0.15886	0.17148	0.01262	7.95
Viscosity						
150	150	0.2	0.15401	0.15636	0.00235	1.53
150	150	0.4	0.15553	0.16038	0.00485	3.12
150	150	0.6	0.15625	0.16362	0.00737	4.72
150	150	0.8	0.15670	0.16659	0.00989	6.30
150	150	1.0	0.15700	0.16945	0.01245	7.94
Inertia terms not included						
100	200	0.2	0.20923	0.21111	0.00188	0.90
100	200	0.4	0.21176	0.21567	0.00391	1.84
100	200	0.6	0.21310	0.21917	0.00607	2.85
100	200	0.8	0.21396	0.22233	0.00837	3.91
100	200	1.0	0.21464	0.22541	0.01077	5.02
Inertia terms included						

TABLE 3a

VARYING INLET TO OUTLET RATIO - NO INERTIA

(i)	$T_s = 150^\circ\text{F}$	$T_p = 150^\circ\text{F}$	\bar{D}	\bar{y}_c	$P_e = 1.0$	$P_e = 6.0$	$T_b (^\circ\text{F})$
m	\bar{W}						
0.25	0.07937	-0.78011	0.55844				157.17
0.50	0.11690	-0.73325	0.60401				156.72
0.75	0.13492	-0.70102	0.64138				156.38
1.00	0.14243	-0.67707	0.67255				156.12
1.25	0.14414	-0.65834	0.69898				155.92
1.50	0.14258	-0.64296	0.72163				155.74
1.75	0.13916	-0.62973	0.74124				155.59
2.00	0.13473	-0.61817	0.75841				155.45
(ii)	$T_s = 150^\circ\text{F}$	$T_p = 150^\circ\text{F}$	\bar{D}	\bar{y}_c	$P_e = 1.0$	$P_e = 1.25$	
0.25	0.07454	-0.73991	0.55653				160.05
0.50	0.11013	-0.69063	0.60121				160.02
0.75	0.12679	-0.65617	0.63790				160.04
1.00	0.13346	-0.63035	0.66854				160.10
1.25	0.13464	-0.60991	0.69448				160.17
1.50	0.13279	-0.59303	0.71671				160.25
1.75	0.12927	-0.57858	0.73593				160.32
2.00	0.12486	-0.56590	0.75270				160.38
(iii)	$T_s = 150^\circ\text{F}$	$T_p = 150^\circ\text{F}$	\bar{D}	\bar{y}_c	$P_e = 1.0$	$P_e = 0.10$	
0.25	0.07040	-0.71668	0.55538				162.22
0.50	0.10508	-0.66848	0.59906				162.26
0.75	0.12081	-0.63414	0.63484				162.38
1.00	0.12672	-0.60808	0.66472				162.56
1.25	0.12730	-0.58710	0.69008				162.76
1.50	0.12502	-0.56951	0.71191				162.97
1.75	0.12119	-0.55429	0.73083				163.18
2.00	0.11662	-0.54084	0.74739				163.40

TABLE 3b

VARYING INLET TO OUTLET RATIO - NO INERTIA

(i)	$T_s = 200^\circ\text{F}$	$T_p = 100^\circ\text{F}$	$\bar{P}_e = 1.0$	$\bar{P}_e = 6.0$
m	\bar{w}	\bar{D}	\bar{w}_c	$T_b (^\circ\text{F})$
0.25	0.055318	-0.70199	0.39678	181.06
0.50	0.085617	-0.64392	0.43024	181.65
0.75	0.10016	-0.59959	0.45837	182.50
1.00	0.10637	-0.56406	0.48254	183.51
1.25	0.10789	-0.53441	0.50359	184.64
1.50	0.10675	-0.50896	0.52225	185.84
1.75	0.10405	-0.48666	0.53912	187.06
2.00	0.10045	-0.46720	0.55471	188.22
(ii)	$T_s = 200^\circ\text{F}$	$T_p = 100^\circ\text{F}$	$\bar{P}_e = 1.0$	$\bar{P}_e = 1.25$
0.25	0.05713	-0.68389	0.39761	182.66
0.50	0.08599	-0.63011	0.43012	183.15
0.75	0.09957	-0.58973	0.45720	183.84
1.00	0.10516	-0.55780	0.48007	184.66
1.25	0.10633	-0.53151	0.49963	185.58
1.50	0.10499	-0.50917	0.51655	186.57
1.75	0.10223	-0.48969	0.53137	187.62
2.00	0.09867	-0.47228	0.54438	188.72
(iii)	$T_s = 200^\circ\text{F}$	$T_p = 100^\circ\text{F}$	$\bar{P}_e = 1.0$	$\bar{P}_e = 0.10$
0.25	0.05619	-0.66536	0.39840	184.58
0.50	0.08533	-0.61616	0.43010	184.89
0.75	0.09879	-0.57932	0.45642	185.40
1.00	0.10414	-0.55027	0.47861	186.05
1.25	0.10504	-0.52645	0.49760	186.78
1.50	0.10348	-0.50625	0.51405	187.58
1.75	0.10059	-0.48878	0.52846	188.42
2.00	0.09700	-0.47333	0.54113	189.29

TABLE 3c
VARYING INLET TO OUTLET RATIO - NO INERTIA

(i)	T_s	T_p	$T_p = 200^\circ\text{F}$	\bar{D}	$\bar{\psi}_c$	P_e	T_b
m	$T_s = 100^\circ\text{F}$	\bar{w}				$P_e = 6.0$	($^\circ\text{F}$)
0.25		0.12494	-0.75248	0.72352			141.90
0.50		0.18236	-0.73949	0.78378			140.09
0.75		0.21113	-0.74252	0.83315			138.22
1.00		0.22432	-0.75330	0.87428			136.32
1.25		0.22875	-0.76805	0.90893			134.40
1.50		0.22811	-0.78460	0.93847			132.49
1.75		0.22456	-0.80276	0.96347			130.60
2.00		0.21648	-0.82911	0.97827			128.23
(ii)	T_s	T_p	$T_p = 200^\circ\text{F}$	\bar{D}	$\bar{\psi}_c$	P_e	T_b
0.25	$T_s = 100^\circ\text{F}$	0.11338	-0.70483	0.71602		$P_e = 1.25$	145.46
0.50		0.16551	-0.67762	0.77303			144.77
0.75		0.18993	-0.66579	0.81939			143.96
1.00		0.19948	-0.66150	0.85789			143.03
1.25		0.20110	-0.66092	0.89035			141.99
1.50		0.19847	-0.66248	0.91821			140.86
1.75		0.19360	-0.66508	0.94242			139.64
2.00		0.18760	-0.66844	0.96359			138.36
(iii)	T_s	T_p	$T_p = 200^\circ\text{F}$	\bar{D}	$\bar{\psi}_c$	P_e	T_b
0.25	$T_s = 100^\circ\text{F}$	0.10184	-0.67818	0.71235		$P_e = 0.10$	147.62
0.50		0.14995	-0.64491	0.76689			147.48
0.75		0.17064	-0.62565	0.81077			147.28
1.00		0.17704	-0.61277	0.84684			146.98
1.25		0.17621	-0.60326	0.87705			146.61
1.50		0.17161	-0.59540	0.90269			146.15
1.75		0.16521	-0.58854	0.92474			145.62
2.00		0.15799	-0.58222	0.94378			145.01

TABLE 4a

DISSIPATION EFFECTS - NO INERTIA

(i) $T_s/T_p = 0.5$		$P_e = 5.0$				
T_s ($^{\circ}\text{F}$)	T_p ($^{\circ}\text{F}$)	PE	\bar{W}	\bar{D}	\bar{W}_c	T_b ($^{\circ}\text{F}$)
55	110	0.5646	0.22167	-0.77857	0.86261	74.044
55	110	1.2704	0.20864	-0.71779	0.85978	76.312
55	110	2.2585	0.19409	-0.65143	0.85600	79.162
55	110	3.5290	0.17837	-0.58442	0.85306	82.370
55	110	5.0817	0.16334	-0.52289	0.84897	85.819
55	110	6.9168	0.14947	-0.46795	0.84438	89.346
55	110	9.0342	0.13734	-0.41988	0.84099	92.894
55	110	11.4340	0.12592	-0.37770	0.83658	96.471
55	110	14.1160	0.11585	-0.34122	0.83244	100.040
55	110	17.0800	0.10722	-0.30977	0.82920	103.460
55	110	20.3270	0.09907	-0.28196	0.82543	106.940
(ii) $T_s/T_p = 1.0$		$P_e = 5.0$				
82.5	82.5	0.56460	0.15021	-0.72206	0.66941	84.701
82.5	82.5	1.27040	0.14030	-0.66314	0.67320	87.175
82.5	82.5	2.25850	0.12931	-0.59758	0.67660	90.176
82.5	82.5	3.52900	0.11817	-0.53438	0.68015	93.549
82.5	82.5	5.08170	0.10800	-0.47838	0.68280	97.060
82.5	82.5	6.91680	0.09881	-0.42857	0.68524	100.700
82.5	82.5	9.03420	0.09037	-0.38439	0.68759	104.310
82.5	82.5	11.43400	0.08299	-0.34623	0.68909	108.000
82.5	82.5	14.11600	0.07691	-0.31373	0.69057	111.650
82.5	82.5	17.08000	0.07149	-0.28624	0.69176	114.960
82.5	82.5	20.32700	0.06616	-0.26156	0.69224	118.380

TABLE 4a (Continued)

(iii) $T_s/T_p = 2.0$		$P_e = 5.0$				
T_s ($^{\circ}\text{F}$)	T_p ($^{\circ}\text{F}$)	PE	\bar{W}	\bar{D}	$\bar{\psi}_C$	T_b ($^{\circ}\text{F}$)
110	55	0.5646	0.11324	-0.60125	0.48631	99.478
110	55	1.2704	0.10466	-0.55727	0.49423	101.710
110	55	2.2585	0.09515	-0.50916	0.50378	104.480
110	55	3.5290	0.08617	-0.46042	0.51194	107.620
110	55	5.0817	0.07759	-0.41546	0.52047	110.940
110	55	6.9168	0.07030	-0.37451	0.52866	114.380
110	55	9.0342	0.06388	-0.33847	0.53611	117.820
110	55	11.4340	0.05804	-0.30716	0.54341	121.320
110	55	14.1160	0.05337	-0.27970	0.55047	124.760
110	55	17.0800	0.04940	-0.25642	0.55577	128.170
110	55	20.3270	0.04617	-0.23636	0.56124	131.320

TABLE 4b
DISSIPATION EFFECTS - NO INERTIA

(i) $T_s/T_p = 0.5$		$P_e = 10.0$				
T_s ($^{\circ}\text{F}$)	T_p ($^{\circ}\text{F}$)	PE	\bar{W}	\bar{D}	$\bar{\psi}_c$	T_b ($^{\circ}\text{F}$)
55	110	0.56460	0.22628	-0.81214	0.86459	72.800
55	110	1.27040	0.21704	-0.76688	0.86449	74.317
55	110	2.25850	0.20596	-0.71347	0.86421	76.289
55	110	3.52900	0.19350	-0.65696	0.86401	78.614
55	110	5.08170	0.18147	-0.60201	0.86421	81.099
55	110	6.91680	0.16954	-0.55006	0.86345	83.791
55	110	9.03420	0.15816	-0.50285	0.86233	86.592
55	110	11.43400	0.14808	-0.46042	0.86205	89.315
55	110	14.11600	0.13839	-0.42230	0.86104	92.146
55	110	17.08000	0.12982	-0.38831	0.85947	95.024
55	110	20.32700	0.12197	-0.35833	0.85918	97.719

(ii) $T_s/T_p = 1.0$		$P_e = 10.0$				
T_s ($^{\circ}\text{F}$)	T_p ($^{\circ}\text{F}$)	PE	\bar{W}	\bar{D}	$\bar{\psi}_c$	T_b ($^{\circ}\text{F}$)
82.5	82.5	0.56460	0.15240	-0.73759	0.66947	83.950
82.5	82.5	1.27040	0.14480	-0.69643	0.67343	85.637
82.5	82.5	2.25850	0.13555	-0.64413	0.67840	87.781
82.5	82.5	3.52900	0.12633	-0.59191	0.68279	90.216
82.5	82.5	5.08170	0.11707	-0.54112	0.68732	92.884
82.5	82.5	6.91680	0.10865	-0.49432	0.69107	95.698
82.5	82.5	9.03420	0.10091	-0.45246	0.69513	98.549
82.5	82.5	11.43400	0.09350	-0.41407	0.69841	101.460
82.5	82.5	14.11600	0.08736	-0.38043	0.70183	104.330
82.5	82.5	17.08000	0.08184	-0.35019	0.70428	107.250
82.5	82.5	20.32700	0.07632	-0.32267	0.70657	110.130

TABLE 4b (Continued)

(iii) $T_s/T_p = 2.0$		$P_e = 10.0$				
T_s (°F)	T_p (°F)	PE	\bar{W}	\bar{D}	$\bar{\Psi}_C$	T_b (°F)
110	55	0.5646	0.11326	-0.60111	0.48805	99.357
110	55	1.2704	0.10620	-0.56881	0.49421	100.920
110	55	2.2585	0.09794	-0.53154	0.50199	102.920
110	55	3.5290	0.08974	-0.49242	0.51011	105.240
110	55	5.0817	0.08212	-0.45310	0.51749	107.790
110	55	6.9168	0.07455	-0.41691	0.52550	110.460
110	55	9.0342	0.06833	-0.38340	0.53288	113.220
110	55	11.4340	0.06264	-0.35289	0.54009	116.010
110	55	14.1160	0.05756	-0.32590	0.54715	118.810
110	55	17.0800	0.05299	-0.30154	0.55401	121.610
110	55	20.3270	0.04956	-0.28005	0.55897	124.450

TABLE 4c
DISSIPATION EFFECTS - NO INERTIA

(i) $T_s/T_p = 0.5$		$P_e = 15.0$				
T_s ($^{\circ}\text{F}$)	T_p ($^{\circ}\text{F}$)	PE	\bar{W}	\bar{D}	$\bar{\psi}_c$	T_b ($^{\circ}\text{F}$)
55	110	0.5646	0.22827	-0.83013	0.86447	72.230
55	110	1.2704	0.22089	-0.79266	0.86556	73.379
55	110	2.2585	0.21149	-0.74799	0.86653	74.886
55	110	3.5290	0.20092	-0.69886	0.86792	76.694
55	110	5.0817	0.19022	-0.64955	0.86986	78.662
55	110	6.9168	0.17961	-0.60160	0.87091	80.816
55	110	9.0342	0.15978	-0.51537	0.87356	85.327
55	110	14.1160	0.15061	-0.47727	0.87405	87.703
55	110	17.0800	0.14236	-0.44281	0.87426	90.064
55	110	20.3270	0.13458	-0.41161	0.87448	92.477

(ii) $T_s/T_p = 1.0$		$P_e = 15.0$				
T_s ($^{\circ}\text{F}$)	T_p ($^{\circ}\text{F}$)	PE	\bar{W}	\bar{D}	$\bar{\psi}_c$	T_b ($^{\circ}\text{F}$)
82.5	82.5	0.5646	0.15360	-0.74540	0.66917	83.579
82.5	82.5	1.2704	0.14749	-0.71444	0.67268	84.855
82.5	82.5	2.2585	0.13936	-0.67224	0.67778	86.508
82.5	82.5	3.5290	0.13120	-0.62640	0.68274	88.454
82.5	82.5	5.0817	0.12272	-0.58121	0.68768	90.560
82.5	82.5	6.9168	0.11468	-0.53828	0.69248	92.839
82.5	82.5	9.0342	0.10704	-0.49774	0.69697	95.211
82.5	82.5	11.4340	0.10031	-0.46153	0.70134	97.637
82.5	82.5	14.1160	0.09374	-0.42754	0.70536	100.080
82.5	82.5	17.0800	0.08815	-0.39714	0.70858	102.570
82.5	82.5	20.3270	0.08308	-0.36985	0.71266	104.980

TABLE 4d
DISSIPATION EFFECTS - NO INERTIA

(i) $T_s/T_p = 0.5$		$P_e = 20.0$				
T_s (°F)	T_p (°F)	PE	\bar{w}	\bar{D}	$\bar{\psi}_c$	T_b (°F)
55	110	0.5646	0.22962	-0.84150	0.86392	71.899
55	110	1.2704	0.22320	-0.80961	0.86542	72.828
55	110	2.2585	0.21519	-0.77049	0.86721	74.056
55	110	3.5290	0.20571	-0.72712	0.86921	75.542
55	110	5.0817	0.19560	-0.68150	0.87224	77.187
55	110	6.9168	0.18595	-0.63730	0.87452	78.998
55	110	9.0342	0.17620	-0.59417	0.87657	80.916
55	110	11.4340	0.16723	-0.55458	0.87922	82.827
55	110	14.1160	0.15871	-0.51762	0.88110	84.834
55	110	17.0800	0.15051	-0.48349	0.88265	86.898
55	110	20.3270	0.14298	-0.45189	0.88370	88.990

(ii) $T_s/T_p = 1.0$		$P_e = 20.0$				
T_s (°F)	T_p (°F)	PE	\bar{w}	\bar{D}	$\bar{\psi}_c$	T_b (°F)
82.5	82.5	0.5646	0.15436	-0.75010	0.66896	83.360
82.5	82.5	1.2704	0.14920	-0.72514	0.67208	84.387
82.5	82.5	2.2585	0.14201	-0.69019	0.67694	85.736
82.5	82.5	3.5290	0.13413	-0.64966	0.68231	87.339
82.5	82.5	5.0817	0.12673	-0.60931	0.68723	89.105
82.5	82.5	6.9168	0.11880	-0.56884	0.69248	91.024
82.5	82.5	9.0342	0.11170	-0.53130	0.69727	93.054
82.5	82.5	11.4340	0.10493	-0.49584	0.70212	95.126
82.5	82.5	14.1160	0.09862	-0.46302	0.70650	97.266
82.5	82.5	17.0800	0.09286	-0.43301	0.71087	99.423
82.5	82.5	20.327	0.08778	-0.40577	0.71546	101.480

TABLE 4d (Continued)

(iii) $T_s/T_p = 2.0$		$P_e = 20.0$				
T_s ($^{\circ}\text{F}$)	T_p ($^{\circ}\text{F}$)	PE	\bar{W}	\bar{D}	$\bar{\psi}_c$	T_b ($^{\circ}\text{F}$)
110	55	0.5646	0.11325	-0.60213	0.49018	99.161
110	55	1.2704	0.10834	-0.58115	0.49419	100.140
110	55	2.2585	0.10211	-0.55541	0.49962	101.410
110	55	3.5290	0.09527	-0.52713	0.50592	102.940
110	55	5.0817	0.08857	-0.49748	0.51243	104.660
110	55	6.9168	0.08219	-0.46726	0.51874	106.530
110	55	9.0342	0.07573	-0.43848	0.52540	108.470
110	55	11.4340	0.07010	-0.41171	0.53207	110.490
110	55	14.1160	0.06493	-0.38632	0.53878	112.550
110	55	17.0800	0.06060	-0.36268	0.54439	114.710
110	55	20.3270	0.05622	-0.34108	0.55075	116.800

TABLE 5a
CONVECTION EFFECTS - NO INERTIA

(i) $T_s/T_p = 0.5$		$PE = 0.39253$			
$T_s (^{\circ}F)$	$T_p (^{\circ}F)$	Pe	\bar{W}	\bar{D}	$T_b (^{\circ}F)$
150	300	1.00	0.22161	-0.75787	206.76
150	300	1.75	0.22725	-0.77595	204.88
150	300	2.50	0.23092	-0.79047	203.35
150	300	3.75	0.23438	-0.80796	201.41
150	300	5.00	0.23658	-0.82122	200.04
150	300	6.25	0.23805	-0.83173	199.03
150	300	10.00	0.24064	-0.85258	197.15
150	300	20.00	0.24385	-0.87895	195.07
(ii) $T_s/T_p = 1.0$		$PE = 0.39253$			
225	225	1.00	0.14896	-0.71744	231.77
225	225	1.75	0.15012	-0.72161	231.16
225	225	2.50	0.15093	-0.72546	230.61
225	225	3.75	0.15185	-0.73101	229.84
225	225	5.00	0.15256	-0.73571	229.23
225	225	6.25	0.15305	-0.73945	228.74
225	225	10.00	0.15416	-0.74713	227.77
225	225	20.00	0.15561	-0.75628	226.64
(iii) $T_s/T_p = 2.0$		$PE = 0.39253$			
300	150	1.00	0.12188	-0.64284	269.11
300	150	1.75	0.12180	-0.64012	269.36
300	150	2.50	0.12162	-0.63781	269.56
300	150	3.75	0.12126	-0.63494	269.79
300	150	5.00	0.12098	-0.63299	269.92
300	150	6.25	0.12083	-0.63169	269.99
300	150	10.00	0.12047	-0.62954	270.04
300	150	20.00	0.11999	-0.62747	269.91

TABLE 5b
CONVECTION EFFECTS - NO INERTIA

(i) $T_s/T_p = 0.5$		PE = 1.59			
T_s (°F)	T_p (°F)	P_e	\bar{W}	\bar{D}	T_b (°F)
105	210	1.00	0.17905	-0.59752	155.80
105	210	1.75	0.19001	-0.62237	153.71
105	210	2.50	0.19777	-0.64383	151.89
105	210	3.75	0.20643	-0.67346	149.39
105	210	5.00	0.21216	-0.69661	147.48
105	210	6.25	0.21630	-0.71538	146.00
105	210	10.00	0.22375	-0.75442	143.10
105	210	20.00	0.23222	-0.80588	139.77
(ii) $T_s/T_p = 1.0$		PE = 1.59			
157.5	157.5	1.00	0.12256	-0.57390	173.64
157.5	157.5	1.75	0.12595	-0.58417	172.51
157.5	157.5	2.50	0.12862	-0.59577	171.29
157.5	157.5	3.75	0.13170	-0.61283	169.60
157.5	157.5	5.00	0.13386	-0.62739	168.21
157.5	157.5	6.25	0.13563	-0.63977	167.08
157.5	157.5	10.00	0.13949	-0.66661	164.75
157.5	157.5	20.00	0.14489	-0.70149	161.90
(iii) $T_s/T_p = 2.0$		PE = 1.59			
210	105	1.00	0.09813	-0.51763	198.67
210	105	1.75	0.09881	-0.52046	198.13
210	105	2.50	0.09918	-0.52302	197.66
210	105	3.75	0.09957	-0.52756	196.91
210	105	5.00	0.09997	-0.53225	196.24
210	105	6.25	0.10042	-0.53673	195.64
210	105	10.00	0.10191	-0.54777	194.27
210	105	20.00	0.10484	-0.56434	192.34

TABLE 5c
CONVECTION EFFECTS - NO INERTIA

(i) $T_s/T_p = 0.5$		PE = 10.89				
T_s ($^{\circ}\text{F}$)	T_p ($^{\circ}\text{F}$)	P_e	\bar{W}	\bar{D}	\bar{Y}_c	T_b ($^{\circ}\text{F}$)
65	130	1.00	0.08443	-0.28158	0.79737	124.45
65	130	1.75	0.09563	-0.30098	0.80653	121.35
65	130	2.50	0.10554	-0.32085	0.81593	118.91
65	130	3.75	0.11806	-0.35099	0.83010	115.48
65	130	5.00	0.12749	-0.37853	0.84132	112.44
65	130	6.25	0.13488	-0.40270	0.85034	109.92
65	130	10.00	0.14993	-0.46045	0.86748	104.38
65	130	20.00	0.16925	-0.55289	0.88451	97.08
(ii) $T_s/T_p = 1.0$		PE = 10.89				
97.5	97.5	1.00	0.06473	-0.27774	0.66928	135.76
97.5	97.5	1.75	0.06930	-0.28857	0.67421	133.74
97.5	97.5	2.50	0.07357	-0.30253	0.67846	131.71
97.5	97.5	3.75	0.07896	-0.32528	0.68426	128.70
97.5	97.5	5.00	0.08278	-0.34565	0.68861	126.10
97.5	97.5	6.25	0.08617	-0.36535	0.69210	123.77
97.5	97.5	10.00	0.09289	-0.41145	0.69734	118.68
97.5	97.5	20.00	0.10384	-0.49169	0.70113	115.90
(iii) $T_s/T_p = 2.0$		PE = 10.89				
130	65	1.00	0.05229	-0.26190	0.53527	149.41
130	65	1.75	0.05370	-0.27004	0.53698	147.57
130	65	2.50	0.05491	-0.27860	0.53784	146.03
130	65	3.75	0.05618	-0.29210	0.53840	143.82
130	65	5.00	0.05725	-0.30505	0.53836	141.87
130	65	6.25	0.05828	-0.31752	0.53781	140.07
130	65	10.00	0.06119	-0.34895	0.53458	135.95
130	65	20.00	0.06852	-0.40445	0.52558	129.84

TABLE 5d
CONVECTION EFFECTS - NO INERTIA

PE = 20.33						
(i) $T_s/T_p = 0.5$						
T_s (°F)	T_p (°F)	P_e	\bar{W}	\bar{D}	$\bar{\psi}_c$	T_b (°F)
55	110	1.00	0.06125	-0.20398	0.77674	121.74
55	110	1.75	0.06949	-0.21613	0.78508	117.31
55	110	2.50	0.07799	-0.23150	0.79530	114.29
55	110	3.75	0.08986	-0.25756	0.81156	110.30
55	110	5.00	0.09907	-0.28196	0.82543	106.94
55	110	6.25	0.10634	-0.30369	0.83662	104.10
55	110	10.00	0.12197	-0.35833	0.85918	97.72
55	110	20.00	0.14298	-0.45189	0.88370	88.99
PE = 20.33						
(ii) $T_s/T_p = 1.0$						
82.5	82.5	1.00	0.04836	-0.20061	0.66876	130.44
82.5	82.5	1.75	0.05311	-0.21187	0.67381	126.92
82.5	82.5	2.50	0.05690	-0.22288	0.67900	124.68
82.5	82.5	3.75	0.06231	-0.24298	0.68626	121.28
82.5	82.5	5.00	0.06616	-0.26156	0.69224	118.38
82.5	82.5	6.25	0.06953	-0.27879	0.69762	115.93
82.5	82.5	10.00	0.07632	-0.32267	0.70657	110.13
82.5	82.5	20.00	0.08778	-0.40577	0.71546	101.48
PE = 20.33						
(iii) $T_s/T_p = 2.0$						
110	55	1.00	0.04004	-0.19430	0.55640	140.55
110	55	1.75	0.04190	-0.20227	0.55844	137.97
110	55	2.50	0.04322	-0.21038	0.55974	136.13
110	55	3.75	0.04471	-0.22308	0.56049	133.67
110	55	5.00	0.04617	-0.23640	0.56124	131.32
110	55	6.25	0.04716	-0.24845	0.56130	129.30
110	55	10.00	0.04956	-0.28005	0.55897	124.45
110	55	20.00	0.05622	-0.34108	0.55075	116.80

TABLE 5e
CONVECTION EFFECTS - NO INERTIA

(i) $T_s/T_p = 0.5$		PE = 43.06			
T_s ($^{\circ}\text{F}$)	T_p ($^{\circ}\text{F}$)	P_e	\bar{W}	\bar{D}	T_b ($^{\circ}\text{F}$)
45	90	1.75	0.04435	-0.13796	118.67
45	90	2.50	0.04927	-0.14274	114.11
45	90	3.75	0.06024	-0.16085	107.67
45	90	5.00	0.06827	-0.18173	103.40
45	90	6.25	0.07434	-0.19969	100.11
45	90	10.00	0.08836	-0.24551	92.65
45	90	20.00	0.10881	-0.32899	82.18
(ii) $T_s/T_p = 1.0$		PE = 43.06			
67.5	67.5	1.00	0.03317	-0.13204	129.97
67.5	67.5	1.75	0.03598	-0.13629	124.08
67.5	67.5	2.50	0.03921	-0.14261	120.58
67.5	67.5	3.75	0.04398	-0.15860	116.10
67.5	67.5	5.00	0.04743	-0.17322	112.74
67.5	67.5	6.25	0.05044	-0.18750	109.85
67.5	67.5	10.00	0.05727	-0.22548	103.15
67.5	67.5	20.00	0.06728	-0.29766	93.04
(iii) $T_s/T_p = 2.0$		PE = 43.06			
90	45	1.75	0.02937	-0.13328	131.15
90	45	2.50	0.03096	-0.13968	128.36
90	45	3.75	0.03270	-0.15044	125.09
90	45	5.00	0.03369	-0.16055	122.64
90	45	6.25	0.03470	-0.17135	120.23
90	45	10.00	0.03718	-0.20041	114.40
90	45	20.00	0.04208	-0.25797	105.19

APPENDIX F

THE COMPUTER PROGRAMS

Written in FORTRAN IV for an IBM 360/67

Computer Using the MTS System


```

      READ(5,597)RF
      IN=0
      MN=0
      M=11
      M1=M-1
      C
      GENERATION OF POINT LOCATIONS IN FLUID FILM AND INITIA
      * SIZE TEMP DIST
      DO 31 I=1,11
      IF(I.EQ.1)GO TO 3
      X(I)=X(I-1)+DX
      3 H(I)=R-X(I)*(R-1.D0)
      DO 4 J=2,N
      Y(J)=Y(J-1)+DY
      4 CONTINUE
      31 CONTINUE
      C
      EVALUATION OF MASS FLOW FOR CONST VISCOSITY
      DO 104 I=1,11
      C(I)=1.D0/X(I)**3
      104 CONTINUE
      CSSUM=0.D0
      DSSUM=0.D0
      DO 107 I=3,11,2
      CSSUM=CSSUM+DX*(C(I)+4.D0*C(I-1)+C(I-2))/3.D0
      DSSUM=DSSUM+DX*(C(I)+4.D0*C(I-1)+C(I-2))/3.D0
      107 CONTINUE
      AFM=CSSUM/DSSUM
      C
      EVALUATION OF PRESS GRADIENT AND STREAM FCN DIST F
      * OR CONST VISCOSITY
      DO 101 I=1,M
      DPDX(I)=C(I)-D(I)*AFM
      DO 38 J=1,N
      S(I,J)= H(I)**3*DPDX(I)*Y(J)*(Y(J)**2/6.D0-Y(J)/3.D0
      * +1.D0/6.D0)/
      * AFM*(2.D0-Y(J))
      C
      EVALUATION OF GRAD'S OF STREAM FCN IN Y DIRE
      * CTION
      SY(I,J)= H(I)**3*DPDX(I)*(Y(J)**2/2.D0-2.D0*Y(J)/3.D
      * 0+1.D0/6.D0)
      * AFM*(2.D0-Y(J))
      SYY(I,J)= H(I)**3*DPDX(I)*(Y(J)-2.D0/3.D0)/AFM-2.D0
      38 CONTINUE
      101 CONTINUE
      DO 212 I=1,M

```



```

      DO 213 J=1,N
      U(I,J)=RE*H(I)*UX(I,J)/H(I)
213  CONTINUE
212  CONTINUE
      NITER=0
      EPVAL=1.00
      GO TO 112
      EVALUATION OF FIRST INTEGRAL
275  IN=IN+1
      MN=MN+1
      ITER=ITER+1
      DO 251 I=1,M
      DO 249 J=1,N
      DSM(I,J)=RE*H(I)**2*(SY(I,J)*UX(I,J)-SX(I,J)*UY(I,J))
249  CONTINUE
C    EVALUATION OF FIRST INTEGRAL
      DSUM(I,1)=0.00
      DO 250 J=2,N
      J2=J/2
      IF(J2*2.NE.J)GO TO 251
      IF(J.NE.2)GO TO 790
      DSUM(I,4)=(DSM(I,1)+3.00*(DSM(I,2)+DSM(I,3))+DSM(I,4))
      *0
      DLSM=(DSM(I,2)+4.00*DSM(I,3)+DSM(I,4))*DY/3.00
      DSUM(I,4)=DSUM(I,4)-DLSM
      GO TO 250
790  DSUM(I,J)=DSUM(I,J-3)+(DSM(I,J)+3.00*(DSM(I,J-1)+DSM(I
      *    ,J-2))+DSM(I
      *    ,J-3))*3.00*DY/8.00
      GO TO 250
251  DSUM(I,J)=DSUM(I,J-1)+DY*(DSM(I,J)+3.00*DSM(I,J-1)+DSM
      *    (I,J-2))/3.0
      *0
250  CONTINUE
251  CONTINUE
      DO 258 I=1,M
      PFSM(I,1)=0.00
      NN=21
C    EVALUATION OF SECOND INTEGRAL
      DO 255 J=2,NN
      J2=J/2
      IF(J2*2.NE.J)GO TO 254
      IF(J.NE.2)GO TO 790
      PFSM(I,4)=(DSUM(I,1)+3.00*(DSUM(I,2)+DSUM(I,3))+DSUM(I
      *    ,4))*3.00*DY
      */8.00
      DPFSM=(DSUM(I,2)+4.00*DSUM(I,3)+DSUM(I,4))*DY/3.00

```



```

      PFSM(I,2)=PFSM(I,4)-DPFSM
      GO TO 255
789 PFSM(I,J)=PFSM(I,J-3)+(DSUM(I,J)+3.D0*(DSUM(I,J-1)+DSU
* M(I,J-2))+
* SUM(I,J-3))*3.D0*DY/8.D0
      GO TO 255
254 PFSM(I,J)=PFSM(I,J-2)+DY*(DSUM(I,J)+4.D0*DSUM(I,J-1)+D
* SUM(I,J-2))/3.D0
255 CONTINUE
258 CONTINUE
C      EVALUATION OF THIRD INTEGRAL
      DO 260 I=1,M
        PFSUM(I,1)=0.D0
        DO 262 J=2,NN
          J2=J/2
          IF(J2*2.NE.J)GO TO 251
          IF(J.NE.2)GO TO 788
          PFSUM(I,2)=(PFSM(I,1)+3.D0*(PFSM(I,2)+PFSM(I,3))+PFSM(I,4))*3.D0*
          *DY/8.D0
          PFSUM(I,2)=PFSUM(I,2)+4.D0*PFSM(I,1)+PFSM(I,3)+PFSM(I,4)*DY/3.D0
          GO TO 262
788 PFSUM(I,J)=PFSUM(I,J-3)+(PFSM(I,J)+3.D0*(PFSM(I,J-1)+P
* FSM(I,J-2))+
* PFSM(I,J-3))*3.D0*DY/8.D0
          GO TO 262
          PFSUM(I,J)=PFSUM(I,J-2)+DY*(PFSM(I,J)+4.D0*PFSM(I,J-1)
          * +PFSM(I,J-2)
          *)/3.D0
262 PFSUM(I,J)=PFSUM(I,J)
        C(I)=6.D0/H(I)**2
        D(I)=6.D0*(PFSM(I,N)-2.D0*PFSUM(I,N)+2.D0)/H(I)**3
260 CONTINUE
      WRITE(6,105) (C(I),I=1,6)
      WRITE(6,151)(C(I),I=7,11)
      WRITE(6,105)(D(I),I=1,6)
      WRITE(6,151)(D(I),I=7,11)
C      EVALUATION OF NEW VALUE FOR MASS FLOW      USING SIMPSON
*      S RULE
      CSSUM=0.D0
      DSSUM=0.D0
      DO 52 I=1,11
        CSSUM=CSSUM+DX*(C(I)+4.D0*C(I-1)+C(I-2))/3.D0
        DSSUM=DSSUM+DX*(D(I)+4.D0*D(I-1)+D(I-2))/3.D0
52 CONTINUE
      AFM=CSSUM/DSSUM

```



```

      C(I)=1
      DO 100 I=1,11
      DPDX(I)=C(I)-D(I)*AFM
      P(I)=(H(I))/2
      C(I)=-(C(I-1))+3*M(I-1)+H(I)*3*DPDX(I)/2+D(I-1)*AFM
C     EVALUATION OF STREAM FCN DIST
      DO 215 J=1,N
      S(I,J)=-(C(I-1)+D(I-1))*3*DPDX(I)*Y(J)+C(I-1)*Y(J)
      * )+C1(I)*Y(J)
      ***2/2.D0+C2(I)*Y(J)
      Y(I,J)=PESUM(I,J)+H(I)*3*DPDX(I)*Y(J)*2/3+C1(I)*Y(J)
      * )+C1(I)*Y(J)
      *+C2(I)
      SYY(I,J)=SYY(I,J)+H(I)*3*DPDX(I)*Y(J)/3+C1(I)
      H(I,J)=H(I)*Y(I)/H(I)
215  CONTINUE
      55  CONTINUE
C     EVALUATION OF PRESS DIST IN FLUID FILM
112  CSUM(1)=0.D0
      DESUM(1)=0.D0
      DO 61 I=2,10
      I2=I/2
      IF(I.EQ.2)GO TO 785
      IF(I.NE.2)GO TO 785
      CSUM(4)=(C(1)+3.D0*(C(2)+C(3))+C(4))*3.D0*DX/8.D0
      DCSCM=(C(2)+4.D0*C(3)+C(4))*DX/3.D0
      CSUM(2)=CSUM(4)-DCSCM
      DESUM(4)=(D(1)+3.D0*(D(2)+D(3))+D(4))*3.D0*DX/8.D0
      DDCSM=(D(2)+4.D0*(D(3)+D(4)))*DX/3.D0
      DESUM(2)=DESUM(4)-DDCSM
      GO TO 64
785  CSUM(I)=CSUM(I-3)+(C(I)+3.D0*(C(I-1)+C(I-2))+C(I-3))*3
      * .D0*DX/8.D0
      DESUM(I)=DESUM(I-3)+(D(I)+3.D0*(D(I-1)+D(I-2))+D(I-3))
      * *3.D0*DX/8.D0
      *0
      GO TO 64
62  CSUM(I)=CSUM(I-2)+DX*(C(I)+4.D0*C(I-1)+C(I-2))/3.
      DESUM(I)=DESUM(I-2)+DX*(D(I)+4.D0*D(I-1)+D(I-2))/3.D0
64  P(I)=CSUM(I)-AFM*DESUM(I)
      IF(MN.EQ.0)GO TO 269
      DPVAL=PA-((C(I)-P(I))/2*(I))
      IF(I.EQ.2)EPVAL=DPVAL
      IF(I.EQ.2)GO TO 269
      IF(DPVAL.GT.FPVAL)EPVAL=DPVAL
269  P(I)=P(I)
      51  CONTINUE
      WRITE(6,793)MN,AFM

```



```

793 FORMAT(' ',//,30X,'ITER  EQUALS',2X,I3,3X,'MASS  FLOW
*  EQUALS',2X,
*D13.5)
WRITE(6,792)MN,EPVAL
792 FORMAT(' ',//,30X,'ITER  EQUALS',2X,I3,3X,'MASS  FLOW
*  EQUALS',2X,D13.5)
*)
WRITE(6,105)(P(I),I=1,6)
WRITE(6,151)(P(I),I=7,11)
270 DO 109 I=1,M
  UY(I,N)=(U(I,N-2)+3.D0*U(I,N)-4.D0*U(I,N-1))/(2.D0*DY)
  UY(I,1)=(4.D0*U(I,2)-3.D0*U(I,1)-U(I,3))/(2.D0*DY)
267 DO 108 J=1,N
C  EVALUATION OF GRAD'S OF STREAM FCN IN X DIRE
*  CTION
  IF(I.EQ.M)SX(I,J)=(S(I-2,J)+3.D0*S(I,J)-4.D0*S(I-1,J))
*  /(2.D0*DX)
  IF(I.EQ.1)SX(I,J)=(4.D0*S(I+1,J)-3.D0*S(I,J)-S(I+2,J))
*  /(2.D0*DX)
  IF(I.NE.1.AND.I.NE.M)SX(I,J)=(S(I+1,J)-S(I-1,J))/(2.D0
*  *DX)
  IF(I.EQ.M)UX(I,J)=(U(I-2,J)+3.D0*U(I,J)-4.D0*U(I-1,J))
*  /(2.D0*DX)
  IF(I.EQ.1)UX(I,J)=(4.D0*U(I+1,J)-3.D0*U(I,J)-U(I+2,J))
*  /(2.D0*DX)
  IF(I.NE.1.AND.I.NE.M)UX(I,J)=(U(I+1,J)-U(I-1,J))/(2.D0
*  *DX)
  IF(J.NE.1.AND.J.NE.N)UY(I,J)=(U(I,J+1)-U(I,J-1))/(2.D0
*  *DY)
108 CONTINUE
109 CONTINUE
  IF(MN.EQ.0)GO TO 445
  IF(EPVAL.LT.EPRES)GO TO 445
  GO TO 275
445 PRINT 211
211 FORMAT(30X,'RESULTS  FOR  VELOCITY  DIST')
  DO 502 I=1,M
    UY(I)=MAX(UY(I,1),UY(I,N))
    WRITE(6,161)(U(I,J),J=1,N)
    WRITE(6,161)(U(I,J),J=13,21)
502 CONTINUE
105 FORMAT(2X,6(D13.6,2X)/)
151 FORMAT(2X,5(D13.6,2X)/)
161 FORMAT(2X,12(F9.4,1X)/)
161 FORMAT(2X,9(F9.4,1X)/)
  IF(MN.GT.0)PRINT 277
277 FORMAT(' ',//,30X,'RESULTS  INCLUDING  INCLINING  (COS(S))
PRINT 140

```



```

140 FORMAT(30X,'FINAL RESULTS FOR PRESS DIST')
WRITE(6,105)(P(I),I=1,6)
WRITE(6,151)(P(I),I=7,11)
PRINT 794
C
* EVALUATION OF LOAD CAPACITY OF BEARING AND FRICTIONAL
* FORCE ON RUNNER
FSUM=0.00
PSUM=0.00
DO 444 I=7,11
PSUM=PSUM+(P(I)+4.00*P(I-1)+P(I-2))*DX/3.00
FDY(I)=FSUM+FDY(I-1)+4.00*FDY(I-1)+FDY(I-2))*DX/3.00
444 CONTINUE
WRITE(6,444) FSUM, PSUM
C
* DRAG EQUAL
* 1.4X, 1.6
IF(MN.EQ.0)GO TO 275
ANS(I1,1)=R
ANS(I1,2)=PSUM
ANS(I1,3)=AFM
ANS(I1,4)=AFM
ANS(I1,5)=RE
1000 CONTINUE
PRINT 698
698 FORMAT('1',/////,30X,'RESULTS OF NUMERICAL ANALYSIS
* *)
DO 691 I1=1,NUM
WRITE(6,700)(ANS(I1,J),J=1,5)
700 FORMAT('1',//3X,5(E13.5,2X))
691 CONTINUE
STOP
END

```

* IN THE SIXTH COLUMN INDICATES
CONTINUATION FROM PREVIOUS LINE

```

C      J.HINDS  COMPUTATIONS FOR THESIS TOPIC ON LUBRICATI
*      CN
C      SOLUTION OF MOMENTUM AND ENERGY EQUATIONS FOR V
*      ARIABLE
*      VISCOSITY AND INCLUDING INERTIA TERMS
C      CALCULATIONS FOR 2-D FLOW THROUGH BEARING USING STR
*      EAM FCN
      IMPLICIT REAL*8 (A-H,C-Z)
      DIMENSION X(11),Y(21),SUM(11,21),SUMY(11,21),DCUM(11,
*      21),FDY(11),
*      LSM(11,21), PF(11,21), PFSM(11,21),P(11),PPDY(11),SY(
*      11,21),
*      SY(11,21),SYY(11,21),SHX(11,21),SHY(11,21),S(11,21),TH
*      ETA(11,21),
*      H(11),F(11,21),FY(11,21),C(11),D(11),CSUM(11),HF(11),T
*      HETB(11,21),
*      B(11,21),BF(11,21),BF(11,21),A(11,21),ALF(11,21),L(11,
*      21),QYP(11),
*      QYS(11),S(11,21),SE(11,21),SB(11,21),SB(11,21),TSE(21)
*      ,ISI(21),
*      SM(11,21),SMY(11,21),DF(11,21),DFY(11,21),TSIM(21),TSE
*      M(21),
*      DESUM(11),DTDYP(11),DTDYS(11),C1(11),C2(11),CN(11),DN(
*      11),
*      PFSUM(11,21),PB(11),T(11,21),THET(11,21),U(11,21),UX(1
*      1,21),
*      UY(11,21),RTHET(11,21),E(11,21),ANS(30,30),V(11,21),T
*      (11),TA(11)
      CALL IEV
      PRINT 994
994  FORMAT('1',30X,'DATA USED IN ANALYSIS',/)
C      READ IN VALUES OF DIMENSIONAL CONSTANTS
      READ(5,996)TK,ROE,CPEC,CPFR,EMUO,TI
996  FORMAT(6E13.5)
      WRITE(6,995)TK,ROE,CPEC,CPFR,EMUO,TI

```



```

995 FORMAT(' ',2X,6(E13.5,2X))
      READ(5,996) DX,DY,X(1),Y(1),P(1),P(11)
      WRITE(6,995) DX,DY,X(1),Y(1),P(1),P(11)
      READ(5,999) ETHET,EPRES,BT,CNTHT
997 FORMAT(4E13.5)
      READ(5,28) TS,TP,VEL,TN,T1,TAA,R,AL,HO
28  FORMAT(3F7.2,6F8.5)
      READ(5,997) N11
997 FORMAT(I2)
      DO 1000 I1=1,NUM
      READ(5,997) R1
597 FORMAT(E13.5)
499 WRITE(6,993) ETHET,EPRES
993 FORMAT(' ',2X,'CONVERGENCE CRITERIA ON TEMP',2X,F6.
* 4,4X,
* 'CONVERGENCE CRITERIA ON PRESSURE',2X,F6.4)
      WRITE(6,29) TS,TP
29  FORMAT(2X,'SLIDED TEMP EQUALS',2X,F6.2,2X,'FAP TEMP
      EQUALS',
* 2X,F6.2,2X)
      WRITE(6,998) R
998 FORMAT(' ',2X,'INLET TO OUTLET RATIO EQUALS',2X,F4
* .2,3X)
      PRINT 276
276 FORMAT(' ',//////,30X,'RESULTS NEGLECTING INERTIA TE
* RMS')
      NA=0
      IN=0
      MN=0
      TAV=(TP+TS)/2.D0
      DT=TAV
      ETDT=31*DT
      ISTP=IS/TP
      N=21
      M=11
      N1=N-1
      N3=N-3
      M1=M-1
      CALL VIS(TAV,EUTAV)
      PRL=CPPR*EUTAV/TK
      EC=VEL**2/(CPEC*DT)
      PEC=PRL*EC
      PE=PRL*RE
      CEDRE=PEC/PE
      RPEC=1.D0/PE
      PEDYS=PE*DY**2
      G=1.D0/PEDYS
      WRITE(6,294) PE,PEC

```



```
294 FORMAT(2X,'PECLET  EQUALS',2X,D13.6,'P*EC  EQUALS',2X,
* D13.6)
```

```
WRITE(6,190) RPEC,CEDFE,PRL
```

```
190 FORMAT(2X,'1.0/PECLET  EQUALS',3X,D13.6,2X,'EC/RE  EQU
* ALS',3X,D13.
```

```
*6,2X,'PRL  EQUALS',2X,E13.6)
```

```
C  GENERATION OF POINT LOCATIONS IN FLUID FILM AND INITIA
* LIFE TEMP DIST
```

```
DO 31 I=1,11
```

```
IF(I.EQ.1)GO TO 3
```

```
X(I)=X(I-1)+DX
```

```
3 H(I)=R-X(I)*(R-1.D0)
```

```
THETA(I,N)=TN
```

```
THETTB(I,N)=THETA(I,N)
```

```
THETA(I,1)=T1
```

```
THETTB(I,1)=THETA(I,1)
```

```
GO 4 J=2,N
```

```
Y(J)=Y(J-1)+DY
```

```
THETA(1,J)=TAA*Y(J)+T1
```

```
THETTB(1,J)=THETA(1,J)
```

```
4 CONTINUE
```

```
31 CONTINUE
```

```
C  EVALUATION OF MASS FLOW FOR CONST VISCOSITY
```

```
DO 104 I=1,11
```

```
C(I)=6.D0/H(I)**2
```

```
D(I)=12.D0/H(I)**3
```

```
104 CONTINUE
```

```
CSSUM=0.D0
```

```
DSSUM=0.D0
```

```
DO 107 I=3,11,2
```

```
CSSUM=CSSUM+DX*(C(I)+4.D0*C(I-1)+C(I-2))/3.D0
```

```
DSSUM=DSSUM+DX*(D(I)+4.D0*D(I-1)+D(I-2))/3.D0
```

```
107 CONTINUE
```

```
AFM=CSSUM/DSSUM
```

```
C  EVALUATION OF PRESS GRADIENT AND STREAM FCN DIST IN
```

```
* OR CONST VISCOSITY
```

```
DO 191 I=1,M
```

```
DPDX(I)=C(I)-D(I)*AFM
```

```
DO 38 J=1,N
```

```
S(I,J)= H(I)**3*DPDX(I)*Y(J)*(Y(J)**2/6.D0-Y(J)/3.D0
```

```
* +1.D0/6.D0)/
```

```
*AFM+Y(J)*(2.D0-Y(J))
```

```
C  EVALUATION OF GRAD'S OF STREAM FCN IN Y DIRE
```

```
* CTION
```

```
SY(I,J)= H(I)**3*DPDX(I)*(Y(J)**2/2.D0-2.D0*Y(J)/3.D
```

```
* 0+1.D0/6.D0)
```

```
*/AFM+2.D0*(1.D0-Y(J))
```

```
SYY(I,J)= H(I)**3*DPDX(I)*(Y(J)-2.D0/3.D0)/AFM-2.D0
```



```

38 CONTINUE
191 CONTINUE
    DO 212 I=1,M
    DO 213 J=1,N
        U(I,J)=AFM*SY(I,J)/H(I)
213 CONTINUE
212 CONTINUE
    NITER=0
    GO TO 112
C    EVALUATION OF TEMP DIST
113 NITER=0
    MM=0
    63 ITER=0
    REVAL=1.D0
    MM=MM+1
25 NN=21
    NITER=NITER+1
    ITER=ITER+1
    DO 46 I=1,M1
    DO 47 J=2,N1
        BF(I,J)=G+HF(I)*AFM*SHY(I,J)/DX
        BE(I,J)=BF(I,J)-2.D0*G
27 AH(I,J)=- (BF(I)*AFM*SHX(I,J)/(4.D0*DY)+G/2.D0)
        A(I,J)=- (G/2.D0-HF(I)*AFM*SHY(I,J)/(4.D0*DY))
        IF(J.EQ.2) W(I,J)=+BF(I,J)
        IF(J.EQ.2) ALF(I,J)=AH(I,J)/W(I,J)
        IF(J.EQ.2) GO TO 47
        W(I,J)=+BF(I,J)-ALF(I,J-1)*A(I,J)
        ALF(I,J)=AH(I,J)/W(I,J)
47 CONTINUE
46 CONTINUE
    DO 75 I=1,M1
    DO 77 J=2,N1
        IF(J.EQ.1) CNST=THETA(I+1,N)*(-AH(I,J))
        IF(J.EQ.2) CNST=THETA(I+1,J-1)*(-A(I,J))
        IF(J.NE.2.AND.J.NE.N1) CNST=0.D0
        IF(NITER.EQ.1) B(I,J)=THETA(I,J-1)*(-A(I,J))+THETA(I,J)
        * ) * BE(I,J) +
        * THETA(I,J+1)*(-AH(I,J))+CEDRE* ((SYY(I,J)+SYY(I+1,J))*A
        * FM/HF(I)) **2
        */4.D0+CNST
        IF(NITER.EQ.1) GO TO 98
        IF(T(I,J).GT.2.3D2) VII=AB(I,J)
        IF(T(I+1,J).GT.2.3D2) VII1=AB(I+1,J)
        IF(T(I,J).LE.2.3D2) VII=V(I,J)
        IF(T(I+1,J).LE.2.3D2) VII1=V(I+1,J)
        E(I,J)=THETA(I,J-1)*(-A(I,J))+THETA(I,J)*BE(I,J)+THETA
        * (I,J+1)*

```



```

* (-AH(I,J)) + CEDRE * ((SYI(I,J) + SYI(I+1,J)) * AFM / HF(I)) ** 2 *
* (VII + VII1) /
* 8. DO + CNST
98 IF (J.EQ.2) Z(I,J) = B(I,J) / W(I,J)
   IF (J.EQ.2) GO TO 77
   Z(I,J) = (B(I,J) - A(I,J) * Z(I,J-1)) / W(I,J)
77 CONTINUE
   THETA(I+1,N1) = Z(I,N1)
   IF (NITER.EQ.1) GO TO 99
   DFVAL = DABS((THETA(I+1,N1) - THETB(I+1,N1)) / THETA(I+1,N1)
* )
   IF (I.EQ.1) EQVAL = DFVAL
   IF (I.EQ.1) GO TO 99
   IF (DFVAL.GT.EQVAL) EQVAL = DFVAL
99 DO 76 K=1,N3
   NK1 = N - (K+1)
   NK = N - K
   THETA(I+1,NK1) = Z(I,NK1) - ALF(I,NK1) * THETA(I+1,NK)
   IF (NITER.EQ.1) GO TO 76
   DFVAL = DABS((THETA(I+1,NK1) - THETB(I+1,NK1)) / THETA(I+1,N
* NK1))
   IF (DFVAL.GT.EQVAL) EQVAL = DFVAL
76 CONTINUE
75 CONTINUE
   DO 117 I=1,M
   DO 116 J=1,N
   THETB(I,J) = THETA(I,J)
   T(I,J) = DT * THETA(I,J)
   TMP = T(I,J)
   IF (T(I,J).GT.2.3D2) GO TO 116
   CALL VIS(TMP,VI)
   V(I,J) = VI / EUTAV
116 CONTINUE
117 CONTINUE
   IF (NITER.EQ.1) GO TO 25
   IF (EQVAL.GT.ETHET) GO TO 25
C   EVALUATION OF INTEGRAL CONSTS FOR STREAM FCN DIST
* REPTITION
   IF (MN.EQ.0) GO TO 252
C   EVALUATION OF CONTRIBUTION DUE TO INERTIA TERMS
175 IN = IN + 1
   MN = MN + 1
   ITER = ITER + 1
   DO 251 I=1,M
   DO 249 J=1,N
   DSM(I,J) = RE * H(I) ** 2 * (SY(I,J) * UX(I,J) - SX(I,J) * UY(I,J))
249 CONTINUE
C   EVALUATION OF FIRST INTEGRAL

```



```

DSUM(I,1)=0.D0
DO 250 J=2,N
J2=J/2
IF(J2*2.NE.J) GO TO 256
IF(J.NE.2) GO TO 790
DSUM(I,4)=(DSM(I,1)+3.D0*(DSM(I,2)+DSM(I,3))+DSM(I,4))
* 3.D0*DY/8.D
*0
DLSM=(DSM(I,2)+4.D0*DSM(I,3)+DSM(I,4))*DY/3.D0
DSUM(I,2)=DSUM(I,4)-DLSM
GO TO 250
790 DSUM(I,J)=DSUM(I,J-3)+(DSM(I,J)+3.D0*(DSM(I,J-1)+DSM(I
* ,J-2))+DSM(I
* ,J-3))*3.D0*DY/8.D0
GO TO 250
256 DSUM(I,J)=DSUM(I,J-2)+DY*(DSM(I,J)+4.D0*DSM(I,J-1)+DSM
* (I,J-2))/3.D0
*0
250 CONTINUE
251 CONTINUE
NN=21
DO 258 I=1,M
PFSM(I,1)=0.D0
C EVALUATION OF SECCND INTEGRAL
DO 255 J=2,NN
J2=J/2
IF(J2*2.NE.J) GO TO 254
IF(J.NE.2) GO TO 789
PFSM(I,4)=(DSUM(I,1)+3.D0*(DSUM(I,2)+DSUM(I,3))+DSUM(I
* ,4))*3.D0*DY
*/8.D0
DPFSM=(DSUM(I,2)+4.D0*DSUM(I,3)+DSUM(I,4))*DY/3.D0
PFSM(I,2)=PFSM(I,4)-DPFSM
GO TO 255
789 PFSM(I,J)=PFSM(I,J-3)+(DSUM(I,J)+3.D0*(DSUM(I,J-1)+DSU
* M(I,J-2))+
* DSUM(I,J-3))*3.D0*DY/8.D0
GO TO 255
254 PFSM(I,J)=PFSM(I,J-2)+DY*(DSUM(I,J)+4.D0*DSUM(I,J-1)+D
* SUM(I,J-2))/
* 3.D0
255 CONTINUE
258 CONTINUE
C EVALUATION OF THIRD INTEGRAL
DO 260 I=1,M
PFSUM(I,1)=0.D0
DO 262 J=2,NN
J2=J/2

```



```

IF (J2*2.NE.J) GO TO 261
IF (J.NE.2) GO TO 788
PFSUM(I,4)=(PFSM(I,1)+3.D0*(PFSM(I,2)+PFSM(I,3))+PFSM(
* I,4))*3.D0*
*DY/8.D0
DPSUM=(PFSM(I,2)+4.D0*PFSM(I,3)+PFSM(I,4))*DY/3.D0
PFSUM(I,2)=PFSUM(I,4)-DPSUM
GO TO 262
788 PFSUM(I,J)=PFSUM(I,J-3)+(PFSM(I,J)+3.D0*(PFSM(I,J-1)+P
* FSM(I,J-2))+
*PFSM(I,J-3))*3.D0*DY/8.D0
GO TO 262
261 PFSUM(I,J)=PFSUM(I,J-2)+DY*(PFSM(I,J)+4.D0*PFSM(I,J-1)
* PFSM(I,J-2)
*)/3.D0
262 CONTINUE
260 CONTINUE
252 DO 18 I=1,M
SM(I,1)=0.D0
SMY(I,1)=0.D0
DO 5 J=1,N
IF (T(I,J).LE.2.3D2) F(I,J)=1.D0/V(I,J)
IF (T(I,J).LE.2.3D2) GO TO 83
F(I,J)=DEXP(BTDT*(THETA(I,J)-1.D0)/(1.D0+DT*(THETA(I,J)
* )-1.D0)
*/CNTHT))
AB(I,J)=1.D0/F(I,J)
83 FY(I,J)=F(I,J)*Y(J)
5 CONTINUE
NN=N
DO 15 J=2,NN
J2=J/2
IF (J2*2.NE.J) GO TO 8
IF (J.NE.2) GO TO 787
SM(I,4)=(F(I,1)+3.D0*(F(I,2)+F(I,3))+F(I,4))*3.D0*DY/8
* .D0
DSMM=(F(I,2)+4.D0*F(I,3)+F(I,4))*DY/3.D0
SM(I,2)=SM(I,4)-DSMM
SMY(I,4)=(FY(I,1)+3.D0*(FY(I,2)+FY(I,3))+FY(I,4))*3.D0
* *DY/8.D0
DSMY=(FY(I,2)+4.D0*FY(I,3)+FY(I,4))*DY/3.D0
SMY(I,2)=SMY(I,4)-DSMY
GO TO 15
787 SM(I,J)=SM(I,J-3)+(F(I,J)+3.D0*(F(I,J-1)+F(I,J-2))+F(I
* ,J-3))*3.D0*
*DY/8.D0
SMY(I,J)=SMY(I,J-3)+(FY(I,J)+3.D0*(FY(I,J-1)+FY(I,J-2)
* )+FY(I,J-3))

```



```

**3.D0*DY/8.D0
GO TO 15
8 SM(I,J)=SM(I,J-2)+DY*(F(I,J)+4.D0*F(I,J-1)+F(I,J-2))/3
* .D0
SMY(I,J)=SMY(I,J-2)+DY*(FY(I,J)+4.D0*FY(I,J-1)+FY(I,J-
* 2))/3.D0
15 CONTINUE
18 CONTINUE
NN=N
C EVALUATION OF LINE INTEGRAL CONST FOR STEFAN F
* CN LIST
DO 180 I=1,M
SUM(I,1)=0.D0
SUMY(I,1)=0.D0
DO 181 J=2,NN
J2=J/2
IF(J2*2.NE.J)GO TO 183
IF(J.NE.2)GO TO 786
SUM(I,4)=(SM(I,1)+3.D0*(SM(I,2)+SM(I,3))+SM(I,4))*3.D0
* *DY/8.D0
DSUMM=(SM(I,2)+4.D0*SM(I,3)+SM(I,4))*DY/3.D0
SUM(I,2)=SUM(I,4)-DSUMM
SUMY(I,4)=(SMY(I,1)+3.D0*(SMY(I,2)+SMY(I,3))+SMY(I,4))
* *3.D0*DY
*/8.D0
DSMMY=(SMY(I,2)+4.D0*SMY(I,3)+SMY(I,4))*DY/3.D0
SUMY(I,2)=SUMY(I,4)-DSMMY
GO TO 181
786 SUM(I,J)=SUM(I,J-3)+(SM(I,J)+3.D0*(SM(I,J-1)+SM(I,J-2)
* )+SM(I,J-3))
**3.D0*DY/8.D0
SMY(I,J)=SMY(I,J-3)+(SMY(I,J)+3.D0*(SMY(I,J-1)+SMY(I
* ,J-2))+SMY
* (I,J-3))*3.D0*DY/8.D0
GO TO 181
183 SUM(I,J)=SUM(I,J-2)+DY*(SM(I,J)+4.D0*SM(I,J-1)+SM(I,J-
* 2))/3.D0
SUMY(I,J)=SUMY(I,J-2)+DY*(SMY(I,J)+4.D0*SMY(I,J-1)+SMY
* (I,J-2))/3.D
* 3
181 CONTINUE
IF(MN.GT.0)GO TO 263
CN(I)=(SUMY(I,NN)-SMY(I,NN))*SM(I,NN)/(SUM(I,NN)-SM(I,
* NN))
DN(I)=SM(I,NN)/(SUM(I,NN)-SM(I,NN))
C(I)=-1.D0/(H(I)**2*(SMY(I,NN)-CN(I)))
F(I)=DN(I)/(H(I)**3*(SMY(I,NN)-CN(I)))
GO TO 180

```



```

263 CN(I)=(SM(I,NN)*(1.D0-PFSUM(I,NN))+PFSM(I,NN)*SUM(I,NN
*   ) ) /
* (SUM(I,NN)-SM(I,NN))
DN(I)=(SUM(I,NN)*SMY(I,NN)-SM(I,NN)*SUMY(I,NN))/(SUM(I
*   ,NN)-SM(I,NN
*))
C(I)=-1.D0/(H(I)**2*DN(I))
D(I)=CN(I)/(H(I)**3*DN(I))
180 CONTINUE
C   EVALUATION OF NEW VALUE FOR MASS FLOW      USING SIMPSON
*   'S RULE
CSSUM=0.D0
DSSUM=0.D0
DO 52 I=3,11,2
CSSUM=CSSUM+DX*(C(I)+4.D0*C(I-1)+C(I-2))/3.D0
DSSUM=DSSUM+DX*(D(I)+4.D0*D(I-1)+D(I-2))/3.D0
52 CONTINUE
AFM=CSSUM/DSSUM
NN=21
DO 55 I=1,11
DPDX(I)=C(I)-D(I)*AFM
C2(I)=D(I)/AFM
IF(MN.GT.0)GO TO 264
C1(I)=- (C2(I) + H(I)**3*DPDX(I)*SMY(I,NN)/AFM)/SM(I,N
*   N)
GO TO 265
264 C1(I)=(1.D0+H(I)**3*DPDX(I)*(SMY(I,NN)-SUMY(I,NN))/AFM
*   + (PFSM(I,NN)
* -PFSUM(I,NN)))/(SUM(I,NN)-SM(I,NN))
C   EVALUATION OF STREAM FCN DIST FOR VARIABLE VISC
*   COSITY
265 DO 215 J=1,NN
IF(MN.GT.0)GO TO 266
C   EVALUATION OF GRAD'S OF STREAM FCN IN Y DIRE
*   CTION
S(I,J)= H(I)**3*DPDX(I)*SUMY(I,J)/AFM+C1(I)*SUM(I,J)
*   +C2(I)*Y(J)
SY(I,J)= H(I)**3*DPDX(I)*SMY(I,J)/AFM+C1(I)*SY(I,J)+
*   C2(I)
SYY(I,J)= H(I)**3*DPDX(I)*FY(I,J)/AFM+C1(I)*F(I,J)
GO TO 215
266 S(I,J)=H(I)**3*DPDX(I)*SUMY(I,J)/AFM+PFSUM(I,J)+C1(I)*
*   SUM(I,J)+
*   C2(I)*Y(J)
C   EVALUATION OF GRADIENTS OF STREAM FCN IN Y DIR
*   ECTION
SY(I,J)=H(I)**3*DPDX(I)*SMY(I,J)/AFM+PFSM(I,J)+C1(I)*S
*   M(I,J)+C2(I)

```



```

      SYX(I,J)=H(I)**3*DPDX(I)*FY(I,J)/AFM+DSUM(I,J)+C1(I)*F
      * (I,J)
215 CONTINUE
55 CONTINUE
      DO 214 I=1,M
      DO 216 J=1,N
      U(I,J)=AFM*SY(I,J)/H(I)
216 CONTINUE
214 CONTINUE
C      EVALUATION OF PRESS DIST IN FLUID FILM
112 CSUM(1)=0.D0
      DESUM(1)=0.D0
      DO 61 I=2,10
      I2=I/2
      IF(I2*2.NE.I) GO TO 62
      IF(I.NE.2) GO TO 785
      CSUM(4)=(C(1)+3.D0*(C(2)+C(3))+C(4))*3.D0*DX/8.D0
      DCSM=(C(2)+4.D0*C(3)+C(4))*DX/3.D0
      CSUM(2)=CSUM(4)-DCSM
      DESUM(4)=(D(1)+3.D0*(D(2)+D(3))+D(4))*3.D0*DX/8.D0
      DDSM=(D(2)+4.D0*D(3)+D(4))*DX/3.D0
      DESUM(2)=DESUM(4)-DDSM
      GO TO 64
785 CSUM(I)=CSUM(I-3)+(C(I)+3.D0*(C(I-1)+C(I-2))+C(I-3))*3
      * .D0*DX/8.D0
      DESUM(I)=DESUM(I-3)+(D(I)+3.D0*(D(I-1)+D(I-2))+D(I-3))
      * *3.D0*DX/8.D0
      *C
      GO TO 64
62 CSUM(I)=CSUM(I-2)+DX*(C(I)+4.D0*C(I-1)+C(I-2))/3.D0
      DESUM(I)=DESUM(I-2)+DX*(D(I)+4.D0*D(I-1)+D(I-2))/3.D0
64 P(I)=CSUM(I)-AFM*DESUM(I)
      IF(ITER.EQ.1.AND.IN.EQ.0) MN=1
      IF(ITER.EQ.1.AND.IN.EQ.0) ITER=0
      IF(IN.EQ.0) GO TO 269
      IF(IN.EQ.1.AND.ITER.EQ.2) MN=1
      IF(IN.EQ.1.AND.ITER.GE.2) GO TO 269
      DPVAL=FAES((P(I)-PB(I))/P(I))
      IF(I.EQ.2) EPVAL=DPVAL
      IF(I.EQ.2) GO TO 269
      IF(EPVAL.GT.DPVAL) EPVAL=DPVAL
269 PB(I)=P(I)
61 CONTINUE
      IF(MN.EQ.0) GO TO 291
      IF(IN.EQ.0) GO TO 291
      IF(IN.EQ.1.AND.ITER.GE.2) GO TO 291
291 CONTINUE
270 DO 109 I=1,M

```



```

      IF (MN.EQ.0) GO TO 267
      UY(I,N) = (U(I,N-2) + 3.DO*U(I,N) - 4.DO*U(I,N-1)) / (2.DO*DY)
      UY(I,1) = (4.DO*U(I,2) - 3.DO*U(I,1) - U(I,3)) / (2.DO*DY)
267 DO 108 J=1,N
C   EVALUATION OF GRAD'S OF STREAM FCN IN X DIRECTION
      IF (I.EQ.M) SX(I,J) = (S(I-2,J) + 3.DO*S(I,J) - 4.DO*S(I-1,J))
      * / (2.DO*DX)
      IF (I.EQ.1) SX(I,J) = (4.DO*S(I+1,J) - 3.DO*S(I,J) - S(I+2,J))
      * / (2.DO*DX)
      IF (I.NE.1.AND.I.NE.M) SX(I,J) = (S(I+1,J) - S(I-1,J)) / (2.DO
      * *DX)
      IF (MN.EQ.0) GO TO 108
      IF (I.EQ.M) UX(I,J) = (U(I-2,J) + 3.DO*U(I,J) - 4.DO*U(I-1,J))
      * / (2.DO*DX)
      IF (I.EQ.1) UX(I,J) = (4.DO*U(I+1,J) - 3.DO*U(I,J) - U(I+2,J))
      * / (2.DO*DX)
      IF (I.NE.1.AND.I.NE.M) UX(I,J) = (U(I+1,J) - U(I-1,J)) / (2.DO
      * *DX)
      IF (J.NE.1.AND.J.NE.N) UY(I,J) = (U(I,J+1) - U(I,J-1)) / (2.DO
      * *DY)
108 CONTINUE
109 CONTINUE
      IF (MN.EQ.0) GO TO 272
      IF (MN.EQ.1) GO TO 12
      IF (IN.EQ.1.AND.ITER.GT.2) GO TO 275
      IF (EPVAL.LT.EPRES) IN=0
      IF (EPVAL.LT.EPRES) GO TO 272
      GO TO 275
C   EVALUATION OF AVERAGE GRAD'S FOR POINTS IN FILM
272 DO 178 I=1,M1
      HF(I) = (H(I) + H(I+1)) / 2.DO
      DO 174 J=1,N
      SHX(I,J) = (SX(I,J) + SX(I+1,J)) / 2.DO
      SHY(I,J) = (SY(I,J) + SY(I+1,J)) / 2.DO
174 CONTINUE
178 CONTINUE
      IF (NITER.EQ.0) GO TO 445
      IF (EQVAL.LT.ETHET.AND.MM.EQ.1) GO TO 12
      GO TO 63
C   EVALUATION OF TEMP DIST
12 PRINT 300
300 FORMAT(30X,'RESULTS FOR TEMP DIST')
      IF (MM.EQ.1) PRINT 138
138 FORMAT(9X,'RESULTS FOR CONST VISCOSITY BASED ON A
      * V PLATE
      TEMPERATURE')
      IF (NITER.GT.1.AND.ITER.EQ.0) PRINT 139

```



```

130 FORMAT(8X,'RESULTS CONSIDERING VARYING VISCOSITY')
IF (NITER.GT.1) WRITE (6,118) NITER,ITER,EQVAL
118 FORMAT(12X,'NITER EQUALS',2X,I3,2X,'ITER EQUALS',2X,
* I3,2X,'EQVAL
* EQUALS',2X,D13.6)
IF (EQVAL.LT.ETHET) WRITE (6,119) ETHET
119 FORMAT(40X,'EQVAL LESS THAN',3X,D13.6)
DO 297 I=1,M
WRITE (6,132) (THETA (I,J),J=1,12)
132 FORMAT(1X,12(F7.4,1X)/)
WRITE (6,155) (THETA (I,J),J=13,21)
155 FORMAT(2X,9(F7.4,1X)/)
297 CONTINUE
PRINT 300
DO 296 I=1,M
WRITE (6,301) (T (I,J),J=1,12)
WRITE (6,302) (T (I,J),J=13,21)
296 CONTINUE
301 FORMAT(2X,12(F7.2,1X)/)
302 FORMAT(2X,9(F7.2,1X)/)
C EVALUATION OF HEAT FLUX AT PAD AND SLIDER AND SHEAR ST
* RESS AT SLIDER
DO 13 I=1,11
QYP(I) = -(THETA (I,1)-2) + 3.00*THETA (I,2) - 4.00*THETA (I,3) -
* 1)) /
* (2.00*DY*H(I))
QYS(I) = (4.00*THETA (I,2) - 3.00*THETA (I,1) - THETA (I,3)) /
* (2.00*DY*H
* (I))
C EVALUATION OF TEMP GRAD'S AT BOUNDARIES
DTDYP(I) = -H(I)*QYP(I)
DTDYS(I) = H(I)*QYS(I)
FDY(I) = AFM*SYI(I,1) / (H(I)**2*F(I,1))
13 CONTINUE
PRINT 195
195 FORMAT(30X,'TEMP GRADIENTS AT PAD')
WRITE (6,197) (DTDYP(I),I=1,M)
197 FORMAT(2X,11(F10.6,1X)/)
PRINT 196
196 FORMAT(30X,'TEMP GRADIENTS AT SLIDER')
WRITE (6,197) (DTDYS(I),I=1,M)
PRINT 143
143 FORMAT(30X,'HEAT FLUX AT PAD')
WRITE (6,197) (QYP(I),I=1,M)
PRINT 144
144 FORMAT(30X,'HEAT FLUX AT SLIDER')
WRITE (6,197) (QYS(I),I=1,M)
PRINT 121

```



```

121 FORMAT(30X,'RESULTS FOR SHEAR FCN DISTRIBUTION')
DO 501 I=1,M
WRITE(6,33) (S(I,J),J=1,12)
WRITE(6,161) (S(I,J),J=13,21)
33 FORMAT(2X,12(F9.4,1X)/)
161 FORMAT(2X,9(F9.4,1X)/)
501 CONTINUE
PRINT 211
211 FORMAT(30X,'RESULTS FOR VELOCITY DIST')
DO 502 I=1,M
WRITE(6,33) (U(I,J),J=1,12)
WRITE(6,161) (U(I,J),J=13,21)
502 CONTINUE
PRINT 145
145 FORMAT(30X,'SHEAR STRESS AT SLIDER')
WRITE(6,197) (FDY(I),I=1,M)
C EVALUATION OF LOAD CAPACITY OF BEARING AND FRICTIONAL
* FORCE ON RUNNER
FSUM=0.D0
PSUM=0.D0
QPSUM=0.D0
QSSUM=0.D0
C EVALUATION OF LOAD CAPACITY OF BEARING
DO 14 I=3,11,2
PSUM=PSUM+(P(I)+4.D0*P(I-1)+P(I-2))*DX/3.D0
FSUM=FSUM+(FDY(I)+4.D0*FDY(I-1)+FDY(I-2))*DX/3.D0
C EVALUATION OF HEAT CONDUCTED AWAY AT BOUNDARIES
QPSUM=QPSUM+(QYP(I)+4.D0*QYP(I-1)+QYP(I-2))*DX/3.D0
QSSUM=QSSUM+(QYS(I)+4.D0*QYS(I-1)+QYS(I-2))*DX/3.D0
14 CONTINUE
QSPER=DABS(QSSUM)/(DABS(QSSUM)+DABS(QPSUM))
145 PRINT 140
140 FORMAT(30X,'FINAL RESULTS FOR PRESS DIST')
WRITE(6,105) (P(I),I=1,6)
105 FORMAT(2X,6(D13.6,2X)/)
WRITE(6,151) (P(I),I=7,11)
151 FORMAT(2X,5(D13.6,2X)/)
IF(NITFP.EQ.0) GO TO 113
PRINT 141
141 FORMAT(2X,'LOAD CAPACITY',10X,'DRAG',10X,'MASS FLOW'
* ,10X,'HT
PTHRU SLIDER')
WRITE(6,142) PSUM,FSUM,AFM,QSPER
142 FORMAT(2X,F13.6,14X,3(F8.4,14X))
PRINT 165
165 FORMAT(2X,'HT CCNUCTED THRU SLIDER',15X,'HT CONDU
* CTED THRU
* PAD',15X,'POWER REQUIRED')

```



```

WRITE(6,166) QSSUM,QPSUM,FSUM
166 FORMAT(11X,F10.5,23X,2(F11.5,23X))
DO 199 J=1,N
C   EVALUATION OF HT CONVECTED INTO BRG
    TSIM(J)=AFM*THETA(1,J)*SY(1,J)
C   EVALUATION OF HT CONVECTED OUT OF BRG
    TSEM(J)=AFM*THETA(M,J)*SY(M,J)
199 CONTINUE
    QISM=0.D0
    QESM=0.D0
    DO 200 J=3,N,2
        QISM=QISM+DY*(TSIM(J)+4.D0*TSIM(J-1)+TSIM(J-2))/3.D0
        QESM=QESM+DY*(TSEM(J)+4.D0*TSEM(J-1)+TSEM(J-2))/3.D0
200 CONTINUE
    WRITE(6,201) QISM,AFM
201 FORMAT(4X,'HEAT CONVECTED INTO BRG EQU',2X,F10.5,'
* AND',F10.5)
    WRITE(6,202) QESM,AFM
202 FORMAT(4X,'HT CONVECTED OUT OF BRG EQU',2X,F10.5,
* 'AND',F10.5)
C   EVALUATION OF AVERAGE TEMP IN BEARING
    DO 799 I=1,M
        US=0.D0
        UTSM=0.D0
        TSM=0.D0
        DO 798 J=3,N,2
            USM=USM+DY*(U(I,J)+4.D0*U(I,J-1)+U(I,J-2))/3.D0
            UTSM=UTSM+DY*(U(I,J)*THETA(I,J)+4.D0*(U(I,J-1)*THETA(I
* ,J-1))
* +U(I,J-2)*THETA(I,J-2))/3.D0
            TSM=TSM+DY*(THETA(I,J)+4.D0*THETA(I,J-1)+THETA(I,J-2))
* /3.D0
798 CONTINUE
        TB(I)=TAV*UTSM/USM
        TA(I)=TAV*TSM
799 CONTINUE
        WRITE(6,105) (TB(I),I=1,6)
        WRITE(6,151) (TB(I),I=7,11)
        WRITE(6,105) (TA(I),I=1,6)
        WRITE(6,151) (TA(I),I=7,11)
        TBSM=0.D0
        TASM=0.D0
        DO 797 I=3,N,2
            TBSM=TBSM+DX*(TB(I)+4.D0*TB(I-1)+TB(I-2))/3.D0
            TASM=TASM+DX*(TA(I)+4.D0*TA(I-1)+TA(I-2))/3.D0
797 CONTINUE
        WRITE(6,784) TBSM,TASM
784 FORMAT(' ',//,30X,'BUICK TEMP EQUALS',2X,E13.5,2X,'AV
* ERAGE TEMP

```



```

*   EQUALS',2X,E13.5)
IF(MM.EQ.1) GO TO 63
NA=NA+1
IF(NA.EQ.1) PRINT 277
277 FORMAT(' ',//,30X,'RESULTS INCLUDING INERTIA TERMS')
IF(NA.EQ.1.AND.IN.EQ.0) GO TO 275
ANS(I1,1)=R
ANS(I1,2)=TS
ANS(I1,3)=TF
ANS(I1,4)=TSTP
ANS(I1,5)=PE
ANS(I1,6)=PEC
ANS(I1,7)=PRL
ANS(I1,8)=DT
ANS(I1,9)=DT*TSTP
ANS(I1,10)=CEDRE
ANS(I1,11)=PSUM
ANS(I1,12)=FSUM
ANS(I1,13)=AFM
ANS(I1,14)=QPSUM
ANS(I1,15)=QSSUM
ANS(I1,16)=QISM
ANS(I1,17)=QESM
ANS(I1,18)=BT
ANS(I1,19)=CNTHT
ANS(I1,20)=RE
ANS(I1,21)=TESM
ANS(I1,22)=IASM
1000 CONTINUE
PRINT 698
698 FORMAT(' ',////////,30X,'RESULTS OF NUMERICAL ANALYSIS
*   ')
DO 691 I1=1,NUM
WRITE(6,700) (ANS(I1,J),J=1,7)
700 FORMAT(' ',//,3X,7(E13.5,2X))
WRITE(6,899) (ANS(I1,J),J=8,14)
899 FORMAT(' ',3X,7(E13.5,2X))
WRITE(6,447) (ANS(I1,J),J=15,22)
447 FORMAT(' ',3X,8(E13.5,2X))
691 CONTINUE
STOP
END
SUBROUTINE INV
IMPLICIT REAL*8 (A-D,F-H,O-Z)
DIMENSION T(67),W(67),ARG(10),VAL(10)
REWIND 2
READ(2)T,W
RETURN

```



```
ENTRY  VIS (TEMP,V)
CALL  DATSM (TEMP,T,W,67,1,ARG,VAL,10)
IF (TEMP.LE.2.3D2) ERR=0.0168E-6
IF (TEMP.LE.1.1D2) ERR=0.14E-6
IF (TEMP.LE.2.5D1) ERR=0.50E-5
CALL  DALI (TEMP,ARG,VAL,V,10,ERR,IER)
RETURN
END
```


B30028